UNIVERSITY OF CALIFORNIA
RIVERSIDE

Understanding and Advancing CELF to Maximize Biofuels and Bioproducts Yields from Lignocellulosic Biomass

A Dissertation submitted in partial satisfaction
of the requirements for the degree of

Doctor of Philosophy

in

Chemical and Environmental Engineering

by

Priyanka Singh

June 2022

Dissertation Committee:
Dr. Charles E. Wyman, Chairperson
Dr. Ian R. Wheeldon
Dr. Charles M. Cai

The Dissertation of Priyanka Singh is approved:

_____

_____

_____

Committee Chairperson

University of California, Riverside

ACKNOWLEDGEMENTS

I am incredibly grateful to all my friends, family, colleagues, and mentors who have been there through every part of this amazing journey.

First and foremost, Dr. Wyman, being your last official student has been an honor. I have learned so many valuable lessons from you throughout both my undergraduate and graduate studies. Your classes have given me an understanding of the field that stretches beyond what happens in lab. You have trusted me to lead collaborations and carryout numerous projects. Your patience, understanding, and most of all jokes on days when Murphy's law would take over, were always comforting. Your constant encouragement before conference presentations and kind words will be the highlight of my graduate career. I am a better engineer having been mentored by you.

Dr. Wheeldon, you have always been a great mentor and professor with whom to work. The first time I ran a bioreactor was in 124 lab, and since then, I have not wanted to do much else. You have always come through with support whether it was for AIChE when you were our advisor or coming to CEE GSA events. I thank you for your advice during my candidacy exam and throughout my studies. I am grateful for the opportunities and coursework that you allowed me to take in the Industrial Biotechnology Program.

Dr. Cai, we have come full circle from you showing me the ropes as an undergraduate student mentor to trusting me to execute projects as a graduate student. I will always carry forth the valuable lessons in experiment design and execution. I'll never start an experiment without a purpose and thanks to you I have truly learned how to do meaningful investigations. Thank you for always encouraging me to keep going.

Outside of my committee, Dr. Kawai Tam has been my mentor through senior design and graduate school. I appreciate that I could always go to you for support and the valuable insights you would always have for me. I hear your voice when using shortcut commands, writing my thesis, and preparing to give talks. I owe you all the accolades I have been given for my presentation skills and preparedness for grad school.

To my CBI colleagues who mentored, taught me, and processed large sample loads, thank you. To Dr. Evert Holwerda, I am so grateful for your master classes on CBP and life in lab in general. Your willingness to always meet and discuss science has been a joy. To Dr. Yannick Bomble, you helped shape much of the CELF-CBP collaborations and supported me as team lead for deconstruction. To Dr. Yining Zeng, I have valued all your feedback especially, in planning the work and analysis reported in Chapters 2 and 3. And Neal, thank you for your help on the Chapter 3 and your constant encouragement. Dr. Maria Pena, you have also been incredibly helpful throughout this process. Your sample analyses greatly improved our understanding in Chapters 3 and 4. To Dr. Yunqiao Pu, who taught me everything I know about HSQC NMR, I thank you for dealing with my sample analysis requests which have greatly contributed to Chapters 2 and 4 of my thesis. I would also like to thank my lab mate Bhogesh Seemala for the willingness to help and to perform X-ray diffraction characterizations to gain further insight in Chapter 3. To Dr. Hyeongmin Seo, thank you for your enthusiasm; it was a pleasure collaborating with you and Dr. Cong Trihn for Chapter 5. A special thank you to Xianzhi Meng, Dr. Ragauskas, and this team on the Azo Dye paper. I would like to thank you all and am grateful to feature the lignin absorbent work in Chapter 7. To Sanchari Ghosh, I appreciate your constant help, feedback, and

support especially towards the end of my thesis. Sarah Hammer, I also appreciate all your support and guidance in the last few months as well. Additionally, to Sandra Notonier and Lilly Amore, I am so thankful for your advice from NREL all the way through my last weeks of grad school.

To my lab mates I am thankful for your guidance and support. Specifically, to Dr. Christian Alcaraz, you are the best lab mate and an even better friend. Grad school would not have been the same if it were not for not for our shenanigans and constant laughter and you passing down valuable mathematical insights for my thesis work. To Leo Ballesteros, Golden Se, Zachary Lyons, and Laura McAllister, undergrads who worked with me, thank you for your great work and dedication. I'd also like to thank my honorary undergrads Juana Sanchez, Raffay Ahmed, and Crystal Pargas for their hard work as well.

To Dr. Abhishek Patri, thank you for teaching me anaerobic shake flask fermentations and your constant mentorship and guidance. Thank you for also being the best doubles partner. Dr. Ninad Kothari for all your CBP and gameboard teaching, Dr. Priya Sengupta for being my favorite member of the PS squad, Glen Svenningsen for always making us laugh, and finally Brent Scheidemantle, for all the support throughout the last decade, your help in the lab was a blessing.

To Jeanette Sanchez and Luis Ortiz, I simply have no idea how I would have done this without you both. I am so thankful I got to come back to Riverside and live with you. Not only did you support, feed, and keep a roof over my head you took me in to your families, always had my back, and kept me laughing. I will never be able repay you for

your love and support, but I owe a large part of getting to the end to both of you. And of course, Ali (Pali) and Mochi (Pochi) for being the best support animals a girl could ask for.

To Kendra Hudzik, I appreciate all the trips you made from Albuquerque for parking lot lunches, quick dinners, and birthday celebrations. You have been the best friend and support system since our days at Lincoln.

To Lakhan Gandhi, I am incredibly lucky for all your support through this. Thank you for pushing me to think critically and advising me when I wanted to carry out large experiment sets. I will never forget all the times you came to Riverside to help me with food and chores when I was running the large experiment sets. Thank you for always making sure I got to my car safely and for driving me to lab for late time points. I especially want to thank you for driving me to lab on Christmas Eve at 4 am, just to find out that I had forgotten my badge.

To Hannah, Christian G. and now my little Axel, thank you for making the trips out to Riverside and always motivating me and helping me. Thank you for all the magical outings and being by my side through the ups and the downs. I value all the lessons you have both taught me throughout my PhD and will carry those into my career.

To Anna Almario, thank you for always pushing me to be the best engineer and teammate I could be and by leading by example. I couldn't have done this without all your encouraging texts and punny cards throughout undergrad and grad school. Our Pri-Anna adventures have always given me perspective outside the lab, beautiful sights, and endless belly laughs, svo gott (the only Icelandic term that stuck).

To the Riverside family forever, Jeanette, Luis O., Lakhan, Naylley, Luis V., Aaron, Christine, Aiden, Yari, Ashley, Juan, and Beatriz, I love you all for your patience and support. Thank you for allowing me to hide in my room or be late to things because of lab work and thesis writing. Thank you for giving me a family of solid supporters and endless memories.

To Lauren & Rigel, thank you for always planning special weekends and trips. To Jenn, the Garling boys, & Caitlyn thank you for giving me Facetime company and laughs during the long lab days and nights. To Sanjana thank you for always checking in with me weekly and cheering on my accomplishments. To Zannain, Marwan, and Kamran thank you for always popping in to check on me. All of you have been supporting my PhD dreams for over 15 years and I am thankful for that.

To my Ce-CERT family Ayla my batchmate and forever support system, Carolyn, Val, Todd, John, and Bernice thank you for allowing me to come to you every day and for all your help.

To my family, you have given me the world. To Shalini and Jessie, I appreciate you both taking care of my mental health and overall health with all the food. To my Nanaji, I admire you and your love for education. I hope that you will read this and feel proud of the values that you and Nani ma have passed down to me.

Finally, to my mom, dad, and brother, when I turn around I see you three. You are my whole heart. I truly appreciate the never-ending love and support. Thank you for giving me this and many other opportunities, motivating me and cheering me on every step to the finish line. I love you all very much.

Last, but certainly not least, to the funding agencies that funded this research: the DOE Basic Energy Science funded Center for BioEnergy Innovation (CBI), National Center for Sustainable Transportation Fellowship, Environmental Protection Agency P3 Phase 2 funding, Graduate Assistance in Areas of National Need (GAANN) Fellowship from UCR, Esther F. Hays Graduate Fellowship at CE-CERT, The Colin E. Hackett Endowed Engineering Research Award at CE-CERT, and the Ford Motor Company Chair in Dr. Wyman's name.

DEDICATION

To Nick Foles and the 2018 Philadelphia Eagles for all we have been through.

And to my Parents, Seema and Rakesh Singh and my Brother, Abhishek Singh, for the same thing.

ABSTRACT OF THE DISSERTATION

Understanding and Advancing CELF to Maximize Biofuels and Bioproducts Yields from Lignocellulosic Biomass

by

Priyanka Singh

Doctor of Philosophy, Graduate Program in Chemical and Environmental Engineering
University of California, Riverside, June 2022
Dr. Charles E. Wyman, Chairperson

Lignocellulosic biomass is a renewable resource with the potential to significantly reduce our dependence on petroleum. However, its recalcitrant nature necessitates robust conversion technologies to enable its conversion into carbon neutral fuels and products. Co-solvent Enhanced Lignocellulosic Fractionation (CELF) employs tetrahydrofuran in solution with aqueous dilute acid to fractionate biomass into its major components. The solids produced by CELF are highly amenable to saccharification, however, the higher enzyme loadings required to achieve high rates along with high yields are cost prohibitive. Anaerobic organisms that combine enzyme production and fermentation in a single unit operation called consolidated bioprocessing (CBP) can eliminate separate enzyme production and thereby dramatically reduce process costs.

This thesis reports on understanding factors that influence the performance of CELF pretreatment of lignocellulosic biomass with subsequent CBP to maximize product yields at low process severity. Results show that CELF and CBP synergistically

deconstructed hardwood Poplar, eliminating the need for external enzymes, with CELF-CBP pairing enabling ~100% glucan solubilization by *C. thermocellum* of solids produced by operation of CELF at a low process severity (2.87). GPC and NMR characterization of residual lignin showed decreases in average molecular weight and a substantial decrease in β-*O*-4 linkage both after CELF and CELF-CBP, suggesting further lignin modification by *C. thermocellum* CBP. CELF-CBP (*C. thermocellum*) pairing was then compared with CELF-fungal cellulase Ctec2 and CELF-*C. thermocellum* secretome combinations. Fractal kinetics were applied to model glucan solubilization rates by each of these three systems, and the rate coefficient k_t and fractal exponent h were compared. Residual xylan from CELF was shown to inhibit *C. thermocellum* activity at high solids loadings (75-100 g/L). However, using *T. thermosaccharolyticum* in combination with *C. thermocellum* in a co-culture strategy minimized xylose accumulation and increased glucan solubilization to >97% at 75g/L solids loadings. The CELF process was then optimized for renewable ester biosynthesis using an appropriately engineered *C. thermocellum*. In addition, CELF pulping of industrial hemp enabled utilization of whole hemp as hemp-fuel and hemp-crete. Finally, aminating lignin from the CELF process was demonstrated to produce an excellent absorbent for toxic dyes. These results demonstrate the versatility of CELF technology and advantageous CELF-CBP synergies for utilization of recalcitrant biomass for production of renewable fuels and other bioproducts.

List of Tables

List of Figures

Table of Contents

Chapter 1: Introduction

1.1 Sustainability: The Critical Need for Renewable Fuels and Chemicals

The world population has reached >7.9 Billion and is projected to increase to >10 billion by the year 2100 (Figure 1-1). Fossil fuels provide > 80% of US energy, and the demand for petroleum is projected to surpass 100 million barrels per day by 2026 (Oil 2021 IEA, 2021). The US transportation sector alone contributes ~ 1/3 of total greenhouse gas emissions (US EPA, 2019) (Figure 1-2). Heavy dependence on fossil fuels and particularly petroleum to meet energy needs results in the release of vast quantities of carbon dioxide, a major greenhouse gas (GHG), whose accumulation is causing global climate change (US EIA, 2019.; Seyboth K. et al., 2011.; Sims, 2004), acidification of oceans (Billé et al., 2013; Doney et al., 2008), rising sea levels (US EPA, 2019.; Titus, 1990; Zickfeld et al., 2017), and other associated problems (*Climate Change and Health*, n.d.; Eckelman & Sherman, 2018; Ohashi et al., 2019) due to the increase of global mean temperature above preindustrial levels (Climate Analytics, n.d.; Hansen et al., 2010). Globally, the transportation sector alone is responsible for about ¼ of total anthropogenic greenhouse gas emissions. Petroleum fuels are inexpensive, energy dense, and easily accessible due to vast infrastructure to support the supply of liquid transportation fuel. Heavy reliance on foreign oil creates energy security concerns in addition to environmental problems. Energy and environmental concerns are two major incentives for developing fuels with low carbon footprints (EIA, 2020; Jeswani et al., 2020; Khan et al., 2021). Petroleum also provides ~90% of commodity and specialty chemicals (Mondal et al., 2011; Petrochemical, Commodity & Specialty Chemicals, 2021.). Burning fossil fuels is linked to climate change (EESI, 2020; Lelieveld et al., 2019). In addition, petrochemical production from a barrel

of oil requires significant energy inputs and further pollutes the environment. Continuing this trend of business as usual is not sustainable. The only way to make finite resources work with the exponential population growth rate and abate climate change and the pollution issue is to resources and adopt stringent green manufacturing practices.

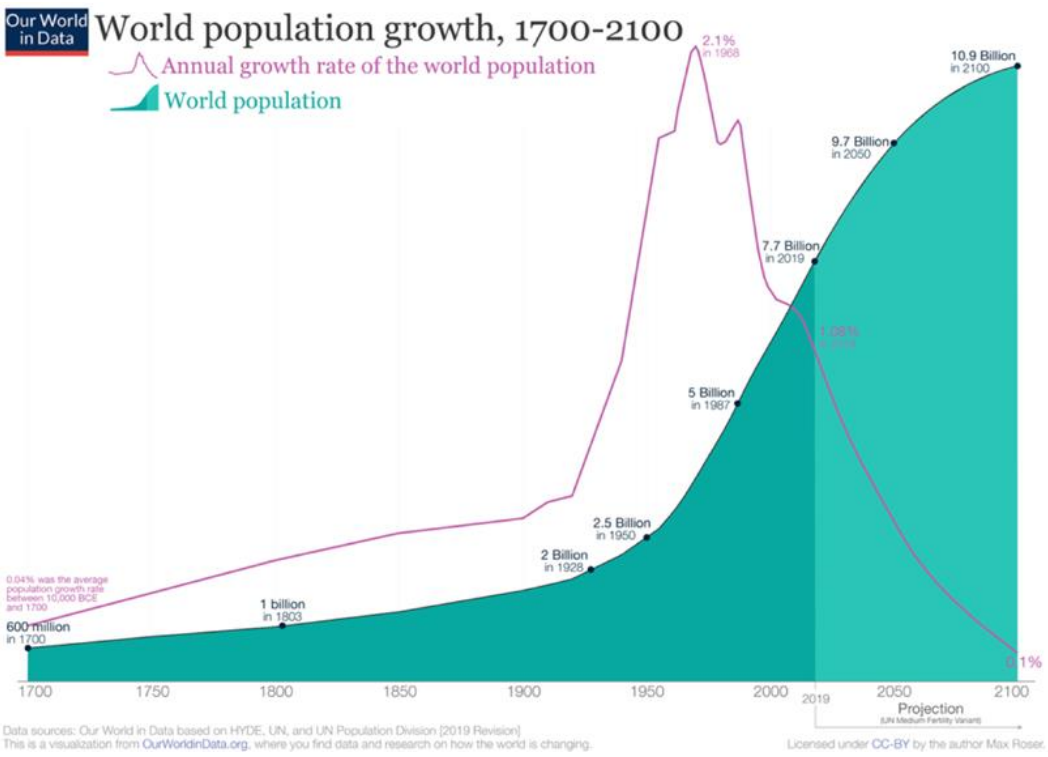

Figure 1-1. World population growth. Max Roser (2013) - "Future Population Growth"

**Published online at OurWorldInData.org*. Retrieved from: https://ourworldindata.org/future-population-growth

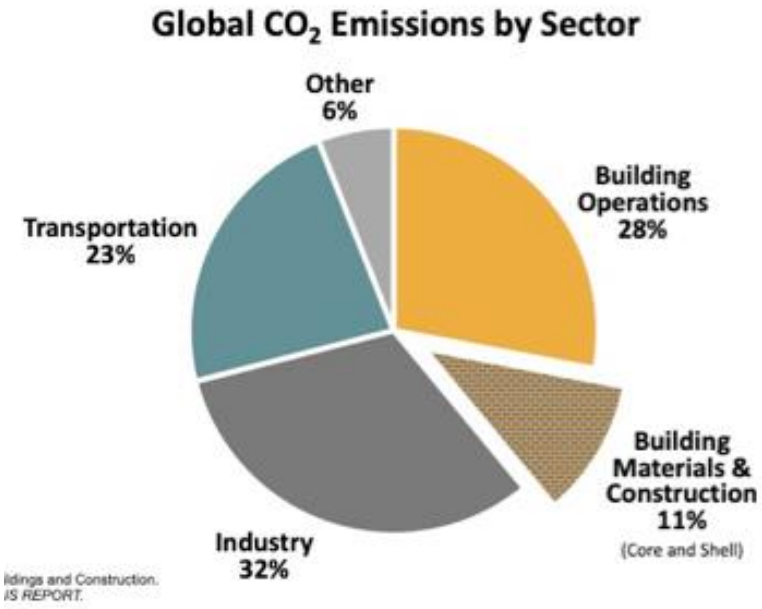

Figure 1-2. Global CO2 emission by sector.*

*Taken from global alliance for Buildings and construction 2018 global status report https://www.iea.org/reports/2018-global-status-report

1.2 Lignocellulosic Biomass as a Sustainable Feedstock

Lignocellulosic biomass has the potential to increase energy security and lessen environmental concerns by enabling production of near or totally carbon neutral fuels and commodity chemicals (Lewandrowski et al., n.d.; Olofsson et al., 2008). Although a variety of technologies are needed to achieve low GHG emissions, lignocellulosic biomass such as agricultural and forestry residues and fast growing grassy and woody energy crops provide a unique low cost and abundant resource for the production of liquid transportation fuels and high value chemicals with a low carbon footprint (Biomass Energy | National Geographic Society, n.d.; Gent et al., 2017). For instance, the Department of Energy estimated that up to 1.6 billion dry tons of biomass could be available annually in the US

at less than $60/dry ton, about equivalent to $20/barrel petroleum (Efroymson et al., 2017; White, 2010). This amount of biomass could displace about 100 billion gallons of gasoline of the 126 billion gallons of gasoline used each year in the US (Use of Gasoline - U.S. Energy Information Administration (EIA), 2020). Lignocellulosic biomass as a renewable, non-food resource to replace finite petroleum is incentivized by the Renewable Fuel Standard (RFS) program put in place under the Energy Policy Act of 2005 to target production of 36 billion gallons of renewable transportation fuel by 2022 (Alternative Fuels Data Center: Renewable Fuel Standard, 2018.; The Renewable Fuel Standard (RFS): An Overview, 2022).

1.3 Need for Efficient Biomass Fractionation Approaches

Although fuels from lignocellulosic biomass are vital to meet GHG reduction targets and reduce dependence on dwindling fossil fuels, lignocellulosic plants resist reaching industrially relevant yields despite many efforts to apply thermochemical and biological processes (Auxenfans et al., 2017; Himmel et al., 2007a; McCann & Carpita, 2015; X. Zhao et al., 2012). Numerous pretreatment and fractionation technologies have been developed for overcoming biomass recalcitrance. The application of the burgeoning field of biotechnology has also resulted in impressive advances in biological systems to overcome this recalcitrance (Holwerda et al., 2019; Lynd et al., 2008). However, major cost barriers are still to be overcome, such as the high cost of pretreatment and high loadings of expensive enzymes needed to realize high product yields (Klein-Marcuschamer et al., 2012). Thus, the key now is to develop efficient pretreatment technologies that overcome recalcitrance and dramatically reduce the amount of enzymes needed to

breakdown the plant cell-wall components into simple sugars and aromatics. To become economically viable, improved biomass processing technologies that lower both capital (CapEx) and operational expenditures (OpEx) are needed (Tao et al., 2014). Pretreatment and fractionation technologies that are not energy intensive and do not require many separations and processing steps to make polysaccharide sugars and lignin amenable to downstream biological and/or catalytic conversion could significantly enhance competitiveness (Kothari et al., 2018; Xu et al., 2016).

1.4 Role of Bioconversion for Biofuels and Chemicals from Lignocellulosic Biomass

Because of high production and purification costs, enzymes for polysaccharide breakdown into monomeric sugars are expensive (Olson et al., 2011). Approaches that could reduce or eliminate the need to add externally generated enzymes for breakdown of polysaccharides into usable monomeric sugars for biological conversion could further enable industrial production of cellulosic fuels (Olson et al., 2011). Consolidated BioProcessing (CBP) that combines enzyme production, release of sugars from polysaccharides (saccharification), and fermentation of those sugars into ethanol in a single unit operation is gaining attention as an attractive route to dramatically reduce lignocellulosic biomass conversion costs (Figure 1b) (Lynd, 2008; Mbaneme-Smith & Chinn, 2015). Because conventional fungal enzyme costs are prohibitive at ~ $0.68-1.47/gallon ethanol produced and fermentation times of pretreated solids at low enzyme loadings are very long (indicating slow kinetics) and incomplete, pretreatment and fractionation technologies are being developed to reduce biomass recalcitrance and enhance enzyme accessibility to cellulose (Tian et al., 2017; Weiss et al., 2019) to rapidly

and almost completely breakdown biomass. It is also important to identify processing conditions that lower energy requirements, minimize biomass degradation, and achieve high product yields.

1.5 Process Intensification- A Must for Biorefinery

Creating renewable fuels and chemicals from lignocellulosic biomass is still challenging. The majority of pretreatment and fractionation processes being investigated are constrained by factors such as low titer and high-water usage. For example, in order to promote efficient distillation and reduce energy inputs, industrial ethanol production requires an ethanol titer of more than 40 g L^{-1}(Olofsson et al., 2008). It is therefore necessary to use a high glucan loading. To achieve high titer, high-gravity (HG) biomass processing has been frequently employed. However, most of the reported processes require large quantities of water for removal of inhibitors from the pretreated biomass before saccharification. Furthermore, the idea of 'no carbon left behind' is challenging because the efficient processing of one polymer at the expense of another has been often observed (Alonso et al., 2017; Carvalheiro et al., 2008). For example, because hemicellulose is very susceptible to degradation at high temperatures and longer times, conditions required for the depolymerization of cellulose and lignin may be too harsh for hemicellulose preservation, rendering sugars from this polymer unavailable for further upgrading. Therefore, it is important to gain insights into how process severity impacts product profiles from the various biomass components are in order to define optimum process scenarios and make the best use of biomass.

1.6 Lignocellulosic Biomass Utilization- Example Applications

Lignocellulosic biomass deconstruction technologies that could be tuned to create substrates and deconstructed products with desired chemistries could truly revolutionize renewable fuels, chemicals, and materials from natural biopolymers in lignocellulosic biomass. Fractionated cellulose, xylan, and lignin polymers and deconstructed sugars and aromatics can serve as important sources of chemicals and materials for a wide range of applications in multiple sectors. For example, cellulose fibers and formulations therefrom (Mannai et al., 2019) for production of nanocellulose (Gupta & Shukla, 2020), renewable aromatics (Mahajan et al., 2020), platform chemicals from glucose/HMF (Assary et al., 2012; Takkellapati et al., 2018), and platform chemicals from xylose/furfural have been demonstrated (Li et al., 2016). The chemical catalysis approach has its own advantages and is being extensively studied. It is important to note that since ethanol production technologies are more mature in comparison to other advanced fuels, starting with ethanol as a platform chemical and its chemical transformation into a multitude of other high value chemicals or high-density fuels seems very promising.

Biological approaches starting with hydrolysates of pure glucose, xylose, and monomeric lignin and mixtures thereof for the bioconversion into high value chemicals or high energy density fuels is also being studied. Although, at a much more fundamental level compared to chemical transformation, numerous success stories are being reported for biological conversion of ligninolysate hydrolysate (Ramos & Duque, 2019). Most importantly, genetic engineering, synthetic biology, and gene editing are already proving microbes to be capable of achieving highly specific chemistry on demand (Johnson et al.,

2019; Kondo et al., 2013; J. W. Lee & Trinh, 2022; Papanek et al., 2015). The modular nature of genes and gene cassettes and the ability to mix and match elements are creating designer super microbes that have the potential to further transform this field.

It is important to note that for both chemical and biological production of fuels, chemicals and materials from recalcitrant lignocellulosic biomass, pretreatment/deconstruction (whether thermochemical, mechanical, biological, or hybrid chemical-biological) will still be required. Therefore, the development of efficient, cost effective, feedstock agnostic, tunable, scalable deconstruction technologies is a must for renewable fuels, chemicals, and materials to reduce GHG emissions and reduce energy and environmental concerns.

1.7 Research Focus

To meet the high volume of renewable fuels and chemicals, a variety of feedstocks will be required. Also, due to the regional and seasonal variability in the availability of the feedstocks for biorefineries, robust feedstock agnostic deconstruction technologies must be developed. To overcome lignocellulosic biomass recalcitrance, plant genetic modifications to lower or modify lignin and xylan linkages are being developed. It is important that pretreatment and fractionation technologies be developed that are flexible to changes in the lignocellulosic biomass attributes. Therefore, it is important to understand how a given pretreatment technology affects physical and chemical characteristics of lignocellulosic biomass and how reaction conditions and processing details (pretreatment temperature, processing time, reaction pressure, reactor design, mixing condition, loadings,

pre-processing, particle size etc.) influence the changes to pretreated lignocellulosic biomass and its downstream bioconversion.

Pretreatment technologies being developed must be low in cost, efficient, feedstock flexible, and scalable. Pretreatment, if efficient, deconstructs plant cell wall and makes the holocellulose more accessible to enzymes and biocatalysts, thereby reducing the amount of enzyme needed and lowering costs. Furthermore, it is also important to understand if the deconstruction process itself leads to deconstructed product(s) that negatively influence enzymes and fermentative microbes. In essence, the development of cost-effective deconstruction technologies and renewables fuels at cost parity with petroleum fuels is complex and very challenging.

Pretreatment of lignocellulosic biomass by Co-solvent Enhanced Lignocellulosic Fractionation (CELF) can be integrated with biological technologies for the breakdown of lignocellulosic biomass into simple sugars (Cai et al., 2013; Nguyen et al., 2015). Integration of pretreatment with simultaneous saccharification and fermentation (SSF) and pretreatment with consolidated bioprocessing (CBP) are being developed to minimize the costs for unit operations, separation, and enzymes (Figure 1-3). As illustrated in Figure 1-4, CELF pretreatment employs tetrahydrofuran (THF) in solution with approximately equal amounts of aqueous dilute sulfuric acid (DSA) at 140-180°C to produce solids that are highly amenable to downstream saccharification with commercial enzymes (Cai et al., 2013b; Holwerda et al., 2019a; Kothari et al., 2018a; Nguyen et al., 2015b; Thomas, Donohoe, et al., 2017a; Thomas, Kothari, et al., 2017b). The susceptibility of CELF solids to deconstruction can be attributed to CELF's ability to fractionate biomass into its major

components of cellulose, hemicellulose, and lignin. Thus, in addition to making highly digestible solids, CELF provides the opportunity to enhance revenues and profitability by utilizing all components of lignocellulosic biomass. Specifically, since lignin valorization is now recognized as a key to low-cost biofuels (Ragauskas et al., 2014), CELF presents the additional advantage of lignin isolation for processing into fuels, chemicals and materials (Wyman et al., 2017).

However, a better understanding of the mechanisms that facilitate these advantages will enable the design of process conditions to control the desired characteristics of breakdown products in various streams and maximize carbon utilization. Such an understanding can also help identify routes to even better systems. CELF process optimization and integration with downstream biological conversion will require a deep understanding of how CELF substrates pretreated at different conditions influence enzyme loading requirements and changes to the metabolism of fermentative microbes and yields of the desired products. The investigation into the advantages and the limitations of various promising biological systems will allow informed decision making when pairing pretreatment technology with a biological system for the desired outcome. Furthermore, bench scale shake flask studies are important for establishing fundamental knowledge and a better understanding of a process being developed. However, understanding scaling limitations and opportunity for process improvement, and optimization at high solids loading to increase the product concentration and minimize energy input needed for product recovery, is a critical next step for the technologies being developed for renewable fuels and chemicals.

Consistent with the need for CELF process optimization at the lowest possible severity, the pairing of the CELF process with a promising biological system that reduces enzyme loading or eliminates the need for exogenous enzyme production by pairing with consolidated bioprocessing biocatalyst furthers CELF optimization for high solids fermentation/CBP. This thesis will focus on understanding the effect of CELF process severity on physio-chemical features of CELF substrates and its influence of the extent on glucan solubilization by biological systems. Specifically, the CELF process will be optimized for a woody biomass Poplar and paired with *Clostridium thermocellum* consolidated bioprocessing to investigate and correlate CELF substrate characteristics with total glucan solubilization. Specific objectives of this thesis are:

1. Gain a better understanding and optimize the CELF process on a woody biomass by understanding how CELF severity impacts Poplar characteristics and the influence of substrate characteristics on glucan solubilization with biological systems.
2. Pair CELF with CBP to understand the synergy of CELF and *C. thermocellum* in order to further optimize the process and maximize glucan solubilization.
3. Compare deconstruction of CELF Poplar using *C. thermocellum* CBP, the secretome from *C. thermocellum*, and fungal cellulase and apply fractal kinetic modeling to understand factors influencing the rate and extent of glucan solubilization.
4. Investigate the impact high of solids loadings of CELF pretreated poplar solids on CBP to understand limits on biological deconstruction.

5. Study high solids CELF-CBP to understand the influence of residual xylan and lignin in the CELF pretreated substrate and explore promising strategies to overcome the inhibition.
6. Investigate and optimize the production of bio-esters from CELF pretreated Poplar using engineered *C. thermocellum*.
7. Determine the extent of CELF applicability for utilization of fiber and hurd in industrial hemp and demonstrate the production of fuel and materials from hemp.
8. Gain a fundamental understanding of what happens to lignin in Poplar during CELF and during biological deconstruction. Track molecular weight and changes to main linkages in lignin during various steps.
9. Explore CELF lignin utilization for green manufacturing of lignin-based dye absorbent.

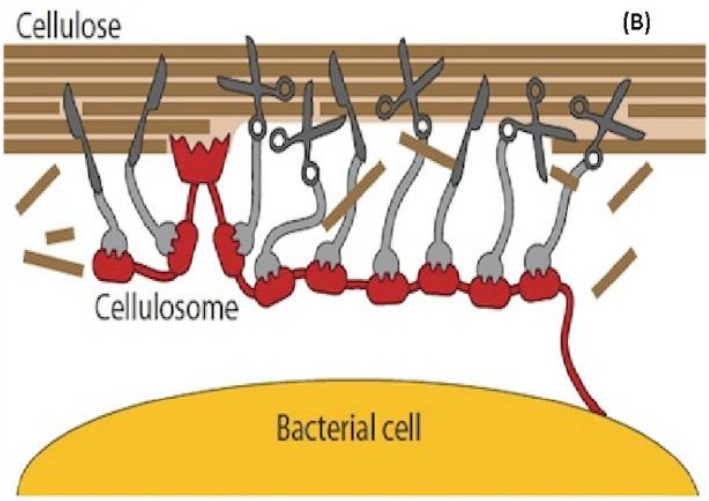

Figure 1-3. Cellulosome- an extracellular multi-enzyme complex from *C. thermocellum* is an order of magnitude more efficient at breaking down cellulose than the current enzyme technologies (Olson et al. 2010).

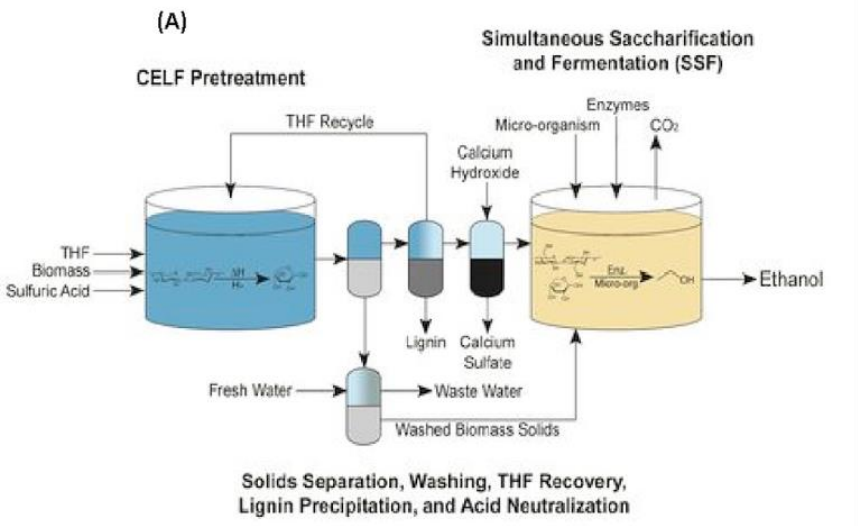

Figure 1-4. Schematic of CELF pretreatment technology developed at UCR. (Nguyen et al., 2015)

1.7 Dissertation Organization

Chapter 2 reports on the optimization of CELF on Poplar (*Populus trichocarpa*) to provide glucan enriched solids for deconstruction by a wild-type *C. thermocellum* strain. The goal was to identify combinations of pretreatment times and temperatures that maximized CBP deconstruction of poplar solids. To gain insights into the synergy between CELF-CBP, X-Ray Diffraction, Stimulated Raman Spectroscopy (SRS) imaging, and NMR were applied to understand the differences between the crystallinity, chemical mapping of the CELF substrate and the amount of lignin linkages in the residue of poplar solids produced by CELF pretreatment at various times and temperatures. Detailed NMR characterization further revealed the fate and nature of lignin and the mode of action of CELF-CBP on major lignin linkages and their degree of polymerization. Chapter 3 focuses on identification of key features of CELF pretreated solids that impact solubilization of CELF pretreated solids by *C. thermocellum* CBP. In addition, a detailed comparison of CELF-CBP using *C. thermocellum* performance to that by fungal enzymes Ctec2 and the *C. thermocellum* secretome was conducted at 5 and 15 mg/g enzyme loadings. Fractal kinetics models were applied to understand the rate and extent of glucan solubilization. 2D NMR characterization of residual lignin in solids and 1D NMR of the broth after biological deconstruction were used to gain a better understanding of the influence of xylan and lignin on deconstruction of Poplar solids produced by CELF pretreatment at varying times.

Based on the high glucan solubilization of CELF pretreated Poplar at low severity, a follow-up investigation of how effectively *C. thermocellum* could solubilize CELF

pretreated poplar at higher solids loadings was conducted. Chapter 4 reports on the impact and limitations of high solids loadings (50-100 g/L) on consolidated bioprocessing by *C. thermocellum* of CELF pretreated poplar. The goal was to identify the mildest CELF condition that would allow C. *thermocellum* to effectively solubilize CELF poplar at a loading of 75 g/L and higher. CBP fermentation rates were compared at higher solids loadings of 50, 75 and 100 g/L to understand glucan solubilization by *C. thermocellum* and correlate it with *C. thermocellum* fermentation activity. The identification of oligosaccharides present in fermentation broths at high solids CBP could lead to a better understanding the influence of residual xylan on *C. thermocelum* CBP, especially since *C. thermocellum* can deconstruct xylan but is unable to metabolize it. To identify oligosaccharides present in the broth, a purpose designed CBP-OMICS was employed. Process intensification to measure the impact of both residual lignin and xylan in the CELF pretreated Poplar solids and its correlation with *C. thermocellum* activity could lead to insights for process refinement and strategy development to overcome xylan and lignin inhibition if any. Research presented in Chapters 2-4 placed major emphasis on insights into CELF-CBP, process optimization, and process intensification for CELF pretreated Poplar with a wild type *C. thermocellum* strain and its ability to solubilize and ferment carbohydrates present in the CELF pretreated Poplar. Through a joint project with the University of Tennessee, Knoxville, Chapter 5 reports on the investigation of the effectiveness of CELF pretreated poplar as a substrate for a C. *thermocellum* strain engineered to produce isobutyl acetate and isobutyl isobutyrate esters. This is the first attempt to biosynthesize these esters from lignocellulosic biomass by in-situ esterification

of C4 alcohols. Further examination and comparison of the Poplar ester titers with those from Avicel helped identification of metabolic stress and advanced our knowledge of the effect of reactor choice.

This thesis further examined the utility of CELF technology for the production of ethanol (hemp-fuel) and biomaterial (hempcrete) from a more sustainable feedstock, industrial hemp. Industrial hemp is a viable cash crop with wide applications in multiple sectors and is being investigated rigorously as a carbon sink and re-forestation crop due to its fast growth (3-4 months compared with decades for hardwood and softwoods) to mitigate greenhouse gases. The availability of industrial hemp is increasing fast, but technologies to pulp cellulose and fibers from hemp and utilize all the carbon in hemp are centuries old and are often hazardous. Chapter 7 explores the utilization of the majority of CELF pretreated Oregon hurd to make “hemp-fuel” and “hempcrete”. This effort includes comparison of CELF pulped hemp with traditional decorticated hemp and examination of ethanol production using *S. cerevisiae* D5A in a simultaneous saccharification and fermentation (SSF) scheme on the CELF pulped substrate.

Finally, in chapter 8, the CELF lignin from corn stover was extensively characterized and then examined as a material for low-cost renewable bio-adsorbents for the removal of toxic dyes from contaminated water. Thermogravimetric analysis (TGA), HSQC (Heteronuclear Single Quantum Coherence), quantitative ^{31}PNMR, and FTIR was applied to characterize and compare CELF and aminated lignin. Aminated CELF lignin was subsequently applied for removal of Methylene Blue and Direct Blue 1 dye from aqueous solution.

The appendix of this thesis features research to understand the impact of removing lignin on the surface of CELF pretreated switchgrass on enzymatic hydrolysis and consolidated bioprocessing with *C. thermocellum.* The effects of CELF hydrolysate on the rate of anaerobic xylose fermentation to ethanol was compared to results with sugar controls. In addition, strain tolerance to glucose and xylose at 1x, 2x, 3x, and 5x concentrations to those present in CELF hydrolysates of switchgrass were tested.

1.8 References

Alonso, D. M., Hakim, S. H., Zhou, S., Won, W., Hosseinaei, O., Tao, J., Garcia-Negron, V., Motagamwala, A. H., Mellmer, M. A., Huang, K., Houtman, C. J., Labbé, N., Harper, D. P., Maravelias, C. T., Runge, T., & Dumesic, J. A. (2017). Increasing the revenue from lignocellulosic biomass: Maximizing feedstock utilization. *Science Advances*, *3*(5). https://doi.org/10.1126/SCIADV.1603301

Alternative Fuels Data Center: Renewable Fuel Standard. (n.d.)., from https://afdc.energy.gov/laws/RFS.html

Assary, R. S., Kim, T., Low, J. J., Greeley, J., & Curtiss, L. A. (2012). This journal is c the Owner Societies. *Phys. Chem. Chem. Phys*, *14*, 16603–16611. https://doi.org/10.1039/c2cp41842h

Auxenfans, T., Terryn, C., & Paës, G. (2017). Seeing biomass recalcitrance through fluorescence. *Scientific Reports 2017 7:1*, *7*(1), 1–8. https://doi.org/10.1038/s41598-017-08740-1

Billé, R., Kelly, R., Biastoch, A., Harrould-Kolieb, E., Herr, D., Joos, F., Kroeker, K., Laffoley, D., Oschlies, A., Gattuso, J.-P., Billé, R., Kelly, R., Biastoch Á Oschlies GEOMAR, A. A., Harrould-Kolieb, E., Herr Á Laffoley, D. D., Kroeker, K., & Gattuso, J. (2013). Taking Action Against Ocean Acidification: A Review of Management and Policy Options. *Environmental Management 2013 52:4*, *52*(4), 761–779. https://doi.org/10.1007/S00267-013-0132-7

Biomass and the environment - U.S. Energy Information Administration (EIA). (2020, December 9). https://www.eia.gov/energyexplained/biomass/biomass-and-the-environment.php

Biomass energy | National Geographic Society. (n.d.)., https://www.nationalgeographic.org/encyclopedia/biomass-energy/

Cai, C. M., Zhang, T., Kumar, R., & Wyman, C. E. (2013). THF co-solvent enhances hydrocarbon fuel precursor yields from lignocellulosic biomass. *Green Chemistry*, *15*(11), 3140–3145. https://doi.org/10.1039/C3GC41214H

Carvalheiro, F., Duarte, L. C., & Gírio, F. M. (2008). Hemicellulose biorefineries: a review on biomass pretreatments. *Journal of Scientific & Industrial Research*, *67*, 849–864.

Climate change and health. (n.d.)., from https://www.who.int/news-room/fact-sheets/detail/climate-change-and-health

Climate Change Indicators: Oceans | US EPA. (n.d.). from https://www.epa.gov/climate-indicators/oceans

Doney, S. C., Fabry, V. J., Feely, R. A., & Kleypas, J. A. (2008). *Ocean Acidification: The Other CO 2 Problem*. https://doi.org/10.1146/annurev.marine.010908.163834

Eckelman, M. J., & Sherman, J. D. (2018). Estimated Global Disease Burden From US Health Care Sector Greenhouse Gas Emissions. *American Journal of Public Health*, *108*(S2), S120–S122. https://doi.org/10.2105/AJPH.2017.303846

Efroymson, R. A., Langholtz, M. H., Johnson, K., Stokes, B., Brandt, C. C., Davis, M. R., Hellwinckel, C., Kline, K. L., Eaton, L. M., Dunn, J., Canter, C. E., Qin, Z., Cai, H., Wang, M., Scott, D. A., Jager, H. I., Wu, M., Ha, M., Baskaran, L. M., … Dale, V. H. (2017). *2016 Billion-Ton Report: Advancing Domestic Resources for a Thriving Bioeconomy, Volume 2: Environmental Sustainability Effects of Select Scenarios from Volume 1*. https://doi.org/10.2172/1340460

Fast Facts on Transportation Greenhouse Gas Emissions | US EPA. (2019). https://www.epa.gov/greenvehicles/fast-facts-transportation-greenhouse-gas-emissions
Fossil Fuels | EESI. (2020). https://www.eesi.org/topics/fossil-fuels/description

Gent, S., Twedt, M., Gerometta, C., & Almberg, E. (2017). Theoretical and applied aspects of biomass torrefaction : for biofuels and value-added products. In *Theoretical and Applied Aspects of Biomass Torrefaction: For Biofuels and Value-Added Products*. Elsevier Inc.
Global warming reaches 1°C above preindustrial, warmest in more than 11,000 years / Climate Analytics. (n.d.). https://climateanalytics.org/briefings/global-warming-reaches-1c-above-preindustrial-warmest-in-more-than-11000-years/

Greenhouse gases' effect on climate - U.S. Energy Information Administration (EIA). (n.d.). 6, 2022, from https://www.eia.gov/energyexplained/energy-and-the-environment/greenhouse-gases-and-the-climate.php

Gupta, G. K., & Shukla, P. (2020). Lignocellulosic Biomass for the Synthesis of Nanocellulose and Its Eco-Friendly Advanced Applications. *Frontiers in Chemistry*, *8*, 1203. https://doi.org/10.3389/FCHEM.2020.601256/BIBTEX

Hansen, J., Ruedy, R., Sato, M., & Lo, K. (2010). Global surface temperature change. *Reviews of Geophysics*, *48*(4). https://doi.org/10.1029/2010RG000345/ABSTRACT

Himmel, M. E., Ding, S. Y., Johnson, D. K., Adney, W. S., Nimlos, M. R., Brady, J. W., & Foust, T. D. (2007). Biomass recalcitrance: Engineering plants and enzymes for biofuels production. *Science*, *315*(5813), 804–807. https://doi.org/10.1126/SCIENCE.1137016/ASSET/53180CC7-C2AC-411F-A286-B238D5DC153A/ASSETS/GRAPHIC/315_804_F3.JPEG

Holwerda, E. K., Worthen, R. S., Kothari, N., Lasky, R. C., Davison, B. H., Fu, C., Wang, Z. Y., DIxon, R. A., Biswal, A. K., Mohnen, D., Nelson, R. S., Baxter, H. L., Mazarei, M., Muchero, W., Tuskan, G. A., Cai, C. M., Gjersing, E. E., Davis, M. F., Himmel, M. E., … Lynd, L. R. (2019). Multiple levers for overcoming the recalcitrance of lignocellulosic biomass. *Biotechnology for Biofuels*, *12*(1), 1–12. https://doi.org/10.1186/S13068-019-1353-7/FIGURES/5

Jeswani, H. K., Chilvers, A., & Azapagic, A. (2020). Environmental sustainability of biofuels: a review. *Proceedings. Mathematical, Physical, and Engineering Sciences*, *476*(2243). https://doi.org/10.1098/RSPA.2020.0351

Johnson, C. W., Salvachúa, D., Rorrer, N. A., Black, B. A., Vardon, D. R., st. John, P. C., Cleveland, N. S., Dominick, G., Elmore, J. R., Grundl, N., Khanna, P., Martinez, C. R., Michener, W. E., Peterson, D. J., Ramirez, K. J., Singh, P., VanderWall, T. A., Wilson, A. N., Yi, X., … Beckham, G. T. (2019). Innovative Chemicals and Materials from Bacterial Aromatic Catabolic Pathways. *Joule*, *3*(6), 1523–1537. https://doi.org/10.1016/J.JOULE.2019.05.011

Khan, N., Sudhakar, K., & Mamat, R. (2021). Role of Biofuels in Energy Transition, Green Economy and Carbon Neutrality. *Sustainability 2021, Vol. 13, Page 12374*, *13*(22), 12374. https://doi.org/10.3390/SU132212374

Klein-Marcuschamer, D., Oleskowicz-Popiel, P., Simmons, B. A., & Blanch, H. W. (2012). The Challenge of Enzyme Cost in the Production of Lignocellulosic Biofuels. *Biotechnol. Bioeng*, *109*, 1083–1087. https://doi.org/10.1002/bit.24370

Kondo, A., Ishii, J., Hara, K. Y., Hasunuma, T., & Matsuda, F. (2013). Development of microbial cell factories for bio-refinery through synthetic bioengineering. *Journal of Biotechnology*, *163*(2), 204–216. https://doi.org/10.1016/J.JBIOTEC.2012.05.021

Kothari, N., Holwerda, E. K., Cai, C. M., Kumar, R., & Wyman, C. E. (2018). Biomass augmentation through thermochemical pretreatments greatly enhances digestion of switchgrass by Clostridium thermocellum. *Biotechnology for Biofuels*, *11*(1), 1–14. https://doi.org/10.1186/S13068-018-1216-7/TABLES/1

Lee, J. W., & Trinh, C. T. (2022). Controlling selectivity of modular microbial biosynthesis of butyryl-CoA-derived designer esters. *Metabolic Engineering*, *69*, 262–274. https://doi.org/10.1016/J.YMBEN.2021.12.001

Lelieveld, J., Klingmüller, K., Pozzer, A., Burnett, R. T., Haines, A., & Ramanathan, V. (2019). Effects of fossil fuel and total anthropogenic emission removal on public health and climate. *Proceedings of the National Academy of Sciences of the United States of America*, *116*(15), 7192–7197. https://doi.org/10.1073/PNAS.1819989116/SUPPL_FILE/PNAS.1819989116.SD02.XLSX

Lewandrowski, J., Project Manager janlewandrowski, U., Pape, D., Project Manager, I., Man, D., Rosenfeld, J., McCurdy, M., Anderson, M., Jaglo, K., Goossen, B., Kaffel, M., Farrell, J. M., Wissell, F., Hendrickson, T., Lukas, J., Buchholz, T., Xiarchos, I. M., Hanson, W., Lewandrowski, J., & Pape, D. (n.d.). *Renewable Energy Trends, Options, and Potentials for Agriculture, Forestry, and Rural America*. fhttps://www.usda.gov/sites/default/files/documents/renewable-energy-trends-2020

Li, X., Jia, P., & Wang, T. (2016). *Furfural: A Promising Platform Compound for Sustainable Production of C 4 and C 5 Chemicals*. https://doi.org/10.1021/acscatal.6b01838

Lynd, L. R., Laser, M. S., Bransby, D., Dale, B. E., Davison, B., Hamilton, R., Himmel, M., Keller, M., McMillan, J. D., Sheehan, J., & Wyman, C. E. (2008). How biotech can transform biofuels. *Nature Biotechnology*, *26*(2), 169–172. https://doi.org/10.1038/NBT0208-169

Mahajan, J. S., O'Dea, R. M., Norris, J. B., Korley, L. S. T. J., & Epps, T. H. (2020). Aromatics from Lignocellulosic Biomass: A Platform for High-Performance Thermosets. *ACS Sustainable Chemistry & Engineering*, *8*(40), 15072–15096. https://doi.org/10.1021/ACSSUSCHEMENG.0C04817

Mannai, F., Elhleli, H., Khiari, R., & Moussaoui, Y. (2019). Cellulosic Fibers from Lignocellulosic Biomass for Papermaking Applications. *Food Preservation and Waste Exploitation*. https://doi.org/10.5772/INTECHOPEN.88388

Mbaneme-Smith, V., & Chinn, M. S. (2015). *Energy and Emission Control Technologies Dovepress Consolidated bioprocessing for biofuel production: recent advances*. https://doi.org/10.2147/EECT.S63000

McCann, M. C., & Carpita, N. C. (2015). Biomass recalcitrance: a multi-scale, multi-factor, and conversion-specific property. *Journal of Experimental Botany*, *66*(14), 4109–4118. https://doi.org/10.1093/JXB/ERV267

Mondal, P., Kumar, A., Agarwal, V., Sharma, N., Vijay, P., Bhangale, U. D., & Tyagi, D. (2011). *Critical Review of Trends in GHG Emissions from Global Automotive Sector*. https://doi.org/10.5281/ZENODO.8442

Nguyen, T. Y., Cai, C. M., Kumar, R., & Wyman, C. E. (2015). Co-solvent Pretreatment Reduces Costly Enzyme Requirements for High Sugar and Ethanol Yields from Lignocellulosic Biomass. *ChemSusChem*, *8*(10), 1716–1725. https://doi.org/10.1002/CSSC.201403045

Ohashi, H., Hasegawa, T., Hirata, A., Fujimori, S., Takahashi, K., Tsuyama, I., Nakao, K., Kominami, Y., Tanaka, N., Hijioka, Y., & Matsui, T. (2019). Biodiversity can benefit from climate stabilization despite adverse side effects of land-based mitigation. *Nature Communications 2019 10:1*, *10*(1), 1–11. https://doi.org/10.1038/s41467-019-13241-y

Oil 2021 – Analysis - IEA. (2021). https://www.iea.org/reports/oil-2021

Olofsson, K., Bertilsson, M., & Lidén, G. (2008). A short review on SSF - An interesting process option for ethanol production from lignocellulosic feedstocks. *Biotechnology for Biofuels*, *1*(1), 1–14. https://doi.org/10.1186/1754-6834-1-7/FIGURES/4

Olson, D. G., Mcbride, J. E., Shaw, A. J., & Lynd, L. R. (2011). Recent progress in consolidated bioprocessing. *Current Opinion in Biotechnology*, *23*, 396–405. https://doi.org/10.1016/j.copbio.2011.11.026

Papanek, B., Biswas, R., Rydzak, T., & Guss, A. M. (2015). Elimination of metabolic pathways to all traditional fermentation products increases ethanol yields in Clostridium thermocellum. *Metabolic Engineering*, *32*, 49–54. https://doi.org/10.1016/J.YMBEN.2015.09.002

Petrochemical, Commodity & Specialty Chemicals | FTI Consulting. (n.d.). https://www.fticonsulting.com/industries/energy-power-and-products/petrochemical-commodity-and-specialty-chemicals

Ragauskas, A. J., Beckham, G. T., Biddy, M. J., Chandra, R., Chen, F., Davis, M. F., Davison, B. H., Dixon, R. A., Gilna, P., Keller, M., Langan, P., Naskar, A. K., Saddler, J. N., Tschaplinski, T. J., Tuskan, G. A., & Wyman, C. E. (2014). *Lignin Valorization: Improving Lignin Processing in the Biorefi nery*. https://doi.org/10.1126/science.1246843

Ramos, J. L., & Duque, E. (2019). Twenty-first-century chemical odyssey: fuels versus commodities and cell factories versus chemical plants. *Microbial Biotechnology*, *12*(2), 200–209. https://doi.org/10.1111/1751-7915.13379

Seyboth K., Eickemeier P., Matschoss P., Hansen G., Kadner S., Schlomer S., Zwickel T., & von Stechow C. (2011). *Renewable Energy Sources and Climate Change Mitigation — IPCC*. https://www.ipcc.ch/report/renewable-energy-sources-and-climate-change-mitigation/

Sims, R. E. H. (2004). Renewable energy: a response to climate change. *Solar Energy*, *76*(1–3), 9–17. https://doi.org/10.1016/S0038-092X(03)00101-4

Takkellapati, S., Li, T., & Gonzalez, M. A. (2018). An Overview of Biorefinery Derived Platform Chemicals from a Cellulose and Hemicellulose Biorefinery. *Clean Technologies and Environmental Policy*, *20*(7), 1615. https://doi.org/10.1007/S10098-018-1568-5

Tao, L., Tan, E. C. D., Mccormick, R., Zhang, M., Aden, A., He, X., & Zigler, B. T. (2014). Techno-economic analysis and life-cycle assessment of cellulosic isobutanol and comparison with cellulosic ethanol and n-butanol. *Biofuels, Bioproducts and Biorefining*, *8*(1), 30–48. https://doi.org/10.1002/BBB.1431

Thanh, Y. N., Cai, C. M., Kumar, R., & Wyman, C. E. (n.d.). *Co-solvent Pretreatment Reduces Costly Enzyme Requirements for High Sugar and Ethanol Yields from Lignocellulosic Biomass*. https://doi.org/10.1002/cssc.201403045

The Renewable Fuel Standard (RFS): An Overview. (2022). https://crsreports.congress.gov

Thomas, V. A., Donohoe, B. S., Li, M., Pu, Y., Ragauskas, A. J., Kumar, R., Nguyen, T. Y., Cai, C. M., & Wyman, C. E. (2017). Adding tetrahydrofuran to dilute acid pretreatment provides new insights into substrate changes that greatly enhance biomass deconstruction by Clostridium thermocellum and fungal enzymes. *Biotechnology for Biofuels*, *10*(1), 1–13. https://doi.org/10.1186/S13068-017-0937-3/FIGURES/6

Thomas, V. A., Kothari, N., Bhagia, S., Akinosho, H., Li, M., Pu, Y., Yoo, C. G., Pattathil, S., Hahn, M. G., Raguaskas, A. J., Wyman, C. E., & Kumar, R. (2017). Comparative evaluation of populus variants total sugar release and structural features following pretreatment and digestion by two distinct biological systems. *Biotechnology for Biofuels*, *10*(1), 1–16. https://doi.org/10.1186/S13068-017-0975-X/FIGURES/11

Tian, D., Chandra, R. P., Lee, J. S., Lu, C., & Saddler, J. N. (2017). A comparison of various lignin-extraction methods to enhance the accessibility and ease of enzymatic hydrolysis of the cellulosic component of steam-pretreated poplar. *Biotechnology for Biofuels*, *10*(1), 1–10. https://doi.org/10.1186/S13068-017-0846-5/FIGURES/4

Titus, J. G. (1990). Greenhouse effect, sea level rise and land use. *Land Use Policy*, *7*(2), 138–153. https://doi.org/10.1016/0264-8377(90)90005-J

Use of gasoline - U.S. Energy Information Administration (EIA). (2021). https://www.eia.gov/energyexplained/gasoline/use-of-gasoline.php

Weiss, N. D., Felby, C., & Thygesen, L. G. (2019). Enzymatic hydrolysis is limited by biomass-water interactions at high-solids: Improved performance through substrate modifications 09 Engineering 0904 Chemical Engineering 09 Engineering 0915 Interdisciplinary Engineering. *Biotechnology for Biofuels*, *12*(1), 1–13. https://doi.org/10.1186/S13068-018-1339-X/FIGURES/6

White, E. M. (2010). *Woody Biomass for Bioenergy and Biofuels in the United States-A Briefing Paper DEPA R TME NT OF AGRIC U LT URE*.

Wyman, C. E., Cai, C. M., & Kumar, R. (2017). Bioethanol from Lignocellulosic Biomass. *Encyclopedia of Sustainability Science and Technology*, 1–27. https://doi.org/10.1007/978-1-4939-2493-6_521-3

Xu, F., Sun, J., Konda, N. V. S. N. M., Shi, J., Dutta, T., Scown, C. D., Simmons Ab, B. A., & Singh, S. (2016). Transforming biomass conversion with ionic liquids: process intensification and the development of a high-gravity, one-pot process for the production of cellulosic ethanol †. | *Energy Environ. Sci*, *9*, 1042. https://doi.org/10.1039/c5ee02940f

Zhao, X., Zhang, L., & Liu, D. (2012). Biomass recalcitrance. Part I: the chemical compositions and physical structures affecting the enzymatic hydrolysis of lignocellulose. *Biofuels, Bioproducts and Biorefining*, *6*(4), 465–482. https://doi.org/10.1002/BBB.1331

Zickfeld, K., Solomon, S., & Gilford, D. M. (2017). Centuries of thermal sea-level rise due to anthropogenic emissions of short-lived greenhouse gases. *Proceedings of the National Academy of Sciences of the United States of America*, *114*(4), 657–662. https://doi.org/10.1073/PNAS.1612066114

Chapter 2: Pairing of Low Severity CELF with *C. thermocellum* CBP Highly Solubilizes Cellulose and Depolymerizes Residual Lignin from Poplar

***** This work was done in collaboration with Dr. Bhogeswararao Seemala (XRD), Dr. Yining Zeng (SRS), Dr. Yunqiao Pu (NMR of solid residuals). The contents of this chapter will be used for publication in a scientific journal in part or in full.

2.1 Abstract

Co-solvent enhanced lignocellulosic fractionation (CELF) has been shown to be a very effective pretreatment of corn stover and switchgrass, and consolidated bioprocessing (CBP) by *Clostrium thermocellum* can almost completely deconstruct cellulosic substrates without adding enzymes. This study reports on optimizing CELF for woody biomass (Poplar) as a substrate for CBP using the bacterium *C. thermocellum* to investigate CELF-CBP synergy and maximize the deconstruction of lignocellulosic biomass. In-depth investigation of CELF pretreated solids (CELF-Solids) and solid residue after CBP (CELF-CBP-Solids), by X-ray diffraction (XRD), Gel Permeation Chromatography (GPC), Stimulated Raman Spectroscopy (SRS), and NMR provided insights into the physio-chemical changes that most influence yields and rates of Poplar glucan solubilization. Application of CBP to solids produced by CELF operation at 150^{o}C for 5 minutes, the shortest pretreatment time that is practical with our experimental system, reached over 90% glucan solubilization within 72 hours. Extending CELF pretreatment times to 15 and 25 minutes resulted in CBP achieving 98.8% and 100% glucan solubilization, respectively, within 48 hours. SRS imaging revealed extensive lignin depolymerization and aggregation that could increase *C. thermocellum* accessibility to glucan and faster kinetics. GPC confirmed extensive lignin depolymerization by comparing the molecular weight of untreated and CELF treated Poplar. NMR revealed an extensive breakdown of β-*O*-4 linkages and lower Syringyl/Guaiacyl (S:G) ratios after CELF at relatively shorter pretreatment times. Most importantly, the comparison of lignin chemical linkages of untreated Poplar, CELF-Solids, and CELF-CBP-Solids after glucan solubilization using

NMR showed that CELF-CBP reduced difficult to break C-C (b-b) linkages and the S:G ratio at the lowest severity (2.17), implying *C. thermocellum* has ligninolytic activity. This study demonstrates the synergy of CELF-CBP pairing as an effective strategy to both lower enzyme costs without compromising glucan solubilization and kinetics and expand opportunities for lignin valorization.

2.2 Introduction

Poplar is a short-rotation woody crop with great potential to feed biorefineries in the Northwest, Lake States, and Mississippi regions of the US. Poplar was included in the 2016 Billion-Ton Report (Perlack, 2011) due to its potential as a dedicated energy crop. The Center for Bioenergy Innovation (CBI), a major Biomass Research Center (BRC) funded by the US Department of Energy, identified Poplar as one of the main feedstocks to further develop desired traits for field growth and biorefinery conversion into biofuels and bioproducts (ORNL, 2018). Many biomass conversion technologies are initially tested on energy grass (e.g., switchgrass) and crop residues (e.g., corn stover), but must be further understood and developed for application to a variety of biomass including woody energy crops. Woody biomass has a different cell wall composition with much higher levels of lignin than grasses and many agricultural residues (Lourenço & Pereira, 2017). Furthermore, the higher lignin content and more recalcitrant linkages in woody biomass renders greater challenges to biological conversion systems (Bhagia et al., 2016; Studer et al., 2011; Tuskan et al., 2019). There is a technology gap and a need to develop cost effective and feedstock agnostic pretreatment and fractionation technologies.

Co-Solvent Enhanced Fractionation (CELF) is a lignocellulosic biomass pretreatment and deconstruction technology developed at UCR (Cai et al., 2013; Kothari et al., 2018; Nguyen et al., 2015). CELF pretreatment applies an aqueous mixture of tetrahydrofuran (THF) solvent in water (1:1 w/w) and dilute sulfuric acid to fractionate lignocellulosic biomass into glucan rich solids that are amenable to biological deconstruction at low enzyme loadings and a liquid hydrolysate containing most of the hemicellulose and lignin. CELF pretreatment followed by hydrolysis by fungal cellulases has been shown to be very effective on switchgrass (Patri et al., 2021a), corn stover (Nguyen et al., 2015), and Poplar (Thomas, Donohoe, et al., 2017b). However, the need for separate pretreatment, enzyme production, saccharification, and fermentation operations and high loadings of expensive cellulase to break-down glucan into fermentable sugar result in high process costs (Volynets et al., 2017).

Consolidated bioprocessing (CBP) by microbes that combine enzyme production, polysaccharide hydrolysis, and fermentation shows great promise to significantly reduce the costs for biological conversion of lignocellulosic biomass into ethanol and other products. *Clostridium thermocellum* is one such CBP thermophilic organism that can be utilized for CBP (Akinosho et al., 2014a; Olson et al., 2012). This organism's ability to solubilize Poplar has been explored and compared against the solubilization performance of commercial fungal cellulases. In that study, the application of commercial cellulases Accelerase 1500 at high enzyme loadings of 65 mg/ g glucan was compared to solids produced by hydrothermal pretreatment of Poplar at a severity >3. The combined sugar release from the fungal cellulase was less than *C. thermocellum* (Thomas, Kothari, et al.,

2017a). Our group has previously demonstrated that pairing of *Clostridium thermocellum* CBP with thermochemical dilute acid or CELF pretreatments is very effective for deconstructing herbaceous biomass and can completely solubilize the glucan in CELF solids from switchgrass within 72-96 hours (Kothari et al., 2018b) .

The goal of this work is to advance the CELF-CBP combination as feedstock agnostic. Specifically, this study focuses on exploiting the synergy of CELF and CBP to maximize glucan solubilization from Poplar biomass at low process severities to maximize product yields. Towards that goal, a better understanding of which changes in physical and chemical characteristics by CELF pretreatment of Poplar can account for enhanced glucan solubilization extents and rates for when CELF conditions are optimized to maximize deconstruction in combination with *Clostridium thermocellum* CBP. Thus, X-Ray Diffraction (XRD), Stimulated Raman Spectroscopy (SRS), Gel Permeation Chromatography (GPC) and Nuclear Magnetic Resonance (NMR) were applied to solids produced by CELF pretreatment of Poplar and residues left after CBP of those solids to gain physio-chemical and structural insights into changes in cellulose and lignin bio-polymers that correlate with the effectiveness of the CELF-CBP combination in deconstructing cellulose and lignin and to suggest strategies for further improving biological conversion of Poplar biomass.

2.3 Materials and Methods

2.3.1 Materials

CBI reference Poplar variant GW-9947 was generously provided by the Center for BioEnergy Innovation (CBI) from Dr. Muchero Wellington's lab. Poplar was knife milled to a uniform particle size of 1 mm using a Wiley Mill (Model 4, Arthur H. Thomas Company, Philadelphia PA). Composition of unpretreated and CELF pretreated Poplar was determined following the NREL Laboratory Analytical Procedure (Version 08-03-2012). The wild type *Clostridium thermocellum* strain DSM 1313 was kindly provided by Dr. Lee Lynd's lab.

2.3.2 Pretreatment

For pretreatment, the CBI Poplar barrel was mixed thoroughly and stored at -20°C between use. Poplar milled was milled by a Thomas Wiley knife mill with and passed through a 1 mm internal sieve. Pretreatments were performed in a 1 L Hastelloy Parr® autoclave reactor (236HC Series, Parr Instruments Co., Moline, IL) equipped with a double stacked pitch blade impeller rotated at 200 rpm. The reactions were prepared by first adding the milled Poplar at 7.5 wt % solid loadings. A mixture of DI water and 0.5 wt% (based on liquid mass) 72 wt % sulfuric acid (Ricca Chemical Company, Arlington, TX). Tetrahydrofuran (>99% purity, Fisher Scientific, Pittsburgh, PA) was added in a 1:1 mass ratio with water in the fume hood. The reactions were left to soak overnight at 4 °C. Temperatures for CELF reactions were 140°C, 150°C and 160°C at times of 35, 25, and 15 minutes identified by optimization reactions for each time. All reactions were

maintained at reaction temperature (± 0.5°C) by convective heating with a 4 kW fluidized sand bath (Model SBL-2D, Techne, Princeton, NJ). The reaction temperature was directly measured by using an in-line K-type thermocouple (Omega Engineering Inc., Stamford, Connecticut). When the reaction was complete, the Parr reactor was submerged into a room temperature water bath until the internal temperature reached 30-40°C. The reaction solids were separated from the liquid by vacuum filtration at room temperature through glass fiber filter paper (Fisher Scientific, Pittsburgh, PA) and washed with 4 liters of deionized room temperature water until the filtrate pH was measured to be neutral. The solids were carefully transferred to a Ziplock bag and weighed with and without the wet filter. The moisture content of the solids was determined by a halogen moisture analyzer (Model HB43, Mettler Toledo, Columbus, OH).

2.3.3 Compositional analysis of the biomass

Compositional analysis of the Poplar before and after CELF pretreatment was done following an established Laboratory Analytical Procedures (LAPs) (version 8-03-2012) from the National Renewable Energy Laboratory (NREL, Golden, CO). After the two-step acid hydrolysis, the resulting solids and liquid were separated using filtering crucibles. The liquid portion was sampled and analyzed against calibration standards and using HPLC Waters Alliance system e2695 (Waters Co., Milford, MA) equipped with an HPX-87H column (Bio-Rad Aminex ®, Bio-Rad Laboratories, Hercules, CA) and a Waters Refractive Index Detector 2414 (Waters Co., Milford, MA). The mobile phase run was a 5 mM sulfuric acid set at a flow rate of 0.6 mL/min. Empower® 3 software package (Empower Software Solutions, Newport Beach, CA) was utilized to collect, view, and

integrate the resulting chromatographs. The glucan and xylan content were calculated and adjusted against internal sugar standards. To determine the amount of acid insoluble or Klason-lignin, the solid residues after the filtration process were dried and weighed. Finally, ash and other insoluble matter were further quantified by utilizing a muffle furnace ramped to 575°C to convert the leftover material in the crucibles into ash.

2.3.4 CBP of CELF pretreated Poplar

A stock culture of *C. thermocellum* DSM 1313 stock cultures were grown in 50 mL culture with a 2% by volume inoculum and a 5 g/L glucan Avicel® PH101 (Sigma Aldrich, St. Louis, MO) for 8-9 hours in a defined MTC media without trace minerals using 2% by volume inoculum. The medium components and concentrations used are shown in the table 1 (see Supporting material). Media components A-D were sterilized by autoclaving at 121°C. The vitamins solution "E" was filter sterilized using 28 mm diameter polyethersulfone (PES) syringe filters with 0.2 μm pores (Corning® Life Sciences, Tewksbury MA). The seed culture was stored overnight in a refrigerator before using it for inoculation the morning. Fermentations were performed in 125 mL bottles (Wheaton, Millville NJ) at 5 grams/L glucan loadings of CELF pretreated Poplar at 150°C (5, 15, 25 minute) substrate in triplicates at a working mass of 50 g. The pretreated substrate was loaded in wet and the remaining water was calculated by accounting for the moisture content. Once the remaining water was added, the bottles containing substrate and water were purged with nitrogen. Nitrogen cycling occurred by 45 seconds application of vacuum with 14 psi nitrogen over a total of 30 minutes. Once purging was complete, the bottles were then sterilized by autoclaving at 121°C for 35 min. Once cooled, the media

components were added aseptically into the bottles via syringe needles. Fermentations were run at 60°C with a shaking speed of 180 rpm in a Multitron Orbital Shaker (Infors HT, Laurel MD). Each time point was run in triplicate and removed at the time point. The residual fermentation solids and liquids were separated via centrifugation at 2400 RPM for 10 minutes. The CBP solids were washed with DI water two times. The residual solids were then carefully poured into aluminum pans to be dried at 35°C and subsequently grinded for compositional analysis to measure solubilization.

2.3.5 Stimulated Raman Spectroscopy (SRS)

For SRS imaging a high-power Nd:YO4 oscillator (HighQ picoTRAIN, Spectra-Physics) producing 7 ps pulse trains at 1064 nm (15 W max) and 532 nm (9 W max) was used. 2 W of the 1064 nm light was used as the Stokes beam. The 532 nm beam was directed to pump an optic parametric oscillator (Levante Emerald, APE GmbH, Germany) to produce 6 ps tunable wavelength pulse train as the pump beam. The wavelength of the pump beam was adjusted for the selected Raman frequency. For example, it was tuned to 909.2 nm for lignin's resonance frequency at 1600 cm−1. The Stokes beam was intensity-modulated by an acoustic optic modulator (3080-122, Crystal Technology) at 10 MHz with 80% modulation depth, and then combined with the pump beams by a long-pass beam combiner (1064dcrb, Chroma). The two beams were routed to a custom modified mirror-scanning microscope system (BX62WI/FV300, Olympus) attached with an Olympus inverted microscope. Typical laser power at the sample plane was 80 mW for each beam, and this allowed for continuous imaging without causing any noticeable photo-damage. The light transmitted through the sample was collected by a high numeric aperture

condenser (1.45 NA O, Nikon), and filtered by an optical filter (CARS980/220, Chroma) to block the Stokes beam completely so that only amplitude modulation on the pump beams due to the SRS process was detected. The pump beam intensity was detected by a large-area silicon PIN photodiode (FDS1010, Thorlabs) back-biased at 70 V. A lock-in amplifier (SR844, Stanford Research Systems) was used to detect the intensity change in the pump beam. 3D SRS imaging was performed by collecting a stack of images along the Z axis and the 3D rendering of the image stack was processed in Matlab.

2.3.6 X-Ray Diffraction (XRD)

XRD spectra of all biomass samples were recorded in the 2θ range of 5° to 60° using an X'pert Pro PANalytical diffractometer (Malvern PANalytical, Empyrean Series 2, Westborough, MA), equipped with a Nickel filtered Cu-Kα radiation source. The unpretreated and CELF pretreated Poplar samples were ground under liquid nitrogen and then characterized by powder X-ray diffraction using an X'pert Pro PANalytical diffractometer (Malvern PANalytical, Empyrean Series 2, Westborough, MA), equipped with a Nickel filtered Cu-Kα radiation source (λ = 0.1546 nm) in the 2θ range of 5° to 60°. Phase identification and quantitative analyses were performed using PANalytical X'Pert Highscore Plus software. The Crystallinity Index for the samples was calculated using Segal's method, Equation (1).

$$Crystalline\ Index\ (CrI) = \frac{I_{200} - I_{am}}{I_{200}} \times 100 \qquad (1)$$

where I_{200} is the maximum intensity of the (200) lattice diffraction, I_{am} is the intensity diffraction of the amorphous band.

2.3.7 Lignin Characterization

2.3.7.1 Gel Permeation Chromatography

Lignin was isolated from the pretreated Poplar after ball-milling in a porcelain jar with ceramic balls via Retsch PM 200 (Newton, PA) at 600 rpm for 2.5 h followed by enzymatic hydrolysis in acetate buffer (pH 4.8, 50°C) for 48 h. The solid residue was isolated by centrifugation and hydrolyzed again with freshly added buffer and enzymes for another 48 h. After filtration, the solid residue was extracted twice with 96% (v/v) 1,4-dioxane/water mixture at room temperature overnight. The extracts were combined, rotary evaporated, and freeze-dried to recover lignin. The lignin samples were then added into acetic anhydride/pyridine (1:1, v/v) mixture and stirred at room temperature for 24 hours. After that, ethanol was added to the reaction mixture, left for 30 min and then removed with a rotary evaporator. The addition and removal of ethanol was repeated at least 3 times until all traces of acetic acid were removed. Acetylated lignin samples were then dissolved in tetrahydrofuran (THF) at a concentration of 1.0 mg/mL. The molecular weight of acetylated lignin was measured by a gel permeation chromatography (GPC) on a PSS-Polymer Standards Service (Warwick, RI, USA) GPC SECurity 1200 system featuring Agilent HPLC 1200 components equipped with four Waters Styragel columns (HR1, HR2, HR4 and HR6) and an UV detector (270 nm). Tetrahydrofuran was used as the mobile phase with a flow rate of 0.3mL/min. A series of standard polystyrene samples with narrow molecular weights were used for establishing the calibration curve. The Polymer Standards Service WinGPC Unity software (Build 6807) was used for data processing for all the samples.

2.3.7.2 Heteronuclear Single Quantum Coherence NMR

Two-dimensional 13C–1H heteronuclear single quantum coherence (HSQC) experiments were performed in a Bruker Advance III HD 500 MHz spectrometer operating at a frequency of 125.12 MHz for the 13C nucleus. A standard Bruker pulse sequence was used on a Prodigy platform cryoprobe. The dry lignin samples were dissolved in deuterated DMSO for HSQC experiments. The spectra acquit ion conditions were: 210 ppm spectral width in F1 (13C) dimension with 256 data points and 11 ppm spectral width in F2 (1H) dimension with 1024 data points, a 90° pulse, a one bond C–H coupling constant of 145 Hz, a 1.0 s pulse delay, and 64 scans. All the data was processed using the TopSpin 3.6 software (Bruker BioSpin). The central DMSO solvent peak was used for chemical shifts calibration (δc 39.5 ppm, δ_H 2.50 ppm). Relative lignin monomer compositions and interunit linkage abundance were estimated semi-quantitatively using volume integration of contours in HSQC spectra. For monolignol compositions of S, G, H, and *p*-hydroxybenzoate (PB) measurements, the $S_{2/6}$, G_2, $H_{2/6}$, and $PB_{2/6}$, were used with G_2 integrals doubled. The Cα cross peak signals of β-aryl ether (β-O-4), phenylcoumaran (β-5) and resinol (β-β) interunit linkages were used for contour integration and expressed per 100 Aromatic rings. Bruker's TopSpin 3.6 software was employed for data processing and integrations.

2.4 Results and Discussions

2.4.1 Optimization of CELF substrate for CBP using *C. thermocellum*

To investigate and exploit the tunability of CELF, to maximize polysaccharide and lignin fractionation in different streams and render the polysaccharide amenable to efficient hydrolysis and further upgrading, a range of temperatures between 140°C – 160°C and times is investigated to identify lowest severity processes that maximize glucan solubilization by the coupled CELF-CBP system.

Pretreatment severity factor is used to define harshness of a pretreatment process (Um & van Walsum, 2012). Um and Walsum defined severity factor log ($R_{0)}$ in terms of the process temperature T and reaction time t as:

$$Severity\ Factor = \log R_0 = \log\left[\mathrm{t} * e^{\frac{(T-100)}{14.75}}\right] \quad (2)$$

Here, the Temperature T is in degree C and time t in minutes.

To take into account of pH effect, combined severity factor (CS) was introduced (Chum et al., 1990)

$$\log (CS) = \log R_0 - \mathrm{pH} \quad (3)$$

The severity factor log R_0 is a simple approach to quantify the reaction harshness, and since the pH of the CELF process was kept constant in this work, severity factor log R_0 was used for relative comparison. Processing temperature and time was used as levers to better understand and optimize synergy between CELF pretreatment and CBP using *C. thermocellum*, we applied CELF pretreatment on Poplar at various process severity to

define the lowest severity condition that could lead to complete glucan solubilization without compromising kinetics and yield of glucan solubilization. CBI reference Poplar was pretreated using CELF at 3 different pretreatment times and temperatures with log R_0 ranging from 2.72- 2.94 (Figure 2-1).

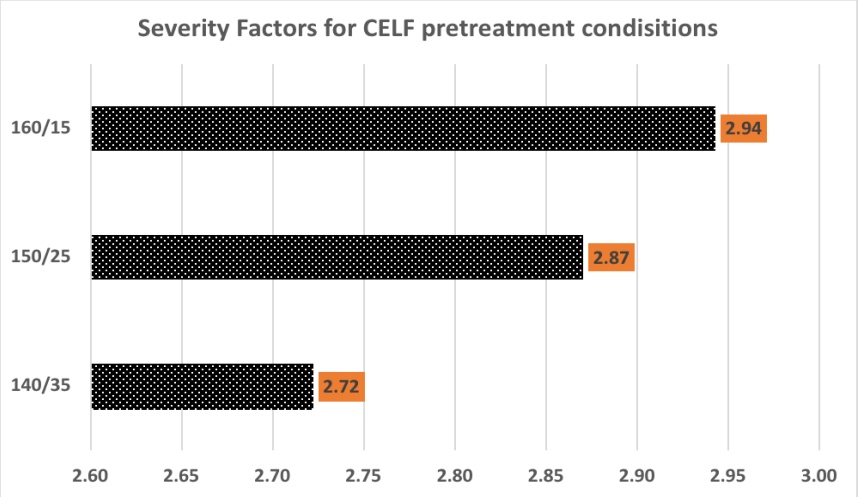

Figure 2-1. Calculated severity factors for the three CELF reaction conditions used in this study. CELF pretreatment temperature was ranged from 140-160 °C and the reaction time was varied from 15-35 minutes.

A better understanding of CELF pretreated Poplar physiochemical traits and its influence on the activity of *C. thermocellum* could lead to a better design of conversion processes, especially in terms of maximizing the whole biomass conversion with high yields and minimum inhibition to *C. thermocellum*. *C. thermocellum* was used for consolidated bioprocessing of CELF pretreated Poplar solids at a glucan loading of 1 wt%. Figure 2-3 shows the percent glucan solubilized during CBP estimated from the amount of remaining glucan in the residual solids as a function of time. Although, the extent of total

glucan solubilization was similar for the Poplar CELF solids pretreated at 140°C, 150°C, 160°C for 35, 25 and 15 minutes respectively, the small differences in CELF pretreatment reaction severity impacted the rate of glucan solubilization. For example, all the CELF process severity ranging from 2.72-2.94 corresponding to the CELF pretreatment temperatures of 140°C, 150°C, 160°C, resulted into complete glucan solubilization at day 3 of CBP. Compared to the untreated Poplar, there was 70% higher glucan solubilization for all the CELF conditions at CBP time of 3 days and longer. At day 1 of CBP, however, the Poplar CELF solids resulted in 48%, 72% and 80% glucan solubilization for 140°C, 150°C and 160°C respectively. In particular, at day 1, there was an increase in glucan solubilization from 39%-71% for 140-160 degrees CELF treated Poplar solids compared to untreated Poplar. The CELF solids generated at the lowest CELF processing temperature of 140°C for 35 minutes, exhibited much slower rate compared to the almost similar rates for 150°C, 25 minutes and 160°C, 15 minutes CELF pretreated CELF solids. Interestingly, the rate of glucan solubilization increased rapidly for the 140°C CELF pretreated Poplar substrate between days 1 and 3, resulting into similar total glucan solubilization for all the CELF processing condition tested in this study.

Based on these results, CELF pretreatment of 150°C was chosen to be further optimized for the CELF - *C. thermocellum* CBP pairing. The goal was to generate CELF pretreated Poplar substrates by pretreating Poplar at 5, 15 and 25 minutes to decipher the subtle differences in the CELF substrate characteristics and its impact on the consolidated bioprocessing using *C. thermocellum*. Figure 2-5 reports on the percent glucan solubilization from this investigation. It is clear that all the pretreatment times (5, 15 and

25 minutes) result into >90% glucan solubilization at longer CBP times of > 3 days, but Poplar CELF pretreated for 5 minutes never reaches complete solubilization. On the other hand, pretreatment times of 15 and 25 minutes both reach to almost complete glucan solubilization by day 2. There is clear evidence of a lag phase with a slow solubilization rate for the 15 minutes CELF pretreated Poplar solid at 12 hours resulting into similar glucan solubilization (27%) as 5 minutes CELF pretreated Poplar solid (26%). However, by day 1 the glucan solubilization rate for the 15 minutes CELF pretreated Poplar solid is accelerated resulting into 82% glucan solubilization compared with 92% for the 25 minutes CELF pretreated Poplar.

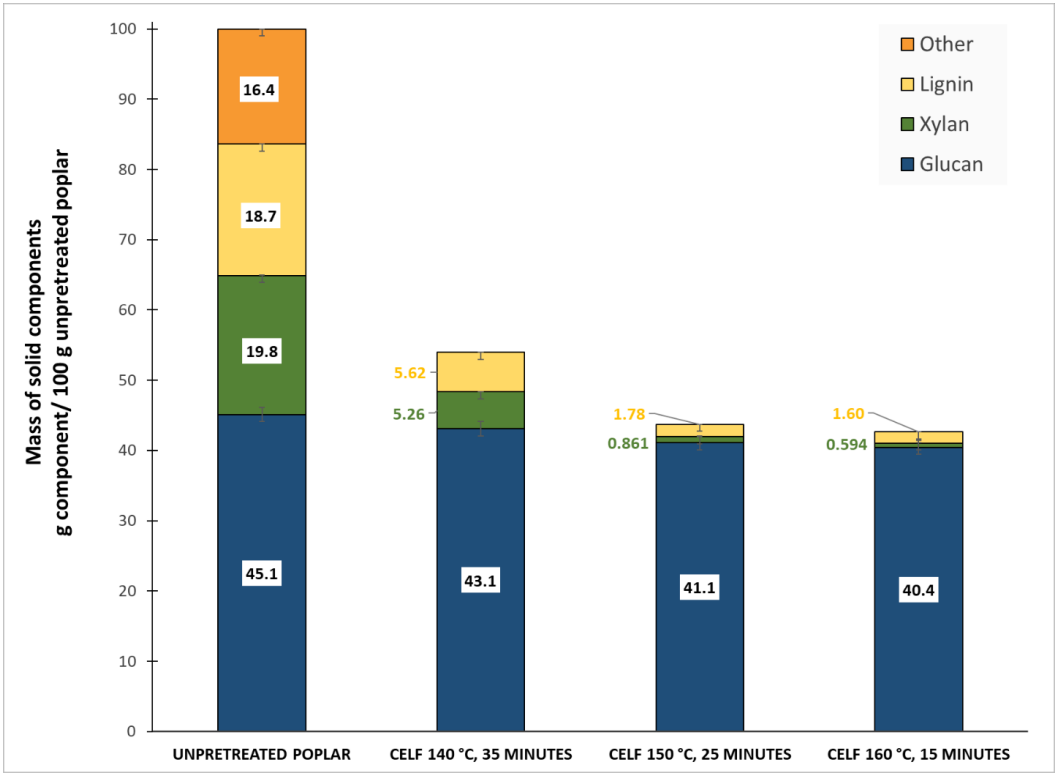

Figure 2-2. Mass of components (glucan, xylan and Klason lignin) in Poplar before and after CELF pretreatment at the chosen reaction conditions to optimize recovery of maximum glucan and xylan yields at varying severities to gain insight into conditions suitable for pairing of CELF process with consolidated bioprocessing using *C. thermocellum*.

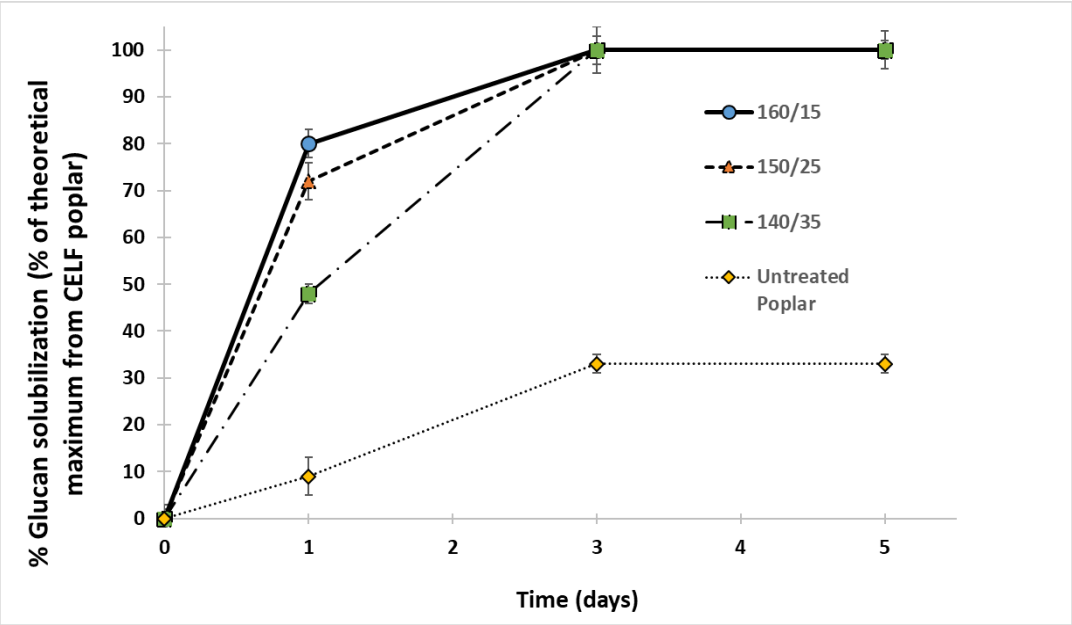

Figure 2-3. Percent glucan solubilization by *C. thermocellum* CBP from solids produced by CELF pretreatment of Poplar at 140°C, 150°C and 160°C for 35, 25, and 15 minutes

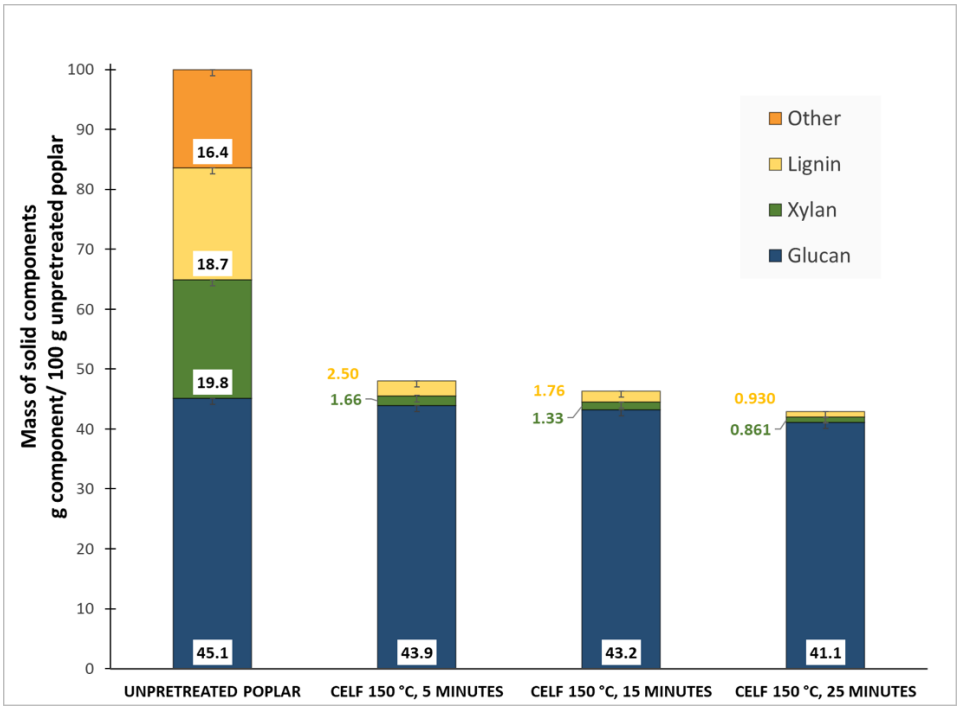

Figure 2-4. Mass of components (glucan, xylan and Klason lignin) in Poplar before and after CELF pretreatment at 150°C for 5, 15 and 25 minutes to further optimize the CELF condition for consolidated bioprocessing using *C. thermocellum* and maximize CELF-CBP synergy.

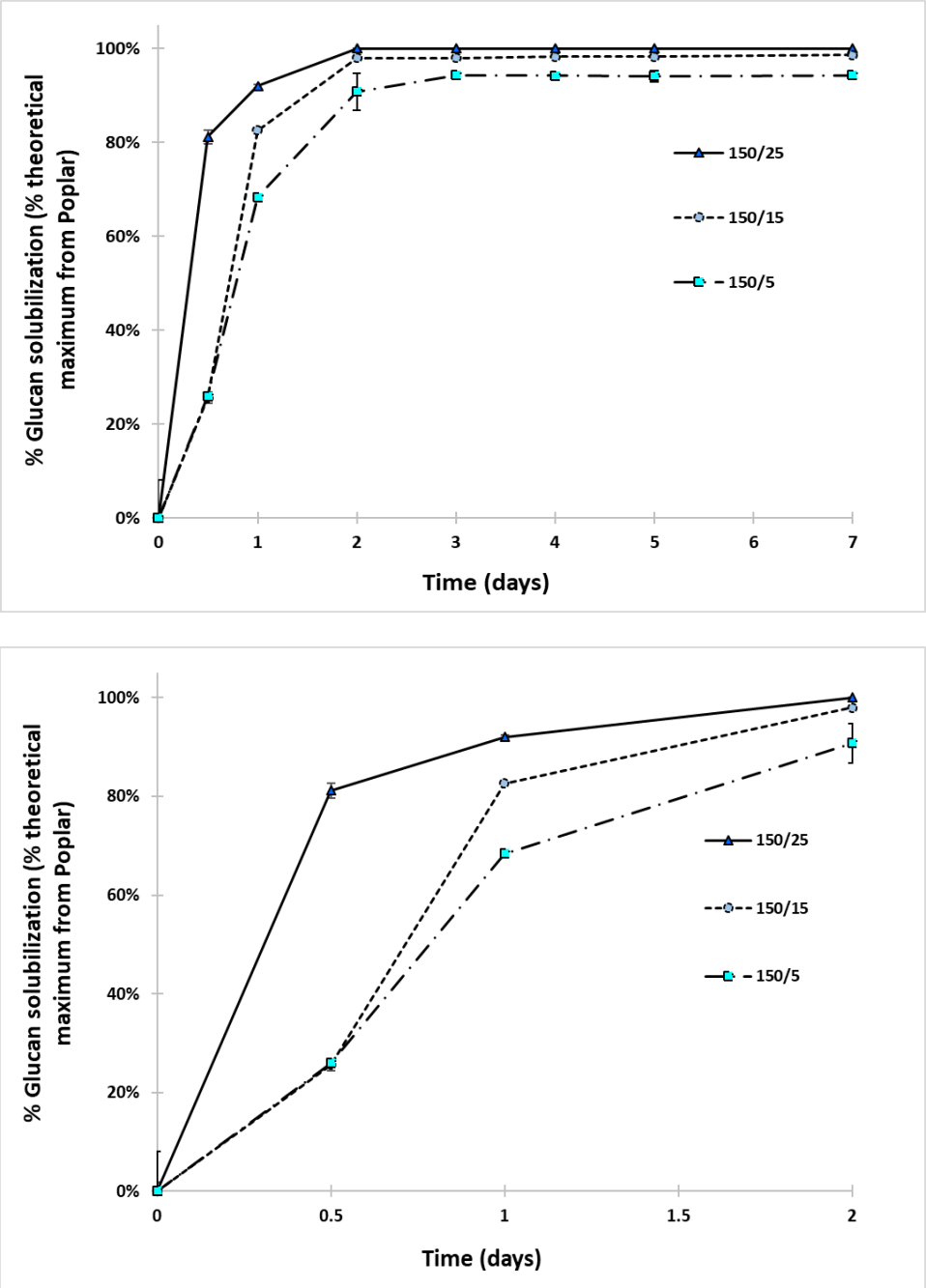

Figure 2-5. (a) Percent glucan solubilization (after consolidated bioprocessing using *C. thermocellum*) as a function of time for Poplar pretreated at 150°C for 5, 15 and 25 minutes. (b) A close up of (a) at the early stage of CBP to show the rate of solubilization for CELF pretreated Poplar at various reaction conditions.

2.4.2 Effect of CELF process severity on physio-chemical and structural features of CELF solids

Lignocellulosic biomass have evolved to be recalcitrant (Aboudi et al., 2021; Merklein et al., 2016; Qian, 2013; Yousuf et al., 2019). The term 'biomass recalcitrance' is defined as the resistance of lignocellulosic biomass to enzymatic digestibility into simple sugars (Himmel et al., 2007b)Type of the biomass (herbaceous or woody etc.), cellulose crystallinity, amount of lignin, lignin chemistry (S:G ratio, C-C and C-O-C linkages etc.)- all contribute to the recalcitrance nature of the biomass. Various pretreatment technologies have been developed to reduce the biomass recalcitrance (Karimi & Taherzadeh, 2016) and enable its utilization for the production of fuels and chemicals from biomass. During pretreatment, lignocellulosic biomass can go through substantial physiochemical changes that influence the downstream hydrolysis and sugar yields (Karimi & Taherzadeh, 2016). Tracking these changes as a function of severity (processing temp and time) allows to gain insight of which factors play key roles for a selected pretreatment and downstream biological system used for saccharifying the pretreated biomass. Pairing of CELF and CBP for a woody biomass has not been studied before, and therefore to maximize carbon conversion from Poplar, a better understanding of this structure-function correlation is essential.

Figure 2-6 reports on the powder XRD pattern of untreated and CELF pretreated Poplar biomass. XRD was done to understand the influence of pretreatment time and temperatures on the crystallinity index of Poplar biomass. The reflections at 2Θ of 22.8°, 15.6° and 18.3° correspond to the crystallographic plane of (200) and (110), and the amorphous phase of cellulose, respectively. One clear observation is the increase of

crystallinity index after CELF pretreated for all the temperature and time tested in this study indicating that CELF pretreatment did not transform the crystalline cellulose into amorphous nature or changed the nature of the cellulose polymorph as seen for other pretreatments (Yao et al., 2018). The change in crystallinity index and polymorph nature influence the glucan digestibility and were reported to be an important factor (Yao et al., 2018). Specially, the accelerated rate of cellulose hydrolysis has been directly linked its transformation into amorphous phase due to pretreatment at high temperatures Chai et al., 2018; Kucharska et al., 2018) However, this XRD result show that the glucan solubilization and the increased hydrolysis rate are not correlated for CELF pretreated but highly crystalline Poplar cellulose. The pairing of CELF-CBP processes using *C. thermocellum* as a host allows solubilization of crystalline cellulose due to its unique ability and preference for crystalline cellulose. Figure S3 (supplementary material) shows XRD reflections of untreated and CELF pretreated Poplar that were pretreated at 150°C for 5, 15 and 25 minutes to further optimize CELF process for Poplar at 150°C and follow similar trend as the 140°C and 160°C pretreated Poplar.

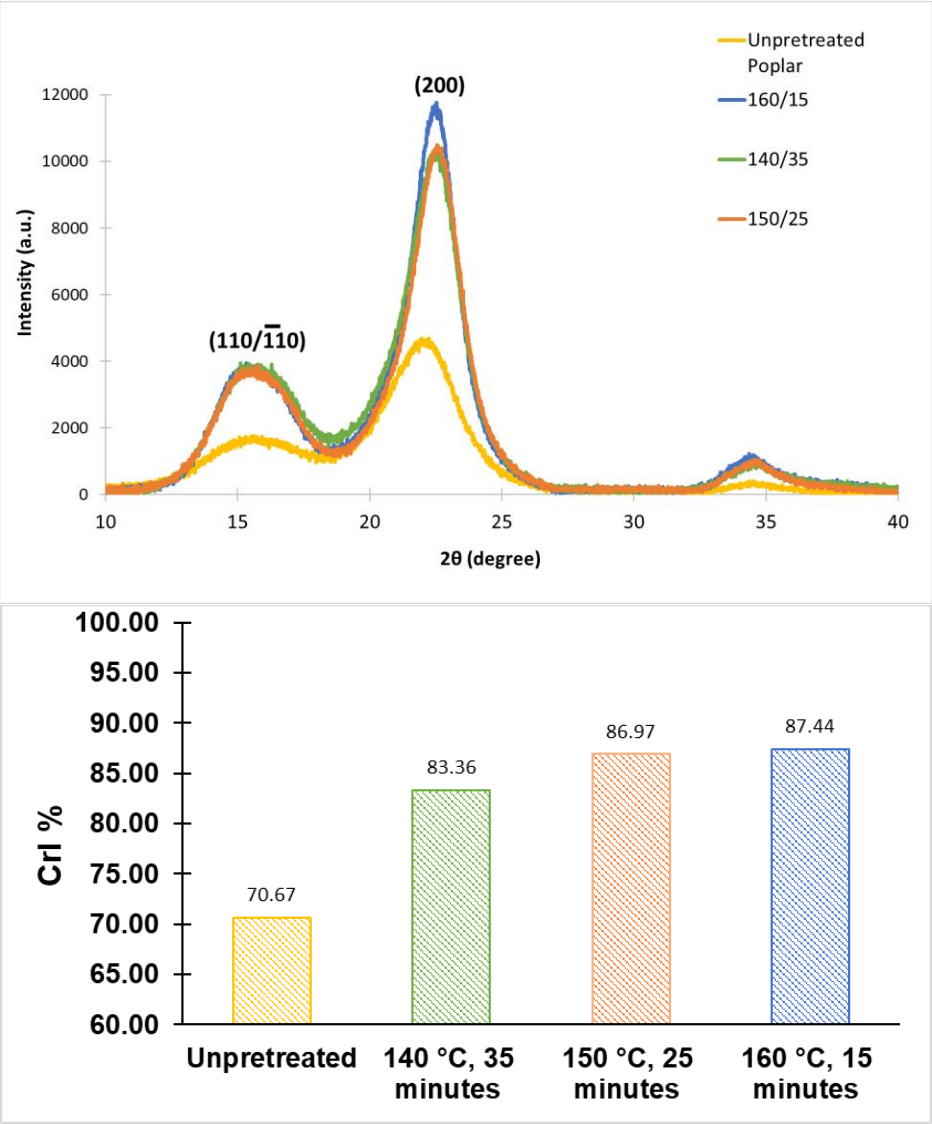

Figure 2-6. (a) XRD patterns of untreated and CELF pretreated Poplar for CELF pretreatment at 140, 150 and 160°C. (b) Crystallinity Index (CrI) calculated by Segal's method of untreated and CELF pretreated solids (pretreatment done at 140°C, 150°C and 160°C for 35, 25 and 15 minutes respectively) for the CELF process severity between 2.72-2.94.

Depending on the type of the biomass, ~15-35% of the lignocellulosic biomass is lignin (Ragauskas et al., 2014.) Lignin is a heterogeneous polymer that serves many purpose including providing structural support, water transport and protection of the plants from pathogenic microbial attack (Q. Liu et al., 2018). However, the presence of lignin in the lignified plant cell wall is a major contributor to its recalcitrance and there have been numerous efforts to investigate physical and chemical nature of lignin that impart the stability to lignocellulosic biomass and makes it difficult to deconstruct (Zoghlami & Paës, 2019). High temperature thermochemical approaches have been developed that can effectively de-lignify the biomass and make them more amenable to enzymatic hydrolysis. However, the high process severity leads to unwanted chemistries and loss of carbon from cellulose, hemicellulose and lignin to other byproducts, condensed products, char etc. (Capolupo & Faraco, 2016)

To understand the impact of CELF process severity on Poplar delignification, quantitation of total lignin was done using compositional analysis method detailed above for the untreated and CELF pretreated Poplar solids (see Figure 2-7a). The lignin content of untreated Poplar was 18.7 g/grams of biomass. After CELF, the remaining lignin content was 5.62g/gram of Poplar biomass for the 140°C, 1.78 g/gram of Poplar biomass for 150°C, and 1.60 g/gram of Poplar biomass for 160°C pretreatments. Compared to the untreated Poplar, the CELF pretreated Poplar at 140 ºC:35 minutes, 150 ºC:25 minutes and 160°C:15 minutes leads to ~ 70%, 91% and 92% delignification respectively.

The CELF pretreatment is reported to be efficient in fractionating solids rich in glucan from the lignocellulosic biomass (Cai et al., 2013a; Pingali et al., 2020). This study

reports on optimizing CELF substrate for the downstream saccharification and fermentation using *C. thermocellum*. The correlation of percent remaining lignin and glucan solubilization show an anti-correlation between the amount of lignin present and the extent of glucan solubilization (Figure 2-7b). The enhanced delignification of the Poplar biomass at the CELF pretreatment temperatures of 150°C and 160ºC compared to the CELF pretreatment at 140 ºC indicates a role of lignin softening or melting at higher temperatures (>150 ºC). Detailed thermal characterization of polymeric lignin from various sources using differential scanning calorimetry (DSC) and thermogravimetric show that lignin glass transition temperature (Tg) is dependent on its molecular weight, moisture content and the type of linkages present (Smith et al., 2016; Wang et al., 2020). On average, the high molecular weight polymeric lignin starts to melt above 150°C. The fractionation of mostly glucan in solid fraction above CELF pretreatment temperatures of 150°C indicates that the processing temperature above lignin Tg may be playing a key role for the Poplar in this study. The gain in the total glucan solubilization is ~ 9% for CELF pretreated Poplar at 160°C at 24 hours (see Figure 2-7 (b), and complete glucan solubilization was seen for all the three CELF pretreatment reaction conditions (see Figure 2-3). This trend is reflected when percent delignification and percent glucan solubilization after CBP using *C. thermocellum* at 24 hours is plotted as a function of CELF severity factor (see Figure 2-7C). A slight increase in the severity factor from 2.72 to 2.87 increased the Poplar delignification by 21 percent. But the increase of severity factor from 2.87 to 2.94 improved the delignification by only 1%.

(a)

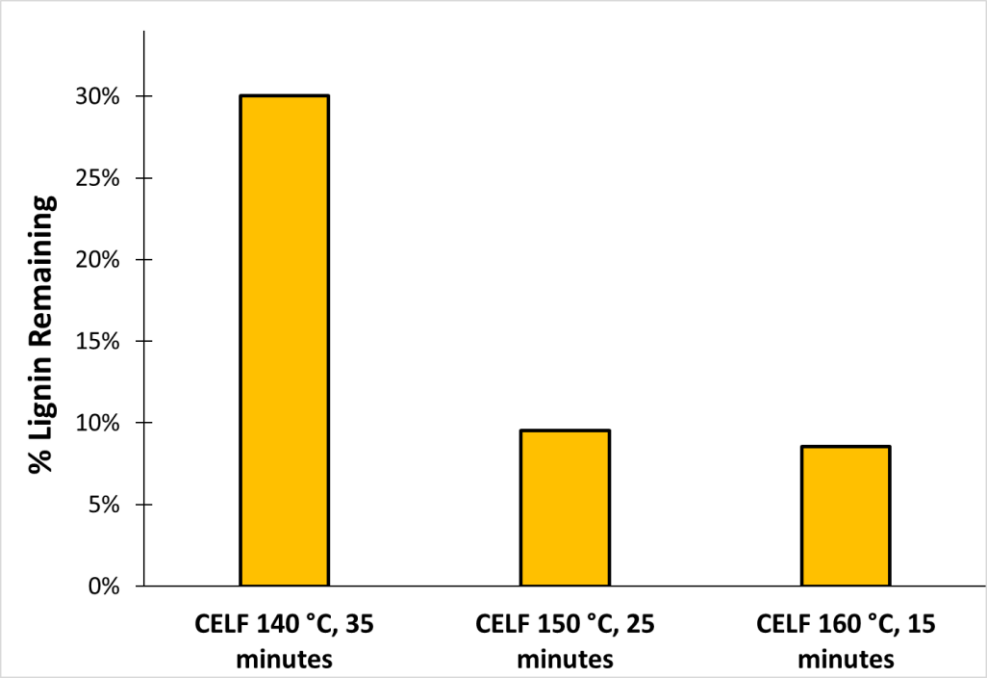
% Lignin Remaining
30%
25%
20%
15%
10%
5%
0%
CELF 140 °C, 35 minutes
CELF 150 °C, 25 minutes
CELF 160 °C, 15 minutes

(b)

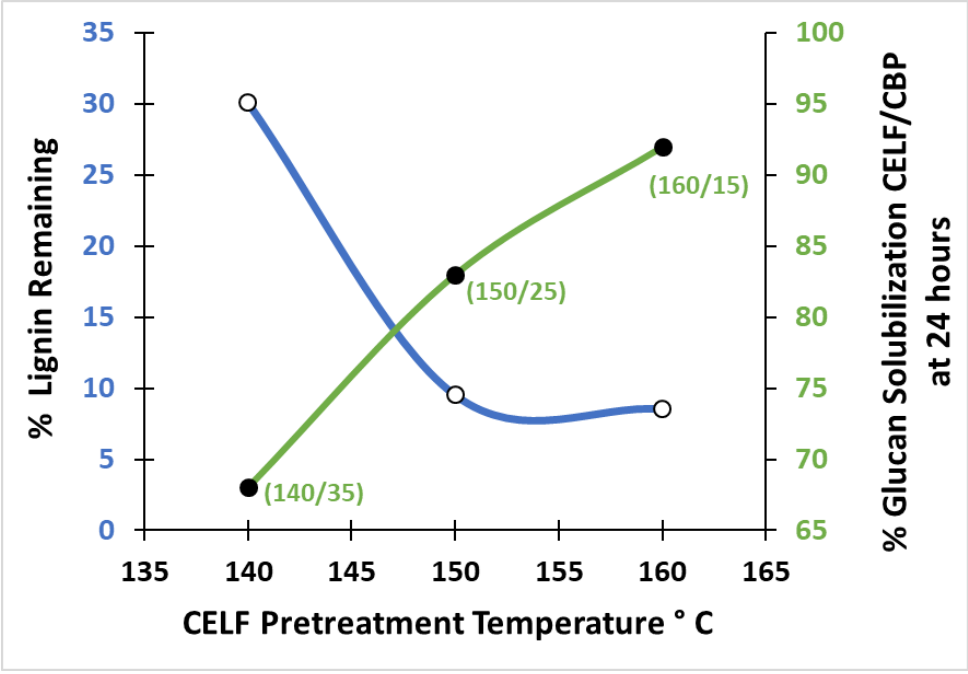
% Lignin Remaining
% Glucan Solubilization CELF/CBP at 24 hours
35
30
25
20
15
10
5
0
100
95
90
85
80
75
70
65
135
140
145
150
155
160
165
(140/35)
(150/25)
(160/15)
CELF Pretreatment Temperature ° C

(c)

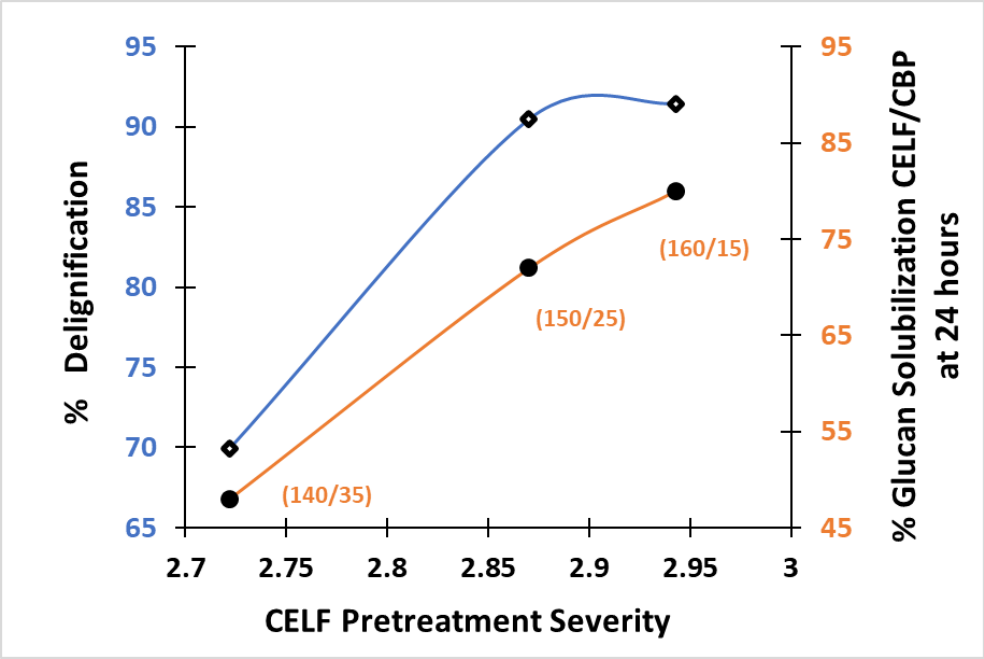

Figure 2-7. (a) Percent remaining lignin in the CELF pretreated solids at the CELF processing temperature of 140, 150 and 160 °C for 35, 25 and 15 minutes respectively. (b) Graph of percent remaining lignin (Y1 axis) and percent glucan solubilization at 24 hours (Y2 axis) as a function of CELF pretreatment severity.

2.4.3 Chemical mapping of Cellulose and Lignin

In order to optimize coupled CELF-CBP, a better understanding of the main factors that contribute to Poplar recalcitrance and features of pretreated solids that impact solubilization of CELF pretreated solids by subsequent biological systems is essential. In addition to XRD and detailed lignin analysis, we used chemical mapping of the CELF pretreated and untreated Poplar to further understand differences in the CELF substrate characteristics and how they correlate with *Clostridium thermocellum* activity to discern differences beyond the total amount of xylan and lignin remaining in solids. Since Stimulated Raman Spectroscopy (SRS) provides a label-free method to interrogate

chemical mapping, SRS was used to image untreated and CELF pretreated Poplar to gain insight into the cellulose and lignin distribution on the surface. Raman spectra of lignocellulosic plant cell walls contain the vibrational modes from cellulose, lignin, and hemicellulose which are the three major cell wall components. Cellulose has broad Raman contributions, but the peaks ~1100 cm^{-1} is the unique Raman peak from cellulose. Primary Raman contribution from lignin is seen around 1600 cm^{-1}. In this study, peaks at 1100 cm^{-1} and 1600 cm^{-1} are used to map cellulose and lignin respectively in the Poplar plant cell walls. Figures 3-8 (a) and (b) reports on representative SRS images of CELF pretreated Poplar at 140°C:35 minutes, 150°C:25 minutes, 160°C:15 minutes and 150°C pretreated Poplar at pretreatment times of 5, 15 and 25 minutes respectively. SRS imaging provided insight of the structural features in addition to the nature of the cellulose and distribution on the surface. Only slight difference in the severity factors ranging from 2.72-2.94 teases out the impact of pretreatment temperature. For example, comparing 140°C:35 minutes CELF pretreatment to 150°C:25 minutes CELF pretreatment, it is clear that there is no difference in cellulose and lignin signatures for 140°C:35 pretreated CELF indicating that lignin is still associated closely with cellulose component. However, lignin signature at 1600 cm^{-1} starts to diminish compared to cellulose signature at 1100 cm^{-1} for both 150°C:25 minutes and 160°C:15 minutes CELF pretreated Poplar. In particular, CELF pretreatment at 160°C:15 clearly show that most of the lignin is now dissociated from cellulose polymer and aggregated on the surface of the Poplar cell wall. When the CELF pretreatment time was shortened to 5 minutes at 150°C, it is again evident from these results that the lignin signature at 1600 cm^{-1} seem evenly distributed at the Poplar cell wall

surface and closely associated with cellulose signature at 1100 cm^{-1}. Compared to 150°C: 5 minutes CELF pretreated Poplar, 150°C:15 minutes CELF pretreated Poplar show diminished intensity of the 1600 cm^{-1} lignin signature and slight aggregation of lignin particulate on the surface. Lignin aggregation that starts above 150°C:5 minutes CELF pretreatment eventually takes the form of aggregated lignin on the cellulose surface and mostly dissociated from cellulosic component at the longer CELF pretreatment time. Recently, the Smith group at ORNL also reported that CELF is effective in removing lignin due to the extended structure of lignin in THF instead of globular structure in water and that THF acts as a barrier between water and lignin (Smith et al., 2016). This finding explains the effectiveness of CELF process in removing lignin that has been long thought to act as barrier between enzymes and cellulose (Patri et al., 2021b).

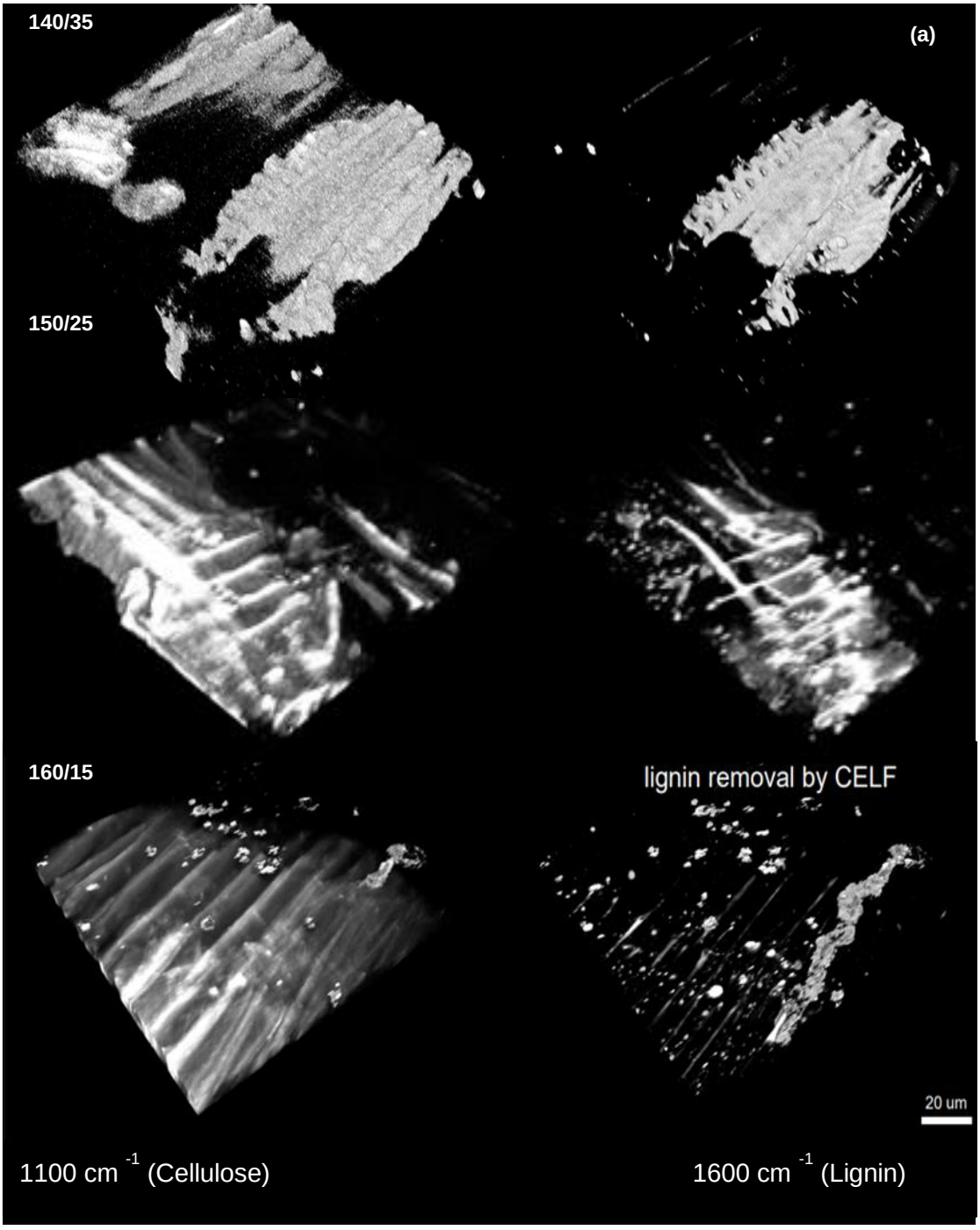
140/35
(a)
150/25
160/15
lignin removal by CELF
20 um
1100 cm -1 (Cellulose)
1600 cm -1 (Lignin)

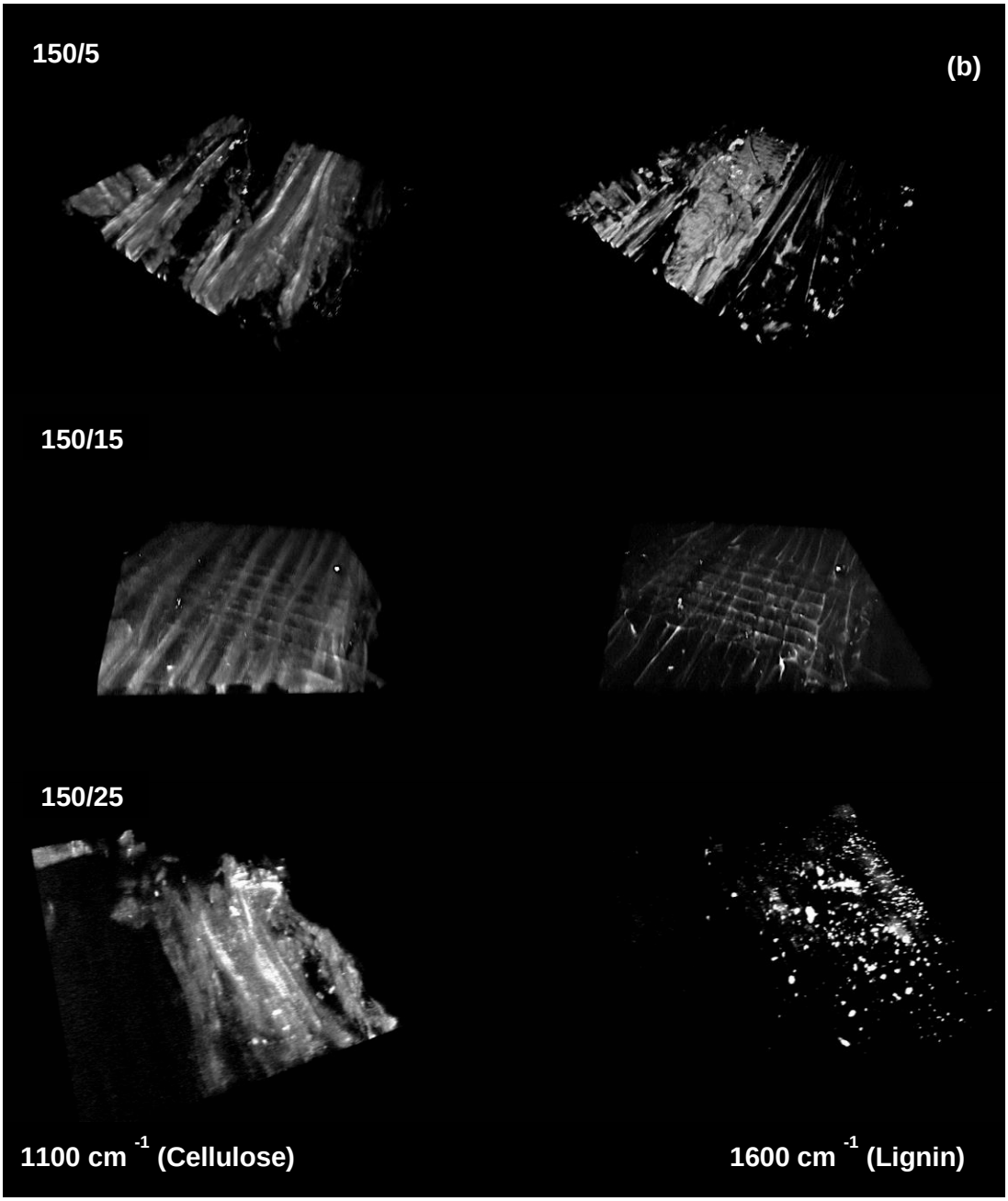

Figure 2-8. (a) Comparison of the SRS map of the cellulose and lignin in the CELF pretreated Poplar for CELF processing temperatures of 140°C, 150°C and 160°C. (b) Comparison of the SRS for the cellulose and lignin distribution in the 5, 15 and 25 minutes CELF pretreated Poplar for CELF processing temperatures of 150°C.

2.4.4 Impact of CELF and CELF-CBP Processes on Residual Lignin

It has been reported that lignin removal during biomass pretreatment results into much higher glucose yields (Lourenço & Pereira, 2017; R. Singh et al., 2014; S. Singh et al., 2015; Wyman et al., 2005. Delignification opens up the biomass structure and provides greater accessibility to cellulose for enzymatic hydrolysis (Baruah et al., 2018). In addition, lignin removal also minimizes enzyme inhibition due to non-productive binding of lignin to cellulolytic enzymes (Gao et al., 2014; Rahikainen et al., 2013; Yarbrough et al., 2015). In the CELF enabled lignin-first strategy, lignin is fractionated first in the liquid stream to leave behind primarily a cellulose rich solid fraction that is suitable for downstream saccharification and fermentation in a CBP process. Although, as shown in this work, the lignin first approach of CELF fractionates most of the lignin (70-92%), about 8-30% residual lignin still remained in the solid polysaccharide by CELF pretreatment of Poplar. We used Gel Permeation Chromatography (GPC) and Heteronuclear Single Quantum Coherence (HSQC) NMR to investigate the nature of this residual lignin and to what extent, if any, it posed a challenge for *C. thermocellum* activity for glucan solubilization during consolidated bioprocessing.

Figure 2-7 details the result of GPC study of residual lignin from untreated Poplar, CELF pretreated Polar and CELF-CBP Poplar at various times for 150°C CELF pretreatment.The weight average molecular weight of Poplar lignin decreased after CELF pretreatment of 5 minutes to ~2247 g/mol from 20500 g/mol in untreated Poplar. Notably, the average molecular weight of lignin further decreased to 7164 g/mol after consolidated bioprocessing using *C. thermocellum*.

The HSQC NMR spectra provide detail insight of the interunit linkages present in untreated, CELF pretreated, and CELF-CBP Poplar (see Figure 2-8 and 2-9). These results indicate that the most prevalent β-O-4 linkage in lignin is not disrupted after CELF pretreatment until severity factor of > 2.8. Quiet remarkably, the HSQC results demonstrate that the integration of CELF pretreatment with CBP using *C. thermocellum* lead to the breakdown of □-O-4 linkages in Poplar even at lowest severity tested (150°C:5 minutes). In particular, detailed NMR characterization show 58% and 75% decrease in β-O-4 linkages after CELF and after CELF-CBP respectively at pretreatment time of 15 minutes. Similarly, there is no indication of breakdown of the difficult to break C-C linkages in Poplar until after integration of CELF pretreatment with consolidated bioprocessing using *C. thermocellum*. These results imply some ligninolytic activity of *C. thermocellum.*

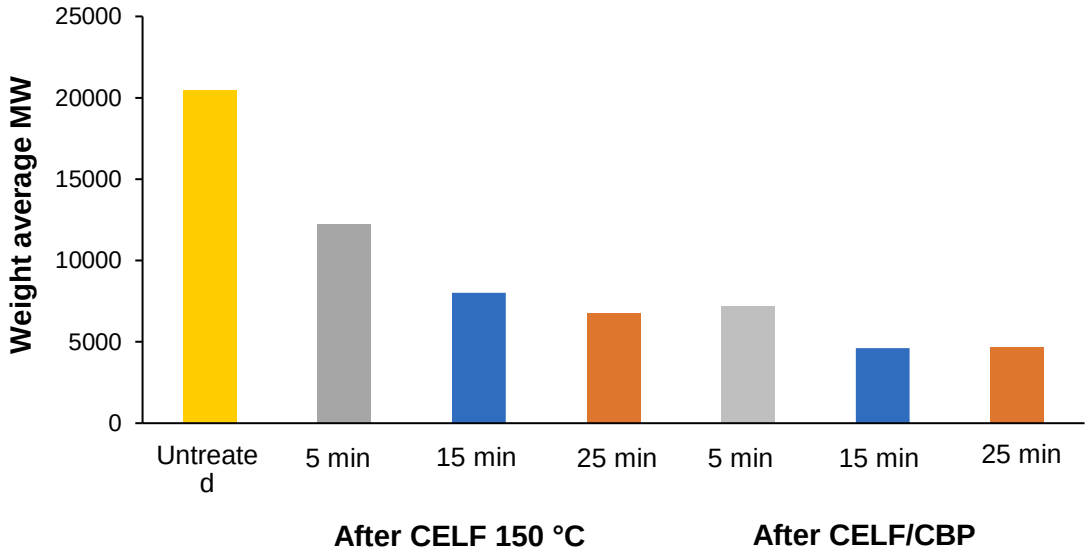

Figure 2-9. Weight-average molecular weights of CELF lignin from Poplar pretreated at 150°C for 5, 15 and 25 minutes and residual lignin after consolidated bioprocessing using *C. thermocellum.*

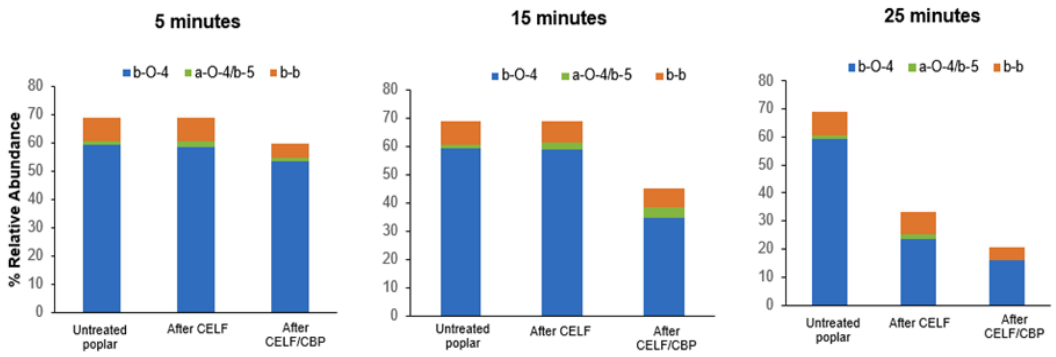

Figure 2-10. Percent relative abundance of various interunit linkages present in Poplar before CELF, after CELF pretreatment at 150°C for 5, 15 and 25 minutes, and after consolidated bioprocessing using *C. thermocellum* of CELF solids pretreated at three different temperatures and times.

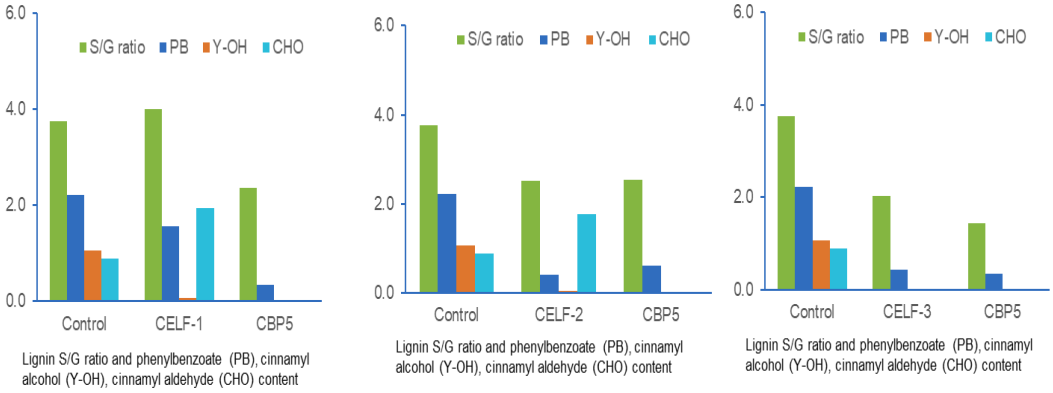

Figure 2-11. Quantitation of Syringyl:Guaiacyl ratios, phenylbenzoate, cinnamyl alcohol and cinnamyl aldehyde in the untreated Poplar, CELF pretreated Poplar at 150°C for 5, 15 and 25 minutes, and remaining solids after consolidated bioprocessing using *C. thermocellum*.

2.5 Conclusions

CELF and CBP synergistically deconstruct biomass, eliminating the need of external enzymes, and CELF-CBP pairings enabled ~100% glucan solubilization by *C. thermocellum* for all tested conditions. Although the 15 and 25 minutes conditions both reached the same percent solubilization, the 25 minute condition resulted in faster kinetics, reaching 81% glucan solubilization within 12 hours, whereas the 15 minute condition only reached 27% glucan solubilization in that time. SRS imaging provided insight that extensive lignin depolymerization and its aggregation allows *C. thermocellum* higher accessibility to glucan and leads to faster kinetics. By varying CELF severity slightly and correlating *C. thermocellum* glucan solubilization to CELF substrate crystallinity, delignification extent and nature of residual lignin aggregate, it is clear that lignin phase change at processing temperatures above lignin glass transition temperature (>150°C) is a key factor. This study also emphasizes the synergy of CELF-CBP pairing- where CELF enables biomass delignification and xylan removal, and *C. thermocellum* efficiently solubilizes crystalline cellulose- together proving to be a highly efficient biomass deconstruction technology that eliminates the need of costly enzymes. GPC and NMR characterization of residual lignin show decreases in average molecular weight and substantial decrease in b-*O*-4 linkage both after CELF and CELF-CBP, suggesting lignin modification during CBP by *C. thermocellum*.

2.6 References

Aboudi, K., Fernández-Güelfo, L. A., Álvarez-Gallego, C. J., & Romero-García, L. I. (2021). Biogas, biohydrogen, and polyhydroxyalkanoates production from organic waste in the circular economy context. *Sustainable Biofuels*, 305–343. https://doi.org/10.1016/B978-0-12-820297-5.00002-5

Ahmed, K. ;, Kershenbaum, L. S., Chadwick, D. ;, Conrad, H., Ertl, G. J., Kippers, J. ;, Latta, E. E., Primet, M., Dalmon, J. A., & Martin, G. A. (2002). Organosolv pretreatment for enzymic hydrolysis of poplars. 2. Catalyst effects and the combined severity parameter. *Industrial and Engineering Chemistry Research*, *29*(2), 156–162. https://doi.org/10.1021/IE00098A003

Akinosho, H., Yee, K., Close, D., & Ragauskas, A. (2014). The emergence of Clostridium thermocellum as a high utility candidate for consolidated bioprocessing applications. *Frontiers in Chemistry*, *2*(AUG), 66. https://doi.org/10.3389/FCHEM.2014.00066/BIBTEX

Baruah, J., Nath, B. K., Sharma, R., Kumar, S., Deka, R. C., Baruah, D. C., & Kalita, E. (2018). Recent trends in the pretreatment of lignocellulosic biomass for value-added products. *Frontiers in Energy Research*, *6*(DEC), 141. https://doi.org/10.3389/FENRG.2018.00141/BIBTEX

Bhagia, S., Muchero, W., Kumar, R., Tuskan, G. A., & Wyman, C. E. (2016). Natural genetic variability reduces recalcitrance in poplar. *Biotechnology for Biofuels*, *9*(1), 1–12. https://doi.org/10.1186/S13068-016-0521-2/FIGURES/5

Cai, C. M., Zhang, T., Kumar, R., & Wyman, C. E. (2013). *Green Chemistry COMMUNICATION THF co-solvent enhances hydrocarbon fuel precursor yields from lignocellulosic biomass †*. https://doi.org/10.1039/c3gc41214h

Capolupo, L., & Faraco, V. (2016). Green methods of lignocellulose pretreatment for biorefinery development. *Applied Microbiology and Biotechnology 2016 100:22*, *100*(22), 9451–9467. https://doi.org/10.1007/S00253-016-7884-Y

Chai, L., Liu, M., Yan, X., Cheng, X., Zhang, T., Si, M., Min, X., & Shi, Y. (2018). Elucidating the Interactive Impacts of Substrate-Related Properties on Lignocellulosic Biomass Digestibility: A Sequential Analysis. *ACS Sustainable Chemistry and Engineering*, *6*(5), 6783–6791. https://doi.org/10.1021/ACSSUSCHEMENG.8B00592/SUPPL_FILE/SC8B00592_SI_001.PDF

Gao, D., Haarmeyer, C., Balan, V., Whitehead, T. A., Dale, B. E., & Chundawat, S. P. S. (2014). Lignin triggers irreversible cellulase loss during pretreated lignocellulosic

biomass saccharification. *Biotechnology for Biofuels*, *7*(1), 1–13. https://doi.org/10.1186/S13068-014-0175-X/TABLES/2

Himmel, M. E., Ding, S. Y., Johnson, D. K., Adney, W. S., Nimlos, M. R., Brady, J. W., & Foust, T. D. (2007). Biomass recalcitrance: Engineering plants and enzymes for biofuels production. *Science*, *315*(5813), 804–807. https://doi.org/10.1126/SCIENCE.1137016/ASSET/53180CC7-C2AC-411F-A286-B238D5DC153A/ASSETS/GRAPHIC/315_804_F3.JPEG

Karimi, K., & Taherzadeh, M. J. (2016). A critical review on analysis in pretreatment of lignocelluloses: Degree of polymerization, adsorption/desorption, and accessibility. *Bioresource Technology*, *203*, 348–356. https://doi.org/10.1016/J.BIORTECH.2015.12.035

Kothari, N., Holwerda, E. K., Cai, C. M., Kumar, R., & Wyman, C. E. (2018). Biomass augmentation through thermochemical pretreatments greatly enhances digestion of switchgrass by Clostridium thermocellum. *Biotechnology for Biofuels*, *11*(1), 1–14. https://doi.org/10.1186/S13068-018-1216-7/TABLES/1

Kucharska, K., Rybarczyk, P., Hołowacz, I., Łukajtis, R., Glinka, M., & Kamiński, M. (2018). Pretreatment of Lignocellulosic Materials as Substrates for Fermentation Processes. *Molecules*, *23*(11). https://doi.org/10.3390/MOLECULES23112937

Liu, Q., Luo, L., & Zheng, L. (2018). Lignins: Biosynthesis and Biological Functions in Plants. *International Journal of Molecular Sciences*, *19*(2). https://doi.org/10.3390/IJMS19020335

Lourenço, A., & Pereira, H. (2017). Compositional Variability of Lignin in Biomass. *Lignin - Trends and Applications*. https://doi.org/10.5772/INTECHOPEN.71208

Merklein, K., Fong, S. S., & Deng, Y. (2016). Biomass Utilization. *Biotechnology for Biofuel Production and Optimization*, 291–324. https://doi.org/10.1016/B978-0-444-63475-7.00011-X

Nguyen, T. Y., Cai, C. M., Kumar, R., & Wyman, C. E. (2015). *Co-solvent Pretreatment Reduces Costly Enzyme Requirements for High Sugar and Ethanol Yields from Lignocellulosic Biomass*. https://doi.org/10.1002/cssc.201403045

Olson, D. G., McBride, J. E., Joe Shaw, A., & Lynd, L. R. (2012). Recent progress in consolidated bioprocessing. *Current Opinion in Biotechnology*, *23*(3), 396–405. https://doi.org/10.1016/J.COPBIO.2011.11.026

ORNL accelerates bioenergy innovation, sharing scientific discoveries in over 1,000 publications | ORNL. (2018). https://www.ornl.gov/blog/ornl-accelerates-bioenergy-innovation-sharing-scientific-discoveries-over-1000-publications

Patri, A. S., Mohan, R., Pu, Y., Yoo, C. G., Ragauskas, A. J., Kumar, R., Kisailus, D., Cai, C. M., & Wyman, C. E. (2021a). THF co-solvent pretreatment prevents lignin redeposition from interfering with enzymes yielding prolonged cellulase activity. *Biotechnology for Biofuels*, *14*(1), 1–13. https://doi.org/10.1186/S13068-021-01904-2/FIGURES/7

Perlack, R. D. S. B. J. et al. (2011). *U.S. Billion-Ton Update: Biomass Supply for a Bioenergy and Bioproducts Industry*.

Pingali, S. V., Smith, M. D., Liu, S. H., Rawal, T. B., Pu, Y., Shah, R., Evans, B. R., Urban, V. S., Davison, B. H., Cai, C. M., Ragauskas, A. J., O'Neill, H. M., Smith, J. C., & Petridis, L. (2020). Deconstruction of biomass enabled by local demixing of cosolvents at cellulose and lignin surfaces. *Proceedings of the National Academy of Sciences of the United States of America*, *117*(29), 16776–16781. https://doi.org/10.1073/PNAS.1922883117

Qian, E. W. (2013). Pretreatment and Saccharification of Lignocellulosic Biomass. *Research Approaches to Sustainable Biomass Systems*, 181–204. https://doi.org/10.1016/B978-0-12-404609-2.00007-6

Ragauskas, A. J., Beckham, G. T., Biddy, M. J., Chandra, R., Chen, F., Davis, M. F., Davison, B. H., Dixon, R. A., Gilna, P., Keller, M., Langan, P., Naskar, A. K., Saddler, J. N., Tschaplinski, T. J., Tuskan, G. A., & Wyman, C. E. (n.d.). *Lignin Valorization: Improving Lignin Processing in the Biorefi nery*. https://doi.org/10.1126/science.1246843

Rahikainen, J. L., Martin-Sampedro, R., Heikkinen, H., Rovio, S., Marjamaa, K., Tamminen, T., Rojas, O. J., & Kruus, K. (2013). Inhibitory effect of lignin during cellulose bioconversion: the effect of lignin chemistry on non-productive enzyme adsorption. *Bioresource Technology*, *133*, 270–278. https://doi.org/10.1016/J.BIORTECH.2013.01.075

Singh, R., Shukla, A., Tiwari, S., & Srivastava, M. (2014). A review on delignification of lignocellulosic biomass for enhancement of ethanol production potential. *Renewable and Sustainable Energy Reviews*, *32*, 713–728. https://doi.org/10.1016/J.RSER.2014.01.051

Singh, S., Cheng, G., Sathitsuksanoh, N., Wu, D., Varanasi, P., George, A., Balan, V., Gao, X., Kumar, R., Dale, B. E., Wyman, C. E., Simmons, B. A., & Bioenergy, J. (2015). *Comparison of different biomass pretreatment techniques and their impact on chemistry and structure*. https://doi.org/10.3389/fenrg.2014.00062

Smith, M. D., Mostofian, B., Cheng, X., Petridis, L., Cai, C. M., Wyman, C. E., & Smith, J. C. (2016). Cosolvent pretreatment in cellulosic biofuel production: effect of tetrahydrofuran-water on lignin structure and dynamics †. *Cite This: Green Chem*, *18*, 1268. https://doi.org/10.1039/c5gc01952d

Studer, M. H., DeMartini, J. D., Davis, M. F., Sykes, R. W., Davison, B., Keller, M., Tuskan, G. A., & Wyman, C. E. (2011). Lignin content in natural Populus variants affects sugar release. *Proc Natl Acad Sci USA*, *108*(15), 6300–6305. https://doi.org/10.1073/pnas.1009252108

Thomas, V. A., Donohoe, B. S., Li, M., Pu, Y., Ragauskas, A. J., Kumar, R., Nguyen, T. Y., Cai, C. M., & Wyman, C. E. (2017). Adding tetrahydrofuran to dilute acid pretreatment provides new insights into substrate changes that greatly enhance biomass deconstruction by Clostridium thermocellum and fungal enzymes. *Biotechnology for Biofuels*, *10*(1), 252. https://doi.org/10.1186/S13068-017-0937-3

Thomas, V. A., Kothari, N., Bhagia, S., Akinosho, H., Li, M., Pu, Y., Yoo, C. G., Pattathil, S., Hahn, M. G., Raguaskas, A. J., Wyman, C. E., & Kumar, R. (2017). Comparative evaluation of Populus variants total sugar release and structural features following pretreatment and digestion by two distinct biological systems. *Biotechnology for Biofuels*, *10*(1), 1–16. https://doi.org/10.1186/S13068-017-0975-X

Tuskan, G. A., Muchero, W., Tschaplinski, T. J., & Ragauskas, A. J. (2019). Population-level approaches reveal novel aspects of lignin biosynthesis, content, composition and structure. *Current Opinion in Biotechnology*, *56*, 250–257. https://doi.org/10.1016/J.COPBIO.2019.02.017

Um, B. H., & van Walsum, G. P. (2012). Effect of pretreatment severity on accumulation of major degradation products from dilute acid pretreated corn stover and subsequent inhibition of enzymatic hydrolysis of cellulose. *Applied Biochemistry and Biotechnology*, *168*(2), 406–420. https://doi.org/10.1007/S12010-012-9784-7

Volynets, B., Ein-Mozaffari, F., & Dahman, Y. (2017). Biomass processing into ethanol: Pretreatment, enzymatic hydrolysis, fermentation, rheology, and mixing. *Green Processing and Synthesis*, *6*(1), 1–22. https://doi.org/10.1515/GPS-2016-0017/ASSET/GRAPHIC/J_GPS-2016-0017_FIG_006.JPG

Wang, Y. Y., Sengupta, P., Scheidemantle, B., Pu, Y., Wyman, C. E., Cai, C. M., & Ragauskas, A. J. (2020). Effects of CELF Pretreatment Severity on Lignin Structure and the Lignin-Based Polyurethane Properties. *Frontiers in Energy Research*, *8*, 149. https://doi.org/10.3389/FENRG.2020.00149/BIBTEX

Wyman, C. E., Dale, B. E., Elander, R. T., Holtzapple, M., Ladisch, M. R., & Lee, Y. Y. (2005). Coordinated development of leading biomass pretreatment technologies. *Bioresource Technology*, *96*(18), 1959–1966. https://doi.org/10.1016/J.BIORTECH.2005.01.010

Yao, L., Yang, H., Yoo, C. G., Pu, Y., Meng, X., Muchero, W., Tuskan, G. A., Tschaplinski, T., & Ragauskas, A. J. (2018). Understanding the influences of different pretreatments on recalcitrance of Populus natural variants. *Bioresource Technology*, *265*(C), 75–81. https://doi.org/10.1016/J.BIORTECH.2018.05.057

Yarbrough, J. M., Mittal, A., Mansfield, E., Taylor, L. E., Hobdey, S. E., Sammond, D. W., Bomble, Y. J., Crowley, M. F., Decker, S. R., Himmel, M. E., & Vinzant, T. B. (2015). New perspective on glycoside hydrolase binding to lignin from pretreated corn stover. *Biotechnology for Biofuels*, *8*(1), 1–14. https://doi.org/10.1186/S13068-015-0397-6/FIGURES/9

Yousuf, A., Pirozzi, D., & Sannino, F. (2019). Fundamentals of lignocellulosic biomass. *Lignocellulosic Biomass to Liquid Biofuels*, 1–15. https://doi.org/10.1016/B978-0-12-815936-1.00001-0

Zoghlami, A., & Paës, G. (2019). Lignocellulosic Biomass: Understanding Recalcitrance and Predicting Hydrolysis. In *Frontiers in Chemistry* (Vol. 7). Frontiers Media S.A. https://doi.org/10.3389/fchem.2019.00874

2.7 Supplementary Material

S1. Media composition for *C. thermocellum* Consolidated Bioprocessing

Solution	Component	Reactor Concentration	Stock Concentration
Solution A	Carbohydrate source	0-100 g/L	
	MOPS (buffer)	5 g/L	100 g/L
	Optional: Yeast extract	5 g/L	
Solution B	Citric Acid Potassium salt [$C_6H_5K_3O_7.H_2O$]	2 g/L	50 g/L
	Citric Acid Monohydrate	1.25 g/L	31.25 g/L
	Na_2SO_4	1 g/L	25 g/L
	KH2PO4	1 g/L	25 g/L
	$NaHCO_3$	2.5 g/L	62.5 g/L
Solution C	NH_4Cl	1.5 g/L	75 g/L
Solution D	$MgCl_2.6H_2O$	1 g/L	50 g/L
	$CaCl_2.2H_2O$	0.2 g/L	10 g/L
	$FeCl_2.4H_2O$	0.2 g/L	5 g/L
	L-cysteine hydrochloride monohydrate	1 g/L	50 g/L
Solution E (Vitamins)	Pyridoxamine dihydrochloride	0.02 g/L	1 g/L
	P-aminobenzoic acid	0.004 g/L	0.2 g/L
	D-biotin	0.002 g/L	0.1 g/L
	Vitamin B12	0.002 g/L	0.1 g/L

S2. Example of fermentation set up for CBP using *C. thermocellum*

S3. XRD patterns of untreated and CELF pretreated Poplar for CELF pretreatment at 150°C. (b) Crystallinity Index (CrI) calculated by Sagel's method.

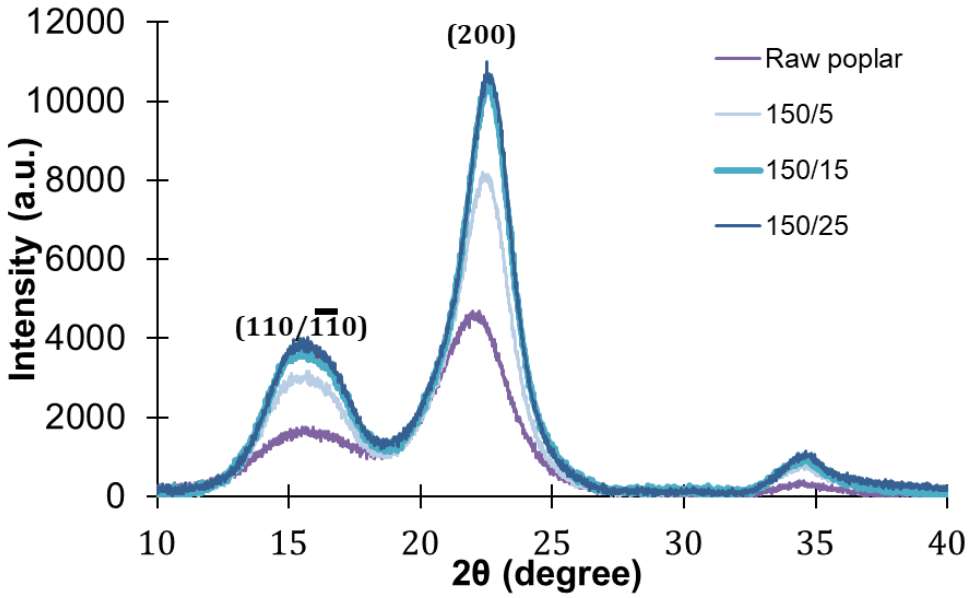

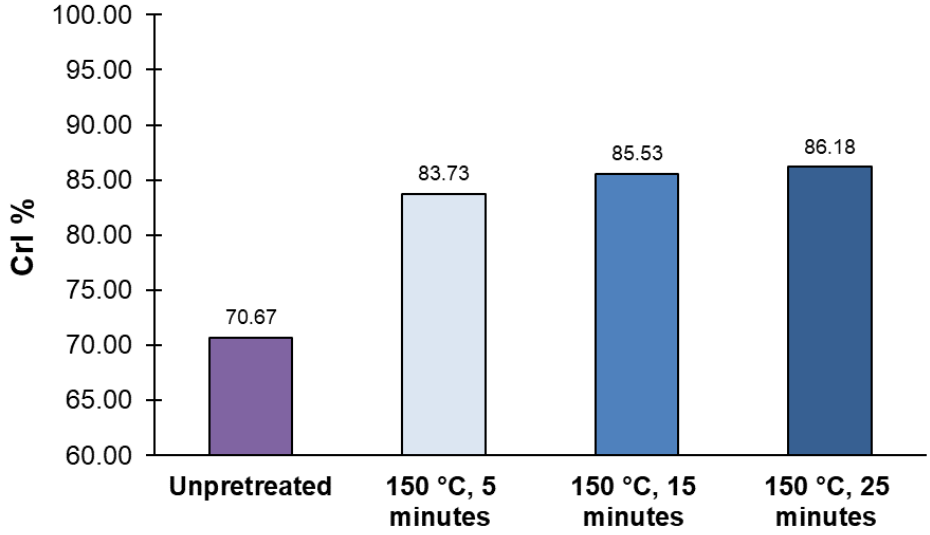

S4. Common interunit linkages present in the lignocellulosic biomass and the associated HSQC signatures.

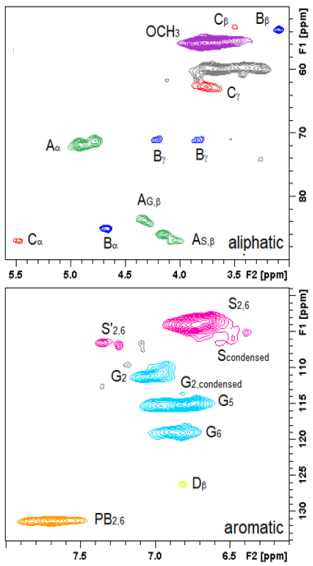

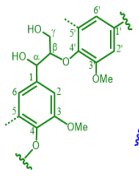

(A) β-*O*-4' alkyl aryl ether

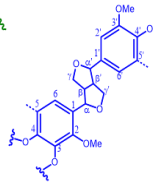

(B) β-β' resinol

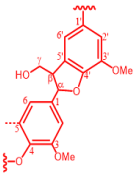

(C) β-5' phenylcoumaran

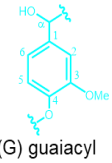

(G) guaiacyl

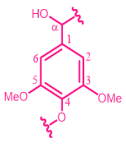

(S) syringyl

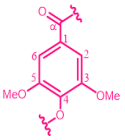

(S') a-oxidized syringyl

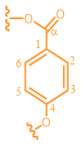

(PB) *p*-hydroxybenzoate

Chapter 3: Deconstruction of CELF Pretreated Poplar by Selected Biological Systems

*This work was done in collaboration with Neal Hengee (secretome study), Dr. Yining Zeng (SRS), Dr. Yannick Bomble, Dr. Maria J. Pena (NMR of fermentation broth), Dr. Yunqiao Pu (NMR of solid residuals). The contents of this chapter will be used for publication in a scientific journal in part or in full.

3.1 Abstract

To overcome the challenges of lignocellulosic biomass recalcitrance, novel fractionation and deconstruction technologies are being developed. Pretreatment, product separation and cellulolytic enzymes, all add to the high cost of lignocellulosic fuel price. To overcome these challenges and enable the non-petroleum renewable fuels from lignocellulosic biomass, extensive research in this field is leading to the development of promising technologies. Co-Solvent Enhanced Lignocellulosic Fractionation (CELF) has shown promise to be a feedstock agnostic process and easier integration with downstream saccharification and fermentation processes. We have recently demonstrated an optimized CELF-Consolidated Bioprocessing (CELF-CBP) process for woody biomass, Poplar, using *Clostridium thermocellum.* This study extends our CELF process optimization research effort and compares the glucan solubilization yields of the CELF-CBP process against fungal cellulose (Ctec2) and with secretome from *C. thermocellum*. The goal was to identify key attributes in CELF pretreated biomass that influence deconstruction with promising selected biological systems. The CELF reaction severity and unique features of each biological system provide two levers to dial and tune CELF process integration with each biological system studied. The lower severity lower enzyme combination revealed similarities between secretomes and *C. thermocellum* in adapting to substrate changes where the fungal cellulase combination was more influenced by pretreatment severity and substrate characteristics than the secretome.

3.2 Introduction

Climate change due to rapid rise in greenhouse gases, especially CO_2, and sustainability issues with our over reliance on petroleum fuels and products have given rise to scientific discourse and focused research in developing alternate non-petroleum-based fuels and chemicals (Binod et al., 2019; "Biomass for Renewable Energy, Fuels, and Chemicals," 1998; Demirbas, 2008; Moghaddam et al., 2016; Siqueira et al., 2020; Su et al., 2020). Novel pretreatment processes that minimize separation cost, maximize product yields, allow integration with downstream biological conversion, and minimize undesired condensation byproducts are some of the challenges that still must be addressed (Antonetti et al., 2020; Chang et al., 2019; Liu et al., 2020; Questell-Santiago et al., 2020). Co-solvent Enhanced Lignocellulosic Fractionation (CELF) has been shown to be efficient in fractionating glucan rich solid fraction that are amenable to downstream biological conversion processes (Cai et al., 2013; Nguyen et al., 2015; Smith et al., 2016). High cost of cellulose hydrolyzing enzymes is another challenge that is limiting the price parity of cellulosic fuels compared with petroleum fuels. Consolidated Bio-Processing using whole cell as biocatalyst is an approach that enables integration of cellulose deconstruction and fermentation of deconstructed sugars into one unit-operation without the need of exogenous enzymes (Akinosho et al., 2014; Lin et al., 2015). In contrast, simultaneous saccharification and fermentation (SSF) process is another approach that consolidate unit operations but still requires addition of external holo-cellulolytic enzymes (Joshi et al., 2021; Shi et al., 2013; van Zyl et al., 2007).

Although CELF process has been demonstrated on a variety of herbaceous and more recently, on woody biomass (Chanoca et al., 2019; Li et al., 2008; Sun et al., 2002; Yu et al., 2016), a more rigorous systems approach on the influence of pretreatment reaction condition on the downstream biological system, specifically, which substrate features positively or negatively influence the biomass solubilization, fermentation and product yields are essential (Chu et al., 2020; Schmatz et al., 2021; Zhai et al., 2018; Zhang et al., 2012).

Clostridium thermocellum, an anaerobic and thermophilic bacterium has been extensively studied due to its ability to secrete holocellulolytic enzymes (Akinosho et al., 2014; Lin et al., 2015) and also its ability to grow on and deconstruct crystalline cellulose (Berger et al., 2007; Boisset et al., 1999). In addition, higher thermos-stability of the secreted enzymes are advantageous for process consolidation with upstream thermochemical processes (Chundawat et al., 2011), enable easier product separation of low boiling products and to lessen the product inhibition (Feng et al., 2021). More recently, ester production in *C. thermocellum* is reported to provide a platform for in-situ production of less toxic esters instead of higher molecular weight alcohols that are more toxic and necessitate engineering efflux pumps to overcome product toxicity (Seo et al., 2019).

3.3 Experimental Section

3.3.1 Materials

CBI reference Poplar variant GW-9947 was generously provided by the Center for BioEnergy Innovation (CBI) from Dr. Muchero Wellington's lab. Poplar was knife milled to a uniform particle size of 1 mm using a Wiley Mill (Model 4, Arthur H. Thomas Company, Philadelphia PA). Composition of unpretreated and CELF pretreated Poplar was

determined following the NREL Laboratory Analytical Procedure (Version 08-03-2012). The wild type *Clostridium thermocellum* strain DSM 1313 was provided by Dr. Lynd's lab at Dartmouth College. Cellic® Ctec2 was provided by Novozymes. The secretome was purified from *C. thermocellum* by our collaborators at NREL.

3.3.2 Pretreatment

For pretreatment, the CBI Poplar barrel was mixed thoroughly and stored in 2 gallon Ziplock bags in between use. Each allocated Poplar bag was then thawed, cut to smaller sizes using gardening scissors and milled by a Thomas Wiley knife mill with and passed through a 1 mm internal sieve. Pretreatments were performed in a 1 L Hastelloy Parr® autoclave reactor (236HC Series, Parr Instruments Co., Moline, IL) equipped with a double stacked pitch blade impeller rotated at 200 rpm. The reactions were prepared by first adding the milled Poplar at 7.5 wt % solid loadings. A mixture of DI water and 0.5 wt% (based on liquid mass) 72 wt % sulfuric acid (Ricca Chemical Company, Arlington, TX). Tetrahydrofuran (>99% purity, Fisher Scientific, Pittsburgh, PA) was added in a 1:1 mass ratio with water in the fume hood. The reactions were left to soak overnight at 4°C. Temperatures for CELF reactions were 140°C, 150°C and 160°C at times of 35, 25, and 15 minutes identified by optimization reactions for each time. All reactions were maintained at reaction temperature (± 0.5°C) by convective heating with a 4 kW fluidized sand bath (Model SBL-2D, Techne, Princeton, NJ). The reaction temperature was directly measured by using an in-line K-type thermocouple (Omega Engineering Inc., Stamford, Connecticut). When the reaction was complete, the Parr reactor was submerged into a room temperature water bath until the internal temperature reached 30-40 °C. The reaction solids

were separated from the liquid by vacuum filtration at room temperature through glass fiber filter paper (Fisher Scientific, Pittsburgh, PA) and washed with 4 liters of deionized room temperature water until the filtrate pH was measured to be neutral. The solids were carefully transferred to a Ziplock bag and weighed with and without the wet filter. The moisture content of the solids was determined by a halogen moisture analyzer (Model HB43, Mettler Toledo, Columbus, OH).

3.3.3 Enzymatic hydrolysis of CELF Poplar using selected biological systems

3.3.3.1 Enzymatic hydrolysis of CELF poplar using fungal cellulases

Enzymatic hydrolysis of CELF pretreated Poplar was carried out in triplicate in 125 mL flasks at working mass of 50 grams. The solids were loaded at 5 g/L glucan and an enzyme loading of Cellic® Ctec2 of 5 and 15 mg/ g glucan (graciously provided by Novozymes Franlinton, NC). A Pierce ™ BCA assay kit was utilized to determine the protein content to be 270 mg/mL. The concentrated enzyme stock was diluted down to a concentration of 54 mg/mL in Mili-Q water prior to addition to the flask. The flasks contained 50 mM of citrate buffer (pH 4.8). The flasks were placed in an orbital shaker incubator set at 50°C and 150 RPM. At the first time point 500 uL of liquid sample was taken, but as fermentation progressed, the sample amount was increased to 650 uL to ensure enough liquid for HPLC analysis. Samples were centrifuged at 15,000 RPM for 12 minutes and transferred to HPLC vials. Cellobiose, glucose, xylose, arabinose concentrations were measured at each time point.

3.3.3.2 Enzymatic hydrolysis of CELF poplar using purified secretome from *C. thermocellum*

Secretomes from *C. thermocellum* were purified for enzymatic digestions from cell-free broth grown on Avicel in a pH controlled bioreactor at 5 g/L solids loadings as described previously (paye 2016 and brice 2014). Digestion preparations were carried out in 20 mM Sodium Acetate,100 mM NaCl, 5 mM CaCl2, 10 mM L-cysteine hydrochloride (pH 5.5).

3.3.4 Consolidated Bioprocessing of CELF poplar using *C. thermocellum*

Consolidated Bioprocessing (CBP) fermentation was first carried out in shake flasks at 50 mL working volume. Fermentation substrate (CELF pretreated Poplar at 5g/L glucan loadings) and MiliQ water was added to 125 mL pressure bottles (Wheaton, Millville NJ) and the oxygen was removed by purging with nitrogen, alternating between nitrogen addition at 14 psi and vacuum at 45 second intervals for 30 minutes. The bottles were then autoclaved at 121°C for 35 minutes. Once cooled, media for Clostridia (MTC) was added at the appropriate volume with ammonium chloride as the component used for media C. Trace minerals were not used in the shake flask experiments. Seed cultures were grown on 5 g/L glucan loading of Avicel® PH-101 (Sigma Aldrich, St. Louis, MO) at 60°C for 8-9 hours and added to the prepared fermentation bottles for CELF pretreated Poplar at 2% (v/v) loadings.

3.4 Results and Discussions

3.4.1 Comparison of CELF Poplar digestibility

The goal of this work was to identify how change in CELF pretreated poplar positively or negatively influences the activity of selected biological systems. Specifically, CELF poplar was pretreated at constant temperature (150°C) for 5, 15 and 25 minutes creating CELF pretreated substrates with subtle physio-chemical differences. The goal was not to create drastic differences by using harsh pretreatment conditions just to understand these factors, which is often the case in published reports. Instead, low severity optimized CELF process (Chapter 2) was used to test the sensitivity of changes. Low severity process minimizes the issue of pseudo-lignin and other byproduct inhibition (He et al., 2020; Kumar et al., 2013; Qing et al., 2010; Shinde et al., 2017; Zhang et al., 2012a) for downstream biological deconstruction and fermentation, as well as minimize glucose and xylose derivatization into furfural, hydroxyl-methyl furfural, and other condensed products from lignin. Three biological systems that were studied and compared include *C. thermocellum,* fungal cellulose Ctec2, and secretome from *C. thermocellum* to further understand the relationship between biomass features and biological deconstruction. The percent composition of the three CELF pretreated Poplar is reported in Table 3-1. As can be seen, the CELF Poplar pretreated at three different severities (ranging from 2.17-2.87) resulted into substrates with percent glucan, xylan and lignin ranging from 76.4-86.7%, 8.3-6% and 13.38-6.4% respectively.

The percent glucan solubilization from 5, 15 and 25 minutes CELF pretreated Poplar by *C. thermocellum*, fungal cellulose Ctec2 and the *C. thermocellum* secretome at

the 5 mg/g enzyme and 15 mg/g enzyme loadings are reported in Figure 3-1 and Figure 3-2 respectively. Glucan solubilization results for the lowest severity CELF pretreated Poplar at the low enzyme loadings of 5 mg/g of glucan show drastic difference in the total solubilized glucan, especially at the early hydrolysis stage of 8 hours. For example, secretome resulted in only 3.31% glucan solubilization compared with 13% by fungal cellulose Ctec2 and 26.2% by *C. thermocellum*. At 48 hours, the glucan solubilization for secretome, fungal cellulose Ctec2 and *C. thermocellum* reached to 15.9%, 31% and 91% respectively. The glucan solubilization for lowest severity CELF pretreated Poplar and low enzyme loading, *C. thermocellum* reached >94% at day 5 compared with 24.6% and 44% respectively for secretome and fungal cellulose Ctec2. The 5 mg/ g glucan enzyme loading condition revealed similarities between the secretomes and C. thermocellum in adapting to substrate changes across all severities whereas the fungal cellulase was more influenced by pretreatment severity and substrate characteristics than the secretome systems.

Examination of the glucan solubilization for the 15 minutes CELF pretreated Poplar at the low enzyme loadings show that at the early stages of hydrolysis, secretome is still not able to hydrolyze much of the of the glucan (only reached 4.7%, an increase of 1% compared with 5 minutes CELF pretreated Poplar), this was the same trend for *C. thermocellum* where glucan solubilization increased by 1% when going from 5 mins to 15 mins of pretreatment. In contrast, the fungal cellulose Ctec2 reached 18.6% (an increase of >5%). At the hydrolysis time of 48 hours, the glucan solubilization for 15 minutes CELF pretreated poplar was 21.7%, 59% and 98% for the secretome, fungal cellulose Ctec2 and *C. thermocellum* respectively. Similarly, for the hydrolysis time of 5 days, the glucan

solubilization was 25%, 82% and 98% for the secretome, fungalcellulase Ctec2 and *C. thermocellum* respectively. Almost complete glucan solubilization was achieved by *C. thermocellum*, but the largest increase was seen for the fungal cellulose Ctec2 (2X increase) when the pretreatment time was increased from 5 minutes to 15 minutes. As the pretreatment time was increased to 25 mins, at the low hydrolysis time and low enzyme loadings of 5 g/mg of glucan, the glucan solubilization by secretome still remained low at 8 hours. By the hydrolysis time of 5 days glucan solubilization reached 27.7%, 100% and 100% for secretome, fungal cellulose Ctec2 and *C. thermocellum* respectively.

At the high 15 mg/g of glucan enzyme loading, the glucan solubilization at 8 hours hydrolysis time for 5 minutes pretreated CELF Poplar show an interesting picture. The increase in glucan solubilization for secretome and fungal cellulase Ctec2 was 3X and 2X when compared with itself at the low enzyme loadings of 5 g/g of glucan loadings. Similar doubling and tripling of glucan solubilization were achieved by secretome and fungal cellulase at the 48 hours hydrolysis time for the 5 minutes CELF pretreated Poplar. This trend continued and the glucan solubilization was increased by 2.5X by both secretome and fungal cellulase Ctec2 at the 5 days hydrolysis time. For 15 minutes pretreated CELF Poplar, at the high enzyme loadings of 15 g/g of glucan, solubilization reached 78.5 and 100% for secretome and fungal cellulase respectively by day 2 and by day 5, the % glucan solubilization was almost completed by all three biological systems (>98%). It is interesting that 25 minutes CELF pretreatment time and high enzyme loadings of 15 g/g glucan at day 2 and day 5 for the secretome and fungal cellulase Ctec2 reached ~80 and 100% for secretome and 100% for both at day 2 and day 5 for fungal celluloase Ctec2.

Figure 3-3 reports on the overall glucan solubilization profiles for CELF poplar substrates at 150°C 5 minutes (square markers), 15 minutes (triangle markers), 25 minute (circle markers) biologically digested by fungal cellulases (green) and the secretome from *C. thermocellum* (yellow) at 5 mg/ g glucan loadings are compared to the solubilization profiles of CBP with *C. thermocellum.* At lower enzyme loadings, neither the fungal cellulases Ctec2 nor secretome are able to fully reach near complete solubilization that can be achieved with the *C. thermocellum* as detailed in figures 4-2 and 4-3 respectively. However, results in figure 4-4 show that both the *C. thermocellum* and the purified secretome from *C. thermocellum* reached similar end point solubilizations despite the pretreatment severity of the pretreated CELF poplar. From these results, it becomes apparent that the secretome alone can adapt to small differences between the compositional variation and is not as affected by the pretreatment severity, but the whole organism is still needed to reach desired levels of high glucan solubilization. However, this is not the case for the fungal enzymes at lower enzyme loadings of 5 mg/g of glucan, as solubilization increases with increasing CELF pretreatment time as shown in the figure 3-4. When the enzyme loadings are increased to 15 mg/ g glucan, the fungal cellulase Ctec2 seems to overcome the inhibition and both the 15 and 25 minutes CELF pretreated Poplar were fully solubilized. Increasing the enzyme loadings for the secretome from *C. thermocellum* also improved glucan solubilization to above 75% for the 15 and 25 minutes CELF pretreated Poplar. Solubilization is also increased by nearly ~40% for 5 minutes CELF pretreated Poplar when the secretome enzyme loading was increased to 15 mg/g of glucan loading.

Overall, results presented in figures 3-1 to 3-4, depict a detailed view of the biological systems studied on the CELF pretreated Poplar at two enzyme loadings.

3.4.2 Correlation of CELF substrate features and Biological Deconstruction

3.4.2.1 Fractal Modeling of Solubilization via Biological Systems

Fractal kinetic models were used to evaluate the rate of percent glucan conversion for the 5, 15 and 25 minutes CELF pretreated Poplar at the enzyme loadings of 5 and 15 mg/g of glucan. The model follows first-order cellulose saccharification kinetics for the conversion of glucan to glucose, and the fractal exponent respectively (equation (1) (Wang and Feng 2010):

$$\frac{dC}{dt} = k_t C \quad \text{where } kt = kt^h \qquad (1)$$

C = Cellulose concentration

k_t, = Time-dependent rate coefficient

k, = Rate constant

t = Time

h = Fractal exponent

The glucan solubilization data from all three biological assays were fit to the model described in equation (2) in which X is percent glucan conversion and t (hours) is time.

$$X = 100 \times \{1 - exp\left[-k(1 + \frac{t^{1-h}-1}{1-h})\right]\} \quad (2)$$

The data was fit in excel using a generalized reduced gradient algorithm generating the rate coefficient (k) and the fractal exponent (h) to minimize the sum of the least squares.

Examining the fractal kinetic parameter kt with respect to glucan conversion can indicate the substrate reactivity. Higher kt values were observed for the higher enzyme loading of 15 mg/ g glucan for all three biological systems, and for CBP for all three CELF Poplar substrates, indicating higher enzymatic rate as shown in the glucan solubilization profiles as well (3-7). For the biological deconstruction of CELF poplar using secretome, a much lower overall kt that decayed with time was observed, indicating a much lower substrate reactivity of the CELF pretreated Poplar for secretome.

The overall kt for CBP is much higher than both fungal enzymes Ctec2 and the secertome (Figure 3-8). However, the overall kt shows rapid decay for the CELF 25 minutes pretreated Poplar. The decay and high kt is likely an indication that the enzymatic rate was much higher in solubilizing glucan leading to inactivation due to substrate availability (Patri et al., 2019; Wojtusik et al., 2020)

The fractal coefficient h has been reported to demonstrate substrate accessibility (Wang et al., 2011; Wang & Feng, 2010). Wang et al. further correlated that smaller h values can be attributed to less lignin inhibition. In Figure 3-9, the calculated h values for all three CELF Poplar substrates at 5 and 15 mg/g glucan enzyme loadings is reported. At the lower enzyme loadings, the fractal coefficient is much higher for all the CELF Poplar substrates tested. The higher h values for secretome suggests lower substrate accessibility. A higher h value is also observed for the for 5 minutes CELF pretreated poplar for fungal

enzymes Ctec2, but not for the 15 and 25 minutes CELF pretreated Poplar even at the low enzyme loading of 5 mg/g of glucan. This implies that composition, specifically the residual lignin may be a factor in accessibility limitations and thus lower solubilization observed for 5 minutes CELF pretreated Poplar.

The fractal kinetics modeling for the experiments at the higher enzyme loadings of 15 mg/g of glucan (Figure 3-7) show reduced h, approaching zero, for all three biological systems (*C. thermocellum*, secretome and fungal cellulase Ctec2) indicating no effect on accessibility and resultant glucan solubilization. The fractal coefficient for CELF 5 minutes poplar is also reduced approximately 40% for secretomes and 73% for fungal cellulases at higher enzyme loadings; however, the h value never drops to 0 as is the case for 15 and 25 minutes CELF pretreated Poplar. Wang et al. have shown that lignin inhibition could be remediated by increasing enzyme loadings and our experimental data and modeling show the residual lignin inhibition for low severity pretreated Poplar can be overcome by higher enzyme loadings.

3.4.2.2 Characterization of fermentation broth and CELF pretreated Poplar by NMR and SRS imaging

In order to investigate further and correlate the glucan solubilization studies with Fractal kinetic modeling, a multimodal approach was taken. The saccharides in the fermentation broth was characterized using 1D NMR. Figure 3-10 reports on the sugar profiles of CELF pretreated Poplar at 5, 15 and 25 minutes hydrolysed by *C. thermocellum* secretome at 5 and 15 mg/g of glucan loadings for the hydrolysis time points of day 1, 2

and 3. As expected and consistent with the glucan solubilization results presented in figures 3-1 and figure 3-2, there is a slow and steady increase in the amount of both free α and β-D- glucose in the fermentation broth as a function of hydrolysis time, pretreatment severity and the amount of added enzyme. No distinct oligomeric sugar was detected and also no xylose can be detected in the sample. Similarly, fungal cellulase Ctec2 only show peaks for free α and β-D-glucose and no xylose or cellulose and xylan oligomers. This is both expected and not expected for the fungal cellulase Ctec2 system since its reported that Ctec2 exhibit some ability to breakdown the glucose. However, since the enzyme did not have htec2 in the cocktail, it is not too surprising to not see any signatures for free xylose, especially considering low amounts of xylan in the high severity CELF poplar substrates. The 1D NMR results of the saccharide characterization of the 5, 15 and 25 minutes CELF pretreated Poplar at the same severities (as C. thermocellum secretome and fungal cellulose Ctec2) at day 3 show very different sugar profile than the other two biological system studied.

In the case of *C. thermocellum*, the 1D NMR show clear signatures of the presence of free β-D-xylose (both reducing and terminal), α-D-xylose (reducing) and free α-D-glucose. Most notably, there is clear evidence of methylated glucuronic acid signature. These results are also consistent with the *C. thermocellum's* ability to breakdown xylan but inability to utilize the pentose sugar (Verbeke et al., 2017). At the day 3 of the fermentation, relatively smaller peaks for free glucose compared to the xylose indicates almost no fermentation inhibition to the *C. thermocellum* due to the presence of xylose in the broth. It is also interesting to note that as the CELF severity was increased, there was decrease in

both the amounts of free xylose, and methyl glucuronic acid. These results are also consistent with the amount of xylan present in the 5, 15 and 25 minutes CELF pretreated Poplar (Table 3-1). The comparison of solid residues of 5 and 25 minutes CELF pretreated Poplar substrate show still intact acetylated methyl glucuronic acids in addition to the methylated glucuronic acids (which was also present in the fermentation broth). The strong peaks for Pectins in the 2D NMR as well as oligomeric Mannan are the hallmark of hardwood Poplar and seem to remain intact in the solid residue after *C. thermocellum* consolidated bioprocessing for the 5 minutes CELF pretreated Poplar substrates.

From the fractal kinetics modeling, we deduce a general understanding of the different modes of actions for these three biological systems. Interestingly, for the conditions, when the glucan solubilization was incomplete despite the fractal kinetics model showing low fractal exponent, h, show the complexity of the system. Multiple physio-chemical factors including, 1) enzyme inactivation, 2) surface obstacles (lignin aggregate) and, 3) changes in substrate accessibility and reactivity, are likely playing a role. To gain further insight, Stimulated Raman Spectroscopy (SRS) imaging and NMR spectroscopy was used. To understand the presence of different amounts of residual lignin and its influence on the glucan solubilization of the three biological systems, the 5, 15 and 25 minutes CELF pretreated Poplar samples were analyzed using SRS imaging. As shown in previous chapter and in Figure 3-12, the highest severity CELF pretreated Poplar substrate show lignin breakdown and the cellulose surface (Raman signature at 2890 cm^{-1}) almost free of lignin (Raman signature at 1600 cm^{-1}) and the residual lignin self aggregated as small particulates. The increase in the extent and rate of glucan solubilization is

consistent with the amount of lignin and its distribution on the cellulose surface. The 5 minutes CELF pretreated Poplar substrate show overlapping signatures of Raman signature at 2890 cm^{-1} and Raman signature at 1600 cm^{-1} representing the chemical maps of cellulose and lignin respectively. The SRS images for 5 minutes CELF pretreated substrate clearly indicate that lignin is still associated with cellulose fibers unlike the chemical distribution of lignin on the cellulose surface showing almost complete disassociation with cellulose, leading to the higher cellulose accessibility by all of the three biological system studied.

3.5 Conclusion

In this work, woody feedstock, Poplar was paired with three selected promising biological systems, namely, *C. thermocellum*, fungal cellulase Ctec2, and *C. thermocellum* secretome, after CELF pretreatment to fractionate glucan rich solids. CELF pretreatment severity was varied between 2.17 to 2.87 to create subtle changes in the physio-chemical attributes of the CELF pretreated Poplar to investigate how each of these biological systems perform. This, 1feedtsock:3 severities:3 biological systems:2 enzyme loadings is a multi-factorial problem and required detailed analysis of the performance metrics (in this case glucan solubilization) via detailed characterization and modeling. Fractal kinetics models were developed and fitted to the time course of % glucan solubilization. The overall rate coefficient, kt for the CBP process using *C. thermocellum* was much higher than both fungal cellulase Ctec2 and the *C. thermocellum* secertome. The SRS imaging and 1D/ 2D NMR of the fermentation broth and solid residue after fermentation provided clues to how each of these biological system act on the CELF pretreated Poplar. The result shows that for the lowest severity CELF pretretement condition tested (150°C/5 minutes), a slower

kinetics was observed for the secretome compared to the *C. thermocellum* and fungal cellulase Ctec2. *C. thermocellum* was found to be least sensitive to the pretreatment severities and the resultant physio-chemical changes. Additionally, the C. *thermocellum* secretome benefitted most from the high enzyme loading (15 mg/g glucan) with enhanced kinetics that almost caught-up with glucan solubilization rates of fungal cellulase Ctec2 with *C. thermocellum*. However, at the high enzyme loading, the difference in the total glucan solubilization by three biological systems started to disappear, especially at the longer fermentation times of >48 hours. Interestingly, *C. thermocellum* secretome's cellulolytic machinery seemed to lack xylanase activity and it was more similar to the fungal cellulase Ctec2 than the *C. thermocellum.* It also appeared to be more impacted by the concentrations of xylan and lignin in the CELF pretreated Poplar substrate. Detailed comparative proteomics of *C. thermocellum* grown on CELF pretreated Poplar with C. *thermocellum* secretome could provide further clarity on these distinctions.

3.6 References

Akinosho, H., Yee, K., Close, D., & Ragauskas, A. (2014). The emergence of Clostridium thermocellum as a high utility candidate for consolidated bioprocessing applications. *Frontiers in Chemistry*, *2*(AUG), 66. https://doi.org/10.3389/FCHEM.2014.00066/BIBTEX

Antonetti, C., Licursi, D., & Galletti, A. M. R. (2020). New Intensification Strategies for the Direct Conversion of Real Biomass into Platform and Fine Chemicals: What Are the Main Improvable Key Aspects? *Catalysts 2020, Vol. 10, Page 961*, *10*(9), 961. https://doi.org/10.3390/CATAL10090961

Berger, E., Zhang, D., Zverlov, V. v., & Schwarz, W. H. (2007). Two noncellulosomal cellulases of Clostridium thermocellum, Cel9I and Cel48Y, hydrolyse crystalline cellulose synergistically. *FEMS Microbiology Letters*, *268*(2), 194–201. https://doi.org/10.1111/J.1574-6968.2006.00583.X

Binod, P., Gnansounou, E., Sindhu, R., & Pandey, A. (2019). Enzymes for second generation biofuels: Recent developments and future perspectives. *Bioresource Technology Reports*, *5*, 317–325. https://doi.org/10.1016/J.BITEB.2018.06.005

Biomass for Renewable Energy, Fuels, and Chemicals. (1998). *Biomass for Renewable Energy, Fuels, and Chemicals*. https://doi.org/10.1016/B978-0-12-410950-6.X5000-4

Boisset, C., Chanzy, H., Henrissat, B., Lamed, R., Shoham, Y., & Bayer, E. A. (1999). Digestion of crystalline cellulose substrates by the Clostridium thermocellum cellulosome : structural and morphological aspects. In *Biochem. J* (Vol. 340).

Cai, C. M., Zhang, T., Kumar, R., & Wyman, C. E. (2013). THF co-solvent enhances hydrocarbon fuel precursor yields from lignocellulosic biomass. *Green Chemistry*, *15*(11), 3140–3145. https://doi.org/10.1039/c3gc41214h

Chang, H., Hussain Motagamwala, A., Huber, G. W., & Dumesic, J. A. (2019). Synthesis of biomass-derived feedstocks for the polymers and fuels industries from 5-(hydroxymethyl)furfural (HMF) and acetone. *Green Chemistry*, *21*. https://doi.org/10.1039/c9gc01859j

Chanoca, A., de Vries, L., & Boerjan, W. (2019). Lignin Engineering in Forest Trees. *Frontiers in Plant Science*, *10*, 912. https://doi.org/10.3389/FPLS.2019.00912/BIBTEX

Chundawat, S. P. S., Beckham, G. T., Himmel, M. E., & Dale, B. E. (2011). Deconstruction of lignocellulosic biomass to fuels and chemicals. *Annual Review of Chemical and Biomolecular Engineering*, *2*, 121–145. https://doi.org/10.1146/ANNUREV-CHEMBIOENG-061010-114205

Chu, Q., Wang, R., Tong, W., Jin, Y., Hu, J., & Song, K. (2020). Improving Enzymatic Saccharification and Ethanol Production from Hardwood by Deacetylation and Steam Pretreatment: Insight into Mitigating Lignin Inhibition. *ACS Sustainable Chemistry & Engineering*, *8*(49), 17967–17978. https://doi.org/10.1021/ACSSUSCHEMENG.0C05583

Demirbas, A. (2008). Present and Future Transportation Fuels. *Http://Dx.Doi.Org/10.1080/15567030701258519*, *30*(16), 1473–1483. https://doi.org/10.1080/15567030701258519

Feng, J., Zhang, J., Ma, Y., Feng, Y., Wang, S., Guo, N., Wang, H., Wang, P., Jiménez-Bonilla, P., Gu, Y., Zhou, J., Zhang, Z. T., Cao, M., Jiang, D., Wang, S., Liu, X. W., Shao, Z., Borovok, I., Huang, H., & Wang, Y. (2021). Renewable fatty acid ester production in Clostridium. *Nature Communications 2021 12:1*, *12*(1), 1–13. https://doi.org/10.1038/s41467-021-24038-3

He, J., Huang, C., Lai, C., Jin, Y., Ragauskas, A., & Yong, Q. (2020). Investigation of the effect of lignin/pseudo-lignin on enzymatic hydrolysis by Quartz Crystal Microbalance. *Industrial Crops and Products*, *157*, 112927. https://doi.org/10.1016/J.INDCROP.2020.112927

Joshi, A., Kanthaliya, B., Meena, S., Khan, F., & Arora, J. (2021). Process consolidation approaches for cellulosic ethanol production. *Sustainable Biofuels*, 43–72. https://doi.org/10.1016/B978-0-12-820297-5.00013-X

Kumar, R., Hu, F., Sannigrahi, P., Jung, S., Ragauskas, A. J., & Wyman, C. E. (2013). Carbohydrate Derived-Pseudo-Lignin Can Retard Cellulose Biological Conversion. *Biotechnol. Bioeng*, *110*, 737–753. https://doi.org/10.1002/bit.24744/abstract

Lin, P. P., Mi, L., Morioka, A. H., Yoshino, K. M., Konishi, S., Xu, S. C., Papanek, B. A., Riley, L. A., Guss, A. M., & Liao, J. C. (2015). Consolidated bioprocessing of cellulose to isobutanol using Clostridium thermocellum. *Metabolic Engineering*, *31*, 44–52. https://doi.org/10.1016/J.YMBEN.2015.07.001

Liu, X., Bouxin, F. P., Fan, J., Budarin, V. L., Hu, C., & Clark, J. H. (2020). Recent Advances in the Catalytic Depolymerization of Lignin towards Phenolic Chemicals: A Review. *ChemSusChem*, *13*(17), 4296–4317. https://doi.org/10.1002/CSSC.202001213

Li, X., Weng, J. K., & Chapple, C. (2008). Improvement of biomass through lignin modification. *The Plant Journal*, *54*(4), 569–581. https://doi.org/10.1111/J.1365-313X.2008.03457.X

Moghaddam, E. A., Ahlgren, S., & Nordberg, Å. (2016). Assessment of novel routes of biomethane utilization in a life cycle perspective. *Frontiers in Bioengineering and Biotechnology*, *4*(DEC), 89. https://doi.org/10.3389/FBIOE.2016.00089/BIBTEX

Nguyen, T. Y., Cai, C. M., Kumar, R., & Wyman, C. E. (2015). *Co-solvent Pretreatment Reduces Costly Enzyme Requirements for High Sugar and Ethanol Yields from Lignocellulosic Biomass*. 1716–1725. https://doi.org/10.1002/cssc.201403045

Patri, A. S., Mostofian, B., Pu, Y., Ciaffone, N., Soliman, M., Smith, M. D., Kumar, R., Cheng, X., Wyman, C. E., Tetard, L., Ragauskas, A. J., Smith, J. C., Petridis, L., & Cai, C. M. (2019). A Multifunctional Cosolvent Pair Reveals Molecular Principles of Biomass Deconstruction. *Journal of the American Chemical Society*, *141*(32), 12545–12557. https://doi.org/10.1021/JACS.8B10242/SUPPL_FILE/JA8B10242_SI_002.MOV

Qing, Q., Yang, B., & Wyman, C. E. (2010). Xylooligomers are strong inhibitors of cellulose hydrolysis by enzymes. *Bioresource Technology*, *101*(24), 9624–9630. https://doi.org/10.1016/J.BIORTECH.2010.06.137

Questell-Santiago, Y. M., Galkin, M. v, Barta, K., & Luterbacher, J. S. (2020). Stabilization strategies in biomass depolymerization using chemical functionalization. *Nature Reviews Chemistry*. https://doi.org/10.1038/s41570-020-0187-y

Schmatz, A. A., Salazar-Bryam, A. M., Contiero, J., Sant'Anna, C., & Brienzo, M. (2021). Pseudo-Lignin Content Decreased with Hemicellulose and Lignin Removal, Improving Cellulose Accessibility, and Enzymatic Digestibility. *Bioenergy Research*, *14*(1), 106–121. https://doi.org/10.1007/S12155-020-10187-8/FIGURES/6

Seo, H., Lee, J. W., Garcia, S., & Trinh, C. T. (2019). Single mutation at a highly conserved region of chloramphenicol acetyltransferase enables isobutyl acetate production directly from cellulose by Clostridium thermocellum at elevated temperatures. *Biotechnology for Biofuels*, *12*(1), 1–13. https://doi.org/10.1186/S13068-019-1583-8/TABLES/2

Shi, J., Gladden, J. M., Sathitsuksanoh, N., Kambam, P., Sandoval, L., Mitra, D., Zhang, S., George, A., Singer, S. W., Simmons, B. A., & Singh, S. (2013). One-pot ionic liquid pretreatment and saccharification of switchgrass. *Green Chemistry*, *15*(9), 2579–2589. https://doi.org/10.1039/C3GC40545A

Shinde, S. D., Meng, X., Kumar, R., & Ragauskas, A. J. (2017). *Recent advances in understanding the pseudo-lignin formation in lignocellulosic 1 biorefinery*. *00*, 1–3. http://energy.gov/downloads/doe-public-access-plan

Siqueira, J. G. W., Rodrigues, C., Vandenberghe, L. P. de S., Woiciechowski, A. L., & Soccol, C. R. (2020). Current advances in on-site cellulase production and application on lignocellulosic biomass conversion to biofuels: A review. *Biomass and Bioenergy*, *132*, 105419. https://doi.org/10.1016/J.BIOMBIOE.2019.105419

Smith, M. D., Mostofian, B., Cheng, X., Petridis, L., Cai, C. M., Wyman, C. E., & Smith, J. C. (2016). Cosolvent pretreatment in cellulosic biofuel production: Effect of tetrahydrofuran-water on lignin structure and dynamics. *Green Chemistry*, *18*(5), 1268–1277. https://doi.org/10.1039/c5gc01952d

Sun, R. C., Sun, X. F., Wang, S. Q., Zhu, W., & Wang, X. Y. (2002). Ester and ether linkages between hydroxycinnamic acids and lignins from wheat, rice, rye, and barley straws, maize stems, and fast-growing poplar wood. *Industrial Crops and Products*, *15*(3), 179–188. https://doi.org/10.1016/S0926-6690(01)00112-1

Su, T., Zhao, D., Khodadadi, M., & Len, C. (2020). Lignocellulosic biomass for bioethanol: Recent advances, technology trends, and barriers to industrial development. *Current Opinion in Green and Sustainable Chemistry*, *24*, 56–60. https://doi.org/10.1016/J.COGSC.2020.04.005

van Zyl, W. H., Lynd, L. R., den Haan, R., & McBride, J. E. (2007). Consolidated bioprocessing for bioethanol production using Saccharomyces cerevisiae. *Advances in Biochemical Engineering/Biotechnology*, *108*, 205–235. https://doi.org/10.1007/10_2007_061

Verbeke, T. J., Garcia, G. M., & Elkins, J. G. (2017). The effect of switchgrass loadings on feedstock solubilization and biofuel production by Clostridium thermocellum. *Biotechnology for Biofuels*, *10*(1), 1–9. https://doi.org/10.1186/S13068-017-0917-7/FIGURES/3

Wang, Z., & Feng, H. (2010). Fractal kinetic analysis of the enzymatic saccharification of cellulose under different conditions. *Bioresource Technology*, *101*(20), 7995–8000. https://doi.org/10.1016/J.BIORTECH.2010.05.056

Wang, Z., Xu, J. H., Feng, H., & Qi, H. (2011). Fractal kinetic analysis of polymers/nonionic surfactants to eliminate lignin inhibition in enzymatic saccharification of cellulose. *Bioresource Technology*, *102*(3), 2890–2896. https://doi.org/10.1016/J.BIORTECH.2010.10.132

Wojtusik, M., Vergara, P., Villar, J. C., Ladero, M., & García-Ochoa, F. (2020). Enzymatic hydrolysis of several pretreated lignocellulosic biomasses: Fractal kinetic modelling. *Bioresource Technology*, *318*, 124050. https://doi.org/10.1016/J.BIORTECH.2020.124050

Yu, Q., Zhuang, X., Wang, W., Qi, W., Wang, Q., Tan, X., Kong, X., & Yuan, Z. (2016). Hemicellulose and lignin removal to improve the enzymatic digestibility and ethanol production. *Biomass and Bioenergy*, *94*, 105–109. https://doi.org/10.1016/J.BIOMBIOE.2016.08.005

Zhai, R., Hu, J., & Saddler, J. N. (2018). The inhibition of hemicellulosic sugars on cellulose hydrolysis are highly dependant on the cellulase productive binding, processivity, and substrate surface charges. *Bioresource Technology*, *258*, 79–87. https://doi.org/10.1016/J.BIORTECH.2017.12.006

Zhang, J., Tang, M., & Viikari, L. (2012a). Xylans inhibit enzymatic hydrolysis of lignocellulosic materials by cellulases. *Bioresource Technology*, *121*, 8–12. https://doi.org/10.1016/J.BIORTECH.2012.07.010

3.7 Figures and Tables

CELF Reaction Conditions	Glucan %	Xylan %	K-lignin
150 °C, 5 minutes	76.4	8.3	13.38
150 °C, 15 minutes	84.3	6.8	9.4
150 °C, 25 minutes	86.7	6	6.4

Table 3-1. Composition of CELF poplar pretreated at 150°C at times of 5, 15 and 25 minutes.

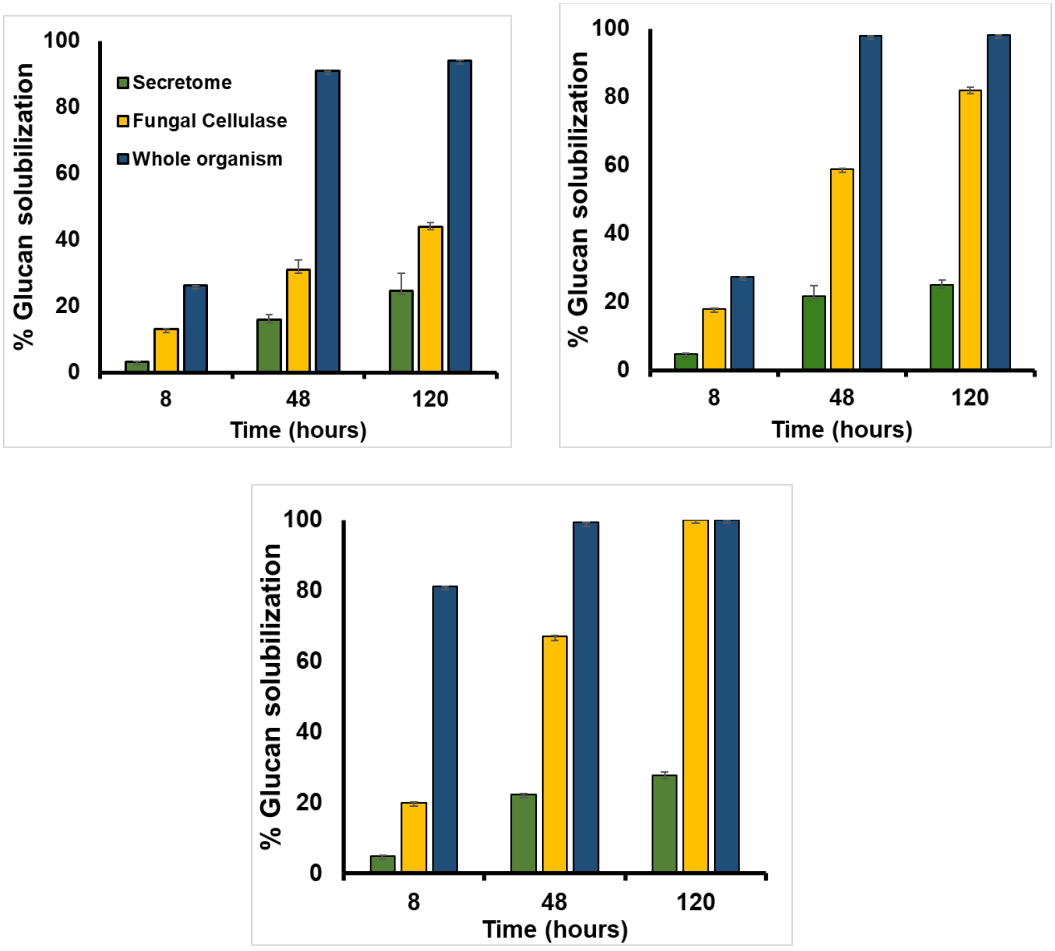

Figure 3-1. Comparison of glucan solubilization of CELF pretreated Poplar by *C. thermocellum, C. thermocellum* secretome (5 mg/ g glucan enzyme loadings) and fungal cellulase Cellic® Ctec2 (5 mg/g enzyme loadings). Top: CELF 150°C, 5 minutes, Middle: CELF 150°C, 15 minutes, and Bottom: CELF 150°C, 25 minutes.

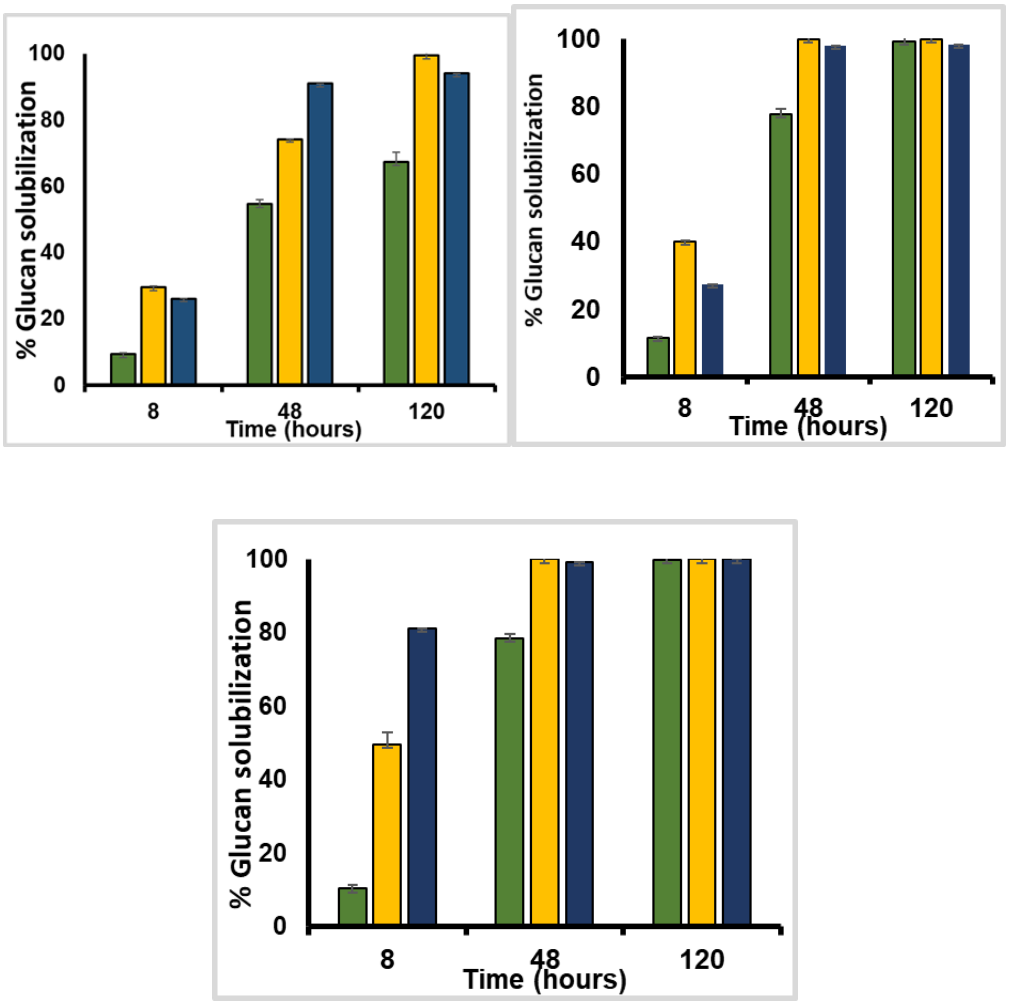

Figure 3-2. Comparison of glucan solubilization of CELF pretreated Poplar by *C. thermocellum, C. thermocellum* secretome (15 mg/ g glucan enzyme loadings) and fungal cellulase Cellic® Ctec2 (15 mg/g enzyme loadings). Top: CELF 150°C, 5 minutes, Middle: CELF 150°C, 15 minutes, and Bottom: CELF 150°C, 25 minutes.

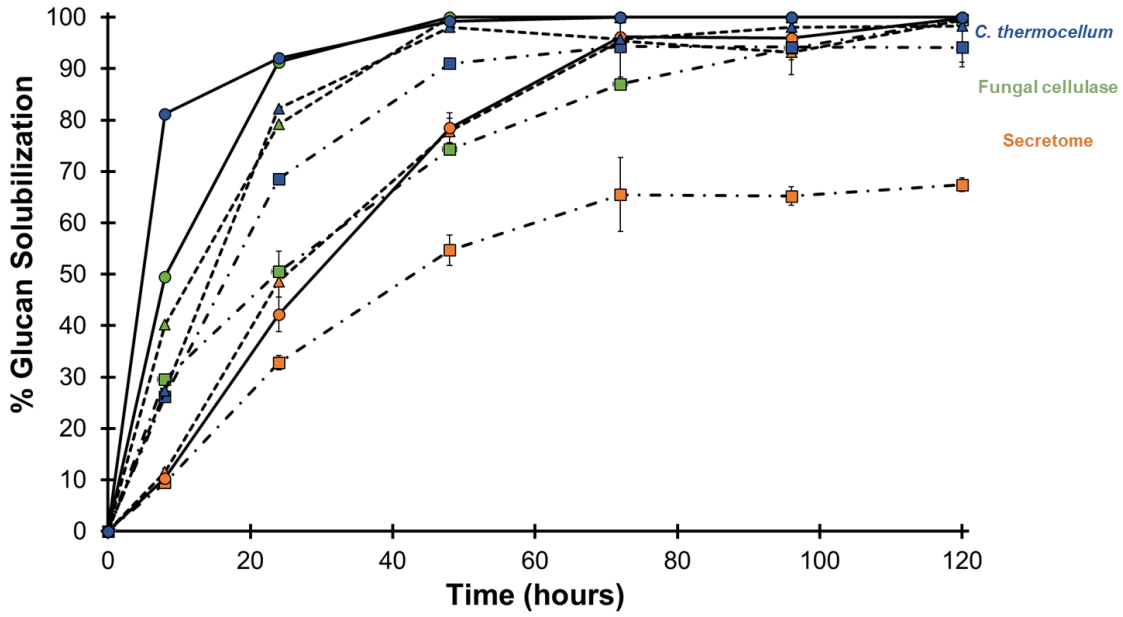

Figure 3-3. Glucan solubilization profiles for CELF pretreated poplar by *C. thermocellum* compared to fungal cellulases and purified secretomes from *C. thermocellum* at 5 mg/ g glucan enzyme loadings.

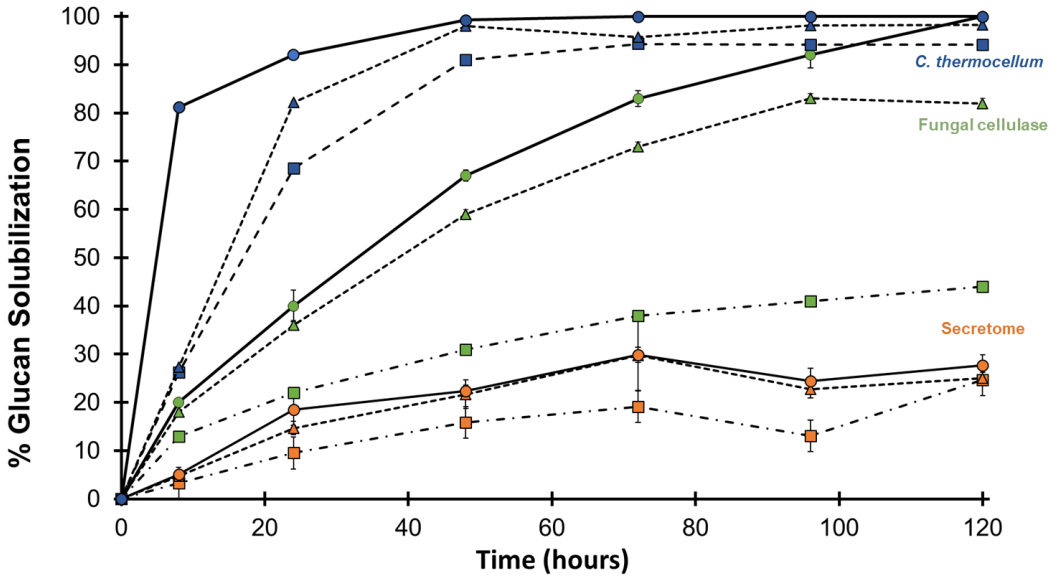

Figure 3-4. Glucan solubilization profiles for CELF pretreated poplar by *C. thermocellum* compared to fungal cellulases and purified secretomes *from C. thermocellum* at 5 mg/ g glucan enzyme loadings.

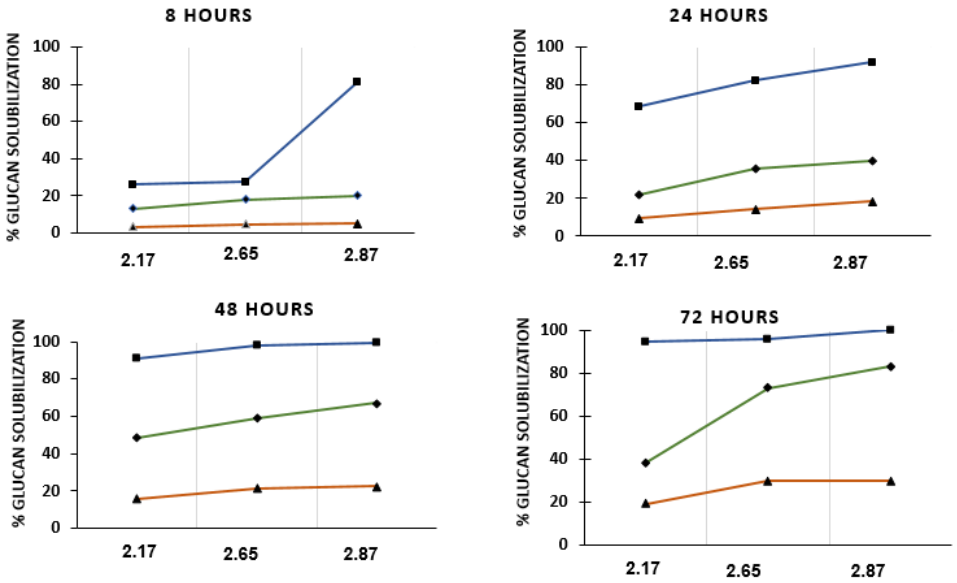

Figure 3-5. Percent glucan solubilization by *C. thermocellum, C. thermocellum* secretome (15 mg/ g glucan enzyme loadings) and fungal cellulase Cellic® Ctec2 (5 mg/g enzyme loadings) at 24, 48 and 72 hours as a function of CELF process severities.

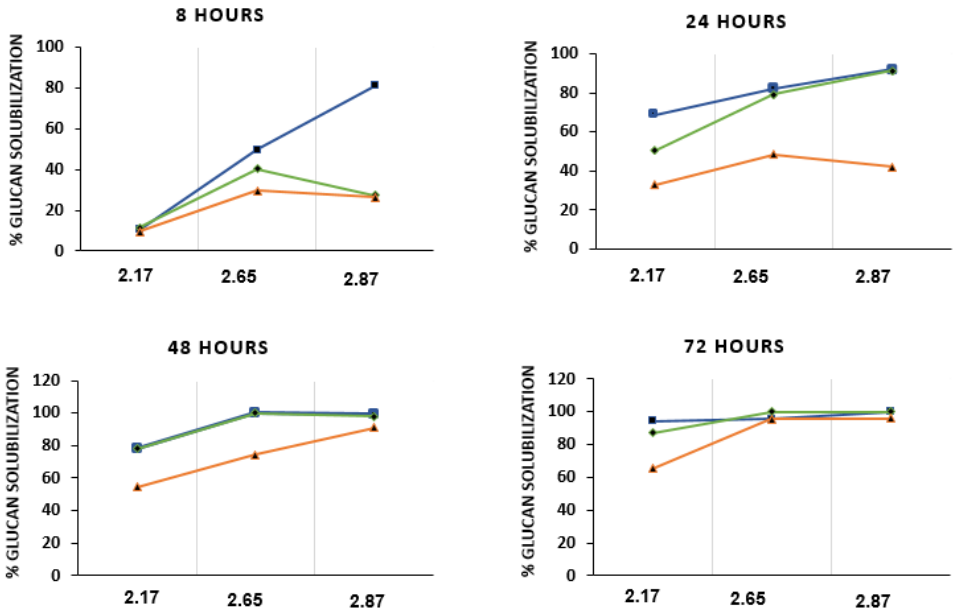

Figure 3-6. Percent glucan solubilization by *C. thermocellum*, *C. thermocellum* secretome (15 mg/ g glucan enzyme loadings) and fungal cellulase Cellic® Ctec2 (15 mg/g enzyme loadings) at 24, 48 and 72 hours as a function of CELF process severities.

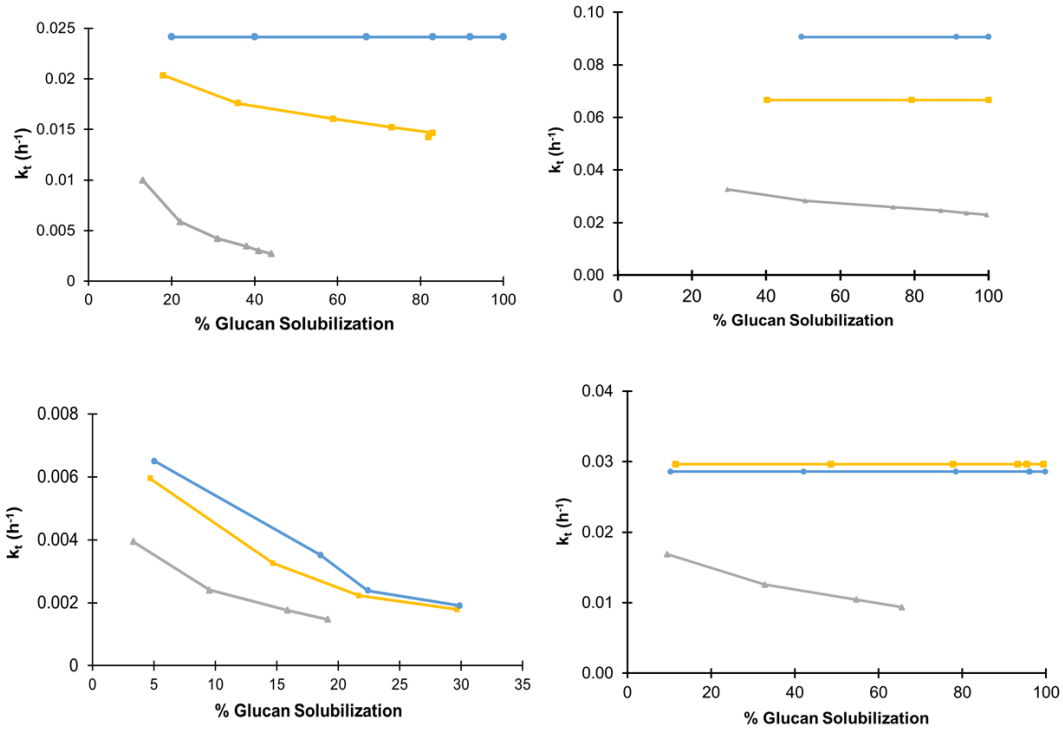

Figure 3-7. Comparison of the fractal rate constant with respect to total glucan solubilization of CELF poplar pretreated at 150 °C at 5 (grey), 15 (yellow) and 25 minutes (blue) by a) Fungal cellulases at 5 mg/ g glucan b) fungal cellulases at 15 mg/ g glucan c) purified secretomes at 5 mg/ g glucan loadings and d) purified secretomes at 15 mg/ g glucan loadings.

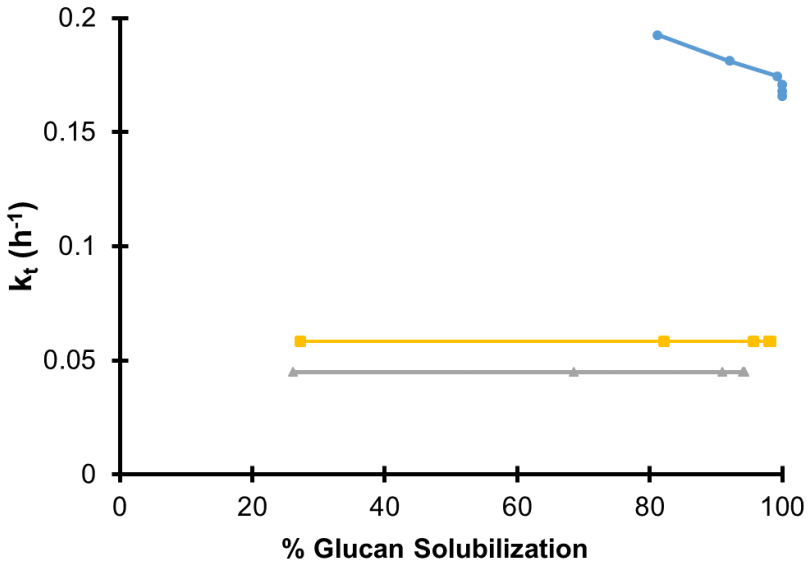

Figure 3-8. Comparison of the fractal rate constant with respect to total glucan solubilization of CELF poplar pretreated at 150 °C at 5 (grey), 15 (yellow) and 25 minutes (blue) by *C. thermocellum.*

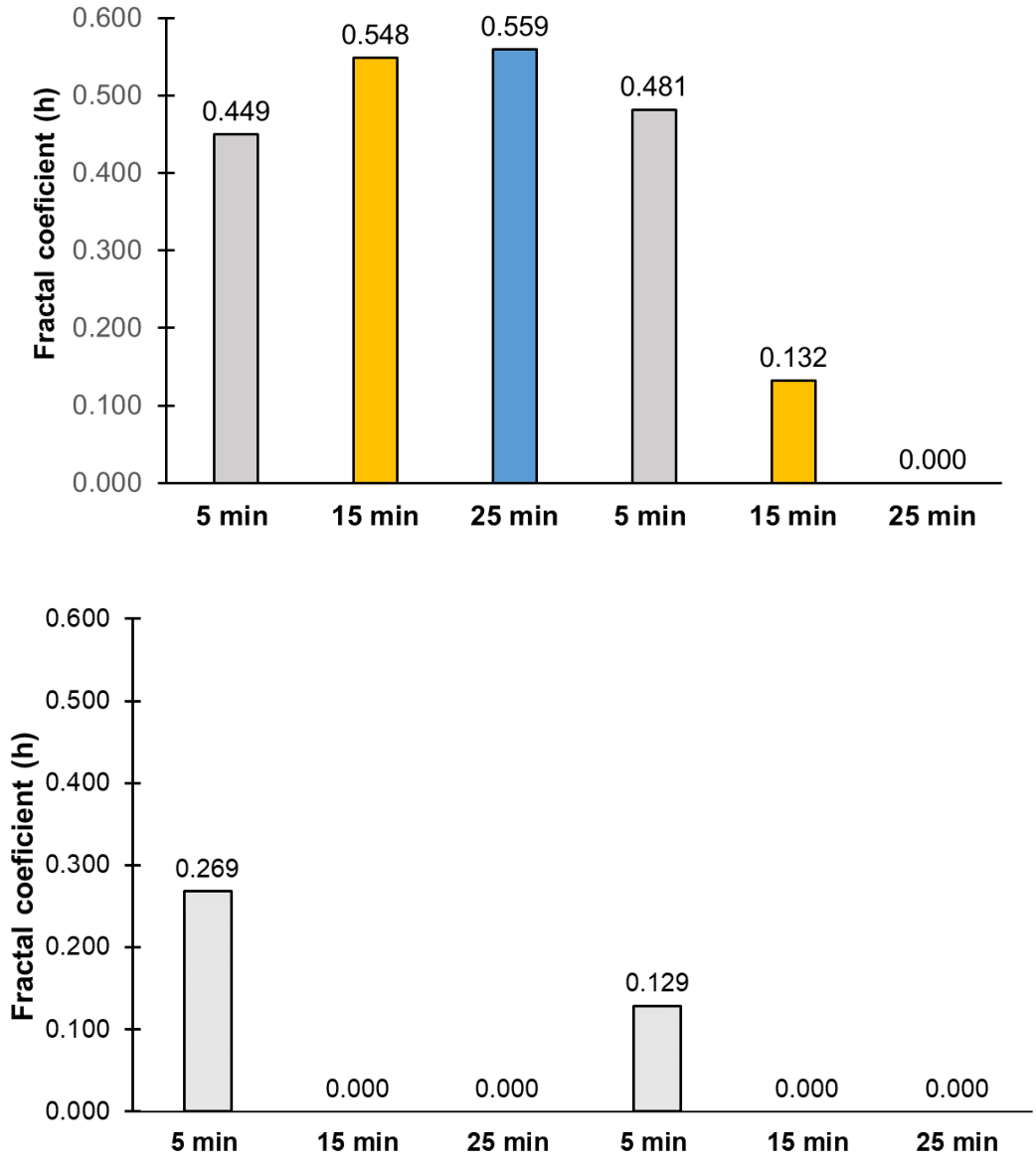

Figure 3-9. Comparison of the fractal rate coefficient h with respect to total glucan solubilization of CELF poplar pretreated at 150 °C at 5 (grey), 15 (yellow) and 25 minutes (blue) by secretomes and fungal cellulases at a) 5 mg/ g glucan and b) 15 mg/g glucan.

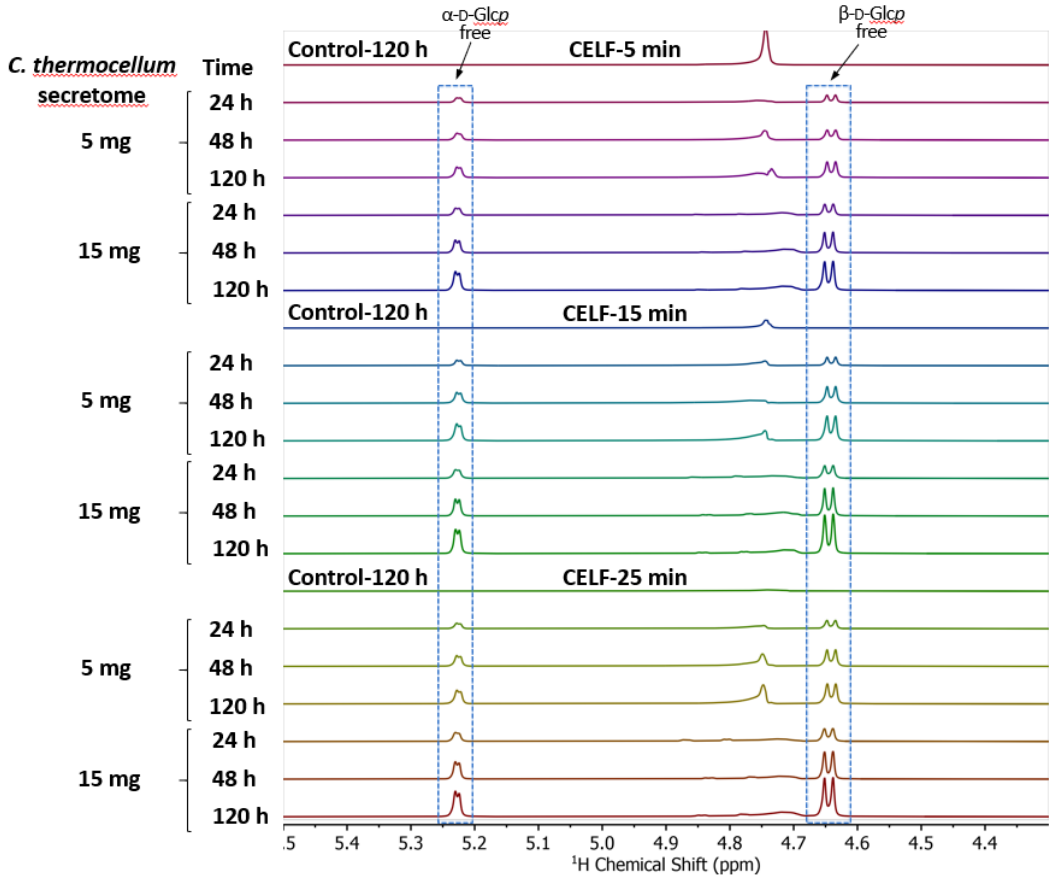

Figure 3-10. 1D NMR Spectra of a) CELF poplar at 5 minutes, b) CELF poplar at 15 minutes, c) CELF poplar at 25 minutes solubilized by purified secretomes at 5 and 15 mg/ g glucan.

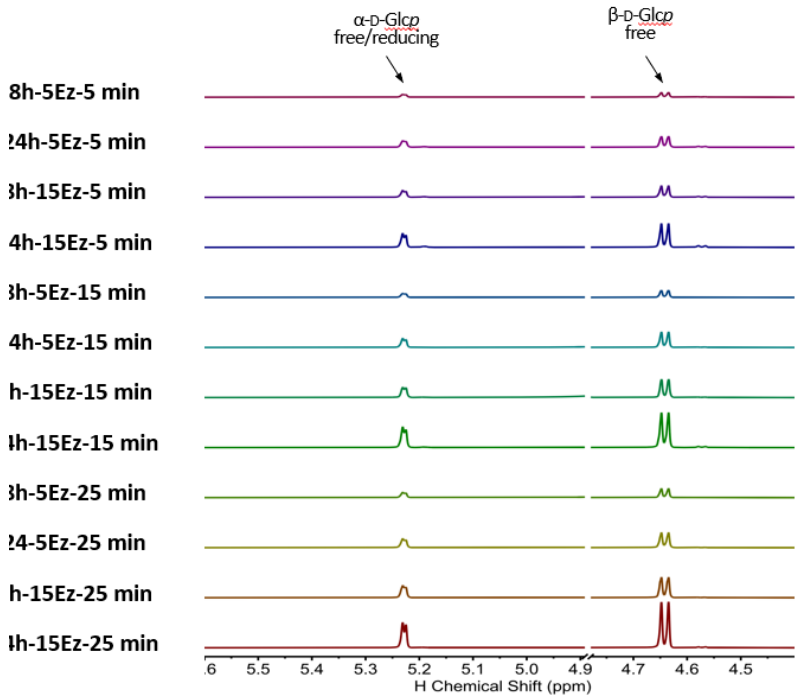

Figure 3-11. 1D NMR Spectra of a) CELF poplar at 5 minutes, b) CELF poplar at 15 minutes, c) CELF poplar at 25 minutes solubilized by fungal cellulases at 5 and 15 mg/ g glucan.

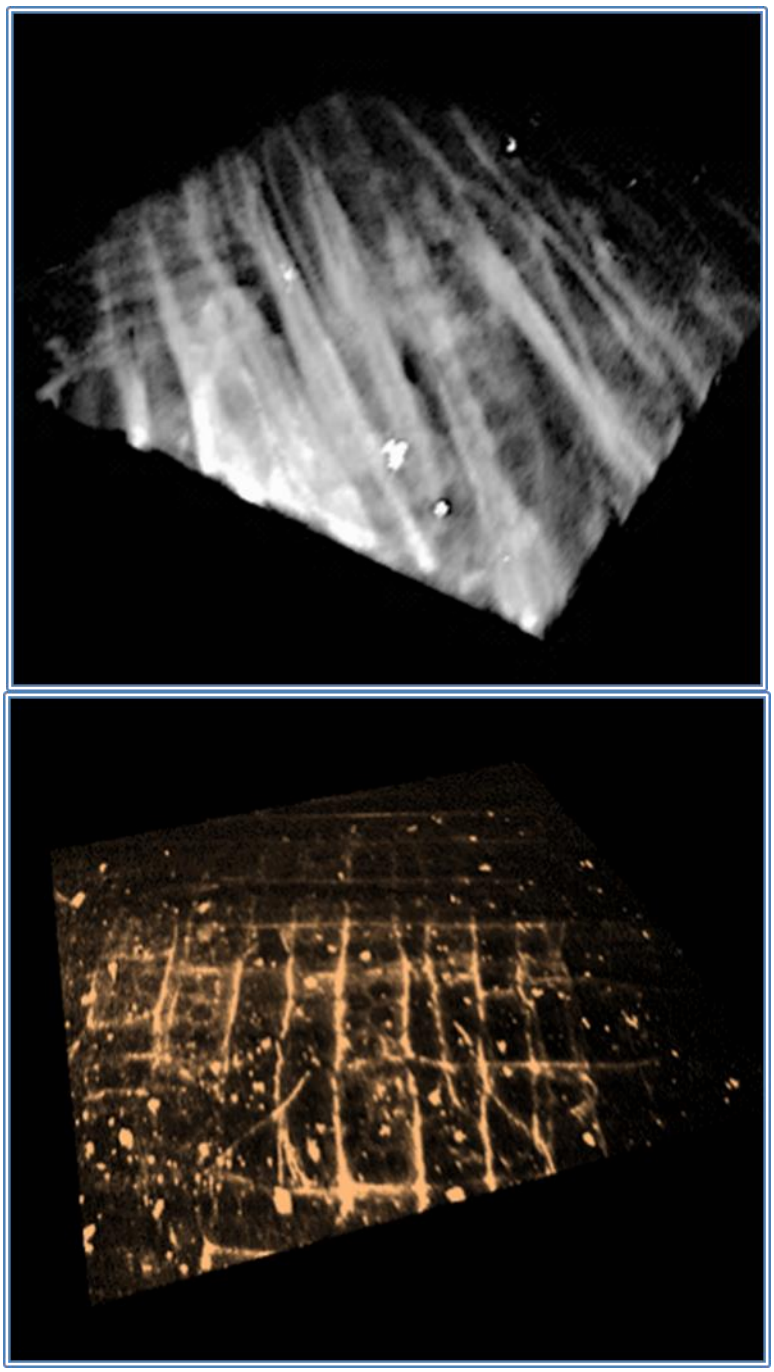

Figure 3-12. Stimulated Raman Spectroscopy of 25 minutes CELF pretreated Poplar. Chemical mapping of cellulose at 2890 (top) and lignin at 1600 cm (bottom).

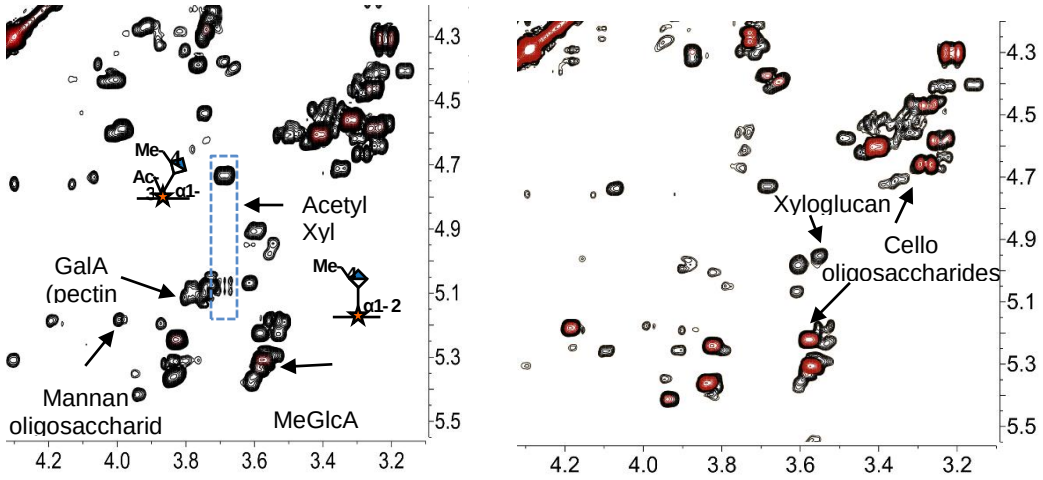

Figure 3-13. 2D NMR spectra of 150 °C, CELF pretreated Poplar 5 minutes (left) and 25 minutes (right) after CBP fermentation broth.

Supplementary Figure

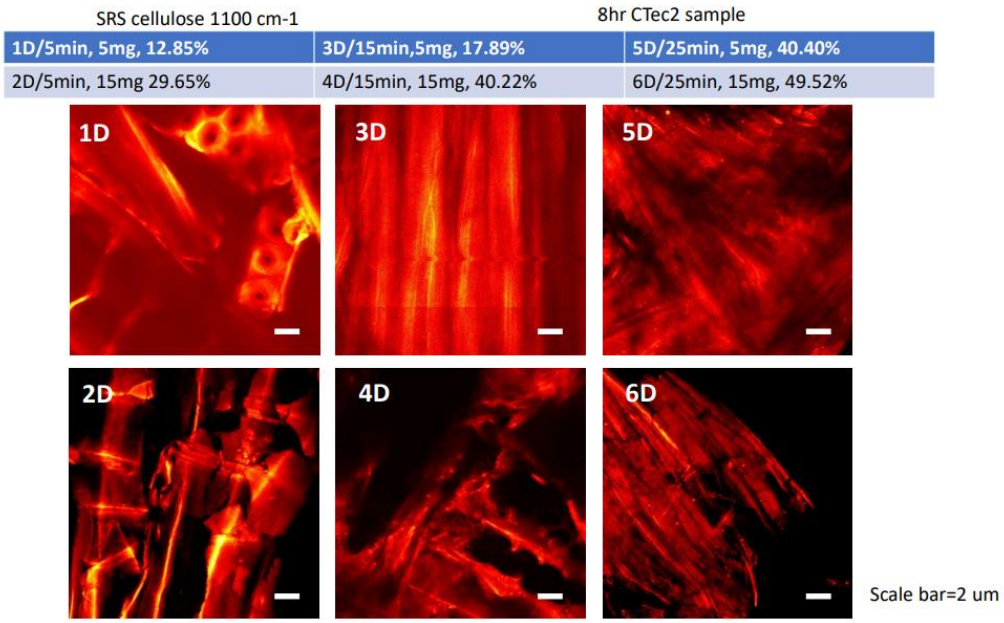

Chapter 4: Integration of CELF-CBP at High Solids Loadings: Understanding and Overcoming Limitations

*This work was done in Collaboration with Dr. Evert Holwerda and Helen Sears at Dartmouth College, Dr. Maria J. Pena at the Complex Carbohydrate Research Center/ University of Georgia. Dr. Evert Holwerda and Helen Sears carried out the fermentations at higher solids loadings. Dr. Maria Pena analyzed the fermentation broth via NMR. The contents of this chapter will be used for publication in a scientific journal in part or in full.

4.1 Abstract

Co-solvent Enhanced Lignocellulosic Fractionation (CELF) of lignocellulosic biomass produces solids that are highly enriched in glucan and a liquid stream containing most of the hemicellulose and lignin. Furthermore, integration of CELF pretreatment with consolidated bioprocessing (CBP) using *C. thermocellum* enables the complete deconstruction of all of the glucan in the CELF solids within 24-48 hours without the need of exogenous commercial enzymes, reducing process cost- providing an added impetus for process intensification to reduce product recovery cost and enable its industrial deployment. To exploit CELF-CBP synergy, and to better understand the limitations of high solids loading of the CELF-CBP integrated process, the extent of total glucan solubilization as a function of solids loadings and as a function of CELF severity is compared. Increasing solids loadings of CELF pretreated Poplar from bench scale (20 g/L glucan) to 50 g/L results in comparable total glucan solubilization (>96%) demonstrating the promise of the integrated CELF-CBP process. Further increasing the solids loadings to 75g/L and 100 g/L for CBP using *C. thermocellum* resulted in a 15-30% drop in glucan solubilization compared to 50 g/L solids loadings. Detailed NMR characterization of the fermentation broth from the high solids loadings CELF-CBP process indicate that the accumulation of oligomeric and monomeric xylose inhibit *C. thermocellum* activity, and that further inhibits glucan solubilization. By employing a co-culture strategy with *C. thermocellum* with a xylose metabolizing *Thermoanaerbacterium thermosaccharolyticum* HG-8, xylose accumulation was minimized, overcoming the decrease of glucan solubilization at very high solids loadings of >75 g/L. This is the first report of an optimized

integrated CELF-CBP process for a woody biomass at high solids loadings that leads to > 97% glucan solubilization from Poplar.

4.2 Introduction

Fossil fuels and natural gas provide > 80% of the energy in the US (Sanchez, 2020). The demand for petroleum is projected to surpass 100 million barrels per day by 2026 (Oil 2021 – Analysis - IEA, 2021). In the US, the transportation sector alone contributes to ~ 1/3 of total greenhouse gas (US EPA, 2019). Lignocellulosic biomass has the potential to lessen both the energy security and environmental concerns by enabling carbon neutral fuels and commodity chemicals. The promise of renewable fuels and chemicals from lignocellulosic sources has gained substantial attention and researchers worldwide are developing technologies to realize lignocellulosic biorefineries (Kim et al., 2020; Lau et al., 2012; Lee et al., 2017; Xu et al., 2016; Yang & Wyman, 2008). One of the many challenges of second-generation fuels from lignocellulosic biomass is their high production cost (Binod et al., 2019; Siqueira et al., 2020; Su et al., 2020). Numerous pretreatment and fractionation technologies have been developed for overcoming biomass recalcitrance (Cai et al., 2013; M. Li et al., 2016; Shi et al., 2016; Uppugundla et al., 2014; Zhao et al., 2020) and there have been efforts to minimize unit operations to further reduce the production cost of biofuels (Joshi et al., 2021a, 2021b; Shi et al., 2013; van Zyl et al., 2007). Short rotation woody crops like hybrid Poplar grow relatively fast and are energy dense compared to agriculture residue (Bryant et al., 2020). However, woody lignocellulosic biomass are more recalcitrant than energy crops and agriculture residues due to the

presence of more difficult to break lignin linkages (Chanoca et al., 2019; Dutta et al., 2014; X. Li et al., 2008; Sun et al., 2002).

Lignin and hemicellulose comprise about two thirds of the lignocellulosic biomass, but when deconstructed with cellulosic component, are known to be inhibitory to the cellulolytic enzymes (Chu et al., 2020; Schmatz et al., 2021; Yu et al., 2016; Zhai et al., 2018; Zhang et al., 2012). Co-Solvent Enhanced Lignocellulosic Fractionation (CELF) has emerged as one of the promising fractionation technologies that lead to a glucan rich solid fraction with varying amounts of residual lignin and hemicellulose, depending on the process severity. The fractionation of oligomeric lignin and hemicellulose makes the CELF process more suitable for integration with downstream saccharification and fermentation processes that utilize enzymes and biocatalysts to produce renewable fuels and bio-based chemicals.

Purified cellulolytic enzymes needed to breakdown the cellulose and cellodextrins fractionated from lignocellulosic biomass are still expensive and contribute to the many challenges of the second-generation fuels from lignocellulosic biomass production cost (Klein-Marcuschamer et al., 2012; Liu et al., 2016). *Clostridium thermocellum* naturally produces active cellulolytic enzymes and has emerged as a high utility biocatalyst due to its ability for the in-situ production of active enzymes and thereby decreasing the added cost of commercial enzymes for the production of biofuels (Hirano et al., 2016)(Hirano et al., 2016). In addition, *Clostridium thermocellum* enables integration of saccharification and fermentation unit operations since it can both breakdown the cellulose and also ferment the sugar produced from the breakdown of the polymeric cellulose (Akinosho et al., 2014;

Lin et al., 2015). *C. thermocellum*'s ability to enable process consolidation has led to recent efforts in optimizing and integrating CELF with consolidated bioprocessing (CBP) using C. *thermocellum* (Chapter 3 of this thesis, Holwerda et al., 2019a; Kothari et al., 2018; Thomas et al., 2017).

The process intensification of fractionation and fermentation processes is a must for high volume biorefinery implementation. Although the CELF-CBP overcomes some of the challenges associated with separation and handing, and minimizes the unit operations, an important next step is to increase product concentrations to sufficient levels to facilitate recovery and further decrease the cost associated with product separation especially at low concentrations (Huang & Percival Zhang, 2011; Torli et al., 2021). Thus, the effect of high mass loading must be investigated to understand challenges and areas of further improvement toward the goal of integrating and optimizing CLEF-CBP. The objective of this work was to understand the limitations of CELF-CBP beyond 5-20 g/L solids loading using CELF pretreated Poplar at high solids loadings of 50 g/L-100 g/L and determine how process severity and solids loadings impact total glucan solubilization using wild type *C. thermocellum* DSM 1313 strain for consolidated bioprocessing. In addition, detailed characterization of the fermentation broth and residual solids was done to identify which components remain after CELF and CBP and their influence on glucan solubilization by *C. thermocellum* at these high solids loadings. Strategies to overcome inhibition due to residual oligomeric sugar from hemicellulose was explored in this work.

4.3 Experimental Section

4.3.1 Materials

CBI reference Poplar variant GW-9947 was generously provided by the Center for BioEnergy Innovation (CBI) from Dr. Muchero Wellington's lab. Poplar was knife milled and passed through an internal sieve to 1mm prior to pretreatment (Model 4, Arthur H. Thomas Company, Philadelphia, PA). Composition of unpretreated and CELF pretreated Poplar was determined following the NREL Laboratory Analytical Procedure (Version 08-03-2012). DSM 1313 wildtype strain and CBP Fermentations were carried out at Dartmouth College. Waters HPLC with an Aminex® HPX-87H column at a flowrate of 0.6 ml/min at a temperature of 65°C.

4.3.2 CELF Pretreatment

For pretreatment, the CBI Poplar barrel was mixed thoroughly and stored in 2 gallon ziplock bags in between use. Each allocated Poplar bag was then thawed, cut to smaller sizes using gardening scissors and milled by a Thomas Wiley knife mill with and passed through a 1 mm internal sieve. Pretreatments were performed in a 1 L Hastelloy Parr® autoclave reactor (236HC Series, Parr Instruments Co., Moline, IL) equipped with a double stacked pitch blade impeller rotated at 200 rpm. The reactions were prepared by first adding the milled Poplar at 7.5 wt % solid loadings. A mixture of DI water and 0.5 wt% (based on liquid mass) 72 wt % sulfuric acid (Ricca Chemical Company, Arlington, TX). Tetrahydrofuran (>99% purity, Fisher Scientific, Pittsburgh, PA) was added in a 1:1 mass ratio with water in the fume hood. The reactions were left to soak overnight at 4°C. Temperatures for CELF reactions were 140°C, 150°C and 160°C at times of 35, 25, and

15 minutes identified by optimization experiments for each of the times. All reactions were maintained at reaction temperature (± 0.5 °C) by convective heating with a 4 kW fluidized sand bath (Model SBL-2D, Techne, Princeton, NJ). The reaction temperature was directly measured by using an in-line K-type thermocouple (Omega Engineering Inc., Stamford, Connecticut). When the reaction was complete, the Parr reactor was submerged into a room temperature water bath until the internal temperature reached 30-40°C. The reaction solids were separated from the liquid by vacuum filtration at room temperature through glass fiber filter paper (Fisher Scientific, Pittsburgh, PA) and washed with 4 liters of deionized at room temperature water until the filtrate pH was measured to be neutral. The solids were carefully transferred to a Ziplock bag and were weighed with and without the wet filter. The moisture content of the solids was determined by a halogen moisture analyzer (Model HB43, Mettler Toledo, Columbus, OH).

4.3.3 Consolidated Bioprocessing

Consolidated Bioprocessing (CBP) fermentation was first carried out in shake flasks at 50 mL working volume. All shake flasks were prepared with 5g/L glucan loadings. Each fermentation substrate and MiliQ water was added to 125 mL pressure bottles (Wheaton, Millville NJ) and the oxygen was removed by purging with nitrogen, and alternating between nitrogen addition at 14 psi and vacuum at 45 second intervals for 30 minutes. The bottles were then autoclaved at 121°C for 35 minutes. Once cooled, media for Clostridia (MTC) was added at the appropriate volume with ammonium chloride as the component used for media C. Trace minerals were not used in the shake flask experiments. Seed cultures were grown on 5 g/L glucan loading of Avicel® PH-101 (Sigma Aldrich, St.

Louis, MO) at 60°C for 8-9 hours and added to the prepared fermentation bottles for CELF pretreated poplar at 2% (v/v) loadings.

For higher solids experiments using monocultures of *C. thermocellum* DSM 1313, consolidated Bioprocessing CBP was performed in 0.5 L Sartorius Qplus bioreactors with a working volume of 300 mL (Sartorius Stedim, Bohemia, NY) at 60°C at 200 rpm. Modified MTC media was used with urea instead of ammonium chloride at 2 g/L. The headspace was purged with nitrogen at 100 ml/min. The pH was maintained at 7 with the automated addition of 2 N KOH. CBP of CELF pretreated poplar was carried out at 50, 75, and 100 1g/L loading in 300 mL at 60°C (Supplementary Figure S1).

Higher solid experiments using co-cultures of *C. thermocellum* DSM 1313 and *Thermoanaerobacterium thermosaccharolyticum* HG-8 ATCC 319600 bioreactor experiments were carried out as described in the previous paragraph. In these experiments, MTC media solutions were supplemented with 2% (v/v) vitamin solution at 2 g/L and a 4% (v/v) vitamin solution containing 0.004 g/L thiamine and 0.004 g/L thiotic acid. The pH was maintained at 6.5 to support the growth of *T. thermosacchacharolyticum*.

4.3.4 Compositional Analysis of CELF and CBP samples

Compositional analysis of the Poplar before and after CELF pretreatment was done following an established Laboratory Analytical Procedures (LAPs) (version 8-03-2012) from the National Renewable Energy Laboratory (NREL, Golden, CO). After the two-step acid hydrolysis, the resulting solids and liquid were separated using filtering crucibles. The liquid portion was sampled and analyzed against calibration standards and using HPLC

Waters Alliance system e2695 (Waters Co., Milford, MA) equipped with an HPX-87H column (Bio-Rad Aminex ®, Bio-Rad Laboratories, Hercules, CA) and a Waters Refractive Index Detector 2414 (Waters Co., Milford, MA). The mobile phase run was a 5 mM sulfuric acid set at a flow rate of 0.6 mL/min. Empower® 3 software package (Empower Software Solutions, Newport Beach, CA) was utilized to collect, view, and integrate the resulting chromatographs. The glucan and xylan content was calculated and adjusted against internal sugar standards. To determine the amount of acid insoluble or Klason-lignin, the solid residues after the filtration process were dried and weighed. Finally, ash and other insoluble matter were further quantified by utilizing a muffle furnace ramped to 575°C to convert the leftover material in the crucibles into ash.

4.3.6 1D/2D NMR Analysis of Carbohydrates in CBP broth

After fermentation, solids and f broths were separated via centrifugation. The soluble residues were shipped to UGA/CCRC where NMR spectroscopy was used to analyze the CBP fermentation broth to identify sugars that accumulated during fermentation. The procedure was similar to that previously reported by our co-authors and summarized here (Beri et al., 2020). Aliquots of the broths were desalted using P-10 columns (GE healthcare, Chicago, USA) using the manufacturer's instructions. The original and the desalted broth samples were lyophilized and dissolved in 0.3 mL of D_2O (99.9%, Cambridge Isotope Laboratories, Tewksbury, MA) then were transferred to a 5 mm NMR tubes. NMR spectra were recorded with a Varian Inova NMR spectrometer (Agilent Technologies) operating at 600 MHz using a 5 mm cold probe and a sample temperature of 25°C. All two-dimensional spectra were recorded using standard Varian

pulse programs. Chemical shifts were measured relative to internal acetone (δH 2.225 and δC 30.89). Data were processed using MestReNova software (Mestrelab Research S.L., Santiago de Compostela, Spain).

4.4 Results and Discussions

4.4.1 Scaled up-CBP Comparison in Bioreactor for various CELF Severity Substrates

Figures 4-1 and 4-2 report on glucan solubilization results from consolidated bioprocessing using *C. thermocellum* on CELF pretreated Poplar substrate at bench scale in shake flasks and at high solids loading of 50 g/L respectively. The CELF processing temperature was 150°C based on our CELF-CBP optimization study reported in chapter 3. For this study, in addition to 5, 15 and 25 minutes, 30 minutes CELF pretreatment was also tested to investigate impact of high solids loadings on glucan solubilization and advantage of longer CELF pretreatment time at high solids loading, if any. When 5, 15, 25 and 30 minutes CELF pretreated Poplar were processed using *C. thermocellum* in the bioreactor, all four tested conditions were effective in solubilizing CELF pretreated Poplar and resulted into more than 90% glucan solubilization (see Figure 5-2 (a)). These results are consistent with our collaborative work done with CBI partners using low lignin engineered Poplar GW-9947 line and also with BESC97 plant line (Holwerda et al., 2019). However, this is the first time CELF-CBP integration using *C. thermocellum* at the solids loading of 50 g/L has been attempted de-risking the scale up issues commonly encounter with saccharification and fermentation unit operations.

The normalized gas production profiles (percentage of each respective maximum gas production value after 140 hours) for the *C. thermocellum* CBP scale up at 50 g/L loading using CELF pretreated Poplar is shown in Figure 5-2 (b). All CELF pretreatment times show similar CBP rates except 5 minutes CELF pretreated Poplar, for which the gas evolution stops 20 hours later and shows residual recalcitrance plays a role mostly in influencing the rate and not the total glucan solubilization yield. A closer look shows 5 mins pretreatment to result into ~ 8% less solubilization than longer pretreatment times ranging from 15-30 minutes.

4.4.2 CBP Fermentation as a function of solids loadings

From our investigation on optimizing CELF pretreatment of Poplar for integration with consolidated Bioprocessing using C. *thermocellum* both at low solids loading of approximately 20 g/L (equivalent to 5 g/L glucan loadings) in the shake flasks at bench scale, and at high solids loading of 50 g/L in the bioreactor, 15 minutes pretreatment the was the shortest pretreatment time for which solubilization was maintained and thus selected to be further investigated at much higher loadings of 75 g/L and 100 g/L. This CELF reaction condition of 150°C and 15 minutes was also the optimum lowest severity CELF process suitable for integration with consolidated bioprocessing using *C. thermocellum* without negatively impacting total glucan solubilization yield or solubilization rate. In addition, CELF pretreatment for longer than 15 minutes did not appear to influence CBP solubilization rate at 50 g/L. Figure 5-3 reports on the results from the comparison of total glucan solubilization at 50 g/L, 75 g/L and 100 g/L solids

loadings from 150°C CELF pretreated Poplar for 15 minutes. Consolidated bioprocessing using *C. thermocellum* at the higher solids loadings of 50g/L, 75 g/L and 100 g/L resulted into 98.5%, 83.1% and 69% total glucan solubilizations respectively. Specifically, when the solids loading was increased from 50 g/L to 75 g/L there was a 15% decrease in total glucan solubilization during CBP. In comparison, the total glucan solubilization decreased by 30% when the solids loading was increased from 50g/L to 100 g/L.

The normalized total gas production profiles (percentage of each respective maximum gas production value after 140 hours) for the *C. thermocellum* CBP scale up at 50 g/L, 75 g/L and 100 g/L solids loadings using CELF pretreated Poplar is shown in Figure 5-3 (b). Interestingly, regardless of the decrease in total glucan solubilization at higher solids loading, all the three solids loadings show similar CBP rates for CELF pretreated Poplar and the fermentation ceases at ~ 60 hours. Since there seems to be incomplete glucan solubilization at 75 g/L and at 100 g/L solids loadings, but there is no further evolution of CO_2 and H_2 after 60 hours indicate inhibition of *C. thermocellum*. Many factors are reported to contribute to incomplete glucan solubilization at high solids loadings including mass transfer issues and accumulation of oligomeric saccharides.

To test whether a higher severity CELF pretreated Poplar may positively impact glucan solubilization by *C. thermocellum* at higher solids loadings of 75 g/L and 100 g/L, another scale-up study was conducted with higher severity (150°C and 25 minutes) pretreated CELF Poplar substrates. Both the fractional total carbohydrate and gas evolution profiles of total cumulative CO_2 and H_2 during fermentation of 50 g/L, 75 g/L and 100 g/L

Poplar show similar trend in the decrease of glucan solubilization as lower severity (150 °C, 15 minutes) pretreated Poplar (Figure 5-4) suggesting diminished solubilization was not caused by Poplar recalcitrance.

4.4.2 Saccharide Characterization of CBP broth as a Function of CELF Severity and CBP Solids Loading

To investigate and understand the accumulation of oligomers and other potential inhibitors present in the fermentation broth of the CELF pretreated Poplar, a "CBP omics" analytical plan was developed (see characterization scheme Figure 5-5). CBP fermentation broth were characterized with 1D and 2D NMR experiments with Gradient –COSY to identify oligosaccharides. In addition, for selected samples fractionation by size exclusion chromatography was used to confirm characterization observations. Figure 5-6 reports on 1D NMR results from the consolidated bioprocessing using *C. thermocellum* at high solids loading of 50 g/L for various CELF pretreatment severities (150°C:5 minutes, 150°C:15 minutes, 150° C:25 minutes, 150°C:30 minutes). The Y1 axis represents pretreatment times of the CELF substrate and the solids loadings for the CBP process using *C. thermocellum*. The Y2 axis lists associated total glucan solubilization for each of the respective CELF and CBP conditions examined.

The results from 1D NMR characterization revealed that except for 5 minutes CELF pretreatment condition, all the conditions which completely solubilized glucan at 50 g/L solids loadings looked fairly the same and showed absence of any oligosaccharide signatures which indicate that the glucan was solubilized and utilized by *C. thermocellum*. (Figure 5-6a). In contrast, distinct oligosaccharide signatures appeared in the fermentation

broth for 5 minutes CELF pretreated Poplar at 50 g/L compared to the CELF 15, 25- and 30-minutes samples (Figure 4-6 a). A close look of the 1D NMR of the replicate bioreactor runs for CELF 5- and 15-minutes Poplar at 50 g/L solids loading show xylo-oligosaccharides to be abundant in the 5 minutes CELF pretreated samples (see Figure 5-6 (b)). In particular, signatures for both terminal and reducing βD-xylose, reducing α-D-xylose, α-D glucose and oligomeric xylose glucuronoxylans can be seen in the fermentation broth of 5 minutes CELF pretreated samples at high solids loadings of 50 g/L. Glucuronoxylans are primary components of hemicellulose found in hardwood trees and contains xylose and glucuronic acid. The 1D NMR signal show the glucuroxylan to be methylated. This is also consistent with the presence of single 4-O-methyl-α-D-glucuronic acid residue (MeGlcA) in hardwood.

Figure 4-7 represents the saccharide characterization of the fermentation broth from the CELF pretreatment of Poplar at higher solids loadings of 75 g/L and 100 g/L consolidated bioprocessing using *C. thermocellum* and compares that with 1D NMR signatures from the 50 g/L fermentation. 1D NMR of the fermentation broth of CELF pretreated poplar at 15 minutes show buildup of glucose and cello-oligomers indicating there may be some inhibition to *C. thermocellum* activity impacting fermentation. In particular, these results indicate that accumulation of saccharification products may inhibit *C. thermocellum* activity and that further inhibits fermentation, leading to glucose and cello-oligosaccharide accumulation. These results are not surprising since *C. thermocellum* is known to not utilize xylose.

Figures 4-8 and 4-9 report on ^{1}H-^{1}H 2D NMR investigation of CBP fermentation broth for 5 minutes CELF pretreated and 15 minutes CELF pretreated Poplar at 50 g/L and 100 g/L solids loading respectively. Correlation Spectroscopy (COSY) 2D NMR technique gives correlations between J-coupled signals by incrementing the delay between two 90º-proton pulses. The resulting 2D spectrum is displayed as a contour plot. Standard COSY experiments are time consuming since it requires phase cycling to remove unwanted signals. To overcome this issue, unwanted magnetization and associated signals is destroyed by utilizing pulse field gradients (gCOSY). The gCOSY was used to understand the correlation between the protons to understand the linkages in the saccharides remaining in the fermentation broth. From these gCOSY result we see clear evidence of xylan oligosaccharides carrying MeGlcA with and without one acetyl group. Mannan, xyloglucan and pectin oligosaccharides are more abundant in the 5 minutes CELF poplar fermentation broth. CELF pretreatment deacetylates and removes uronic acid from poplar, enabling *C. thermocellum* to solubilize the majority of the carbohydrates at 50 g/L solids loadings. Compared to the residual sugars from 50 g/L solid loading for 5 mins CELF pretreated Poplar, the 2D NMR of residual sugars from the 100 g/L solids loading for 15 minutes CELF pretreated samples show much cleaner spectra. However, in comparison, it also indicates the buildup of xylo-and cello-oligomers. The 2D NMR data for the CELF 5 minutes condition at 50 g/L solids loading again showed the evidence of the xylan oligosaccharides carrying 4-O-methyl-α-D-glucopyranosyl urinate with and without one acetyl group. We also see mannan and pectin oligosaccharides as being more abundant in the 5 minutes CELF pretreated Poplar.

4.4.3 Strategy to Reduce Xylan/Xylose inhibition for *C. thermocellum*

Prior studies have demonstrated xylose, xyloglucan, and xylo-oligomers negatively impact Avicel utilization, rate, and reduction of OD by *C. thermocellum* (Beri et al., 2020, 2021; Qing et al., 2010) To remedy the inhibitor issue due to *C. thermocellum* inability to ferment xylose and xylooligomers, we looked into different strategies to reduce the presence of xylan/xylose. It has been reported that xylose, xyloglucan and xylo-oligmores negatively impact avicel (pure polymeric cellulose) utilization rate, and growth of *C. thermocellum* (decreased OD). However, this problem was overcome by using a microbial co-culture that can utilize the remaining xylose and in turn prevented xylose accumulation and related inhibition (Beri et al., 2020).

Both 1D and 2D NMR clearly show accumulation of xylo-oligomers in the fermentation broth and provide a detail understanding of the nature of oligomers (for low CELF pretreatment time of 5 minutes) and cello-oligomers in addition to xylo-oligomers (for CBP done at higher solids loadings of 75 g/L and 100 g/L).

We hypothesized that solubilization limitations are not due to recalcitrance but to xylose/xylo-oligomer accumulation inhibiting *C. thermocellum.* To examine the fermentation broth composition and quantitate the major sugars remaining post CBP in the fermentation broth of the CELF pretreated Poplar, carbohydrates from fermentation broth were hydrolyzed using mild acid hydrolysis and quantified as monomers. The residual sugars in the fermentation broth of *C. thermocellum* from 25 minutes CELF pretreated

Poplar at high loadings of 50 g/L, 75 g/L and 100 g/L are reported in Figure 4-10 (a). We clearly observed a buildup of xylose and glucose and, to a lesser extent arabinose. Interestingly, the amount of glucose in the 75 g/L and 100 g/L were 2X and 3X higher than xylose (9.56 g/L and 13.56 g/L of glucose compared to 4.36 g/L and 4.61g/L xylose). In contrast, the xylose accumulation was >2X higher than glucose accumulation for the 50 g/L CBP. The amount of arabinose was .12 g/L, .78 g/L and .88 g/L respectively in the CBP broth of CELF pretreated Poplar at 50 g/L, 75 g/L and 100 g/L solids loadings. The residual sugar quantitation after mild acid hydrolysis for the 15 minutes CELF pretreated Poplar at 75 g/L solids loading was compared to the 25 minutes CELF pretreated Poplar at the same solids loading of 75 g/L and the result show comparable total glucose, xylose, and arabinose for both conditions (Figure 4-10 (b)).

Figure 4-11 (a) and (b) depict the results of the co-culture strategy to overcome xylose and oligomeric xylose inhibition to *C. thermocellum* using *T. thermosaccharolyticum*. Changing the 75 g/L loadings high solids consolidated bioprocessing from a monoculture of *C. thermocellum* to co-culture of *C. thermocellum*-*T. thermosaccharolyticum* improved total glucan solubilization by ~16 %, reaching to almost complete glucan solubilization for both the 15 and 25 minutes pretreated CELF Poplar (Figure 4-11 (a)). Cumulative CO_2 and H_2 gas evolution profiles for 15 and 25 minutes CELF pretreated Poplar show almost similar profiles regardless of whether mono (*C. thermocellum*) or co-cultures (*C. thermocellum and T. thermosaccharolyticum*) CBP was done. In addition, cumulative CO_2 and H_2 gas evolution profiles for consolidated bioprocessing with co-cultures show delayed fermentation compared to the mono-culture

CBP for both 15 and 25 minutes CELF pretreated Poplar. The slow co-growth of the co-cultures, however, did not negatively impact the total glucan solubilization and the sugar yields indicating the co-culture to be a promising strategy.

Figure 4-12 reports on the measurement of the residual monomeric and oligomeric sugars after mild acid hydrolysis in *C. thermocellum* mono-culture and *C. thermocellum* and *T. thermosaccharolyticum* co-culture broths. Using the co-cultures of *C. thermocellum* and *T. thermosaccharolyticum* to enable the utilization of both cellulose and xylose, a reduction of 45% in xylose accumulation was observed compared to *C. thermocellum* mono-culture for consolidated bioprocessing of 25 minutes CELF pretreated Poplar at 75 g/L solids loading. These results again confirm the utility of co-culture strategy by using a xylose metabolizing *T. thermosaccharolyticum* to overcome xylose and oligomeric xylose accumulation in the fermentation broth, and in turn minimize its inhibition to *C. thermocellum*, leading to almost complete glucan solubilization at very high solids loadings of low severity CELF pretreated Poplar.

4.5 Conclusions

CELF process optimization for woody lignocellulosic biomass (GW- 9947) and its integration with consolidated bioprocessing using wild type *C. thermocellum* at high solids loadings of 50 g/L, 75 g/L and 100 g/L was investigated for the first time. Combining CELF-CBP with *C. thermocellum* was advantageous as very high solubilization was achieved in 3-4 days even at higher solid loadings. For the lowest severity CELF pretreatment of 5 minutes, residual xylo-oligomers contributed to recalcitrance. Increasing pretreatment time to 25 minutes did not improve solubilization at 75g/L and 100 g/L,

indicating the drop in solubilization at high loading was most likely not due to remaining Poplar recalcitrance. In addition to xylo-oligomers, buildup of cello-oligomers was observed when solids loading was increased from 75 g/L to 100 g/L. The incomplete solubilization and accumulation of oligomeric sugars at high solids loading was hypothesized to be from xylose and xylo-oligomer inhibition to *C. thermocellum* due to its inability to utilize hemicellulose. Co-culture strategy to utilize a xylose metabolizing organism *T. thermosaccharolyticum* with *C. thermocellum* to avoid xylo- and cello-oligomer accumulation and related inhibition resulted into a reduction of xylose accumulation by 45%, improving total glucan solubilization to >97% at high solids loadings of 75 g/L.

4.6 References

Akinosho, H., Yee, K., Close, D., & Ragauskas, A. (2014). The emergence of Clostridium thermocellum as a high utility candidate for consolidated bioprocessing applications. *Frontiers in Chemistry*, *2*(AUG), 66. https://doi.org/10.3389/FCHEM.2014.00066/BIBTEX

Beri, D., Herring, C. D., Blahova, S., Poudel, S., Giannone, R. J., Hettich, R. L., & Lynd, L. R. (2021). Coculture with hemicellulose-fermenting microbes reverses inhibition of corn fiber solubilization by Clostridium thermocellum at elevated solids loadings. *Biotechnology for Biofuels*, *14*(1), 1–13. https://doi.org/10.1186/S13068-020-01867-W/FIGURES/7

Beri, D., York, W. S., Lynd, L. R., Peña, M. J., & Herring, C. D. (2020). Development of a thermophilic coculture for corn fiber conversion to ethanol. *Nature Communications 2020 11:1*, *11*(1), 1–11. https://doi.org/10.1038/s41467-020-15704-z

Binod, P., Gnansounou, E., Sindhu, R., & Pandey, A. (2019). Enzymes for second generation biofuels: Recent developments and future perspectives. *Bioresource Technology Reports*, *5*, 317–325. https://doi.org/10.1016/J.BITEB.2018.06.005

Bryant, N. D., Pu, Y., Tschaplinski, T. J., Tuskan, G. A., Muchero, W., Kalluri, U. C., Yoo, C. G., & Ragauskas, A. J. (2020). Transgenic Poplar Designed for Biofuels. *Trends in Plant Science*, *25*(9), 881–896. https://doi.org/10.1016/J.TPLANTS.2020.03.008

Cai, C. M., Zhang, T., Kumar, R., & Wyman, C. E. (2013). THF co-solvent enhances hydrocarbon fuel precursor yields from lignocellulosic biomass. *Green Chemistry*, *15*(11), 3140–3145. https://doi.org/10.1039/C3GC41214H

Chanoca, A., de Vries, L., & Boerjan, W. (2019). Lignin Engineering in Forest Trees. *Frontiers in Plant Science*, *10*, 912. https://doi.org/10.3389/FPLS.2019.00912/BIBTEX

Chu, Q., Wang, R., Tong, W., Jin, Y., Hu, J., & Song, K. (2020). Improving Enzymatic Saccharification and Ethanol Production from Hardwood by Deacetylation and Steam Pretreatment: Insight into Mitigating Lignin Inhibition. *ACS Sustainable Chemistry & Engineering*, *8*(49), 17967–17978. https://doi.org/10.1021/ACSSUSCHEMENG.0C05583

Dutta, S., Wu, K. C. W., & Saha, B. (2014). Emerging strategies for breaking the 3D amorphous network of lignin. *Catalysis Science & Technology*, *4*(11), 3785–3799. https://doi.org/10.1039/C4CY00701H

Fast Facts on Transportation Greenhouse Gas Emissions | US EPA. (2019). https://www.epa.gov/greenvehicles/fast-facts-transportation-greenhouse-gas-emissions

Hirano, K., Kurosaki, M., Nihei, S., Hasegawa, H., Shinoda, S., Haruki, M., & Hirano, N. (2016). Enzymatic diversity of the Clostridium thermocellum cellulosome is crucial for the degradation of crystalline cellulose and plant biomass. *Scientific Reports 2016 6:1*, *6*(1), 1–9. https://doi.org/10.1038/srep35709

Holwerda, E. K., Worthen, R. S., Kothari, N., Lasky, R. C., Davison, B. H., Fu, C., Wang, Z. Y., DIxon, R. A., Biswal, A. K., Mohnen, D., Nelson, R. S., Baxter, H. L., Mazarei, M., Muchero, W., Tuskan, G. A., Cai, C. M., Gjersing, E. E., Davis, M. F., Himmel, M. E., … Lynd, L. R. (2019a). Multiple levers for overcoming the recalcitrance of lignocellulosic biomass. *Biotechnology for Biofuels*, *12*(1), 1–12. https://doi.org/10.1186/S13068-019-1353-7/FIGURES/5

Holwerda, E. K., Worthen, R. S., Kothari, N., Lasky, R. C., Davison, B. H., Fu, C., Wang, Z. Y., DIxon, R. A., Biswal, A. K., Mohnen, D., Nelson, R. S., Baxter, H. L., Mazarei, M., Muchero, W., Tuskan, G. A., Cai, C. M., Gjersing, E. E., Davis, M. F., Himmel, M. E., … Lynd, L. R. (2019b). Multiple levers for overcoming the recalcitrance of lignocellulosic biomass. *Biotechnology for Biofuels*, *12*(1), 1–12. https://doi.org/10.1186/S13068-019-1353-7/FIGURES/5

Huang, W. D., & Percival Zhang, Y. H. (2011). Analysis of biofuels production from sugar based on three criteria: Thermodynamics, bioenergetics, and product separation. *Energy & Environmental Science*, *4*(3), 784–792. https://doi.org/10.1039/C0EE00069H

Joshi, A., Kanthaliya, B., Meena, S., Khan, F., & Arora, J. (2021a). Process consolidation approaches for cellulosic ethanol production. *Sustainable Biofuels*, 43–72. https://doi.org/10.1016/B978-0-12-820297-5.00013-X

Joshi, A., Kanthaliya, B., Meena, S., Khan, F., & Arora, J. (2021b). Process consolidation approaches for cellulosic ethanol production. *Sustainable Biofuels*, 43–72. https://doi.org/10.1016/B978-0-12-820297-5.00013-X

Kim, S., Zhang, X., Reddy, A. D., Dale, B. E., Thelen, K. D., Jones, C. D., Izaurralde, R. C., Runge, T., & Maravelias, C. (2020). Carbon-Negative Biofuel Production. *Environmental Science and Technology*, *54*(17), 10797–10807. https://doi.org/10.1021/ACS.EST.0C01097/SUPPL_FILE/ES0C01097_SI_001.PDF

Klein-Marcuschamer, D., Oleskowicz-Popiel, P., Simmons, B. A., & Blanch, H. W. (2012). The challenge of enzyme cost in the production of lignocellulosic biofuels. *Biotechnology and Bioengineering*, *109*(4), 1083–1087. https://doi.org/10.1002/BIT.24370

Kothari, N., Holwerda, E. K., Cai, C. M., Kumar, R., & Wyman, C. E. (2018). Biomass augmentation through thermochemical pretreatments greatly enhances digestion of

switchgrass by Clostridium thermocellum. *Biotechnology for Biofuels*, *11*(1), 1–14. https://doi.org/10.1186/S13068-018-1216-7/TABLES/1

Kubis, M. R., Holwerda, E. K., & Lynd, L. R. (2022). Declining carbohydrate solubilization with increasing solids loading during fermentation of cellulosic feedstocks by Clostridium thermocellum: documentation and diagnostic tests. *Biotechnology for Biofuels and Bioproducts 2022 15:1*, *15*(1), 1–16. https://doi.org/10.1186/S13068-022-02110-4

Lau, M. W., Bals, B. D., Chundawat, S. P. S., Jin, M., Gunawan, C., Balan, V., Jones, A. D., & Dale, B. E. (2012). An integrated paradigm for cellulosic biorefineries: utilization of lignocellulosic biomass as self-sufficient feedstocks for fuel , food precursors and saccharolytic enzyme production. *Energy & Environmental Science*, *5*(5), 7100–7110. https://doi.org/10.1039/C2EE03596K

Lee, C. R., Sung, B. H., Lim, K. M., Kim, M. J., Sohn, M. J., Bae, J. H., & Sohn, J. H. (2017). Co-fermentation using Recombinant Saccharomyces cerevisiae Yeast Strains Hyper-secreting Different Cellulases for the Production of Cellulosic Bioethanol. *Scientific Reports 2017 7:1*, *7*(1), 1–14. https://doi.org/10.1038/s41598-017-04815-1

Li, M., Pu, Y., & Ragauskas, A. J. (2016). Current understanding of the correlation of lignin structure with biomass recalcitrance. *Frontiers in Chemistry*, *4*(NOV), 45. https://doi.org/10.3389/FCHEM.2016.00045/BIBTEX

Lin, P. P., Mi, L., Morioka, A. H., Yoshino, K. M., Konishi, S., Xu, S. C., Papanek, B. A., Riley, L. A., Guss, A. M., & Liao, J. C. (2015). Consolidated bioprocessing of cellulose to isobutanol using Clostridium thermocellum. *Metabolic Engineering*, *31*, 44–52. https://doi.org/10.1016/J.YMBEN.2015.07.001

Liu, G., Zhang, J., & Bao, J. (2016). Cost evaluation of cellulase enzyme for industrial-scale cellulosic ethanol production based on rigorous Aspen Plus modeling. *Bioprocess and Biosystems Engineering*, *39*(1), 133–140. https://doi.org/10.1007/S00449-015-1497-1/TABLES/3

Li, X., Weng, J. K., & Chapple, C. (2008). Improvement of biomass through lignin modification. *The Plant Journal*, *54*(4), 569–581. https://doi.org/10.1111/J.1365-313X.2008.03457.X

Oil 2021 – Analysis - IEA. (2021). https://www.iea.org/reports/oil-2021

Qing, Q., Yang, B., & Wyman, C. E. (2010). Xylooligomers are strong inhibitors of cellulose hydrolysis by enzymes. *Bioresource Technology*, *101*(24), 9624–9630. https://doi.org/10.1016/J.BIORTECH.2010.06.137

Sanchez, B. (2020). *Fossil fuels account for the largest share of U.S. energy production and consumption - Today in Energy - U.S. Energy Information Administration (EIA)*. https://www.eia.gov/todayinenergy/detail.php?id=45096

Schmatz, A. A., Salazar-Bryam, A. M., Contiero, J., Sant'Anna, C., & Brienzo, M. (2021). Pseudo-Lignin Content Decreased with Hemicellulose and Lignin Removal, Improving Cellulose Accessibility, and Enzymatic Digestibility. *Bioenergy Research*, *14*(1), 106–121. https://doi.org/10.1007/S12155-020-10187-8/FIGURES/6

Shi, J., Gladden, J. M., Sathitsuksanoh, N., Kambam, P., Sandoval, L., Mitra, D., Zhang, S., George, A., Singer, S. W., Simmons, B. A., & Singh, S. (2013). One-pot ionic liquid pretreatment and saccharification of switchgrass. *Green Chemistry*, *15*(9), 2579–2589. https://doi.org/10.1039/C3GC40545A

Shi, J., Pattathil, S., Parthasarathi, R., Anderson, N. A., Kim, J. I., Venketachalam, S., Hahn, M. G., Chapple, C., Simmons, B. A., & Singh, S. (2016). Impact of engineered lignin composition on biomass recalcitrance and ionic liquid pretreatment efficiency. *Green Chemistry*, *18*(18), 4884–4895. https://doi.org/10.1039/C6GC01193D

Siqueira, J. G. W., Rodrigues, C., Vandenberghe, L. P. de S., Woiciechowski, A. L., & Soccol, C. R. (2020). Current advances in on-site cellulase production and application on lignocellulosic biomass conversion to biofuels: A review. *Biomass and Bioenergy*, *132*, 105419. https://doi.org/10.1016/J.BIOMBIOE.2019.105419

Sun, R. C., Sun, X. F., Wang, S. Q., Zhu, W., & Wang, X. Y. (2002). Ester and ether linkages between hydroxycinnamic acids and lignins from wheat, rice, rye, and barley straws, maize stems, and fast-growing poplar wood. *Industrial Crops and Products*, *15*(3), 179–188. https://doi.org/10.1016/S0926-6690(01)00112-1

Su, T., Zhao, D., Khodadadi, M., & Len, C. (2020). Lignocellulosic biomass for bioethanol: Recent advances, technology trends, and barriers to industrial development. *Current Opinion in Green and Sustainable Chemistry*, *24*, 56–60. https://doi.org/10.1016/J.COGSC.2020.04.005

Thomas, V. A., Donohoe, B. S., Li, M., Pu, Y., Ragauskas, A. J., Kumar, R., Nguyen, T. Y., Cai, C. M., & Wyman, C. E. (2017). Adding tetrahydrofuran to dilute acid pretreatment provides new insights into substrate changes that greatly enhance biomass deconstruction by Clostridium thermocellum and fungal enzymes. *Biotechnology for Biofuels*, *10*(1), 252. https://doi.org/10.1186/S13068-017-0937-3

Torli, M., Geer, L., Kontogeorgis, G. M., & Fosbøl, P. L. (2021). Benchmarking of Separation Methods for Bioethanol (<5 wt %) Recovery. *Industrial and Engineering Chemistry Research*, *60*(16), 5924–5944. https://doi.org/10.1021/ACS.IECR.1C00087/SUPPL_FILE/IE1C00087_SI_001.PDF

Uppugundla, N., da Costa Sousa, L., Chundawat, S. P. S., Yu, X., Simmons, B., Singh, S., Gao, X., Kumar, R., Wyman, C. E., Dale, B. E., & Balan, V. (2014). A comparative study of ethanol production using dilute acid, ionic liquid and AFEX^{TM} pretreated corn stover. *Biotechnology for Biofuels*, *7*(1), 1–14. https://doi.org/10.1186/1754-6834-7-72/FIGURES/5

van Zyl, W. H., Lynd, L. R., den Haan, R., & McBride, J. E. (2007). Consolidated bioprocessing for bioethanol production using Saccharomyces cerevisiae. *Advances in Biochemical Engineering/Biotechnology*, *108*, 205–235. https://doi.org/10.1007/10_2007_061

Xu, F., Sun, J., Konda, N. V. S. N. M., Shi, J., Dutta, T., Scown, C. D., Simmons, B. A., & Singh, S. (2016). Transforming biomass conversion with ionic liquids: process intensification and the development of a high-gravity, one-pot process for the production of cellulosic ethanol. *Energy & Environmental Science*, *9*(3), 1042–1049. https://doi.org/10.1039/C5EE02940F

Yang, B., & Wyman, C. E. (2008). Pretreatment: the key to unlocking low-cost cellulosic ethanol. *Biofuels, Bioproducts and Biorefining*, *2*(1), 26–40. https://doi.org/10.1002/BBB.49

Yu, Q., Zhuang, X., Wang, W., Qi, W., Wang, Q., Tan, X., Kong, X., & Yuan, Z. (2016). Hemicellulose and lignin removal to improve the enzymatic digestibility and ethanol production. *Biomass and Bioenergy*, *94*, 105–109. https://doi.org/10.1016/J.BIOMBIOE.2016.08.005

Zhai, R., Hu, J., & Saddler, J. N. (2018). The inhibition of hemicellulosic sugars on cellulose hydrolysis are highly dependant on the cellulase productive binding, processivity, and substrate surface charges. *Bioresource Technology*, *258*, 79–87. https://doi.org/10.1016/J.BIORTECH.2017.12.006

Zhang, J., Tang, M., & Viikari, L. (2012). Xylans inhibit enzymatic hydrolysis of lignocellulosic materials by cellulases. *Bioresource Technology*, *121*, 8–12. https://doi.org/10.1016/J.BIORTECH.2012.07.010

Zhao, C., Shao, Q., & Chundawat, S. P. S. (2020). Recent advances on ammonia-based pretreatments of lignocellulosic biomass. *Bioresource Technology*, *298*, 122446. https://doi.org/10.1016/J.BIORTECH.2019.122446

4.7 Figures and Tables

Mass of solid components (g component/ 100 g unpretreated Poplar)	Unpretreated Poplar	CELF 150 °C, 5 minutes	CELF 150 °C, 15 minutes	CELF 150 °C, 25 minutes	CELF 150 °C, 30 minutes
Glucan	45.1	43.9	43.2	41.1	39.9
Xylan	19.8	1.66	1.33	0.861	0.0852
Lignin	18.7	2.50	1.76	0.930	0.921

Table 4-1 Composition of CELF Poplar pretreated at 150°C for 5, 15, 25 and 30 minutes.

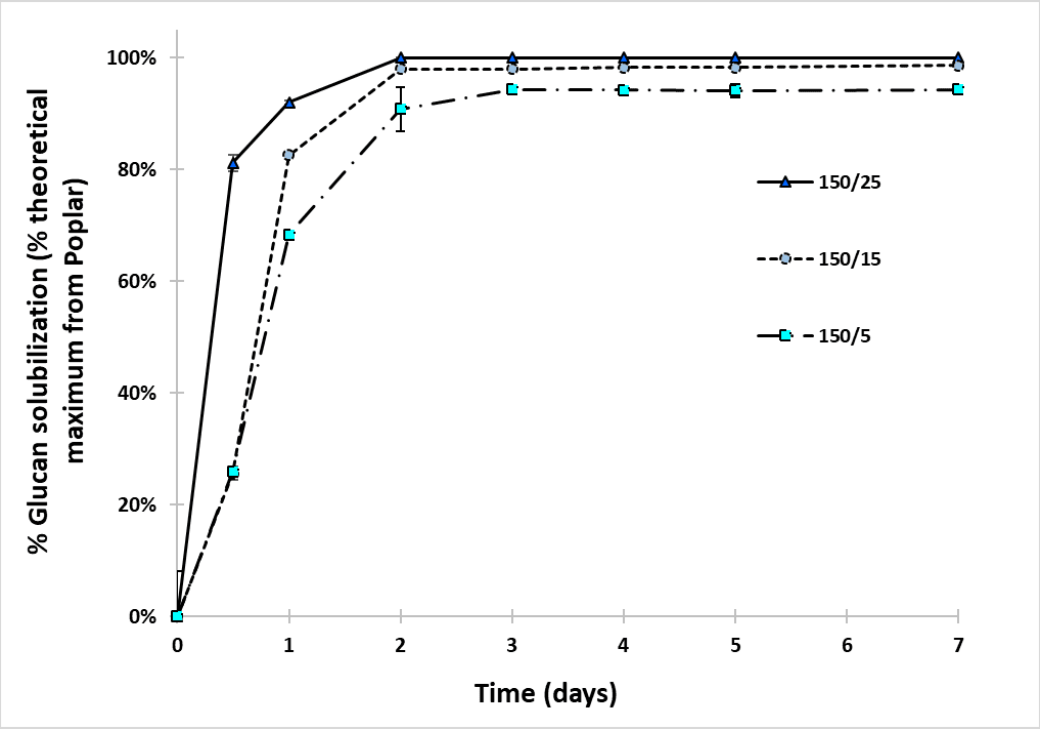

Figure 4-1. Percent glucan solubilization from integrated CELF-CBP using *C. thermocellum* at 5 g/L glucan loadings in shake flasks.

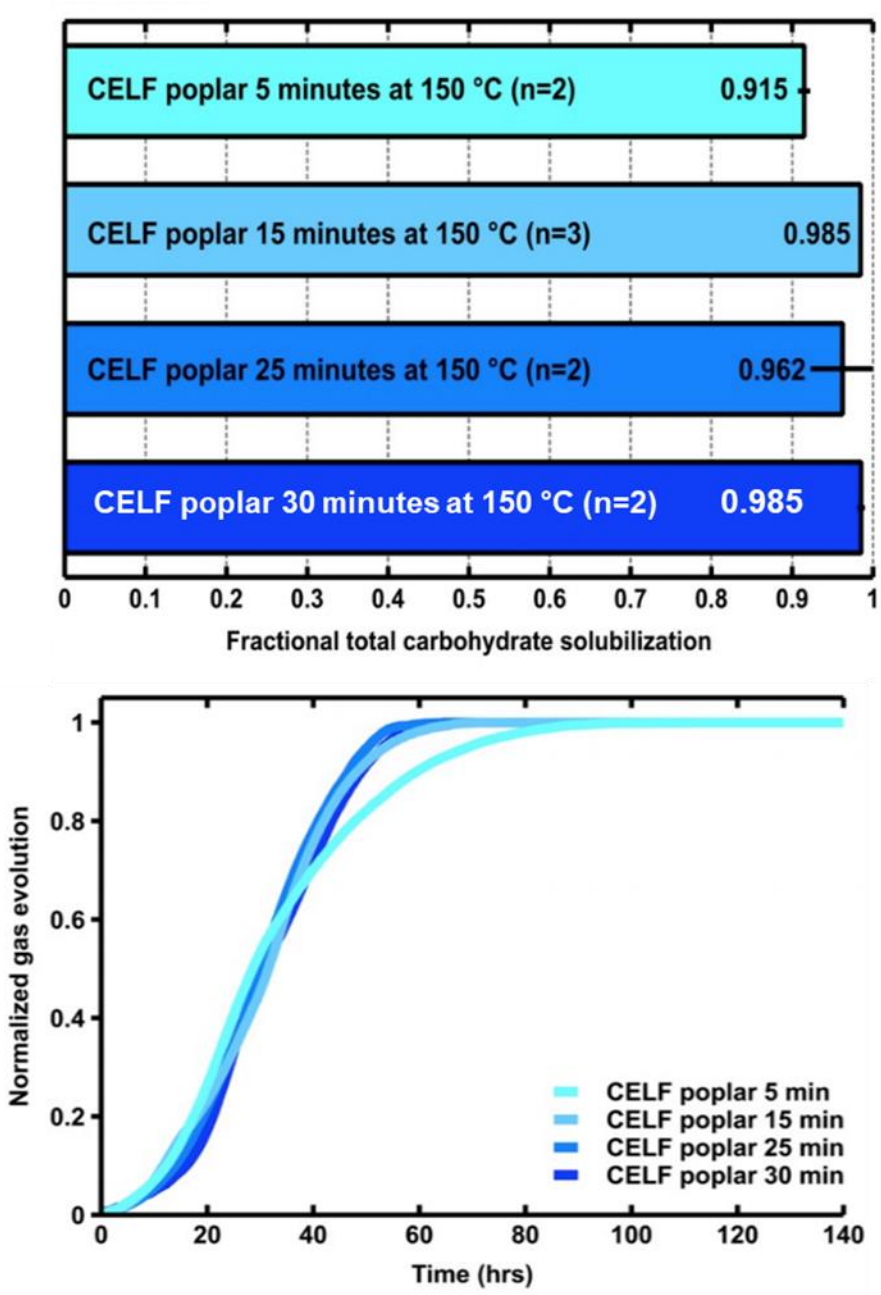

Figure 4-2. Fractional total carbohydrate solubilization of 150°C 5, 15, 25 and 30 minutes CELF pretreated Poplar by *C. thermoceullum* at 50 g/L total solids loadings.

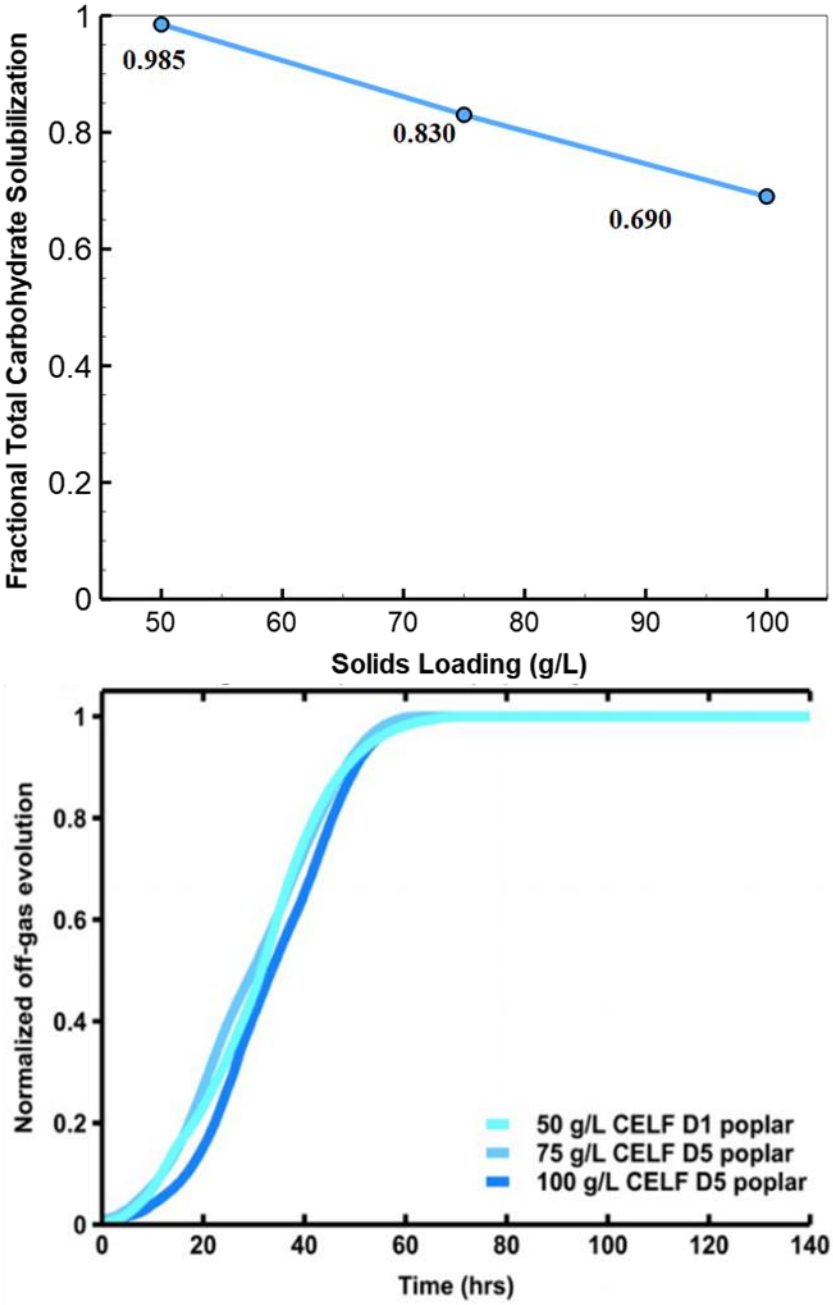

Figure 4-3. Fractional total carbohydrate from integrated CELF-CBP process using *C. thermocellum* as a function of solids loading for 150°C, 15 minutes CELF pretreated Poplar.

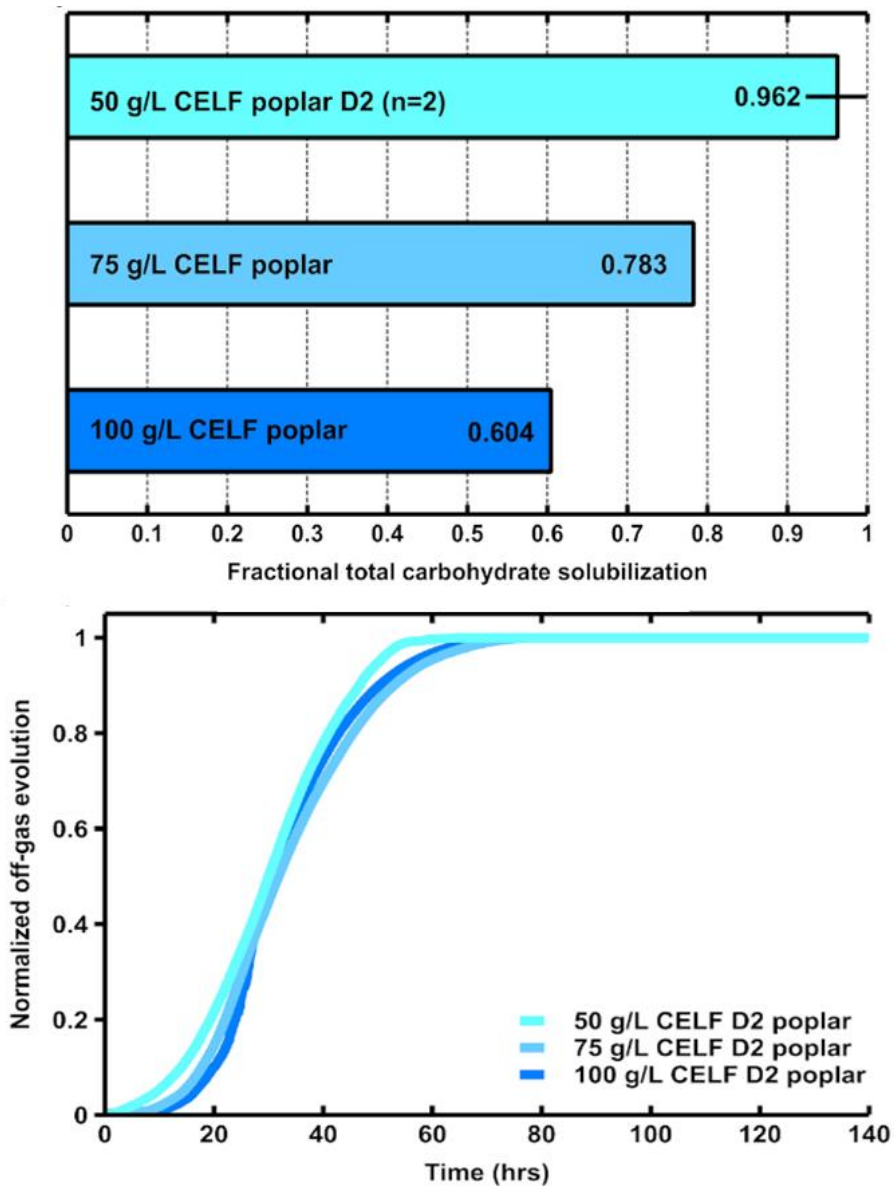

Figure 4-4. CELF pretreated at 150°C for 25 minutes at increasing solids loadings of 50, 75, 100 g/L.

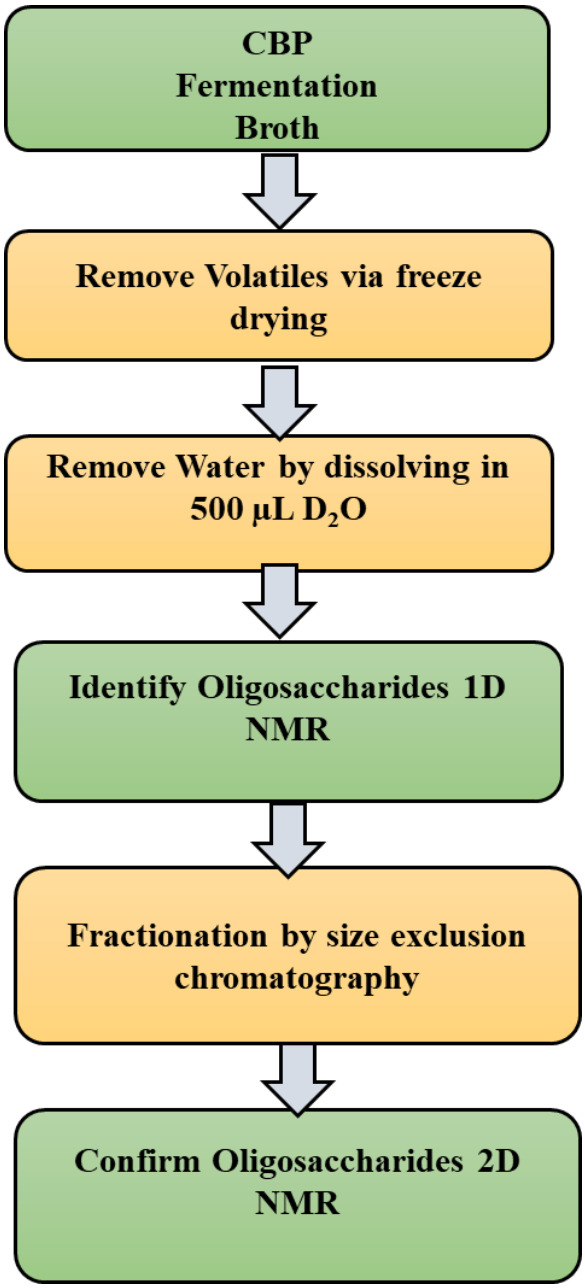

Figure 4-5. CBP-omics Process Flow for identification and quantitation of inhibitors in present in the fermentation broth.

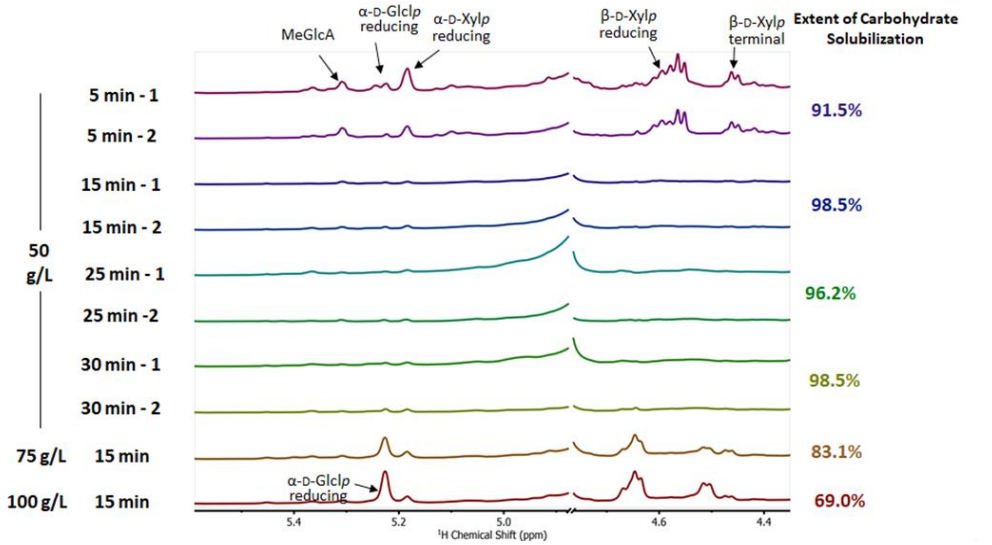
MeGlcA
α-D-Glcp reducing
α-D-Xylp reducing
β-D-Xylp reducing
β-D-Xylp terminal
Extent of Carbohydrate Solubilization
5 min - 1
5 min - 2
15 min - 1
15 min - 2
25 min - 1
25 min -2
30 min - 1
30 min - 2
50 g/L
75 g/L 15 min
100 g/L 15 min
91.5%
98.5%
96.2%
98.5%
83.1%
69.0%
5.4
5.2
5.0
4.6
4.4
¹H Chemical Shift (ppm)

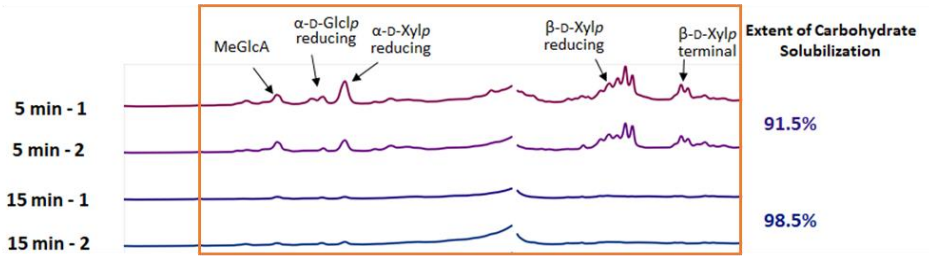
MeGlcA
α-D-Glcp reducing
α-D-Xylp reducing
β-D-Xylp reducing
β-D-Xylp terminal
Extent of Carbohydrate Solubilization
5 min - 1
5 min - 2
15 min - 1
15 min - 2
91.5%
98.5%

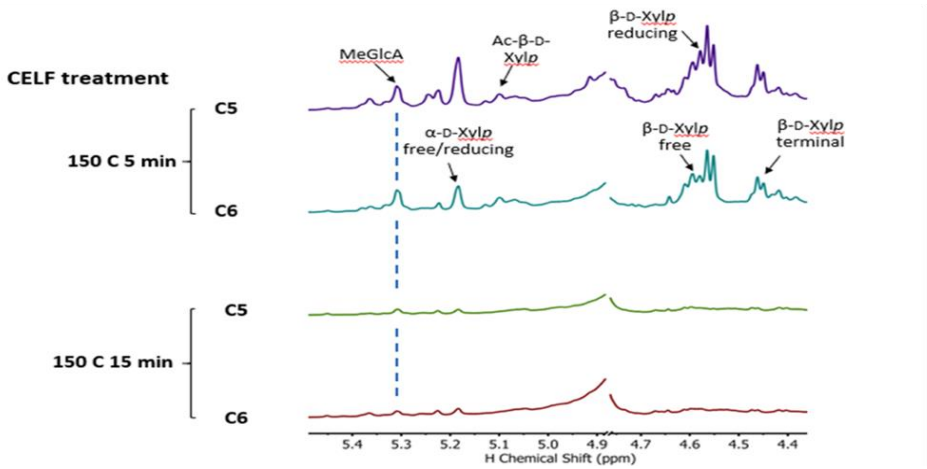
CELF treatment
MeGlcA
Ac-β-D-Xylp
β-D-Xylp reducing
α-D-Xylp free/reducing
β-D-Xylp free
β-D-Xylp terminal
C5
C6
150 C 5 min
150 C 15 min
5.4
5.3
5.2
5.1
5.0
4.9
4.7
4.6
4.5
4.4
H Chemical Shift (ppm)

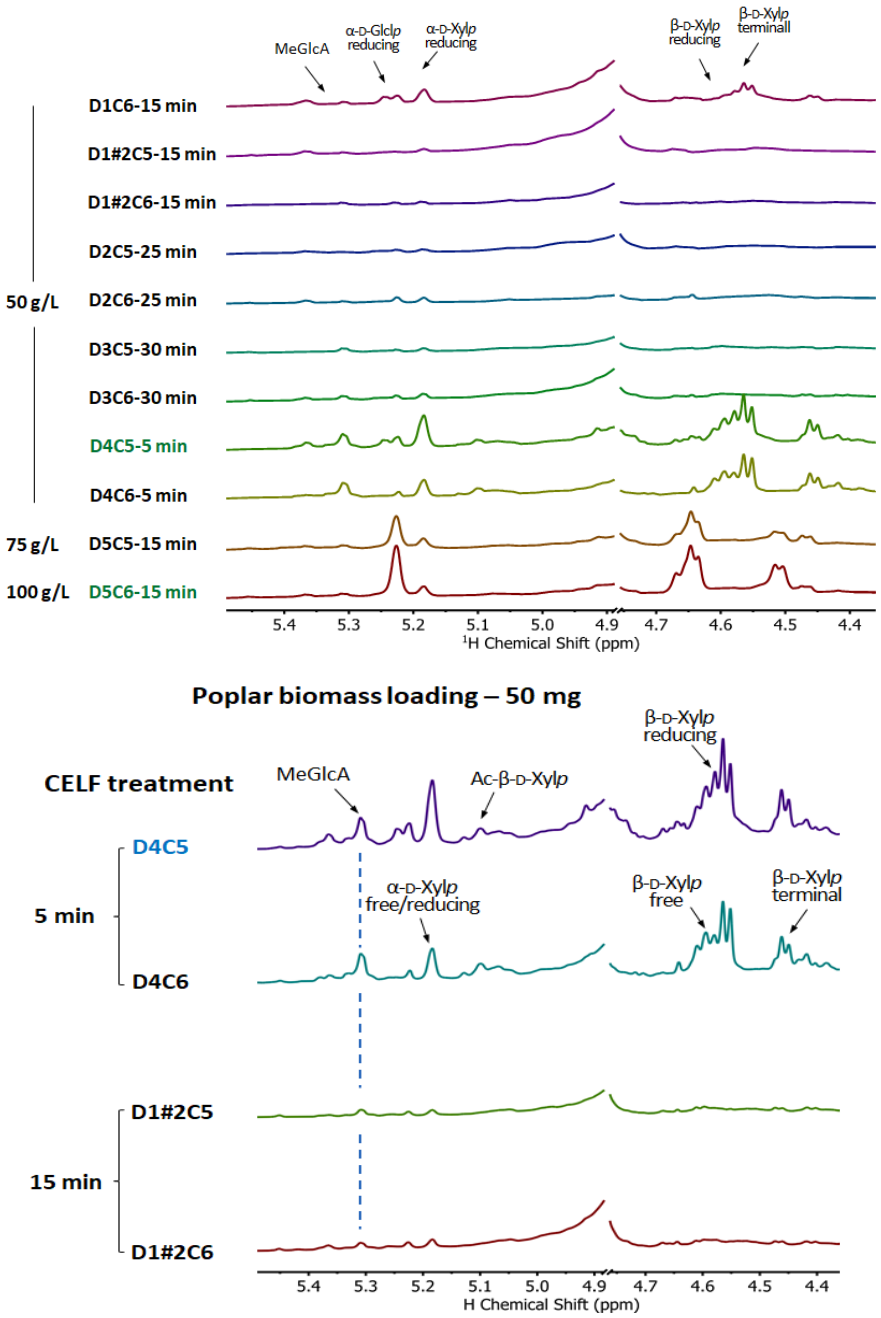

Figure 4-6. Comparison of duplicate runs of the oligosaccharides that accumulated in the fermentation broth of biomass at different CLEF pretreatment times and at different solid loadings. At 50 g/L more oligosaccharides accumulated in the samples with 5 min pretreatment than the one with 15 min.

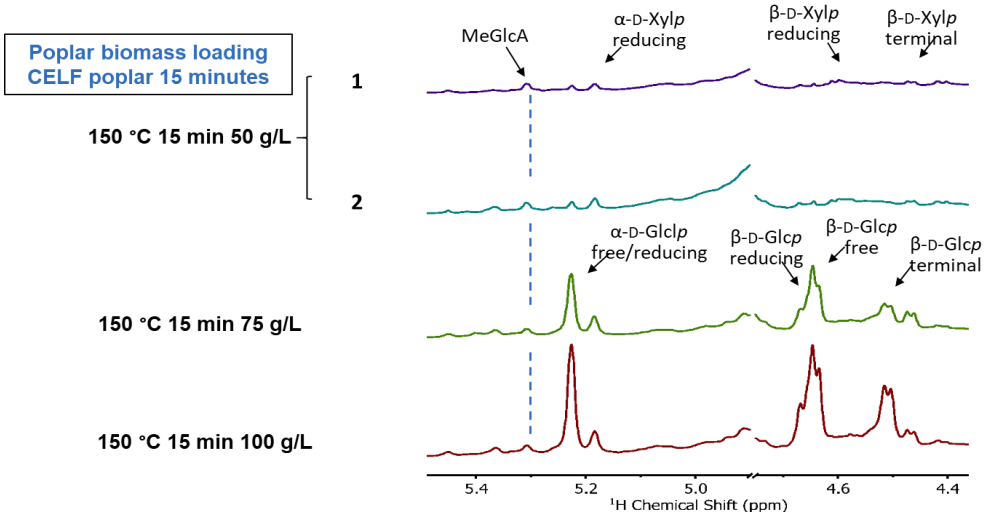

Figure 4-7. Comparison of amount xylo- and cello- oligomers that accumulated in the CBP broth as a function of CBP loading.

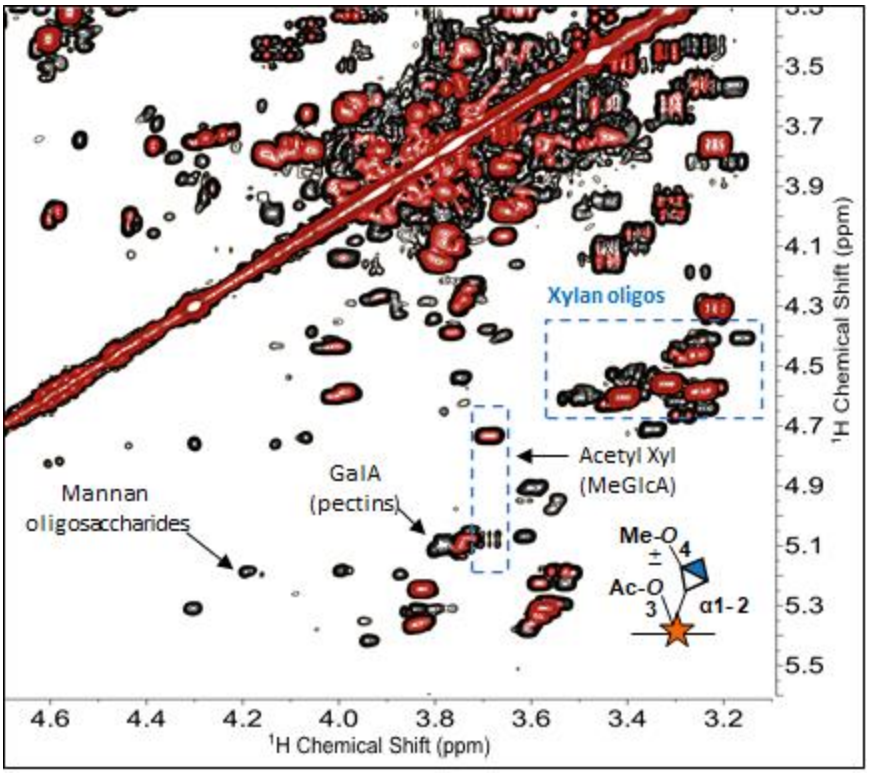

Figure 4-8. Partial 2D spectrum of the fermentation broth of 50 g/L loading at 5 min CELF pretreatment. Acetylated xylan oligosaccharides and pectin are present in the broth but were not detected when the duration of the pretreatment increased.

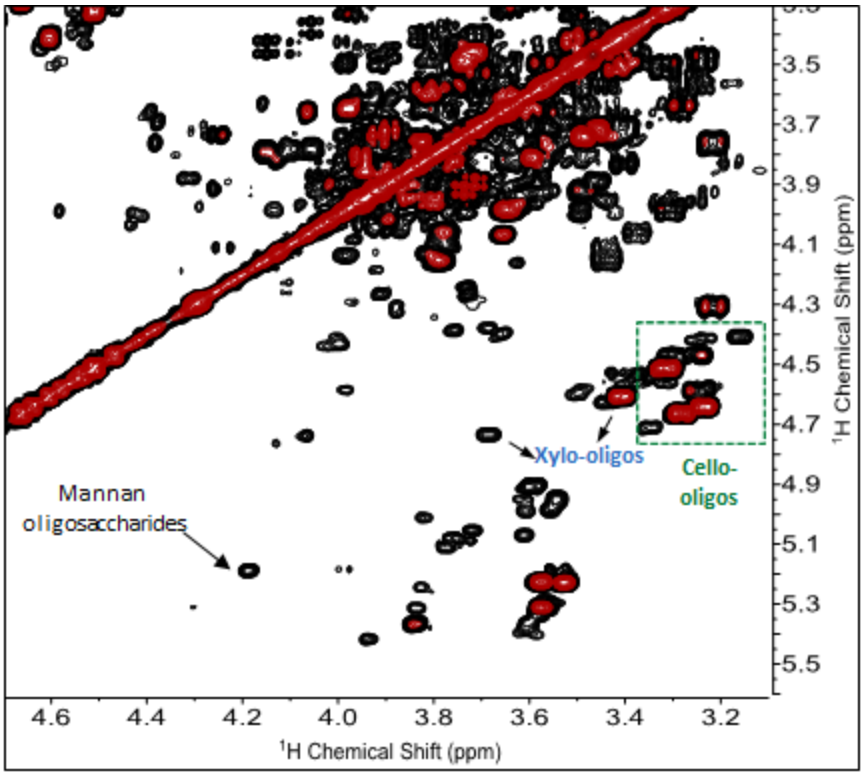

Figure 4-9. 100 g/L solids loading @ 15 minutes Different types of oligosaccharides accumulated in the broths depending on CELF treatment times and biomass loadings. At high loadings of 100 g/L, in addition to xylo-oligomers, cello-oligomers accumulate in the broth Comparing this with the 2D NMR for CELF 15 at 100 g/L we see a much cleaner spectra but qualitatively see the buildup of xylo-and cello-oligomers.

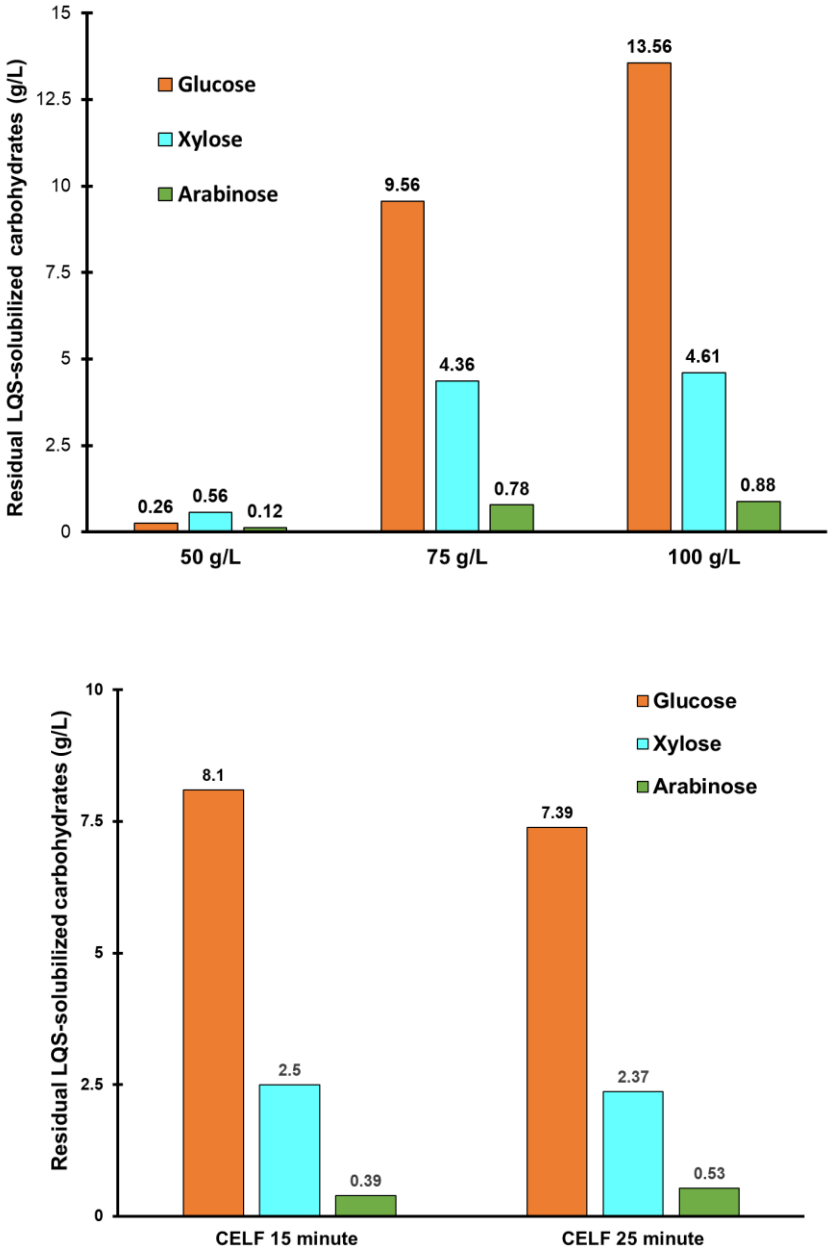

Figure 4-10. Quantitation of remaining carbohydrates in the fermentation broth of 75 g/L solids loading CBP using CELF pretreated Poplar (top: 150°C/15, bottom: 150°C/25 minutes).

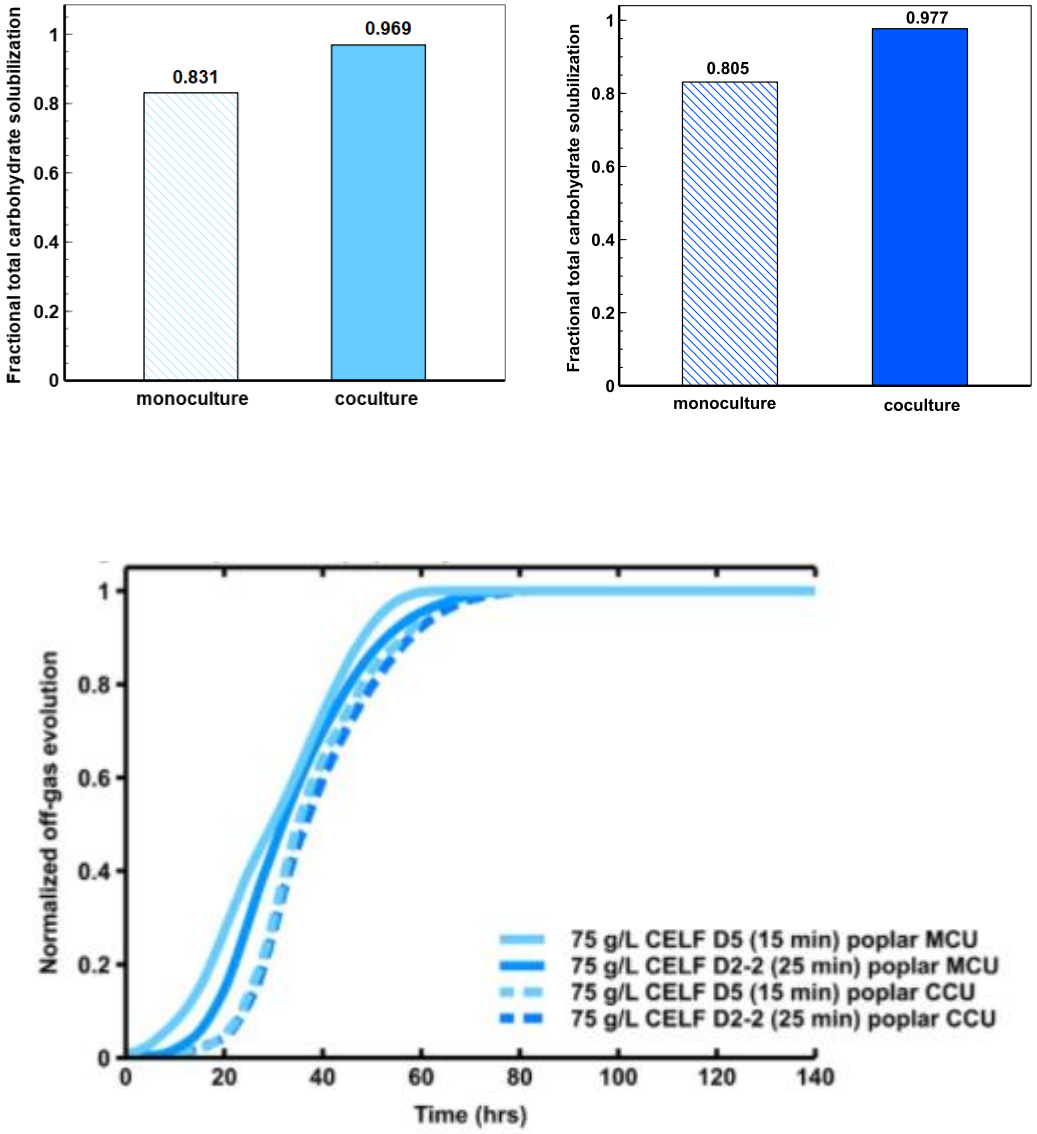

Figure 4-11. Mono and co-culture comparison for CELF 15 and 25 minutes pretreated Poplar.

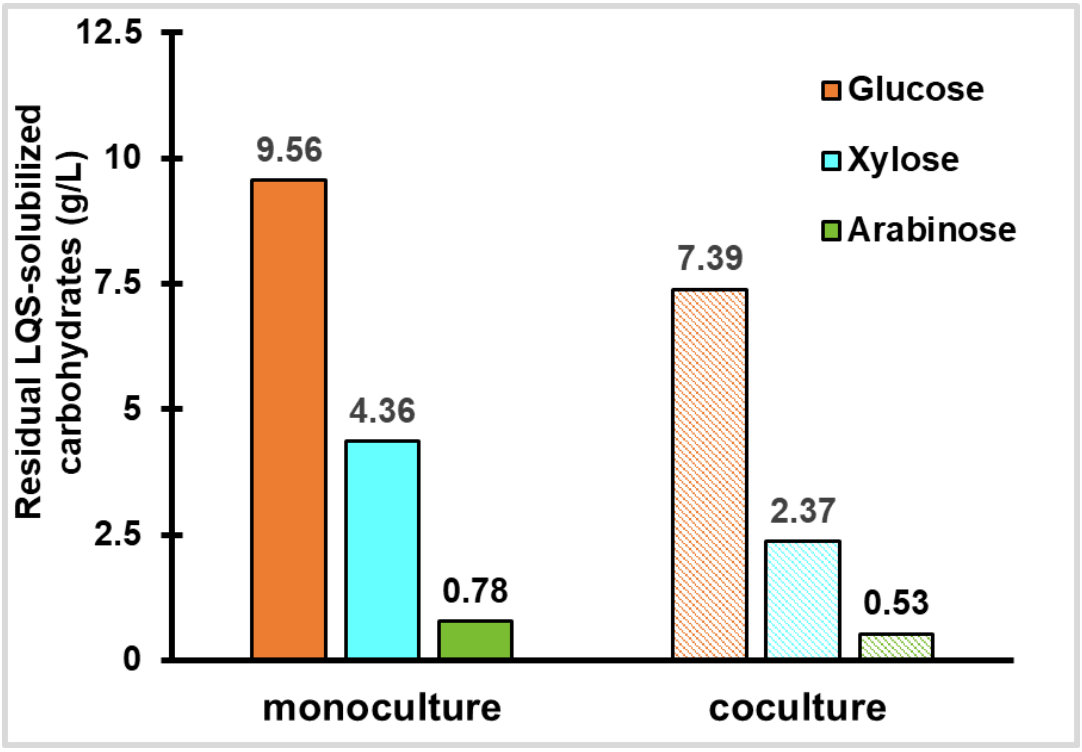

Figure 4-12. Comparison of broth of mono and co-culture residual sugars for 25 minutes at 75 grams/L loading.

Supplementary Figure

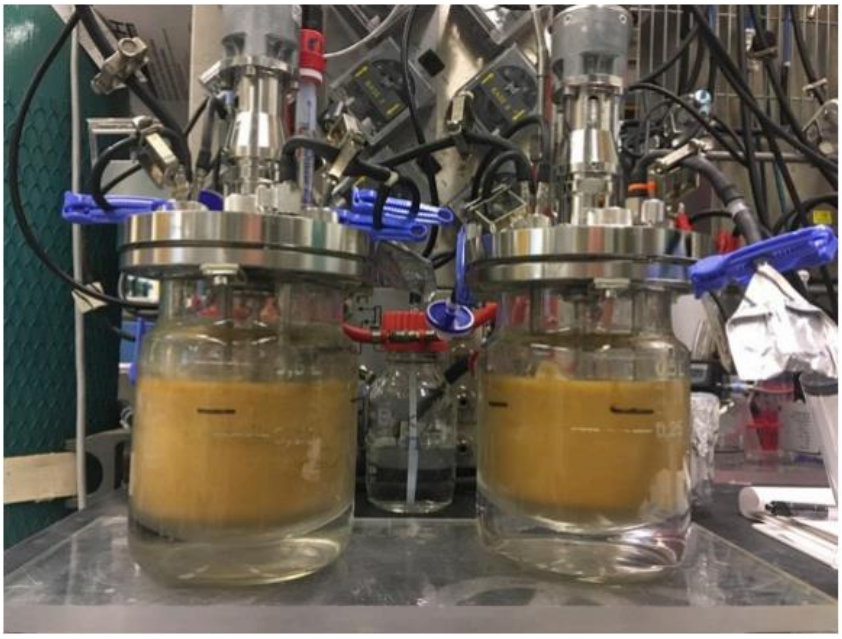

Chapter 5: Renewable Esters from CELF-Pretreated Poplar Wood using Engineered *C. thermocellum*

*This work was done in collaboration with Dr. Cong Trihn and Dr. Hyeongmin Seo at the University of Tennessee Knoxville. Strain engineering and CBP fermentation was carried out by Dr. Hyeongmin Seo. The contents of this chapter will be used for publication in a scientific journal in part or in full.

5.1 Abstract

Esters serve numerous high volume and high value end use industries. Global demand of non-petroleum bioesters is on the rise. Microbial synthesis of renewable esters from lignocellulosic biomass is greener and more sustainable. This work investigated the production of medium chain esters directly from a woody lignocellulosic biomass, Poplar, using an engineered *Clostridium thermocellum* (*C. thermocellum*) in a consolidated bioprocessing. Ethanol, acetic, lactic and ester intermediates, as well as ethyl- and isobutyl-isobutyrate and acetates were biosynthesized from Co-solvent Enhanced Lignocellulosic Fractionation (CELF) pretreated Poplar with varying amounts of glucan, xylan and lignin content. Cell density for fermentation was improved by *C. thermocellum* strain adaptation on the CELF pretreated Poplar to improve the ester biosynthesis capability of the engineered *C. thermocellum* from Poplar. The percent relative ester production increased from 70% to 100% as the CELF process severities were increased and the xylan and lignin content were minimized. This is the first reported study on ester biosynthesis from a lignocellulosic biomass. Future detailed multi-omics studies can provide insight on the correlation of type and the amount of components in lignocellulosic biomass, with changes in protein and gene expression, metabolite fate and the impact on esters titer, rate and yield.

5.2 Introduction

Esters have wide applications in the food, chemical, pharmaceuticals, personal care, packaging and textiles end use industries. The global market size of esters is projected to increase to ~US $147 Billion by 2029 (Esters Market | Global Sales Analysis Report - 2029, n.d.). Esters are produced mostly from petroleum or extracted from plants. Plants usually have small amounts of esters, and solvent extractions are not cost effective or green (Murador et al., 2019; SÁ et al., 2017). There is also a growing demand for greener products and a shift towards green manufacturing (Dornfeld, 2014; Kostadinova, n.d.; Peneda de Oliveira & Sousa, 1 C.E.). Microbial production of esters is advantageous since the process could be scaled up to meet the high-volume demand. In addition, since esters are more volatile at higher temperatures, the cost of product separation could also be minimized if ester biomanufacturing utilized thermophilic microorganisms. In addition to its wide applications in numerous sectors, due to their lower toxicity, short chain esters could also serve as platform chemicals for the synthesis of other high value or high-volume chemicals that cannot be bio-manufactured.

Clostridium thermocellum is an anaerobic thermophilic ethanol producer utilized in consolidated bioprocessing due to its ability to deconstruct and ferment the cellulosic substrates without the need of exogenous commercial cellulolytic enzymes (Akinosho et al., 2014; Cornet et al., 1983; Joliff et al., 1986; Lamed & Bayer, 1988; Ng et al., 1977). The wild-type *C. thermocellum* strain mainly utilizes the resulting glucose from cellulose solubilization towards the production of ethanol, acetic, lactic acid at solids loadings <10-

20 g/L. However, a recent study reported that when the wild-type *C. thermocellum* strain is grown on solids loadings of 100 g/L Avicel (a model cellulose substrate), the overflow metabolism increases the amount of other pyruvate conversion pathways towards isobutanol and butanediol (Holwerda 2014, Thompson 2017). Seo et al. and Lee et al. also demonstrated that the deletion of key esterase genes could enable the biosynthesis of esters in *C. thermocellum* (Lee & Trinh, 2020; Seo et al., 2019).

In chapter 2 of this thesis, results from the optimization of CELF and *C. thermocellum* consolidated bioprocessing pairing are presented. The CELF-CBP pairing led to almost complete glucan solubilization from a woody biomass Poplar at very low process severities. The CELF-CBP synergy to produce cellulosic substrate from lignocellulosic biomass using CELF, and almost complete glucan solubilization using *C. thermocellum* could be leveraged to produce renewable esters. Although, we demonstrated effective deconstruction of glucan and total carbohydrate solubilization of CELF pretreated poplar using *C. thermocellum*, metabolite production was not explored. The intermediates of the *C. thermocellum* metabolites are medium chain esters that also have several advantages towards advanced biofuels and platform chemicals. In this study, the potential of renewable ester biomanufacturing directly from CELF pretreated Poplar using an engineered *C. thermocellum* is explored.

5.3 Experimental Section

5.3.1 Materials

CBI reference Poplar variant GW-9947 was generously provided by the Center for BioEnergy Innovation (CBI) from Dr. Muchero Wellington's lab. Poplar was knife milled to a uniform particle size of 1 mm using a Wiley Mill (Model 4, Arthur H. Thomas Company, Philadelphia PA). Composition of unpretreated and CELF pretreated Poplar was determined following the NREL Laboratory Analytical Procedure (Version 08-03-2012). The wild type *Clostridium thermocellum* strain DSM 1313 was engineered at the University of Tennessee Knoxville toward the production of Esters.

5.3.2 CELF pretreatment

For pretreatment, the CBI Poplar barrel was mixed thoroughly and stored in 2 gallon Ziplock bags in between use. Each allocated Poplar bag was then thawed, cut to smaller sizes using gardening scissors and milled by a Thomas Wiley knife mill with and passed through a 1 mm internal sieve.

5.3.2.1 CELF Pretreatments in the Parr Reactor

Pretreatments were performed in a 1 L Hastelloy Parr® autoclave reactor (236HC Series, Parr Instruments Co., Moline, IL) equipped with a double stacked pitch blade impeller rotated at 200 rpm. The reactions were prepared by first adding the milled Poplar at 7.5 wt % solid loadings. A mixture of DI water and 0.5 wt% (based on liquid mass) 72 wt % sulfuric acid (Ricca Chemical Company, Arlington, TX). Tetrahydrofuran (>99% purity, Fisher Scientific, Pittsburgh, PA) was added in a 1:1 mass ratio with water in the

fume hood. The reactions were left to soak overnight at 4 °C. Temperatures for CELF reactions were 140°C, 150°C and 160°C at times of 35, 25, and 15 minutes identified by optimization reactions for each time. All reactions were maintained at reaction temperature (± 0.5°C) by convective heating with a 4 kW fluidized sand bath (Model SBL-2D, Techne, Princeton, NJ). The reaction temperature was directly measured by using an in-line K-type thermocouple (Omega Engineering Inc., Stamford, Connecticut). When the reaction was complete, the Parr reactor was submerged into a room temperature water bath until the internal temperature reached 30-40°C. The reaction solids were separated from the liquid by vacuum filtration at room temperature through glass fiber filter paper (Fisher Scientific, Pittsburgh, PA) and washed with 4 liters of deionized room temperature water until the filtrate pH was measured to be neutral. The solids were carefully transferred to a Ziplock bag and weighed with and without the wet filter. The moisture content of the solids was determined by a halogen moisture analyzer (Model HB43, Mettler Toledo, Columbus, OH).

5.3.2.2 CELF Pretreatments in the Steam Jacketed Reactor

CELF pretreatments were performed in a 1 gallon hastelloy steam jacketed reactor. Each reaction was prepared at a total loading of 2800 grams. Poplar was milled to 1 mm as described above. Poplar was added at a solid loading of 7.5 wt% to an aqueous tetrahydrofuran solution (1:1 w/w) containing 0.5 wt% sulfuric acid (Ricca Chemical Company, Arlington, TX). The solution was stored at 4°C overnight prior to pretreatment to allow the poplar biomass to soak and minimize solvent evaporation. Reactions were performed at 150, 160 and 170°C for a target time of 15 minutes. After the desired reaction

time of 15 minutes, the contents of the reactor were released into a collection tank. The 1 gallon collection tank contained 19 mLs of ammonium hydroxide. When the pretreated slurry is introduced to the tank with the ammonium hydroxide the pH of the slurry increases to roughly 3 when measured via pH indicator strips. The collection tank is cooled for 5 minutes under running water. The reaction slurry was then vacuum filtered at room temperature to separate the CELF solids from the liquids. The solids were then further washed with deionized water. The resulting solids were analyzed for compositional differences and were subjected to fermentation utilizing the engineered *C. thermocellum* strain.

5.3.3 Compositional Analysis

Compositional analysis of the Poplar before and after CELF pretreatment was done following an established Laboratory Analytical Procedures (LAPs) (version 8-03-2012) from the National Renewable Energy Laboratory (NREL, Golden, CO). After the two-step acid hydrolysis, the resulting solids and liquid were separated using filtering crucibles. The liquid portion was sampled and analyzed against calibration standards and using HPLC Waters Alliance system e2695 (Waters Co., Milford, MA) equipped with an HPX-87H column (Bio-Rad Aminex®, Bio-Rad Laboratories, Hercules, CA) and a Waters Refractive Index Detector 2414 (Waters Co., Milford, MA). The mobile phase run was a 5 mM sulfuric acid set at a flow rate of 0.6 mL/min. Empower® 3 software package (Empower Software Solutions, Newport Beach, CA) was utilized to collect, view, and integrate the resulting chromatographs. The glucan and xylan content were calculated and adjusted against internal sugar standards. To determine the amount of acid insoluble or Klason-

lignin, the solid residues after the filtration process were dried and weighed. Finally, ash and other insoluble matter were further quantified by utilizing a muffle furnace ramped to 575°C to convert the leftover material in the crucibles into ash.

5.3.4 Engineering *C. thermocellum* whole-cell biocatalysts for C4-derived alcohols and esters

Engineering efforts to enable ester production from *C. thermocellum* DSM 1313 was carried out by our collaborators (Seo et al., 2021). The first strain, HSCT2108 was tested on both CELF Poplar generated in the Parr and Steam Jacketed reactors. The engineering efforts on HSCT2108 is detailed by Seo et al. and has two esterase deletions and a CATec3 Y20F expression for ester production. Further engineering efforts were done on this previous strain to delete a ldhA (lactate dehydrogenase) and expresses a gene specific to ester production which will be published soon.

5.4 Results and Discussion

In chapter 3, results from the investigation of CELF and *C. thermocellum* consolidated bioprocessing pairing is presented. CELF-CBP pairing led to almost complete glucan solubilization from a woody biomass Poplar at very low process severity. The CELF-CBP synergy was also demonstrated to be critical in scaling up the *C. thermocellum* CBP fermentation at high solids loadings with relatively higher glucan solubilization than other methods reported for a woody biomass (chapter 5). Recently, Holwerda et al. reported overflow metabolism of wild type *C. thermocellum* at high cellulose loadings and high amount of isobutanol production (Holwerda et al., 2014). Furthermore, Seo et al. have successfully engineered chloramphenicol acetyltransferase from *Staphylococcus aureus* (CAT_{Sa}) to overcome thermos-stability issue of alcohol acetyltransferases for microbial

ester biosynthesis that limited its utility only to mesophilic microbes(Seo et al., 2019). The engineered CATsa were heterologously expressed in *C. thermocellum* and production of isobutyl acetate was demonstrated with model cellulose substrate (Avicel). In this study, ester biosynthesis from an engineered *C. thermocellum* grown on CELF pretreated lignocellulosic biomass is investigated.

Ester production from consolidated bioprocessing was compared for the engineered *C. thermocellum* strain grown on two CELF pretreated poplar substrates (Supporting Figure S2) with slightly different compositions of glucan, xylan and lignin to understand the influence of chemical composition of the pretreated Poplar and how C. thermocellum responds to CELF treated biomass in comparison to Avicel. CELF1 sample was processed in a 1-L Hastelloy parr reactor at 150°C for 25 minutes (reaction severity of 2.87) while CELF2 was processed in a steam-jacketed reactor for 160°C for 15 minutes (reaction severity of 2.94). Both CELF1 and CELF2 substrates showed the synthesis of isobutyl acetate and isobutyl isobutyrate from the engineered *C. thermocellum* strain and the data is reported in Figure 6-1. The amount of esters produced were 32 mg/L (CELF1) for the CELF Poplar processed in the parr reactor compared to the 57 mg/L (CELF2) for the CELF2 Poplar processed in a steam jacketed reactor. The ester titers from Poplar CELF substrates for both, parr reactor and steam jacketed reactors, were lower than reported for the engineered *C. thermocellum* strain grown on pure commercial cellulose substrate (Supporting Figure S3). A detail comparison of the amounts of isobutyl isobutyrate, isobutyl acetate, ethyl isobutyrate and ethyl acetate esters biosynthesized using engineered *C. thermocellum* from Poplar CELF processed in the parr reactor and steam jacketed

reactors are presented in Figure 6-2. From these results, it is clear that except for ethyl acetate, all three esters- isobutyl acetate, isobutyl isobutyrate, and ethyl isobutyrate- titers were consistently higher for the Poplar CELF processed in the steam jacketed reactor.

To understand the differences in the amounts of ester biosynthesis and the factors affecting the *C. thermocellum* metabolism, compositional analysis of the Poplar CELF processed in the parr and steam jacketed reactors were conducted. The relative compositions of glucan, xylan and lignin for the CELF processed Poplar substrates are presented in Figure 6-3. Both of the CELF processed Poplar substrates are rich in glucan (>80%). The Poplar substrate from parr reactor consists of 4% more glucan, 4% more xylan and 8% less lignin than the Poplar processed in the steam jacketed reactor. In general, due to 8% lower lignin, the composition of the CELF processed Poplar from the parr reactor seem more similar to pure cellulose than the Poplar substrate from the steam jacketed reactor and should have resulted into higher amounts of ester. Correlating the xylan and lignin contents of these two samples to the total ester production, indicate higher amount of xylan to be more detrimental to *C. thermocellum* than the higher amount of lignin. Negative correlation of xylan content and wild type *C. thermocellum* consolidated bioprocessing of CELF processed Poplar was also evident for the CBP at high solids loadings (chapter 5). In addition, there has been reports on the impact of xylose and xylo-oligomers on *C. thermocellum* fermentation of glucose (Beri et al., 2020; Jin et al., 2012; Verbeke et al., 2017). Interestingly, comparison of major metabolites produced by engineered *C. thermocellum* strain grown on CELF pretreated Poplar show that the poplar processed in steam jacketed reactor resulted into lower percent xylan, preformed more

closely to the pure Avicel in terms of metabolite (Figure 6-4). Both of the CELF poplar samples show less lactate titer than Avicel, and all the major metabolites titers were consistently higher for CELF poplar processed in the steam jacketed reactor.

In order to further improve ester titers and to tease out the impact of lignin amount, further engineering was done and three different CELF processed Poplar samples were generated by changing the process severities (Supporting Figure S1). The compositional details of the three substrates resulting from CELF pretreatment of Poplar for 15 minutes at 150, 160 and 170°C are presented in Figure 6-5. All three CELF processed Poplar have >80% of glucan. The xylan content is less (by 1%) in Poplar samples at processing temperatures of >160°C. The measured lignin content is 16%, 14% and 12% for the 150°C, 160°C and 170°C respectively. Next, cell growth was measured on these three CELF processed Poplar substrates at 19 g/L glucan loadings via a pellet protein Bradford assay. The result shows a lag phase of 2 days when compared against growth of engineered *C. thermocellum* on Avicel (Figure 6-6). The cell mass increased as the CELF severity was increased by increasing the CELF processing temperature. The 170°C CELF process resulted into Poplar substrates that support cell growth similar to that of pure cellulose, Avicel (Table 6-1). To further trigger the overflow metabolism properties, more active cells were needed as demonstrated previously to increase ester titers (Seo et al., 2019). Therefore, a one passage strain adaptation of the *engineered C. thermocellum* on CELF pretreated Poplar was carried out. The adaptation improved the cell growth and protein pellet of *C. thermocellum* as shown in Figure 5-7.

The ethanol, acetic, lactic and ester intermediates were measured. We observed that as the reaction severity was increased, the ethanol, acetate, and lactate titers remained similar with slight differences. In particular, 0.4 g/L more acetate was produced for the CELF Poplar pretreated at 160°C when compared to the CELF pretreated Poplar at 150 °C which then dropped by ~0.7g/L when the processing temperature was raised by 10°C to 170°C. The percent relative ester production also increased by 30% for the 160°C CELF pretreated Poplar compared to the 150°C Pretreated CELF poplar and by 50% when the ester production for the 160°C CELF pretreated Poplar was compared with the 170°C CELF pretreated CELF poplar. Total increase of 100% was observed when the relative ester production for the highest severity (3.24) pretreated CELF Poplar in the steam jacketed reactor was compared against the Poplar CELF pretreated at 150°C in the parr reactor (reaction severity 2.87). These results demonstrate the tunability of the CELF process and impact of substrate compositional differences on the *C. thermocellum* cell physiology, metabolite production and the biosynthesis of esters via consolidated processing using engineered *C. thermocellum.*

5.5 Conclusions

Current production of esters requires energy intensive esterification processes. In this work, we demonstrated biosynthesis of isobutyl isobutyrate, isobutyl acetate, ethyl isobutyrate and ethyl acetate esters using an engineered *C. thermocellum* capable of consolidating glucan solubilization, in-situ fermentation and esterification of fermented alcohols and acids from glucan rich CELF pretreated Poplar. This study shows that composition of lignocellulosic components is an important factor that dictates metabolism and productivity of *C. thermocellum* for ester biosynthesis. Lignin removal was correlated

with higher cell biomass and higher esters production. However, xylan content was found to be more problematic than lignin content. Iterative design, build, test, optimize cycle to further explore the metabolic and proteomic changes to *C. thermocellum* on a variety of pretreated lignocellulosic substrates will be necessary to realize the promise of *C. thermocellum* as a robust biocatalyst for the large scale production of bioesters from a variety of lignocellulosic biomass.

5.6 References

Akinosho, H., Yee, K., Close, D., & Ragauskas, A. (2014). The emergence of Clostridium thermocellum as a high utility candidate for consolidated bioprocessing applications. *Frontiers in Chemistry*, *2*(AUG), 66. https://doi.org/10.3389/FCHEM.2014.00066/BIBTEX

Beri, D., York, W. S., Lynd, L. R., Peña, M. J., & Herring, C. D. (2020). Development of a thermophilic coculture for corn fiber conversion to ethanol. *Nature Communications 2020 11:1*, *11*(1), 1–11. https://doi.org/10.1038/s41467-020-15704-z

Cornet, P., Millet, J., Beguin, P., & Aubert, J. P. (1983). Characterization of Two Cel (Cellulose Degradation) Genes of Clostridium Thermocellum Coding for Endoglucanases. *Bio/Technology 1983 1:7*, *1*(7), 589–594. https://doi.org/10.1038/nbt0983-589

Dornfeld, D. A. (2014). Moving towards green and sustainable manufacturing. *International Journal of Precision Engineering and Manufacturing-Green Technology 2014 1:1*, *1*(1), 63–66. https://doi.org/10.1007/S40684-014-0010-7

Esters Market | Global Sales Analysis Report - 2029. (n.d.). https://www.futuremarketinsights.com/reports/esters-market

Holwerda, E. K., Thorne, P. G., Olson, D. G., Amador-Noguez, D., Engle, N. L., Tschaplinski, T. J., van Dijken, J. P., & Lynd, L. R. (2014). The exometabolome of Clostridium thermocellum reveals overflow metabolism at high cellulose loading. *Biotechnology for Biofuels*, *7*(1), 1–11. https://doi.org/10.1186/S13068-014-0155-1/FIGURES/4

Jin, M., Gunawan, C., Balan, V., & Dale, B. E. (2012). Consolidated bioprocessing (CBP) of AFEX™-pretreated corn stover for ethanol production using Clostridium phytofermentans at a high solids loading. *Biotechnology and Bioengineering*, *109*(8), 1929–1936. https://doi.org/10.1002/BIT.24458

Joliff, G., Béguin, P., Juy, M., Millet, J., Ryter, A., Poljak, R., & Aubert, J. P. (1986). Isolation, Crystallization and Properties of a New Cellulase of Clostridium thermocellum Overproduced in Escherichia coli. *Bio/Technology 1986 4:10*, *4*(10), 896–900. https://doi.org/10.1038/nbt1086-896

Kostadinova, E. (n.d.). *Sustainable Consumer Behavior: Literature Overview*.
Lamed, R., & Bayer, E. A. (1988). The Cellulosome of Clostridium thermocellum. *Advances in Applied Microbiology*, *33*(C), 1–46. https://doi.org/10.1016/S0065-2164(08)70203-X

Lee, J. W., & Trinh, C. T. (2020). Towards renewable flavors, fragrances, and beyond. *Current Opinion in Biotechnology*, *61*, 168–180. https://doi.org/10.1016/J.COPBIO.2019.12.017

Murador, D. C., Salafia, F., Zoccali, M., Martins, P. L. G., Ferreira, A. G., Dugo, P., Mondello, L., de Rosso, V. v., & Giuffrida, D. (2019). Green Extraction Approaches for Carotenoids and Esters: Characterization of Native Composition from Orange Peel. *Antioxidants 2019, Vol. 8, Page 613*, *8*(12), 613. https://doi.org/10.3390/ANTIOX8120613

Ng, T. K., Weimer, P. J., & Zeikus, J. G. (1977). Cellulolytic and physiological properties of Clostridium thermocellum. *Archives of Microbiology 1977 114:1*, *114*(1), 1–7. https://doi.org/10.1007/BF00429622

Peneda de Oliveira, C., & Sousa, B. M. (1 C.E.). Green Consumer Behavior and Its Implications on Brand Marketing Strategy. *Https://Services.Igi-Global.Com/Resolvedoi/Resolve.Aspx?Doi=10.4018/978-1-5225-9558-8.Ch004*, 69–95. https://doi.org/10.4018/978-1-5225-9558-8.CH004

SÁ, A. G. A., Meneses, A. C. de, Araújo, P. H. H. de, & Oliveira, D. de. (2017). A review on enzymatic synthesis of aromatic esters used as flavor ingredients for food, cosmetics and pharmaceuticals industries. *Trends in Food Science & Technology*, *69*, 95–105. https://doi.org/10.1016/J.TIFS.2017.09.004

Seo, H., Lee, J. W., Garcia, S., & Trinh, C. T. (2019). Single mutation at a highly conserved region of chloramphenicol acetyltransferase enables isobutyl acetate production directly from cellulose by Clostridium thermocellum at elevated temperatures. *Biotechnology for Biofuels*, *12*(1), 1–13. https://doi.org/10.1186/S13068-019-1583-8/TABLES/2

Verbeke, T. J., Giannone, R. J., Klingeman, D. M., Engle, N. L., Rydzak, T., Guss, A. M., Tschaplinski, T. J., Brown, S. D., Hettich, R. L., & Elkins, J. G. (2017). Pentose sugars inhibit metabolism and increase expression of an AgrD-type cyclic pentapeptide in Clostridium thermocellum. *Scientific Reports 2017 7:1*, *7*(1), 1–11. https://doi.org/10.1038/srep43355

5.7 Figures and Tables

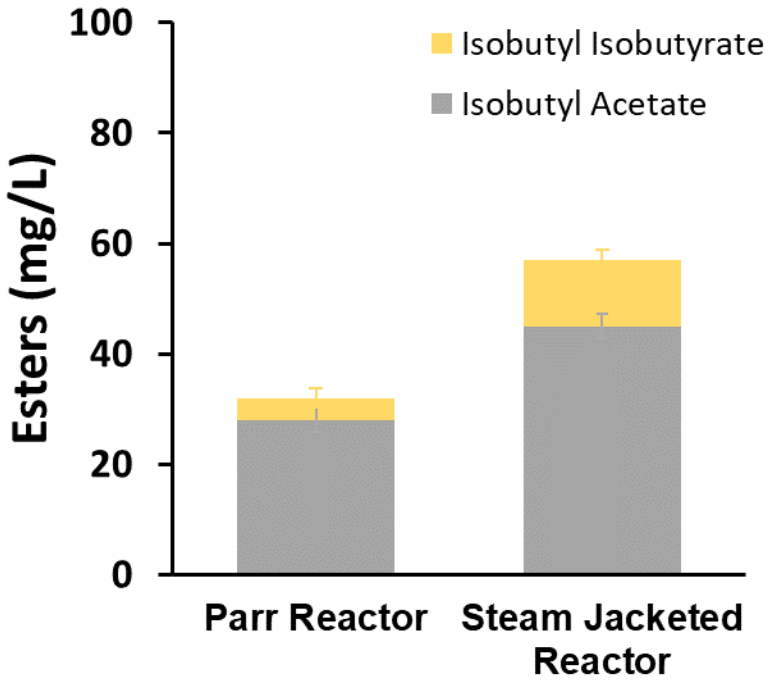

Figure 5-1. Biosynthesis of isobutyl acetate and isobutyl isobutyrate from CELF pretreated Poplar (CELF1= 150° C: 25 minutes in a parr reactor; CELF2= 150° C:15 minutes in a steam jacketed reactor) using engineered *C. thermocellum* strain HSCT2108.

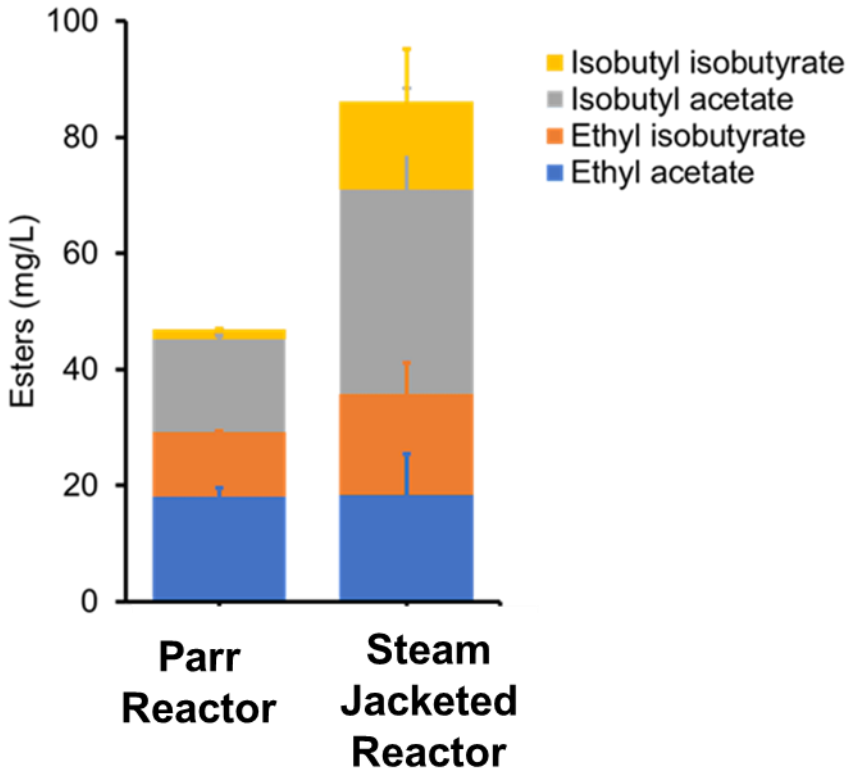

Figure 5-2. Comparison of the total esters (sum of isobutyl isobutyrate, isobutyl acetate, ethyl isobutyrate and ethyl acetate) biosynthesized from CELF pretreated Poplar (CELF1= 150°C: 25 minutes in a parr reactor; CELF2= 150°C:15 minutes in a steam jacketed reactor) using engineered *C. thermocellum* strain HSCT2108.

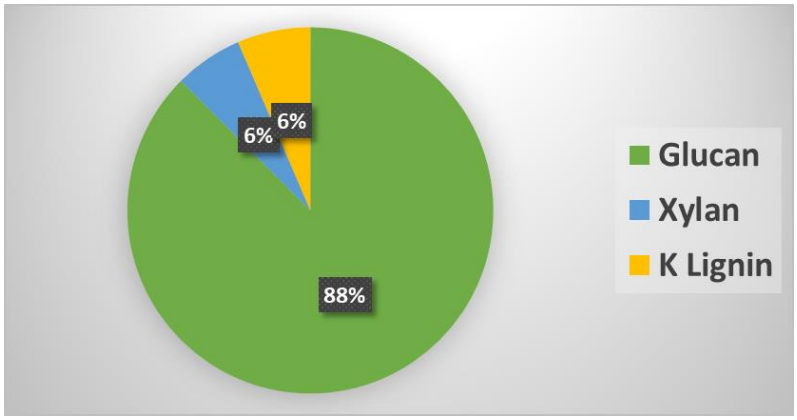

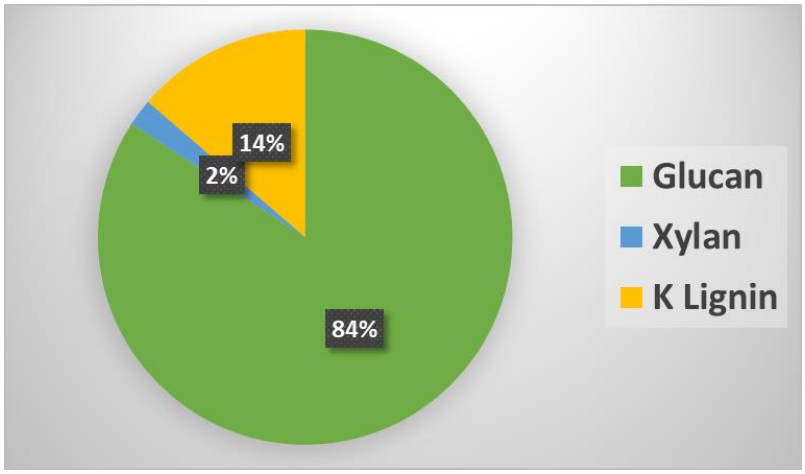

Figure 5-3. Relative compositions of Glucan, Xylan and K-lignin in CELF 1 (150 °C: 25 minutes in a parr reactor- top) and CELF2= 160°C:15 minutes in a steam jacketed reactor-bottom) pretreated poplar.

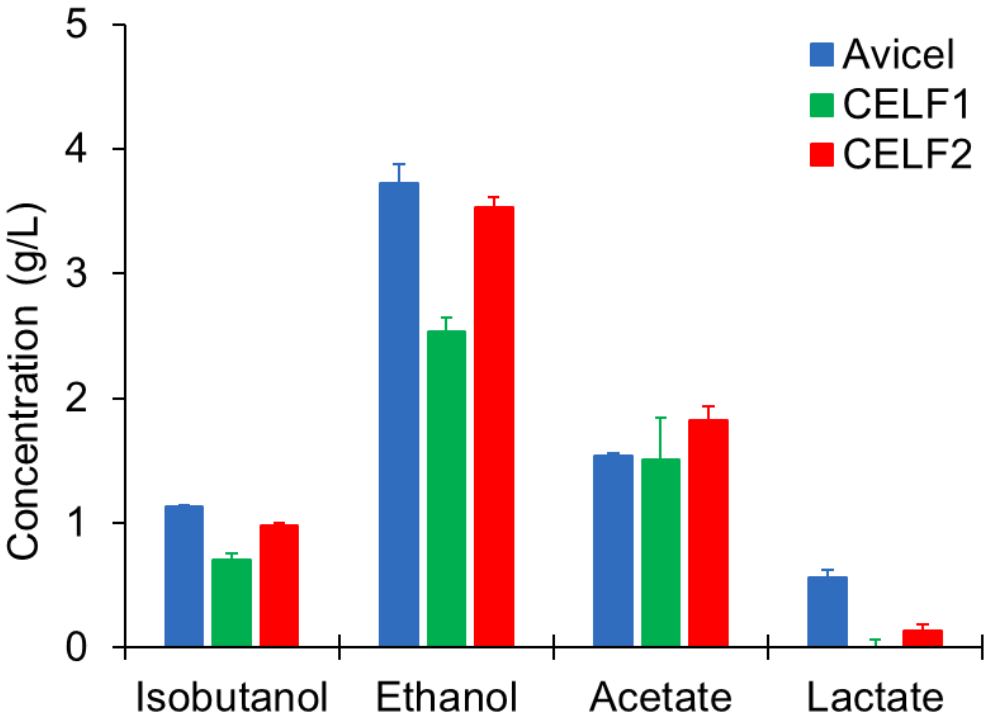

Figure 5-4. Comparison of major metabolites produced by engineered *C. thermocellum* strain HSCT3111 gown on CELF pretreated Poplar (CELF1= 150°C: 25 minutes in a parr reactor; CELF2= 150°C:15 minutes in a steam jacketed reactor) and Avicel.

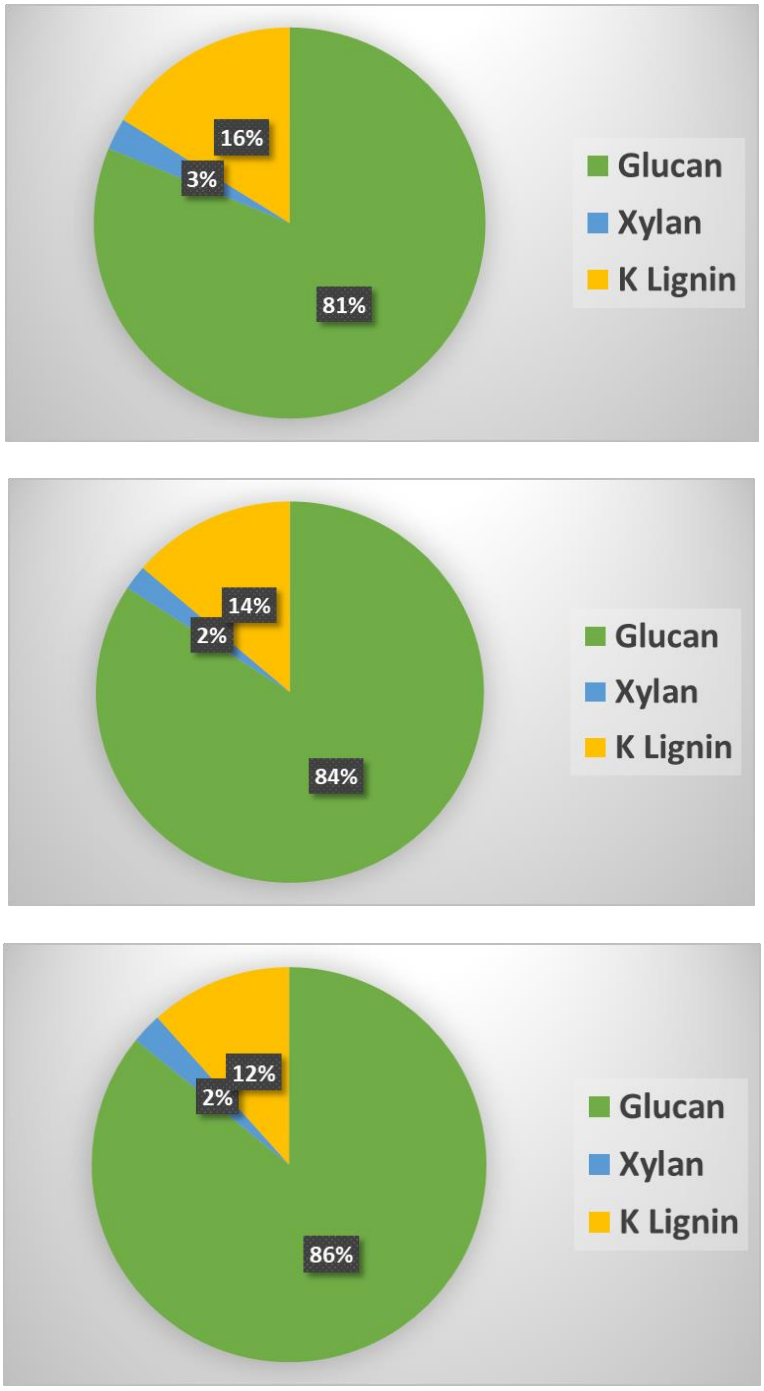

Figure 5-5. Relative compositions of Glucan, Xylan and K-lignin in 150°C (top), 160°C (middle) and 170°C (bottom), 15 minutes CELF pretreated Poplar.

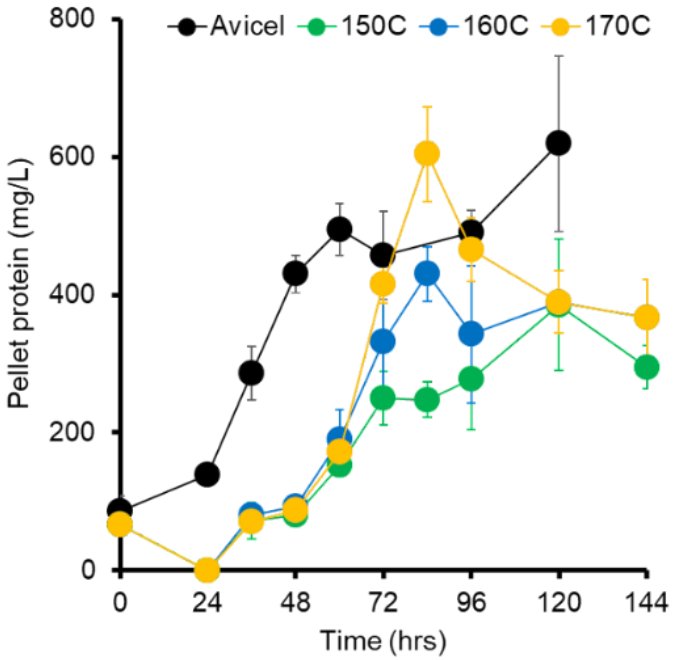

Figure 5-6. Comparison of protein pellet of engineered *C. thermocellum* grown on Avicel, and 150°C, 160°C, and 170°C, 15 minutes CELF pretreated Poplar.

.

	Avicel	**150°C 15 minutes**	**160°C 15 minutes**	**170°C 15 minutes**
Pellet protein @ stationary phase (mg/L)	498 +/- 94	290 +/- 85	374 +/ 82	468 +/- 96

Table 5-1. Resulting protein contents measured by Bradford assay at stationary phase for Avicel and 150°C, 160°C, and 170°C, 15 minutes CELF pretreated Poplar.

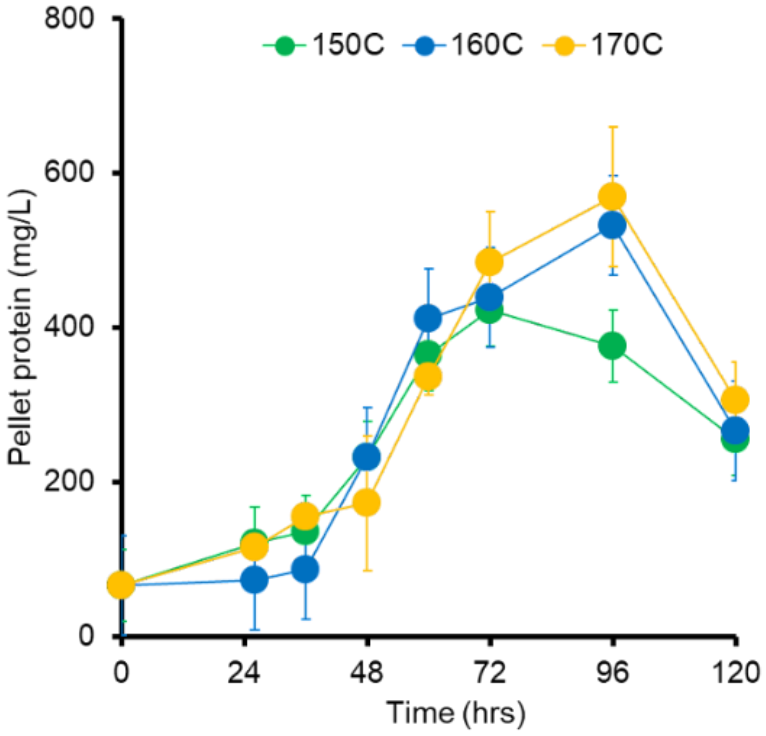

Figure 5-7. Comparison of protein pellet of engineered *C. thermocellum* grown on Avicel, and 150°C, 160°C, and 170°C, 15 minutes CELF pretreated Poplar after a one passage adaptation to improve cell activity on CELF poplar.

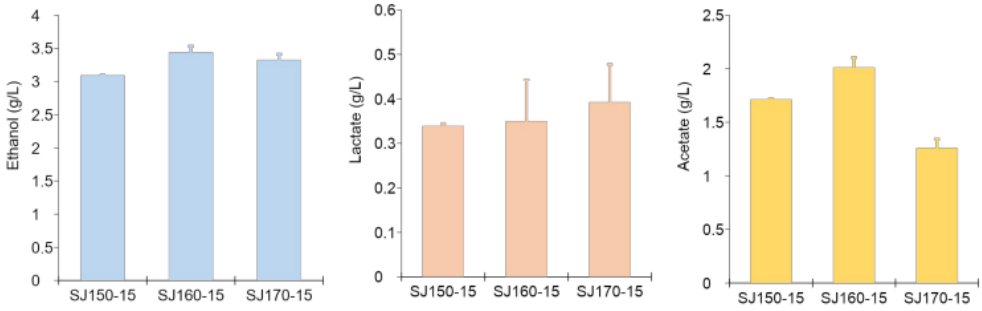

Figure 5-8. Comparison of Ethanol, Lactate and Acetate titers produced by engineered *C. thermocellum* strain HSCT3111 gown on 150°C (SJ150-15), 160°C (SJ160-15), and 170°C (SJ170-15), 15 minutes CELF pretreated Poplar.

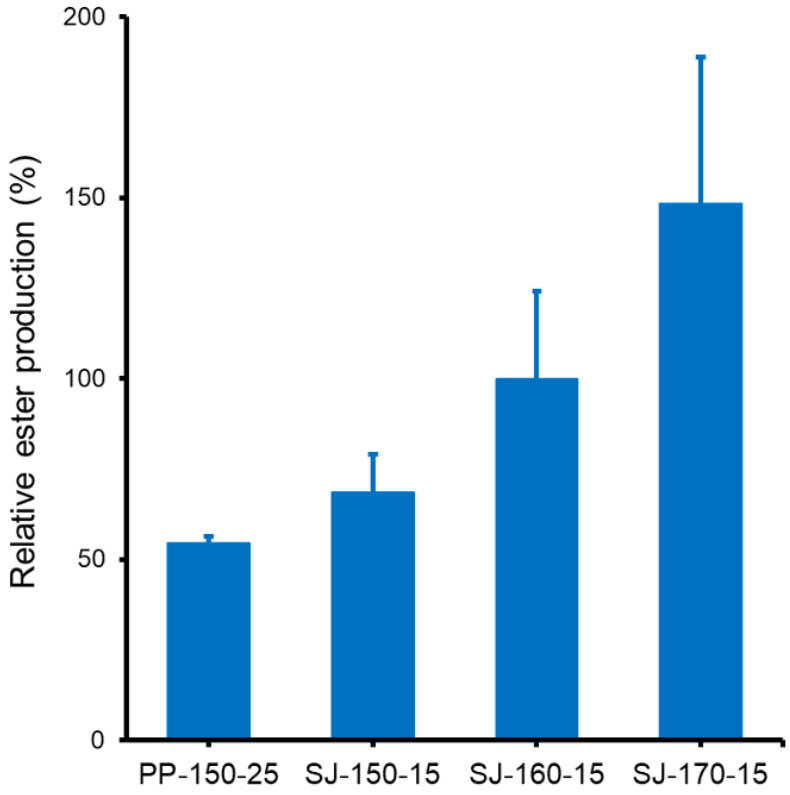

Figure 5-9. Relative total esters (sum of isobutyl isobutyrate, isobutyl acetate, ethyl isobutyrate and ethyl acetate) biosynthesized using engineered *C. thermocellum* strain HSCT3111 grown on 150°C (SJ150-15), 160°C (SJ160-15), and 170°C (SJ170-15), 15 minutes CELF pretreated Poplar. Total esters biosynthesized for the CELF pretreated Poplar 150°C: 25 minutes in a parr reactor (PP-150-25) is shown for comparison.

Supplementary Information

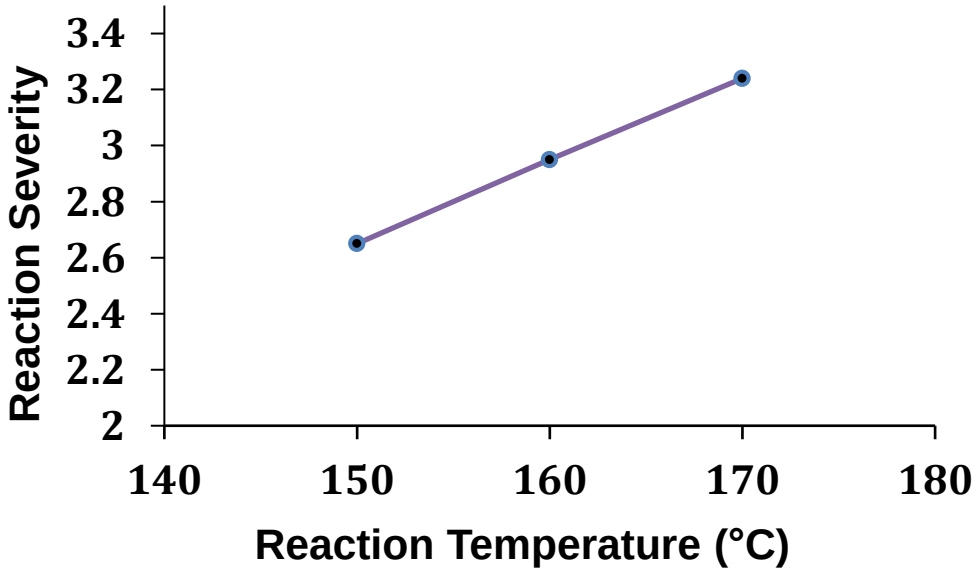

Figure S-1. Severity factor for the three CELF pretreatment conditions tested in the steam jacketed reactor for the ester biosynthesis.

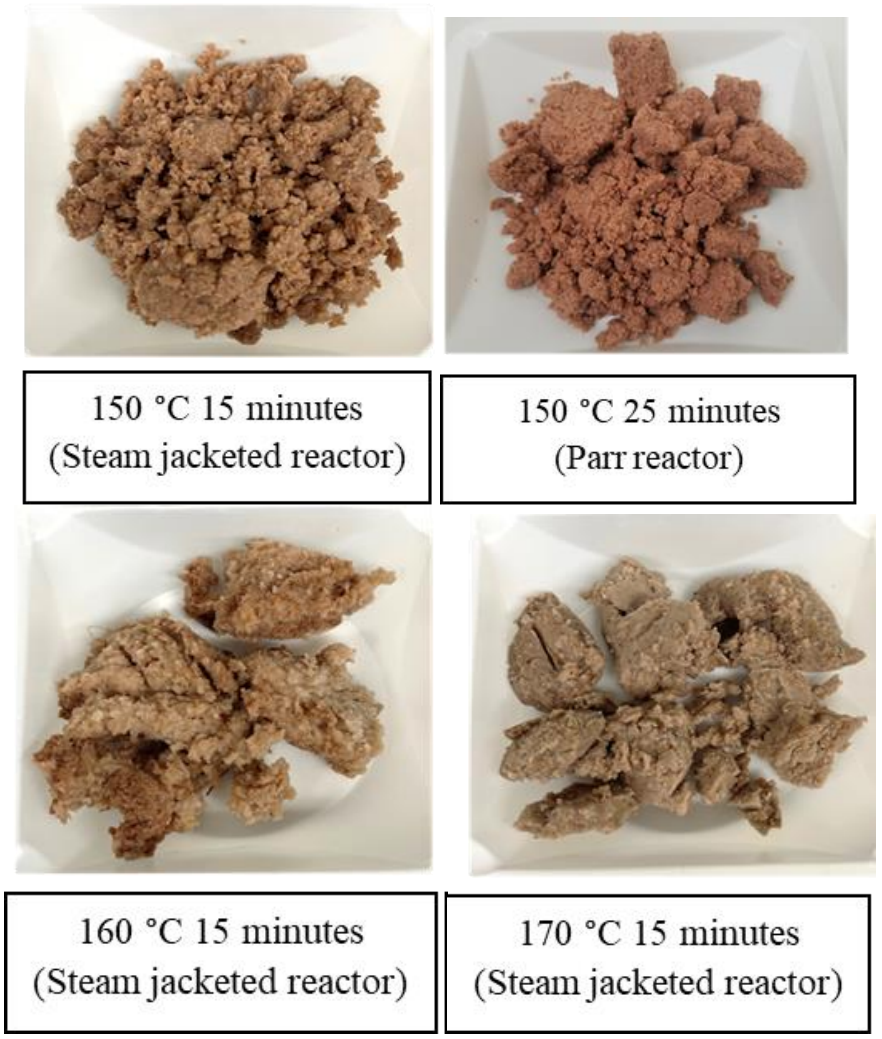

Figure S-2. CELF Pretreated Poplar (in parr and steam jacketed reactors) used in this study to investigate biosynthesis of esters using engineered *C. thermocellum*.

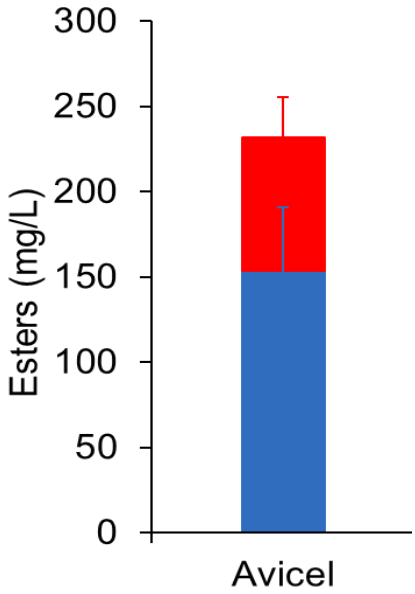

Figure S-3. Total esters (sum of isobutyl isobutyrate, isobutyl acetate, ethyl isobutyrate and ethyl acetate) biosynthesized using engineered *C. thermocellum* strain HSCT3111 grown on Avicel.

Chapter 6: CELF Enabled Hemp-Fuel and Hemp-Crete

6.1 Abstract

Our aim for this study was to use CELF pretreatment as an alternative green chemistry approach to pulp hemp and fractionate cellulose from newly-legalized industrial hemp in the US, without producing any toxic waste stream such as black liquor. Processing raw hemp stalks using CELF can utilize the entire hemp plant without decortication while producing purer hemp intermediates for the newer applications of green renewable fuels and green manufacturing. We examined the production of hemp-based sugars and hemp-fuel, as well as hemp-crete from the whole hemp plant. Simultaneous saccharification and fermentation (SSF) and enzymatic hydrolysis (EH) was investigated in order to understand the impact of CELF pulping on the sugar breakdown from the industrial hemp. High solids ethanol fermentation was carried out on CELF pulped hemp using Saccharomyces cerevisiae D5A at a glucan-from-solids loading of 10 wt%. The CELF pulped hemp was also used to produce 2”x2” sized briquettes of “enhanced” hemp-crete which was noticeably denser, harder, and less brittle than conventional hempcrete produced directly from decorticated hemp hurd.

6.2 Introduction

Deforestation accounts for a significant amount of anthropogenic greenhouse gas emission (Von Uexkull & Buhaug, 2021). Since re-forestation is an important carbon sink strategy that can directly reduce atmospheric concentration of carbon dioxide, alternate non-woody fast-growing feedstock are being investigated. Industrial hemp shows promise due to its carbon sequestration properties, and multiple applications in the paper industry, the textile industry, the cosmetic industry, and the building sector etc. (Small & Marcus, 2002)and can be an important strategy as a fast rotation, high yielding crop (~12 tons/hectare cellulose and ~25 tons/hectare fiber material) that requires less fertilizer to grow. In addition, hemp can be harvested in four months after cultivation compared to the woody biomass (hardwood, softwood) that take decades to grow (Lu & Oza, 2013; Lynch, 2020; Schluttenhofer & Yuan, 2017). Reforestation using industrial hemp and use of hemp as a commercial crop are opening new opportunities. Therefore, development of more efficient and greener approaches to enable the utilization of whole hemp plant is critical.

Hemp fibers, like other plant lignocellulosic fibers, contain mostly cellulose. Cellulose is extremely strong, boasting high lateral tensile strength, durability, and strength-to-weight ratio (Lu & Oza, 2013). The two current methods for isolating fibers from hemp is either by acid or Kraft pulping (Manian et al., 2021). Although pulping is very effective at removing lignin to improve fiber purity and strength, the pulping processes produces toxic black liquors that require a substantial effort to treat and dispose (Hubbe et al., 2016; Vakkilainen, 2017). In many cases, each ton of fiber pulp produced also introduces 7 tons of black liquor (States et al., 1991). Because of its high toxicity, the

lignin-rich black liquor requires expensive chemical treatment and the waste product is then burned in a kiln, releasing organic sulfides, H_2S, SO_2, VOCs, NOx, and other pollutants into the atmosphere.

Furthermore, there are about 1,269,000 homes built in the US per year, contributing to the annual consumption of millions of tons of largely non-renewable materials that have an adverse effect on the environment in both their production and utilization (Epstein et al., 2011). Many of the materials used in construction are produced from fossil petroleum resulting in significant greenhouse gas (GHG) emissions during production (Abdellatef et al., 2020; Piot et al., 2017). Hempcrete, a bio-composite of lime binder and hemp fibers, is a renewable and natural wall-in material with unique advantages over existing wall materials such as drywall, particle board, plastic, fiberglass, and concrete. Hempcrete is not only a strong material, but it can also participate in moisture and temperature regulation. In many instances, buildings made from hempcrete have demonstrated substantial reduction in energy consumption related to temperature and moisture control (Abdellatef et al., 2020; Müssig et al., 2020). However, traditional methods of producing quality hemp fibers suitable for use in hempcrete either rely on mechanical separation, known as decortication, or chemical pulping and retting that in turn releases toxic and corrosive waste streams (National Academies of Sciences Engineering Medicine, 1999).

Decortication is an alternate method to provide hemp herds for direct incorporation into hempcrete, but the process has traditionally represented a mechanical challenge that is unreliable, expensive to scale up, and the resulting hempcrete is not densely packed resulting in poor wind isolating properties and limited structural strength, destined to be

mostly used as fill-in wall material. Traditional forms of hempcrete production are energy intensive due to the use of conventional mechanical equipment. Furthermore, traditional pulping produces highly toxic black liquor streams that is expensive to clean up (Hubbe et al., 2016; National Academies of Sciences Engineering Medicine, 1999). Furthermore, since not all the hemp that undergoes processing could be used for green construction materials, a potential use-case for the production of high value co-products, such as fuel ethanol is needed.

The goal of this work was to optimize CELF to fractionate hemp fiber and hemp hurd from the hemp plant and examine the utility of hemp hurd for conversion into hemp fuel (ethanol) using commercial enzyme cocktail in a simultaneous saccharification and fermentation scheme, and to demonstrate the utility of hemp fibers for hempcrete formulation. This approach of whole hemp conversion into fuels and material could enable renewable fuels and green manufacturing from hemp, and also maximize the utilization of hemp carbon by expanding the product portfolio for this ancient crop.

6.3 Experimental Section

6.3.1 Materials

Oregon Hemp Hurd (CBB) was provided by Columbia Basin Bioscience (Hermiston, Oregon). The material was not milled prior to CELF pretreatment. Cellic® Ctec2 was provided by Novozymes. *S. cerevisiae* D5A provided by NREL.

6.3.2 Analytical procedures

Standardized analytical laboratory procedures (LAPs) from the National Renewable Energy Laboratory were used for chemical analysis as well as enzymatic saccharification, simultaneous saccharification, and fermentation procedures. Sugars and

fermentation products were quantified using the proper calibration standards via High performance liquid chromatography (HPLC) analysis utilizing a Bio-Rad Aminex HPLX-87H column.

6.3.3 CELF Pretreatment

CELF pretreatment of Oregon Hurd was carried out in a steam jacketed reactor at 160°C for 15 minutes. The Oregon hurd was soaked and left overnight at 4°C at 7.5 wt% solids loading, 0.5 wt % sulfuric acid (72 wt %) and deionized water and THF at 1:1 ratio (w/w) mixture for a total loading of 2,800 grams.

6.3.4 Composition of Hemp before and after Pulping

Compositional analysis of the Poplar before and after CELF pretreatment was done following an established Laboratory Analytical Procedures (LAPs) (version 8-03-2012) from the National Renewable Energy Laboratory (NREL, Golden, CO). After the two step acid hydrolysis, the resulting solids and liquid were separated using filtering crucibles. The liquid portion was sampled and analyzed against calibration standards and using HPLC Waters Alliance system e2695 (Waters Co., Milford, MA) equipped with a HPX-87H column (Bio-Rad Aminex ®, Bio-Rad Laboratories, Hercules, CA) and a Waters Refractive Index Detector 2414 (Waters Co., Milford, MA). The mobile phase run was a 5 mM sulfuric acid set at a flow rate of 0.6 mL/min. Empower® 3 software package (Empower Software Solutions, Newport Beach, CA) was utilized to collect, view, and integrate the resulting chromatographs. The glucan and xylan content were calculated and adjusted against internal sugar standards. To determine the amount of acid insoluble or Klason-lignin, the solid residues after the filtration process were dried and weighed.

Finally, ash and other insoluble matter were further quantified by utilizing a muffle furnace ramped to 575°C to convert the leftover material in the crucibles into ash.

6.3.5 Enzymatic Hydrolysis (EH)

Enzymatic hydrolysis of CELF pretreated Oregon Hurd was carried out in duplicate in 125 mL flasks at working mass of 50 grams. The solids loading was selected to be 100 g/L glucan (10 wt%) or 5 g of glucan with an enzyme loading of Cellic® Ctec2 of 15 mg/ g glucan (graciously provided by Novozymes). A Pierce ™ BCA assay kit was utilized to determine the protein content to be 270 mg/mL. The concentrated enzyme stock was diluted down to a concentration of 54 mg/mL in Mili-Q water prior to addition to the flask. The flasks contained 50 mM of citrate buffer (pH 4.8). The flasks were placed in an orbital shaker incubator set at 50°C and 150 RPM. At the first time point 500 uL of liquid sample was taken, but as fermentation progressed, the sample amount was increased to 650 uL to ensure enough liquid for HPLC analysis. Samples were centrifuged at 15,000 RPM for 12 minutes and transferred to HPLC vials. Cellobiose, glucose, xylose, arabinose concentrations were measured at each time point.

6.3.6 Simultaneous Saccharification and Fermentation (SSF)

SSF of CELF pretreated hemp was carried out in duplicate in 125 mL flasks at working mass of 50 grams. The solids loading was selected to be 100 g/L glucan (10 wt%) or 5 g of glucan with an enzyme loading of Cellic® Ctec2 of 15 mg/ g glucan. The yeast selected for this fermentation was *S. cerevisiae* D5A (provided by NREL) and was inoculated at an OD (600 nm) of 0.5. The remaining contents of the flask was 50 mM citrate buffer (pH 4.8), 10 g/L yeast extract, 20 g/L peptone, and 40 mg/L tetracycline. The

flasks were placed in an orbital shaker incubator set at 37°C and 130 RPM. After the 48-hour time, samples were taken daily for analysis. At the first time point, 500 uL of liquid sample was taken, but as fermentation progressed, the sample amount was increased to 650 uL to ensure enough liquid for HPLC analysis. Samples were centrifuged at 15,000 RPM for 12 minutes and transferred to HPLC vials. Cellobiose, glucose, xylose, arabinose, lactic acid, acetic acid, and ethanol concentrations were measured at each time point.

6.3.7 Production of Hemp-Crete after CELF pulping

Hemp was pretreated at 160°C for 15 minutes to evaluate the effect of CELF on the resulting composition and integrity of the hemp stalk to be used as a building material. After the CELF pulping process, the hemp solids were separated from the liquids via liquid filtration using a Buchner funnel. The resulting solids were washed with DI water and samples were then dried overnight to reduce the moisture content. Hemp-Crete was made by mixing the samples with a 1:3:3 volume ratio of hemp:lime:water. Hemp-Crete was molded in a heating tray and left over night at 45°C to dry.

6.4 Results and Discussions

6.4.1. Composition Analysis of CELF Pulped Hemp

Compositional analysis of the raw and 160°C:15 minutes CELF pretreated industrial hemp was preformed according to the National Renewable Energy Laboratory (LAPs) in triplicates. The glucan, xylan, Klason lignin, extractives and ash contents of the raw and CELF pulped industrial hemp is shown in table 6-1. As can be seen, the glucan, xylan, Klason lignin contents of the raw and CELF pulped industrial hemp changed quite substantially after CELF pulping. The glucan content of the industrial hemp increased by

>30%, whereas, a reduction of 7% in the Klason lignin content is seen. The xylan and extractives contents also reduced by >10% and 9% respectively. The ash content of the CELF pulped hemp was not determined. This result shows CELF pulped hemp to increase the glucan content substantially at the relatively lower temperatures reported in the the literature (Bokhari et al., 2021). The CELF pretreated hemp initially had a moisture content of 90%, but was pressed down to remove excess water from the fiber to a final moisture content of 76.32%.

6.4.2 Production of Hemp-based Sugars and Hemp-Fuel

In order to evaluate CELF pulped hemp as a substrate for fermentation the sugar release and ethanol yields were measured. We performed both simultaneous saccharification and fermentation (SSF) and enzymatic hydrolysis (EH) in order to understand the impact of sugar breakdown by EH and ethanol fermentation performance by SSF of the combined system using both enzymes and yeast culture. In this study, EH runs were used as an internal control to prove viability of the enzymes for releasing fermentable sugars to be consumed by the yeast strain during SSF. The experimental details of the EH and SSF fermentation study is provided in Table 6-2. Due to a limited batch of hemp initially, the experiments to determine sugar release (a control for simultaneous saccharification and fermentation), and SSF was carried out in duplicate. Since the EH and SSF were done at high solids loadings of 10% (Supplementary figure S-1), the sampling was not possible earlier than 48 hours (mostly solid state until day 2). The sampling started at 48 hours and continued for 7 days for EH, and 14 days for SSF at one day intervals.

The glucose release upon enzymatic hydrolysis of the 160°C CELF pretreated Oregon Hurd using an enzyme loading of 15mg/g Cellic® Ctec2 is shown in Figure 6-2. Due to the high solids loading and high moisture content of the CELF pulped hemp substrate, sampling was started at 48 hours when the enzyme had begun to drastically liquefy the hemp material. In only 2 days, 50 grams/L of glucose had been released. Enzymatic hydrolysis on CELF pretreated Oregon Hurd released a total of 80 g/L glucose, resulting in total glucan solubilization of 72% after 7 days of enzymatic hydrolysis (Figure 3). The high glucose concentration from a relatively low severity CELF pretreatment process show the efficiency of the CELF process in overcoming the recalcitrance of the industrial hemp. The composition of the liquid fraction from the CELF pretreatment is presented in Table 6-3. As can be seen, the xylose concentration in the liquid fraction is high (>20 g/L) and is consistent with CELF process hydrolyzing majority of the xylan during CELF pretreatment into xylose. The glucose concentration in the CELF liquid fraction was measured to be 6.79 g/L. The combined sugar from solid (after the enzymatic hydrolysis of the CELF pretreated hemp solid) and the liquid fraction (after the CELF pretreatment) from the CELF+EH processing of industrial hemp is >107 g/L. Since the CELF process resulted into a glucan rich solid, and since the enzymatic hydrolysis of performed at high solids loading of 10 wt%, the total fermentable sugar from this relatively milder process is in the industrially relevant range (Ou et al., 2021). In addition,4.80 g/L of 1,4 butanediol was also detected in the liquid fraction from the CELF pretreatment of the hemp (Table 6-3).

In order to achieve high ethanol titers as a metric for industrial relevance, the solids loadings for the SSF was chosen to be 10 wt%. The resulting ethanol concentrations from the high solids fermentation over 14 days of culture are shown in Figure 6-4. Simultaneous saccharification and fermentation (SSF) at 10 wt%, of the CELF pretreated Oregon Hurd, using Cellic® Ctec2 at 15 mg/g glucan loading and using *S. cerevisiae* D5A, resulted into an ethanol titer of 39.7 g/L. Furthermore, the high solids fermentation resulted in a theoretical ethanol yield of 65% after 7 days of fermentation (Figure 6-5).

Prior to the CELF pretreatment, the Oregon Hurd substrate was not milled down to a small particle size. Despite this, the recalcitrant Oregon Hurd began to solubilize within 48 hours during both EH and SSF. Further improvement to sugar and ethanol yields may be achieved by milling the Hurd prior to pretreatment. In addition, if the moisture content of the CELF pretreated Oregon Hurd can be reduced down even further using a hydraulic press, the enzyme and yeast may be able to act upon the biomass earlier, and slightly higher ethanol titers could be achievable.

6.4.2 Formulation of CELF Hemp-Crete

Figure 6-6 shows hempcrete briquettes made from both raw hemp hurd and CELF-pulped hemp stalk at identical compositions of biomass:binder:water ratios of 1:1:3. CELF-pulped hemp stalk was shown to produce consistent 2”x2” briquettes. Briquettes produced from CELF hemp were more easily moldable resulting in a more compact and sturdy material as compared to the briquettes made from the untreated hemp. Moisture absorptivity was tested for briquettes made from untreated hemp and CELF pulped hemp by soaking the resulting hemp-crete in water and subsequently measuring the moisture

retained by the briquettes. Hemp-Crete made from untreated hemp retained 3.53 milliliters of water per gram of dry biomass. CELF treated hemp-crete retained 10.94 milliliters of water per gram of reacted fibers. The increased moisture absorptivity is a positive characteristic for building materials and has been attributed to the glucan rich nature of the CELF pretreated hemp (Piot et al., 2017).

Furthermore, CELF-pulped hempcrete was noticeably denser, less porous, less brittle, harder, and conformed better as it cured inside the briquette mold as compared to the traditional hempcrete. We anticipate that CELF-pulped hempcrete to have better insulating properties, higher compressive strength, improved durability, and less friable than traditional hempcrete. In order to understand how CELF pulped hemp fibers can be used as green construction materials, more research is needed to determine the extent of its properties in the real world setting. Towards that goal, more research is needed on how to optimize CELF for hemp to increase the utilization of industrial hemp.

6.5 Conclusions

CELF is a lower-temperature chemical pulping process that has demonstrated high reliability when scaled up; ideal for processing large quantities of underutilized industrial hemp resources. At larger scales, the feasibility for producing renewable 2nd generation fuel ethanol from CELF pulped hemp is an important feature to reduce waste generation and greenhouse gas emissions. Here, we report on our work on utilizing CELF process to produce multiple potential product streams from industrial hemp while eliminating the need for mechanical decortication. CELF pretreatment resulted into hemp pulp that was >70% cellulose, and resulted into a total glucan solubilization of 70% during enzymatic

hydrolysis using Cellic® Ctec2 enzymes at 15 mg/g of glucan loading. Simultaneous saccharification and fermentation at 10 wt%, using *S. cerevisiae* D5A resulted into ethanol concentration of 50g/L and >70% ethanol yield. The hemp-crete was formulated at the biomass:binder:water ratios of 1:1:3 and the molded briquettes was shown to retain 10.94 milliliters of water per gram of reacted fibers- an important property for building material. The briquettes were also noticeably denser, less porous, and less brittle compared to the briquettes molded from the raw decorticated hemp, and also conformed to the mold during the curing process.

6.6 References

Abdellatef, Y., Khan, M. A., Khan, A., Alam, M. I., & Kavgic, M. (2020). Mechanical, Thermal, and Moisture Buffering Properties of Novel Insulating Hemp-Lime Composite Building Materials. *Materials 2020, Vol. 13, Page 5000*, *13*(21), 5000. https://doi.org/10.3390/MA13215000

Bokhari, S. M. Q., Chi, K., & Catchmark, J. M. (2021). Structural and physico-chemical characterization of industrial hemp hurd: Impacts of chemical pretreatments and mechanical refining. *Industrial Crops and Products*, *171*, 113818. https://doi.org/10.1016/J.INDCROP.2021.113818

Epstein, P. R., Buonocore, J. J., Eckerle, K., Hendryx, M., Stout, B. M., Heinberg, R., Clapp, R. W., May, B., Reinhart, N. L., Ahern, M. M., Doshi, S. K., & Glustrom, L. (2011). Full cost accounting for the life cycle of coal. *Annals of the New York Academy of Sciences*, *1219*(1), 73–98. https://doi.org/10.1111/J.1749-6632.2010.05890.X/PDF

Hubbe, M. A., Metts, J. R., Hermosilla, D., Blanco, M. A., Yerushalmi, L., Haghighat, F., Lindholm-Lehto, P., Khodaparast, Z., Kamali, M., & Elliott, A. (2016). Pulp & paper effluent. *BioResources*, *11*(3), 7953–8091
.

Lu, N., & Oza, S. (2013). A comparative study of the mechanical properties of hemp fiber with virgin and recycled high density polyethylene matrix. *Composites Part B: Engineering*, *45*(1), 1651–1656. https://doi.org/10.1016/J.COMPOSITESB.2012.09.076

Lynch, P. (2020). *Hemp vs. Trees: Why Switch to Hemp and Save the Planet*. https://wayofleaf.com/hemp/hemp-vs-trees-why-we-should-switch-to-hemp

Manian, A. P., Cordin, M., & Pham, T. (2021). Extraction of cellulose fibers from flax and hemp: a review. *Cellulose 2021 28:13*, *28*(13), 8275–8294. https://doi.org/10.1007/S10570-021-04051-X

Müssig, J., Amaducci, S., Bourmaud, A., Beaugrand, J., & Shah, D. U. (2020). Transdisciplinary top-down review of hemp fibre composites: From an advanced product design to crop variety selection. *Composites Part C: Open Access*, *2*, 100010. https://doi.org/10.1016/J.JCOMC.2020.100010

National Academies of Sciences Engineering Medicine. (1999). *Industrial Environmental Performance Metrics: Challenges and Opportunities*. https://www8.nationalacademies.org/onpinews/newsitem.aspx?RecordID=9458

Ou, L., Dou, C., Yu, J. H., Kim, H., Park, Y. C., Park, S., Kelley, S., & Lee, E. Y. (2021). Techno-economic analysis of sugar production from lignocellulosic biomass with

utilization of hemicellulose and lignin for high-value co-products. *Biofuels, Bioproducts and Biorefining*, *15*(2), 404–415. https://doi.org/10.1002/BBB.2170

Piot, A., Béjat, T., Jay, A., Bessette, L., Wurtz, E., & Barnes-Davin, L. (2017). Study of a hempcrete wall exposed to outdoor climate: Effects of the coating. *Construction and Building Materials*, *139*, 540–550. https://doi.org/10.1016/J.CONBUILDMAT.2016.12.143

Schluttenhofer, C., & Yuan, L. (2017). Challenges towards Revitalizing Hemp: A Multifaceted Crop. *Trends in Plant Science*, *22*(11), 917–929. https://doi.org/10.1016/J.TPLANTS.2017.08.004

Small, E., & Marcus, D. (2002). *Hemp: A New Crop with New Uses for North America*. https://www.hort.purdue.edu/newcrop/ncnu02/v5-284.html

States, U., Alexander, S., & Greber, B. (1991). *Environmental Ramifications of Various Materials Used in Construction and Manufacture in the United States*.

Vakkilainen, E. K. (2017). Recovery Boiler. *Steam Generation from Biomass*, 237–259. https://doi.org/10.1016/B978-0-12-804389-9.00011-3

von Uexkull, N., & Buhaug, H. (2021). Security implications of climate change: A decade of scientific progress. *Journal of Peace Research*, *58*(1), 3–17. https://doi.org/10.1177/0022343320984210

6.7 Figures and Tables

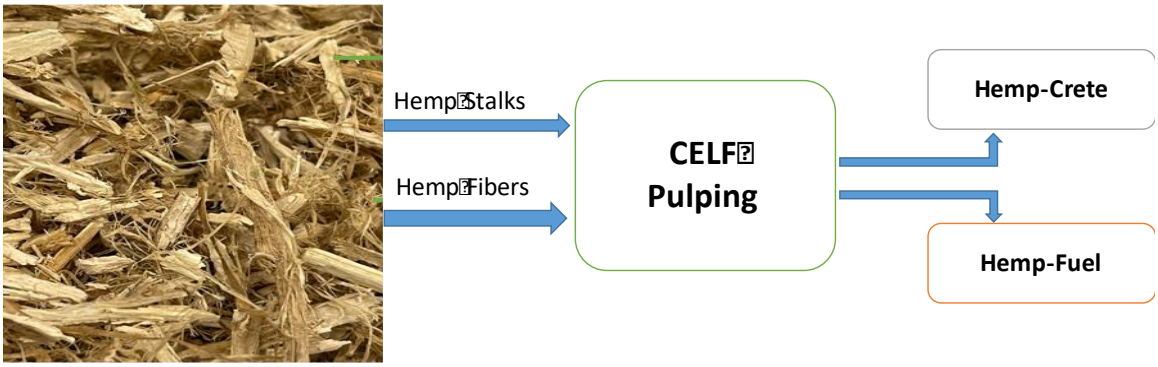

Figure 6-1. Schematic of a CELF process flow to maximize production of fuel ethanol and hemp-crete from industrial hemp.

Sample	Glucan (%)	Xylan (%)	Lignin (%)	Extractives (%)	Ash (%)
Oregon hemp hurd stalk (raw)	39.1	18.0	25.8	12	5.1
Oregon hemp hurd stalk (CELF pulped)*	69.4	7.3	18.8	2.8	*

Table 6-1. Compositional analysis of raw and CELF pulped hemp solid after CELF pretreatment at 160°C for 15 minutes. *undetermined.

	Flask 1 (EH)	Flask 2 (EH)	Flask 3 (SSF)	Flask 4 (SSF)
Enzyme	Cellic® Ctec2 enzymes at 15 mg/g-glucan loading	Cellic® Ctec2 enzymes at 15 mg/g-glucan loading	Cellic® Ctec2 enzymes at 15 mg/g-glucan loading	Cellic® Ctec2 1 enzymes at 15 mg/ mg/g-glucan loading
Glucan Loading	10 wt% glucan loading	10 wt% glucan loading	10 wt% glucan loading	10 wt% glucan loading
Yeast strain	N/A	N/A	*S. cerevisiae* D5A	*S. cerevisiae* D5A

Table 6-2. Experimental overview of enzymatic hydrolysis and simultaneous saccharification and fermentation of CELF-pulped hemp stalk to produce hemp-sugar and hemp-ethanol.

	Glucose (g/L)	**Xylose (g/L)**	**1,4-BDO (g/L)**	**THF (g/L)**
Oregon hurd hemp liquid after CELF pulping	6.79	20.45	4.80	61.99

Table 6-3. Composition of the liquid fraction from the CELF pretreatment of the Oregon hurd (hemp reaction liquid).

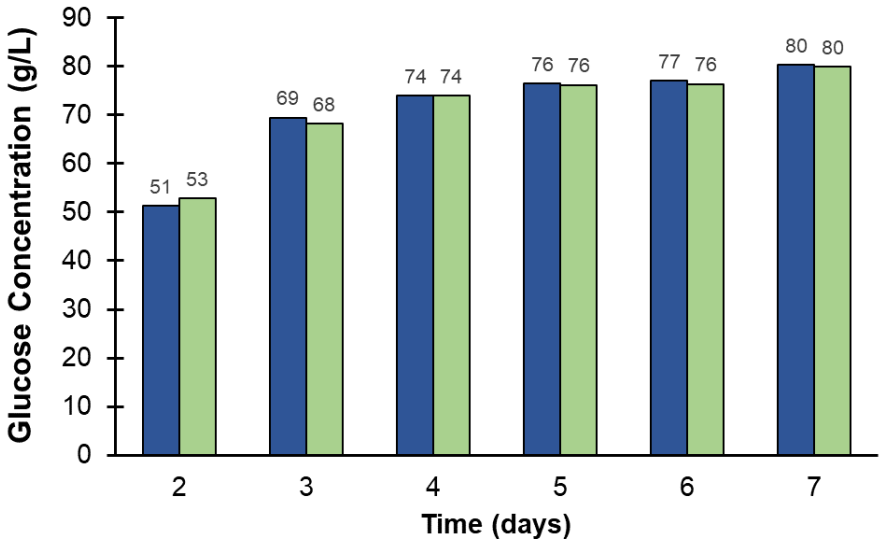

Figure 6-2. Concentration of glucose in g/L during enzymatic hydrolysis of CELF Hurd at 10 wt% solids loadings (clustered bars show measurement from the duplicate flasks).

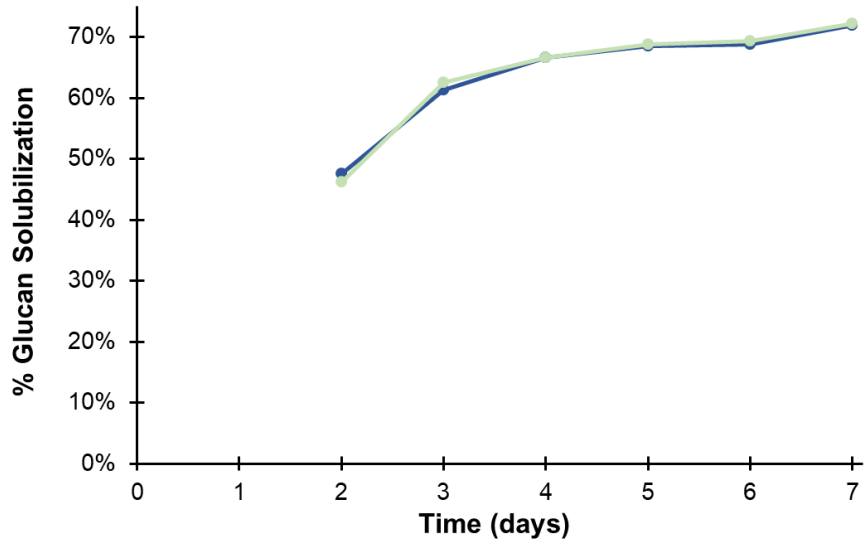

Figure 6-3. Percent glucan solubilization of the CELF pulped hemp as a function of time. Enzymatic hydrolysis of CELF hemp was performed under conditions identical to SSF ethanol fermentations at 10 wt % glucan loadings.

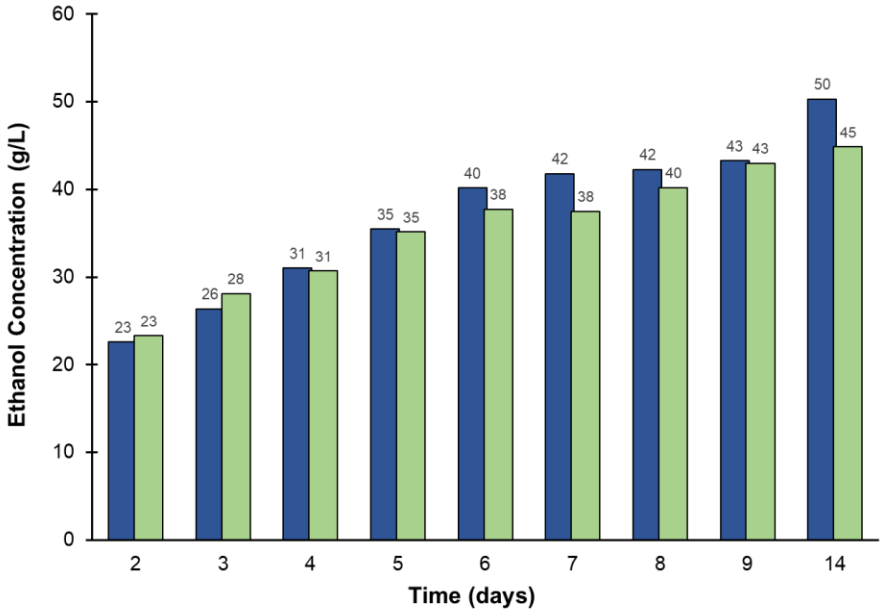

Figure 6-4. Ethanol titers (g/L) measured during SSF of CELF hemp hurd at 10 wt% solids loading and 15 mg/ g glucan enzyme loading using S. cerevisiae D5A.

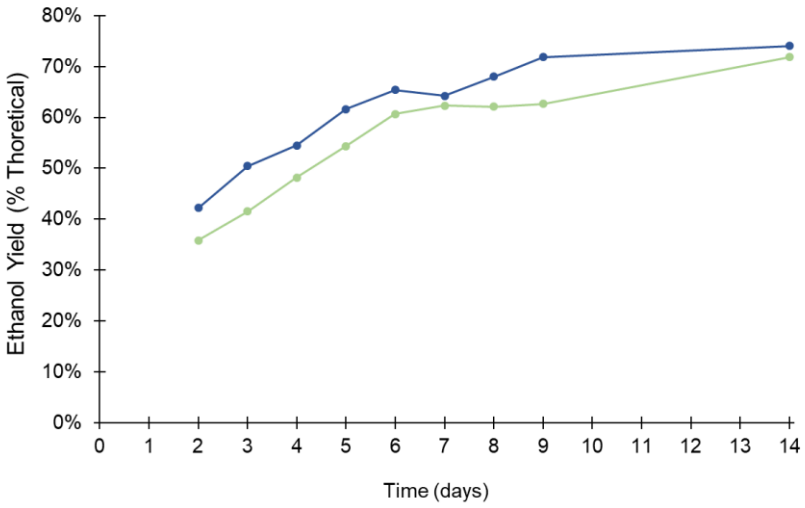

Figure 6-5. Ethanol yield during SSF using S. cerevisiae D5A., of CELF hemp at 10 wt% solids loading and 15 mg/ g glucan enzyme loadings.

Figure 6-6. Hemp-crete made from raw decorticated hemp hurd (top), and CELF pulped hemp stalk (bottom).

Supplementary Figures

Figure S-1. Fermentation shake flasks at Day 0 (Top), Day 2 (Middle), and day 7 (bottom).

Chapter 7: CELF Enabled Renewable Lignin-Based Adsorbent for Effective Removal of Azo Dye

This chapter was published in its entirety in *ACS Omega* (2020), 5, 6, 2865–2877
Xianzhi Meng[†*], Brent Scheidemantle[‡,§], Mi Li[†], Yunyan Wang[†], Xianhui Zhao[⊥], Miguel Toro-González[#], Priyanka Singh[‡,§], Yunqiao Pu[∥], Charles E. Wyman[‡,§], Soydan Ozcan[∇,Ω], Charles M. Cai[‡,§], Arthur J. Ragauskas. *"Synthesis, characterization, and utilization of a lignin-based adsorbent for effective removal of azo dye from aqueous solution."ACS Omega* 2020, 5, 6, 2865–2877.

7.1 Abstract

How to effectively remove toxic dyes from the industrial wastewater using green low-cost lignocellulose-based adsorbent such as lignin has become a topic of great interest but remains quite challenging. In this study, Co-solvent Enhanced Lignocellulosic Fractionation (CELF) pretreatment and Mannich reaction were combined to generate aminated CELF lignin which is subsequently applied for removal of Methylene Blue (MB) and Direct Blue (DB) 1 dye from aqueous solution. ^{31}P NMR was used to track degree of amination, and an orthogonal design was applied to determine the relationship between extent of amination and reaction parameters. The physicochemical, morphological, and thermal properties of the aminated CELF lignin were characterized to confirm the successful grafting of DETA onto the lignin. The aminated CELF lignin proved to be an effective azo dye-adsorbent, demonstrating considerably enhanced dye decolorization, especially toward DB 1 dye (>90%). It had a maximum adsorption capacity of DB 1 dye of 502.7 mg/g, and the kinetic study suggested the adsorption process conformed to a pseudo-second-order kinetic model. The isotherm results also showed that the modified lignin-based adsorbent exhibited monolayer adsorption. The adsorbent properties were mainly attributed to the incorporated amine functionalities as well as the increased specific surface area of the aminated CELF lignin.

7.2 Introduction

The demand for clean water is likely to increase driven by the rapid urbanization, expanding industrial activities, energy generation, and water pollution. Due to the limited fresh water resources on earth, this demand should be addressed by developing promising water purification techniques. The presence of organic dyes in industrial wastewater could cause some serious environmental concerns due to their poor biodegradability and toxicity to the exposed plants, living organisms, and even human being. As a result, those toxic dyes should be removed from the wastewater as much as possible before being discharged to land or water sources in an environmentally friendly manner (Budnyak et al., 2018). The textile industry consumes organic dyes which represent 60% of the world's dye consumption, and it was reported that 10-25% of water-soluble dyes are lost during the dyeing process and 2-20% of dyes are released as effluent into the water system after the dyeing process (Abdelhamid & Zou, 2018). Azo dyes are known as dyes containing –N=N– groups, representing 60-70% of commercially available dyes in the world (S. Wang et al., 2018). They are extensively used in the textile industry, and become part of the textile effluents. Therefore, how to cost-effectively remove these toxic azo dyes from the industrial wastewater has become a topic of great interest. Adsorption is considered as an alternative method to the traditional combination of chemical and biological processes for the removal of dyes from aqueous solutions (Peng et al., 2016; Zambare et al., 2017). Dye adsorption by various adsorbents is considered to occur primarily via π interaction, hydrogen bonding, and electrostatic interactions. Several organic and inorganic materials including zeolite, (Abdelhamid & Zou, 2018; Mirzaei et al., 2018). lignocellulosic

substrate, (Sohni et al., 2019; Zhang et al., 2019), activated carbon (Singh et al., 2017), graphite (Oliveira et al., 2019), and graphene oxide have been all tested and shown to have different adsorption activities toward organic dyes in wastewater (Konicki et al., 2017; Mahmoodi et al., 2017). Some of these adsorbents have a rather high dye removal efficiency, however, low-cost renewable green bio-adsorbents are still rare for this field of application and further studies are urgently required (Alatalo et al., 2016).

The biorefinery concept has received considerable attention in the last decade due to advances in biotechnology and genetic engineering, offering a renewable and sustainable alternative to the production of common petrochemicals (Ragauskas et al., 2006). Abundant lignocellulosic biomass is a second-generation non-food feedstock that, when used by future biorefineries, has the potential to significantly offset the carbon footprint of the traditional refining (Amore et al., 2016). As one of the most important renewable fractions found in biomass, lignin is still significantly underutilized in the current biorefinery industries, which has mainly focused on transforming biomass carbohydrates to liquid fuels (Ragauskas et al., 2014). It is anticipated that with the growing demand of biomass for production of fuels, the production of lignin would also substantially increase, potentially serving as a versatile platform for the production of biopolymers and renewable high-performance materials. The Renewable Fuel Standard (RFS) established in 2005 and further expanded in 2007 by the Energy Independence and Security Act (EISA) aims to ascend to 36 billion gallons of renewable fuel in 2022. Assuming a yield of 335 liters per dry Mg of biomass, 223 million Mg of biomass will be used annually, producing about 62 million Mg of lignin (Langholtz et al., 2014). To avoid using lignin as a low-grade boiler

fuel, new thermal and chemical processes are needed to generate value-added products from lignin.

Lignin macromolecule contains various amounts of functional groups including carbonyl, methoxy, carboxyl, and hydroxyl groups, which offers promising opportunities to take advantage of its versatile functionality for multiple applications (Gillet et al., 2017). Without any further chemical treatments, lignin could be directly incorporated into a polymeric matrix to be served as an antioxidant (Gadioli et al., 2016), a flame retardant (L. Liu et al., 2016), dye adsorbent (Domínguez-Robles et al., 2018; Yu et al., 2016) and a UV stabilizer (Andrady et al., 2019). Given the diversity of lignin, variability in performance as a functionalized polymer is expected to depend on the plant sources, lignin isolation methods, and physicochemical structures of lignin. Thus, chemical modifications of lignin to improve its valorization have attracted growing attentions (Buono et al., 2016; Figueiredo et al., 2018). Lignin amination refers to a process that introduces an amine group into the lignin structure. One of the bases of lignin amination is the Mannich reaction which refers to the reaction between lignin and amine in the presence of formaldehyde. The obtained aminated lignin, has properties that make it ideal for use in several applications, including surfactants (Z. Liu et al., 2013), dispersants (Ye et al., 2017), heavy metal adsorbents (Ge et al., 2015), and asphalt emulsifiers (Z. Liu et al., 2016; Sun et al., 2014). Due to its aromatic/phenolic nature and cationic side chain, aminated lignin could have great potential as a low-cost bio-adsorbent for the removal of organic dyes especially azo dyes that are typically anionic in charge in wastewater.

Here, we used a Co-solvent Enhanced Lignocellulosic Fractionation (CELF) method as a highly effective lignin-first pretreatment approach capable of extracting highly pure technical-grade lignin from corn stover. CELF applies aqueous mixture of tetrahydrofuran (THF) and dilute acid to greatly enhance the fractionation of lignin, hemicellulose, and cellulose fractions in biomass while promoting lignin fragmentation by limiting certain lignin condensation reactions typically suffered at high reaction severities. The obtained CELF lignin is depolymerized, containing lower aryl ether linkages and higher phenolic hydroxyl groups than typical native milled wood lignin (MWL), cellulolytic enzyme lignin (CEL), or Kraft lignin, which favors the subsequent amination process (Meng et al., 2019; Seemala et al., 2018). The isolated CELF lignin was then aminated by diethylenetriamine (DETA) in the presence of formaldehyde under acid conditions via the Mannich reaction. An orthogonal array system was also applied to test the optimal conditions for the Mannich reaction. The obtained final aminated lignin was thoroughly characterized by various analytical techniques including Fourier-transform Infrared Spectroscopy (FTIR), Nuclear Magnetic Resonance spectroscopy (NMR), Scanning Electron Microscopy (SEM), Thermal Gravimetric Analysis (TGA), and Brunauer-Emmett-Teller (BET) surface area analysis. Finally, the performance of the obtained aminated CELF lignin as a bio-renewable adsorbent for the removal of methylene blue and direct blue dyes was evaluated and compared to other reported adsorbents from literature. The combinatorial process takes advantage of the selectivity of the Mannich chemistry and the unique versatile functionality of CELF lignin such as low ether linkages and high phenolic OH content. It is fully expected that this study will provide a baseline

for future studies to synthesis renewable lignin-based dye adsorbent in advanced wastewater treatment systems.

7.3 Experimental Section

7.3.1 Materials Feedstocks and Chemical

Kramer corn stover was provided by the National Renewable Energy Laboratory (NREL, Golden, CO). The corn stover was knife milled to pass through a 1 mm particle size interior sieve using a laboratory mill (Model 4, Arthur H. Thomas Company, Philadelphia, PA). All the chemicals used in this study were used as received from Sigma-Aldrich without any further purification.

7.3.2 Production of CELF lignin

CELF pretreatment of corn stover was performed in a custom built 1 L Hastelloy Parr reactor (Parr instruments Company, Moline, IL) at 7.5 wt% solids loading and 0.5wt% H_2SO_4 acid loading. The CELF reaction was sustained at 180 ^oC for 25 min in an equivolume mixture of THF and water. After pretreatment, the reactor was quenched in a 25 °C water bath and the liquid phase was separated from the pretreated solids through vacuum paper filtration. CELF lignin was then isolated from the liquid phase by first neutralization with ammonium hydroxide followed by THF evaporation and subsequent vacuum filtration of the precipitated lignin from the neutralized liquor. The obtained CELF lignin was washed with water and diethyl ether and dried at 45°C in an incubator. Once dried, the lignin was finally crushed to a fine powder in a mortar & pestle and stored in a container prior to further test and modification.

7.3.3 Amination of CELF lignin

Corn stover CELF lignin (~200 mg) was mixed with 2 mL of dioxane in a round-flask under constant stirring for 20 min at room temperature until the lignin was fully dissolved. Specified amounts of DETA, acetic acid, and formaldehyde were then added into the solution with continuous stirring. Formaldehyde was added stepwise to avoid unnecessary crosslinking reactions. Subsequently, the flask was heated in a sand bath, kept at a specified temperature (45, 60, 75, and 90 °C) and stirred for a specified time (1, 2, 3, and 4 h). Afterward, the reaction mixture was evaporated under reduced pressure to remove the majority of the organic solvent followed by dialysis with a molecular weight cut off of 1000 Da. The obtained aminated CELF lignin was finally freeze-dried and store at room temperature before further characterization.

7.3.4 Lignin characterization before and after amination. FTIR analysis

The IR spectra were collected using a Spectrum One FTIR spectrophotometer (PerkinElmer, Wellesley, MA) equipped with a diamond-composite attenuated total reflectance (ATR) cell from 1000 to 4000 cm^{-1} with 128 scans at 4 cm^{-1} resolutions.

NMR analysis

NMR experiments were acquired with a Bruker Avance III HD 500 MHz spectrometer equipped with a 5 mm N_2 cryogenically cooled BBO H&F probe according to previously published literatures (Ataeefard et al., 2016; Hosseinnezhad et al., 2017)A standard Bruker pulse sequence (hsqcetgpspsi2.2) and an inverse-gated decoupling pulse sequence (Waltz-16) were applied for HSQC and ^{31}P NMR experiment, respectively.

SEM analysis

The morphology of lignin samples was observed with a scanning electron microscopy (SEM, Zeiss Auriga, Germany) at an accelerating voltage of 5 kV. The samples were sputter-coated with Au using an SPI-Module Sputter Coater for 50 s. Imaging was subsequently captured at various magnifications from 2K to 20K.

Thermal gravimetric analysis

The TGA was performed by a TGA Q50 thermo-gravimetric analyzer (TA instruments, UDA). Lignin samples (~5 mg) were loaded to a Platinum sample pan (TA instruments) and heated in nitrogen from 25 to 105 °C at 20 °C/min. After incubating at 105 °C for 10 min, it was heated further from 105 to 800 °C at a heating rate of 20 °C/min. *Zeta potential analysis.* The zeta potential of lignin suspensions was measured at different hydrogen ion concentrations while keeping a concentration of 1 mg/mL, using a ZetaPALS (Brookhaven Instruments Corporation, NY). The mean zeta potential of each suspension were calculated from 10 measurements.

Surface area and pore size analysis

The N_2 adsorption-desorption measurement of samples was carried out at 77 K on a Quantachrome Autosorb iQ. The samples were first degassed at 353K for ~17 h before being loaded into the analysis station. The pore volume and pore size distribution were determined using a Barrett−Joyner−Halenda (BJH) method. The specific surface area was calculated using Brunauer−Emmett−Teller (BET) in the P/P0 range of 0.05−0.30.

7.3.5 Dye decolorization study

Various amounts of CELF lignin and aminated lignin were mixed with 25 mL of MB or DB 1 dye solution with a concentration of 50 mg/L. The mixture was left in an incubator at 25 °C and 150 rpm for 24 h. The concentration of dye in the supernatant of the solution at the equilibrium was determined by a UV spectrophotometer. The amount of dye adsorbed (q_e) by lignin substrates was calculated based on the following Equation 5:

$$q_e = \frac{v(Co-Ce)}{m} \quad (5)$$

where c_o and c_e represent the initial and equilibrium concentrations of dye solution (mg/L), respectively. v is the volume of the total solution (mL), and m is the dry weight of the lignin sample (g). The maximum wavelength for MB and DB 1 dye was set at 663 and 624 nm, respectively. The extinction coefficient of MB and DB 1 dye was determined to be 149.3 and 12.3 L mol^{-1} cm^{-1} based on the Beer's law calibration (Fig. S1 and S2). The decolorization efficiency (η) is defined by:

$$\eta = \frac{Co-C}{Co} \times 100\% \quad (6)$$

where c_o represents the initial concentration, and c is the concentration of dye in the supernatant after decolorization. The adsorption isotherms of DB 1 dye onto aminated lignin were measured with varying concentrations of dye ranging from 0.05 to 1 mg/mL at 25 °C. To further investigate the kinetics of dye adsorption, the equilibrium concentrations of dye solution were measured from 5 min to 8 h after mixing 20 mg of aminated lignin with 40 mL of DB 1 with an initial concentration of 1 mg/mL. The effect of initial pH on dye adsorption was studied by mixing ~10 mg of lignin with 25 mL of initial DB 1 dye

with a concentration of 50 mg/mL at 25 ºC. ~0.1M HNO_3 and 0.01M of NaOH were used to adjust the pH between 4 and 10. For recycling experiment, dilute NaOH (pH=10) was used to release the adsorbed dye from adsorbent. The adsorption of the dye by the regenerated lignin was repeated four times by mixing ~20 mg of solid with 25 mL of MB or DB 1 dye solution with a concentration of 50 mg/L.

7.4 Result and Discussion

7.4.1 Synthesis and characterization of adsorbents. Orthogonal experiments.

Systematic experimental designs such as response surface methodology and orthogonal arrays are widely used to obtain the optimal response (Ataeefard et al., 2016; Hosseinnezhad et al., 2017). An orthogonal experiment design (L16, 5^4) including five factors (A: temperature, B: time, C: amine content, D: formaldehyde content, and E: acetic acid content) at four different levels were first applied to determine the optimal Mannich reaction conditions. The Mannich reaction can only occur between a high electron density carbon and an immonium ion formed from formaldehyde and an amine, thus the amine groups are expected to be introduced only at the *ortho* or *para* position of a phenolic hydroxyl group, converting H or G types of free phenolic hydroxyl group (or both) to C_5 substituted hydroxyl groups (Fig. 1) (Du et al., 2014). This provides a unique opportunity to determine the extent of lignin amination by tracking the content of free H and G phenolic hydroxyl groups. Quantitative ^{31}P NMR technique was used to track the content of free H and G phenolic hydroxyl groups, aiming to assess the extent of lignin amination. Table 1 shows the conversion of H and G types of free phenolic hydroxyl for each experiment of the designed orthogonal array. As indicated by the Table 1, the effect of each experiment

parameter on the extent of lignin amination increases in this order: acetic acid content (E) < reaction time (B) < DETA content (C) < formaldehyde content (D) < reaction temperature (A) according to the extremum of each factor (R value). The reaction temperature was found to be the most important factor, and the extent of amination appears to achieve its maximum at 75 °C. This could be because the Mannich reaction is an endothermic reaction thus it can be promoted by increasing the temperature. A further increase in temperature has been shown to have a negative effect on animation, which could be due to unnecessary formaldehyde and DETA evaporation thus resulting in a decrease of reaction efficiency (Qiao et al., 2018; Zhou et al., 2017). In conclusion, the optimal combination parameters of the experiment are 75 ^{o}C, 4 h, 4 mmol DETA, 16 mmol formaldehyde, 0.20 mL acetic acid according to the average values of each factor at different levels (K value). A large scale batch reaction was then performed at this optimal condition, and the obtained aminated CELF lignin was subsequently characterized by several state-of-the-art analytical techniques.

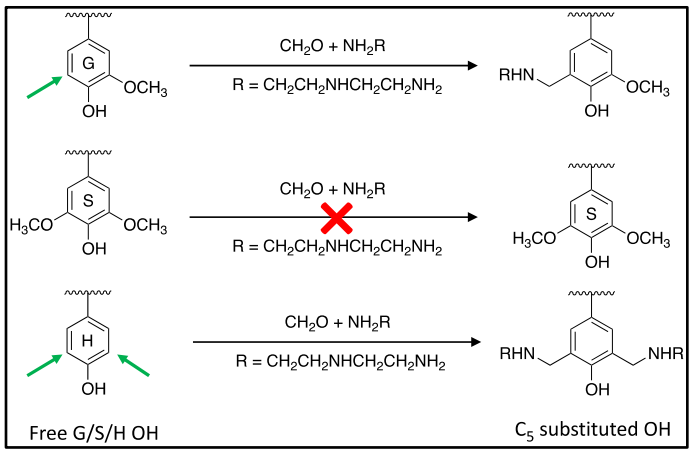

Figure 7-1. Mannich reaction between phenolic G/S/H lignin and DETA, leading to the formation of phenolic C5 substituted lignin units.

Experiment**	Temp. (A)	Time (B)	DETA (C)	Formal. (D)	Acid (E)	(G+H) phenolic conversion (%)
1	A1	B1	C1	D1	E1	43.8
2	A1	B2	C2	D2	E2	46.9
3	A1	B3	C3	D3	E3	52.5
4	A1	B4	C4	D4	E4	55.6
5	A2	B1	C2	D3	E4	57.1
6	A2	B2	C1	D4	E3	81.0
7	A2	B3	C4	D1	E2	59.4
8	A2	B4	C3	D2	E1	61.1
9	A3	B1	C3	D4	E2	84.3
10	A3	B2	C4	D3	E1	85.0
11	A3	B3	C1	D2	E4	89.8
12	A3	B4	C2	D1	E3	77.1
13	A4	B1	C4	D2	E3	48.9
14	A4	B2	C3	D1	E4	63.4
15	A4	B3	C2	D4	E1	78.3
16	A4	B4	C1	D3	E2	90.8
K1***	49.7	58.5	76.3	60.9	67.0	
K2	64.6	69.1	64.9	61.7	70.3	
K3	84.0	70.0	65.3	71.3	64.9	
K4	70.4	71.1	62.2	74.8	66.4	
R****	34.3	11.6	13.1	13.9	2.1	
Best quality level	A3	B4	C1	D4	E2	
Optimal combination	**75 °C, 4 h, 4 mmol DETA, 16 mmol Formal aldehyde, 0.2 mL acetic acid**					

Table 7-1. $L_{16}(P5)^{L4}$ orthogonal experiment design of the Mannich reaction between CELF lignin and DETA under acid conditions.*

*For each run, 200 mg of lignin was dissolved in 2 mL of dioxane.
**Temperature A1-A4: 45, 60, 75, and 90 °C; Time B1-B4: 1, 2, 3, and 4 h; DETA content C1-C4: 4, 8, 12, and 16 mmol; Formaldehyde content D1-D4: 4, 8, 12, and 16 mmol; Acetic acid content E1-E4: 0.1, 0.2, 0.3, and 0.4 mL.
***K: average value of each factor at different levels;
****R: extremum of each factor.

FTIR analysis

The structural characteristics of the CELF lignin and aminated lignin were analyzed by FTIR as shown in Fig. 2. Results showed that aminated CELF lignin exhibited some basic adsorption peaks of CELF lignin, which indicates that the skeleton structure of lignin remains basically intact during the Mannich reaction. For example, hydroxyl group stretch (3400 cm^{-1}), asymmetrical stretching vibrations of $-CH_3$ and $-CH_2-$ (2937 cm^{-1}), and symmetrical stretching vibrations of $-CH_3$ and $-CH_2-$ (2844 cm^{-1}) are observed in both lignin samples. Nonetheless, there exist obvious differences between the lignin and aminated lignin samples. For example, the intensity of FTIR peaks associated with the aromatic C–H vibrations including 1603 cm^{-1} and 1512 cm^{-1} from the aminated lignin is significantly lower than that from the original CELF lignin. This is because the Mannich reaction mainly occurred in the aromatic region of lignin.[37] In addition, the intensity of FTIR peaks associated with G units including 1267 cm^{-1} (C-O stretch), 1113 cm^{-1} (deformation vibrations of C–H), and 1030 cm^{-1} (aromatic C-H in-plane deformation) and H units such as 1164 cm^{-1} (C-O stretch) is decreased after amination reaction.[38] On the other hand, the intensity of syringyl C-O stretch (1325 cm^{-1}) remains relatively strong after Mannich reaction (Zhou et al., 2017). This is because the amine group could be only introduced at C_3 or C_5 position of H lignin and C_5 position of the G units. Finally, a strong peak around 1650 cm^{-1} representing the N–H bending vibrations in amine structure (NH_2) appeared in the aminated lignin, validating the successful addition of the amine (Chatterjee et al., 2016; X. Wang et al., 2014). The peak of carbonyl group around 1680 cm^{-1} also

disappears after Mannich reaction possibly due to the reaction between C=O and primary amines to form imine derivatives known as Schiff bases. (Chatterjee et al., 2016).

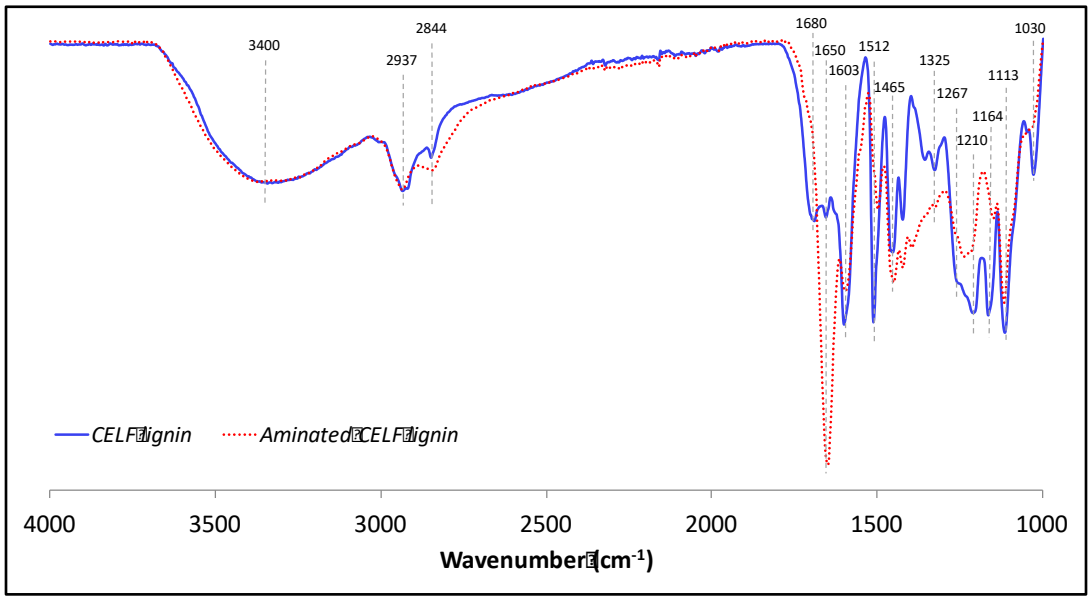

Figure 7-2. FTIR spectra of corn stover CELF lignin and aminated CELF lignin.

2D HSQC analysis

Two-dimensional HSQC NMR has been comprehensively used in lignin characterization due to its versatility in offering structural insight into the lignin subunits and inter-linkages (Constant et al., 2016). The reaction mechanism of Mannich reaction and the chemical structural transformation of CELF lignin during the amination reaction was further characterized by 2D HSQC NMR in this study. As shown in **Fig. 3**, CELF lignin possesses typical structural aromatic patterns of corn stover lignin. Peaks related to S, G, H, p-coumaric acid (pCA) ferulic acid (FA), and tricin (T) are all well defined in the aromatic region (Meng et al., 2017). Condensed S and G signals were also found in CELF

lignin, which are commonly observed from lignin isolated by cosolvent pretreatment at temperature conditions of 180 ºC or higher with acid (S. Sun et al., 2016; X. Wang et al., 2017; Yoo et al., 2017). However, there exist dramatic differences between the original CELF lignin and modified lignin in both the aromatic and aliphatic regions. Specifically, it was found that the cross peaks associated with G and H lignin unit were significantly altered during the Mannich reaction, while the signal of the S lignin units remained relatively stable. In addition, there are two Mannich reactive sites in tricin namely T_6 and T_8 which also disappeared in the aminated lignin due to the reaction of DETA and formaldehyde at these activate aromatic sites. Several intense signals were observed in CELF lignin at δ_C/δ_H 178/9.5-9.6 ppm and δ_C/δ_H 123/7.5 ppm, representing the aldehyde (C_α) and furanic C-H (C_3) signal of the 5-substituted furfural derivatives, respectively (Constant et al., 2016). It has been reported that these types of furfural derivatives such as 5-hydroxymethyfurfural or 5-(methoxymethyl)furfural which arose from sugar dehydration reactions could be condensed with lignin structure during the acid catalyzed organosolv pretreatments (Wildschut et al., 2013). These types of structure were absent after the Mannich reaction possibly due to the reaction between aldehydes and primary amines to form Schiff bases (Chatterjee et al., 2016)

In the aliphatic region, lignin interlinkages especially the β-O-4 linkages were dramatically cleaved during the CELF pretreatment process and in fact, these linkages could be only detected at a noise level (data not shown). This is consistent with previous studies that reported CELF pretreatment performed at high severities (180 ºC) was capable of achieving near-complete removal of its native β-aryl ether linkages without hydrogen

input or further heterogeneous catalytic processing (Jiao et al., 2019; Meng et al., 2019). This process is expected to generate a substantial amount of phenolic hydroxyl groups that favors the subsequent amination process. Methoxyl group remain as the pronounced functional group in both lignin spectra. Compared to unmodified CELF lignin, a significant amount of new signals appeared in the phenolic lignin side chain of aminated lignin, which was mainly ascribed to the methylene bridge of DETA introduced during the Mannich reaction. Our HSQC analysis also reveals that both the primary and secondary amines are capable of activating the formaldehyde. As shown in Fig. 3, there still exist plenty of secondary amines in our proposed aminated lignin structure, which means as new formaldehyde is activated by these protons, additional reactive phenolic G and H units could be subsequently grafted onto these partially aminated lignins until all the protons on the N atoms are replaced. A schematic diagram of Mannich reaction and the structural transformation of CELF lignin during the amination reaction is shown in Fig. S3. The unmodified and aminated lignin was also subjected to a qualitatively visual Ninhydrin test (Fig. S4). The original CELF lignin had a negative/orange color indicating the absence of amines, while the change of color in the aminated lignin proved the existence of primary and secondary amine groups.

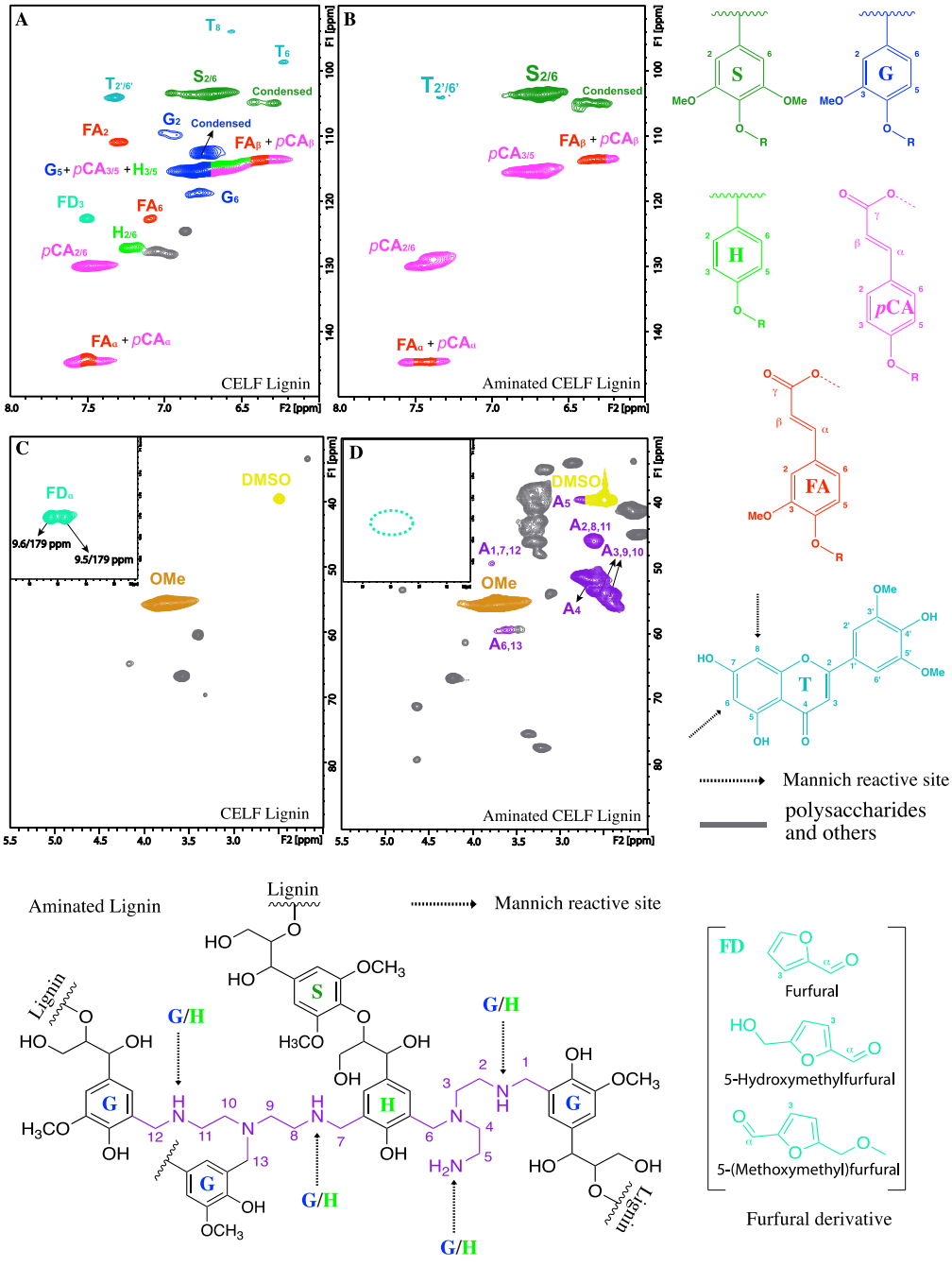

Figure 7-3. HSQC analysis of the original CELF lignin and its aminated product. (A). CELF lignin aromatic region; (B) aminated lignin aromatic region; (C). CELF lignin aliphatic region; (D). aminated lignin aliphatic region.

^{31}P NMR analysis. Quantitative ^{31}P NMR technique was further employed to determine different types of hydroxyl groups including aliphatic, phenolic, and carboxylic acid in CELF lignin and aminated lignin and the results are shown in Fig. 4. The phosphitylation reaction of various OHs in lignin structural units with TMDP is shown in Fig. S5. According to a recent study, S hydroxyl group and condensed G hydroxyl groups are not fully baseline resolved and therefore are combined into C_5 substituted hydroxyl groups in this study to avoid any possible overestimation of S and underestimation of G condensed unit (Balakshin & Capanema, 2015). As compared to the original CELF lignin, a noticeable decrease in phenolic G and H hydroxyl groups was observed in the aminated CELF lignin after Mannich reaction. By contrast, the content of phenolic C_5 substituted hydroxyl groups including the S and condensed G and H units were considerably higher in the modified lignin than that in the original CELF lignin. The ^{31}P results also indicated that the reactivity of the reaction sites in G lignin units was higher than that in H lignin, as a result, the proportion of the G unit decreased more obviously than H unit. The slight loss of aliphatic hydroxyl group may result from the possible loss of hydrophilic lignin fragment during the dialysis of aminated lignin.

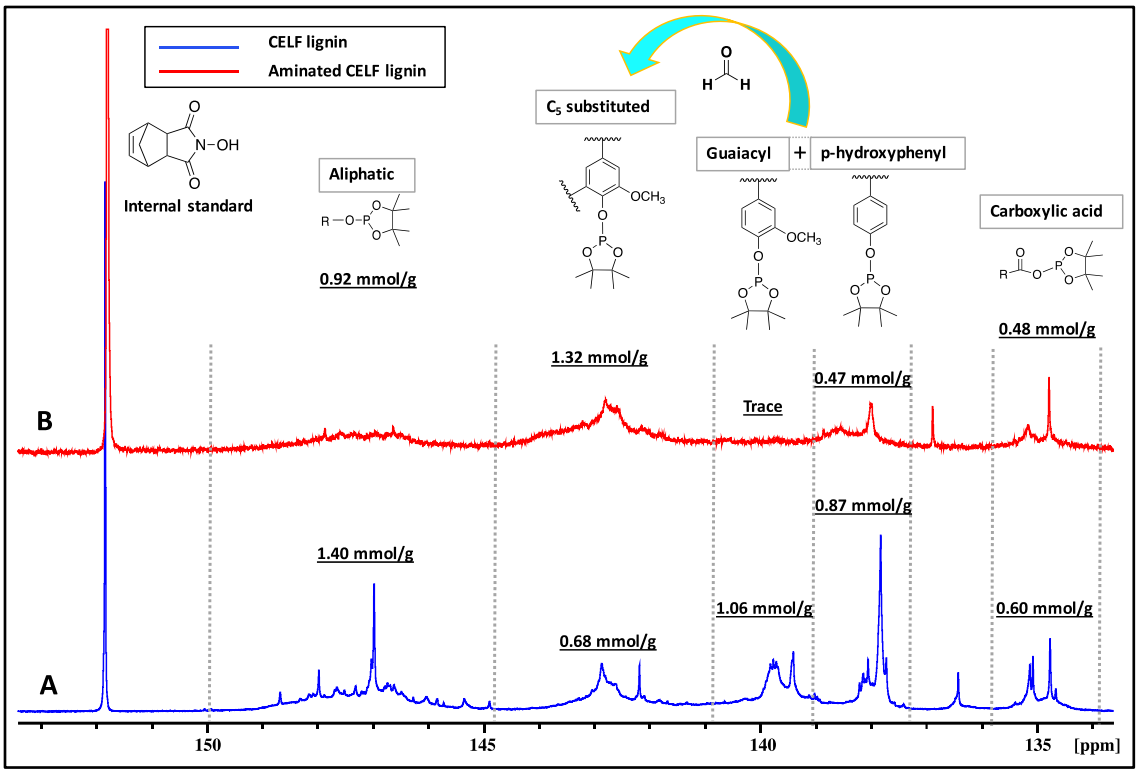

Figure 7-4. Quantitative 31PNMR spectra of the (A) CELF lignin and (B) aminated lignin.

SEM analysis

The modified lignin sample was obtained by rotatory evaporation, centrifugation followed by extended dialysis and freeze-drying. After repeated vacuum evaporation and centrifugation, the formation of a turbid suspension suggesting the possible presence of aminated lignin nanoparticles. The morphological changes of CELF lignin during Mannich reaction are monitored by SEM and displayed in Fig. 5. The unmodified CELF lignin in the solid state has a much larger particle size compared to the aminated lignin and appears granulated with irregular grains of compact structure. The surface of aminated lignin is

much smoother than that of the original lignin. The nano-spheric particles also aggregated into a micron-sized cluster with undefined shapes in aminated lignin, which were possibly induced by the freeze-drying process (Bian et al., 2017).

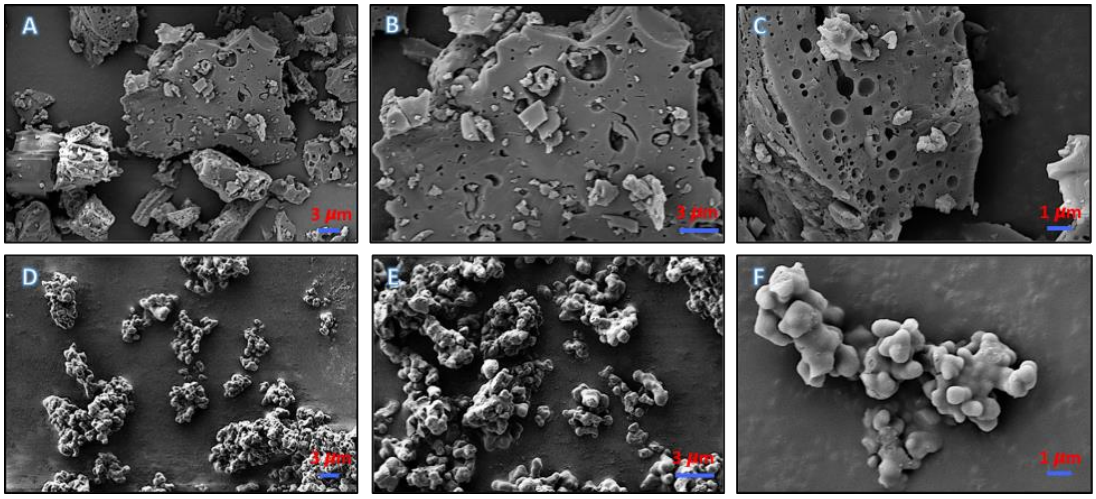

Figure 7-5. Scanning electron microscopy images of lignin (top) and aminated lignin (bottom). (A) and (D): Mag. = 5K; (B) and (E): Mag. = 10K; (C) and (F): Mag. = 20K.

Thermal gravimetric analysis

The first derivative of the thermogravimetric (DTG) curves of the original CELF lignin and its aminated products exhibited different thermal degradation stages in N_2 (Fig. 6). Overall, the aminated CELF lignin degraded faster than the unmodified lignin. In the pyrolysis range (200 °C to 600 °C), the DTG curve for CELF lignin exhibits a single decomposition step with a decomposition peak temperature of 395 °C, while the curve for the aminated CELF lignin exhibits two composition steps which are around 243 °C and 317 °C. The decomposition step above 300 °C is probably due to the cleavage of the C – C linkages and the demethoxylation of aromatic ring (Jiao et al., 2019; Y. Y. Wang et al., 2018). The lower degradation temperature for aminated lignin is probably due to the lower

C – N bond energy compared to C – C bond. The decomposition step around 243°C could be due to the degradation and evaporation of small molecular weight lignin fragments such as aliphatic side chains. The final degradation step around 600°C is probably due to the crack of C – C/H bond of the charcoal that was formed during the pyrolysis (Cao et al., 2013).

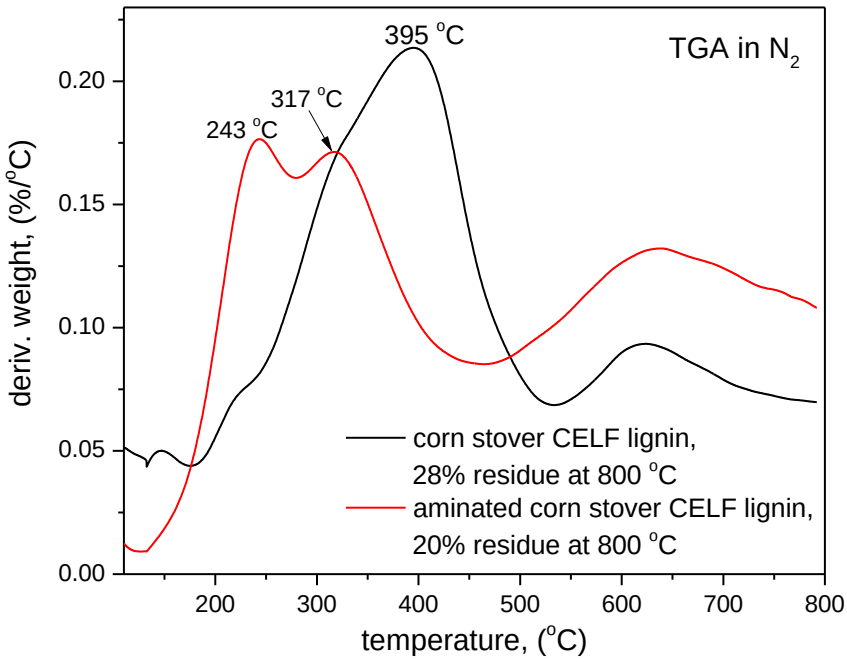

Figure 7-6. The derivative thermogravimetric curves of CELF lignin and aminated lignin.

BET surface area analysis

Table 2 summarizes the BET specific surface areas (S_{BET}) and BJH pore volumes (V_{BJH}) of the lignins before and after amination. Results indicated that the aminated lignin exhibited higher S_{BET} and V_{BJH} than those of the original CELF lignin. For example, the S_{BET} values were 4.2 and 5.9 m^2/g for CELF lignin and aminated lignin, respectively. In addition, the mesoporosity of these lignin samples is also confirmed by the pore size

distribution analysis (Fig. S6). Since the aminated lignin had a larger surface area, it provided more adsorption sites and hence enhanced dye removal can be anticipated.

Sample	BET surface area (m^2/g)	BJH pore volume (cm^3/g)
CELF lignin	4.2	0.002
Aminated CELF lignin	5.9	0.006

Table 7-2. Surface area and pore volume of CELF lignin and aminated lignin as determined by physisorption analysis.

Removal of dye by adsorbent

To demonstrate the potential dye-adsorption property of the modified CELF lignin, two types of dyes were tested in the lignin-dye adsorption experiment: a cationic dye MB and an anionic azo dye DB 1. The qualitative and quantitative effect of lignin loading on the dye decolorization efficiency for the original and aminated lignin is shown in Fig. 7. These results indicated that the aminated lignin showed drastically improved decolorization efficiency for both dyes especially the anionic DB 1 dye. For example, the amination process increased the DB 1 dye removal efficiency from <5% to >90% even at extremely low lignin loadings. The decolorization efficiency for MB dye is proportional to the dose of lignin, while no correlation could be obtained between the efficiency of DB 1 dye removal and the concentration of lignin. This might be attributed to the unmodified lignin's inability to adsorb DB 1 dye even at extremely high lignin dose and the aminated lignin's strong ability to adsorb DB 1 dye even at low lignin loadings. The effect of amino content on the adsorptivity of the aminated CELF lignin was further investigated, and the results indicated that the dye decolorization efficiency was positively correlated to the

amino content of the modified CELF lignin (Fig. S7). The modified lignin has much higher decolorization efficiency toward the anionic dye (DB 1) compared to the cationic dye (MB). This could be mainly due to the electrostatic coupling between the cationic side chain (amine group) of the aminated lignin and the anionic sites of the DB 1 dye.[52] It is well known that pH affects the adsorption of most organic pollutants as well as the surface charges of adsorbents. To further confirm that electrostatic interactions is a key mechanism of adsorptive removal of dyes in DB 1 dye in aqueous solutions, the effect of initial pH on the dye decolorization efficiency and zeta potential of aminated CELF lignin was evaluated within the pH range of ~4.0 and 10.0 (Fig. 8). At extreme acidic or basic conditions (pH<3 or >12), lignin samples were found to be partially or completely dissolved in aqueous solutions, thus their adsorption and surface charge behaviors were not investigated at those conditions. These results also indicated that high pH values resulted in a decrease in the adsorptivity of aminated CELF lignin, which could be due to the increase of the magnitude of the negative zeta potential as pH increases. The aminated CELF lignin has a point of zero charge (pH_{PZC}) around 4.5, and its magnitude of zeta potential at each tested pH value (-2 to -25 mV) is significantly lower than that of the unmodified CELF lignin ranging from -68 to -75 mV (Fig. 8). This is due to the addition of the cationic amine group onto the side chain of aminated lignin. DB 1 dye has four sulfonate groups, thus it remains negatively charged at basic conditions and even at highly acidic solutions as these protonated sulfonate groups have a pK_a value lower than zero (Prola et al., 2013). Therefore, the increase of the net negative zeta potential could further cause a decrease of the electrostatic interactions between the cationic lignin side chain and the negatively charged DB 1 dye in aqueous

solution. This suggests that electrostatic force is a major interaction for DB 1 dye adsorption at lower pH. Furthermore, the decolorization efficiency is still above 60% even at high pH, although there exists substantial electrostatic repulsion between the modified lignin and DB 1 dye. This indicates that mechanisms other than electrostatic interaction such as hydrogen bonding and π-π stacking are also operative for the DB 1 dye adsorption on the aminated CELF lignin.[54] On the other hand, hydrogen bonding, π-interaction, and limited electrostatic interaction between lignin dissociated carboxyl/hydroxyl groups and the cationic sites of the dye molecule are believed to be responsible for the MB dye adsorption (Budnyak et al., 2018). Fig. 9 shows a proposed scheme for the MB and DB 1 dye binding to the unmodified CELF lignin and aminated lignin surface.

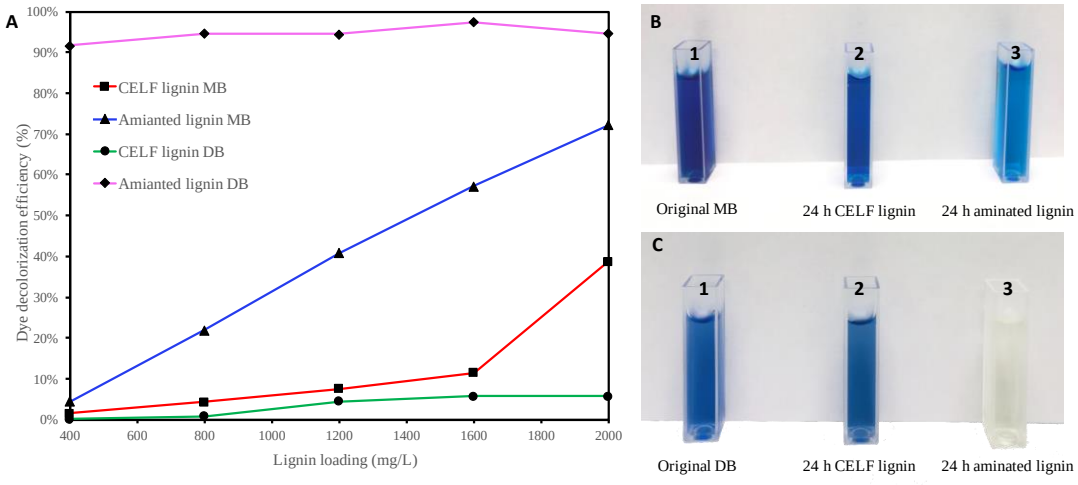

Figure 7-7. Dye adsorption capacity of the CELF lignin and aminated lignin. (A). The effect of lignin loading on dye decolorization efficiency. (B). MB dye before (1) and after (2,3) 24 h lignin adsorption. (C). DB 1 dye before (1) and after (2,3) 24 h lignin adsorption.

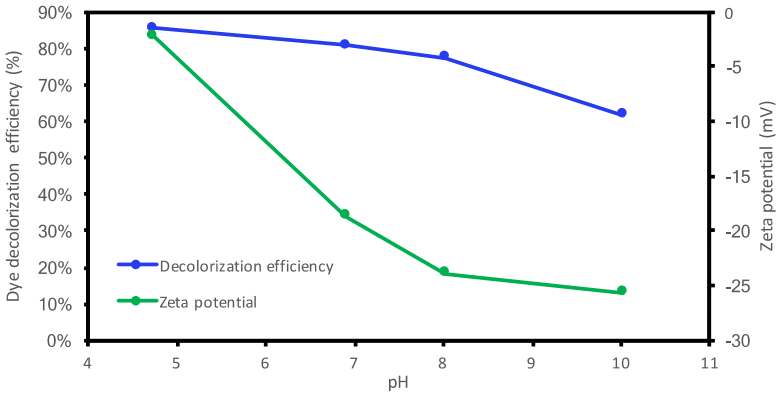

Figure 7-8. The effect of pH on the zeta potential and adsorptivity of the modified lignin toward direct blue dye.

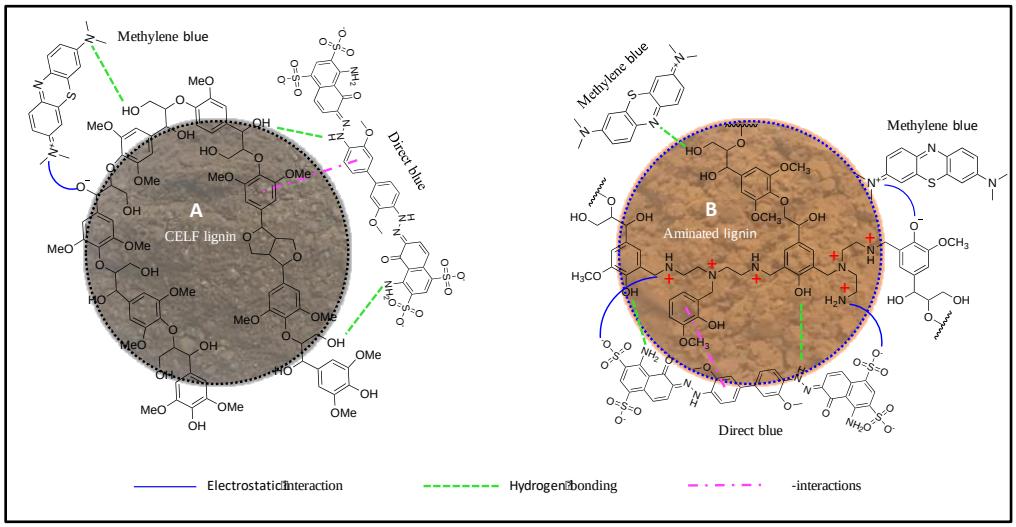

Figure 7-9. A proposed scheme of Direct blue and Methylene blue dye binding to the CELF lignin (A) and aminated lignin (B).

The Langmuir and Freundlich model were used to study the adsorption isotherms of azo-dyes, and their equations (Eq. 1 and 2) are shown below:

$$\frac{Ce}{Qe} = \frac{Ce}{Qm} + \frac{1}{QmKL} \quad (1)$$

$$logQe = log\,KF + \frac{1}{n} logCe \quad (2)$$

where c_e (mg/mL) is the equilibrium concentration, Q_e (mg/g) is the equilibrium adsorption capacity, Q_m (mg/g) is the maximum adsorption capacity of the Langmuir isotherm model, K_L (mL/mg) is a Langmuir adsorption coefficient, K_F (mL/mg) is the Freundlich constant, and 1/n is an indicator that reflects the nonlinear degree of adsorption. Fig. 10 shows the Langmuir (A) and Freundlich (C) adsorption isotherms curves, and the linear analysis (B and D) indicated that the observed dye adsorption data for aminated CELF lignin were better described by the Langmuir isotherm model as confirmed by the higher coefficient R^2. The Langmuir fitting results suggested that the adsorption process between lignin and the azo dye could be characterized as a monolayer type of adsorption. The Langmuir isotherm analysis indicated that the maximum adsorption capacity of the aminated CELF lignin is 502.7 mg/g for DB 1 dye. A direct comparison of the maximum adsorption capacities of different anionic azo dyes on various previously reported adsorbents is presented in Table 3. Based on our literature survey, it was found that the adsorption capacity of aminated CELF lignin is higher than that of all other adsorbents except carbon nanospheres. It should be noted that these adsorbents include commercial activated carbon, anion exchange membrane, and multi-wall-carbon nanotubes which are all well-known for their high aspect ratio, natural porosity, and strong ability to adsorb pollutants from

aqueous system. This suggests that the aminated CELF lignin, as a low-cost renewable resource, is highly suitable for the removal of azo-dyes from the aqueous solutions.

Adsorbent	Dye adsorbate	Maximum Capacity (mg/g)	Reference
Granular activated carbon	Congo Red	9.1	55
Zeolite	Direct Blue 71	13.7	6
Graphene oxide	Acid Orange 8	29.0	11
Chitosan Halloysite Nanotubes	Congo Red	41.5	56
Multi-wall-carbon nanotube	Tartrazine	84.0	57
$Mn_{0.4}Zn_{0.6}Fe_2O_4$ nanoparticles	Tartrazine	90.8	58
$Mn_{0.4}Zn_{0.6}Fe_2O_4$ nanoparticles	Ponceau 4R	101.4	58
SEG modified starch	Direct Red 23	129.9	59
SEG modified starch	Acid Blue 92	147.1	59
Lignin amine coated Fe_3O_4	Acid scarlet GR	176.5	54
Chitosan	Tartrazine	350	60
Multi-wall-carbon nanotube	Direct Blue 53	409.4	53
Graphene oxide sponge	Direct red 80	501.3	5
Aminated CELF lignin	***Direct Blue 1***	***502.7***	***Present***
Chitosan-based hydrogel	Erichrome black T	520	61
Carbon nanospheres	Acid Red 88	555.6	62
$Fe(OH)_3$@Cellulose hybrid fibers	Congo Red	689.7	63

Table 7-3. The adsorption performance of different adsorbents towards azo-dyes as characterized by the maximum adsorption capacity (mg dye/g substrate)

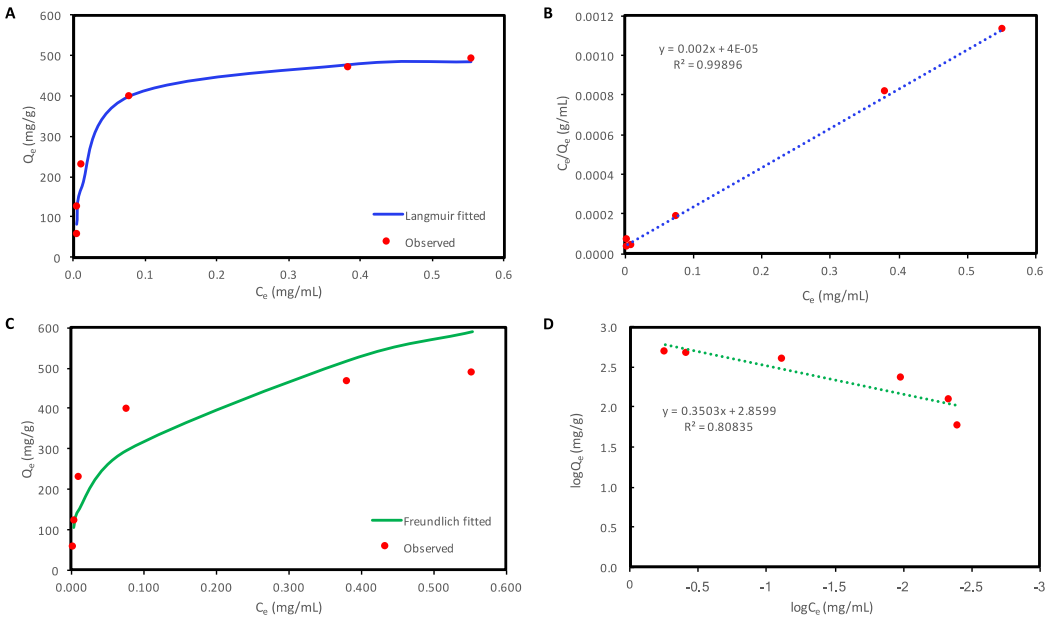

Figure 7-10. Adsorption isotherms of Direct blue 1 by aminated CELF lignin. (A) Langmuir fitted adsorption isotherm curve; (B) The linear fit of Langmuir model R^2 = 0.99); (C) Freundlich fitted adsorption isotherm curve; (D) The linear fit of La Freundlich model (R^2 = 0.81).

The rate of the adsorption process is an important factor that determines if the sorbent could be used on large scales in industrial applications, and it can be determined by kinetic studies. In the study of solid-liquid static adsorption kinetics, the relationship between the time and the amount of adsorption is typically fitted through dynamic models (X. Wang et al., 2014). Two mathematical models are usually adapted to analyze the dynamic models of adsorption process, namely pseudo first-order (Eq. 3) and pseudo second-order (Eq. 4) equation:

$$log(Qe - Qt) = log\ Qe - \frac{K1t}{2.303} \quad (3)$$

$$\frac{t}{Qt} = \frac{t}{Qe} + \frac{1}{Qe^2K2} \quad (4)$$

where Q_e and Q_t are adsorption capacity (mg/g) at equilibrium time and any instant of adsorption time t (min), K_1 and K_2 are the rate constant of the pseudo-first-order and second-order adsorption, respectively. The study about the effect of time on the adsorption process, as shown in Fig. S8, suggests that the amount of dye adsorbed by the adsorbent increases rapidly at the beginning for 30 min, and then the adsorption efficiency becomes slow for 240 min until the adsorption equilibrium is reached. The pseudo first and second kinetic models assume that the adsorption process is governed by diffusion and chemical adsorption mechanism, respectively. The observed experimental data were fitted to the pseudo-first-order and second-order equations, and their linear fitted plots and the parameters of the kinetic model were shown in Fig. 11 and Table 4, respectively. It was found that the correlation coefficient (R^2) of pseudo second-order equation kinetic model was higher than that of the pseudo-first-order model, suggesting the pseudo-second-order kinetic model may be more suitable for describing the kinetics of the adsorption process of

the DB 1 dye on the aminated CELF lignin. This suggested that the adsorption behaviors of azo-dye onto the modified lignin are dominated by chemical adsorption instead of diffusion process. It has been reported that the adsorption process is generally divided into three main stages, including film diffusion stage, Intraparticle diffusion stage, and the final actual adsorption stage (X. Wang et al., 2014). To further test if the intraparticle diffusion is the only rate determining step of the adsorption process, the intraparticle diffusion kinetic model is also fitted with the experimental data (Fig. S9), and results indicated that the adsorption process has more than one speed controlling step. In addition, the relatively large boundary layer thickness as reflected by the large intercept of the linear plot ($t^{1/2}$ vs. q_t) suggests that membrane diffusion might also have a great effect on the adsorption process.[65]

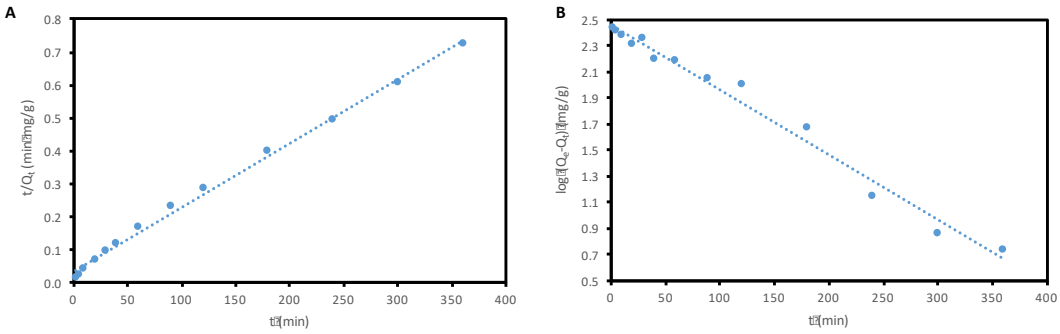

Figure 7-11. Pseudo-second order plot (A) and Pseudo-first order plot (B) for the Direct blue dye adsorption kinetics by aminated CELF lignin.

Kinect model	q_e (mg g^{-1})	K_1 (min^{-1}) or K_2 (g mg^{-1} min^{-1})	R^2
Pseudo-first order	285.8	0.01152	0.984
Pseudo-second order	511.7	0.00013	0.996

Table 7-4. Parameters of adsorption kinetic model.

Reusability of the adsorbent represents an important aspect to minimize the cost of the overall adsorption process. The recycle performances of aminated CELF lignin for DB 1 dye removal were also investigated in this study. The results, as shown in Fig. 12, show that no significant reduction in the adsorption efficiency is found for three cycles compared with that of the fresh adsorbent, although there is a gradual decrease in the dye removal efficiencies possibly due to the incomplete of dye desorption. The dye removal efficiency decreased to 65% for the fourth use, probably due to the saturation of the adsorbent surface. Thus, the recycle study demonstrated that the aminated CLEF lignin remained as an efficient adsorbent even after multiple reuses.

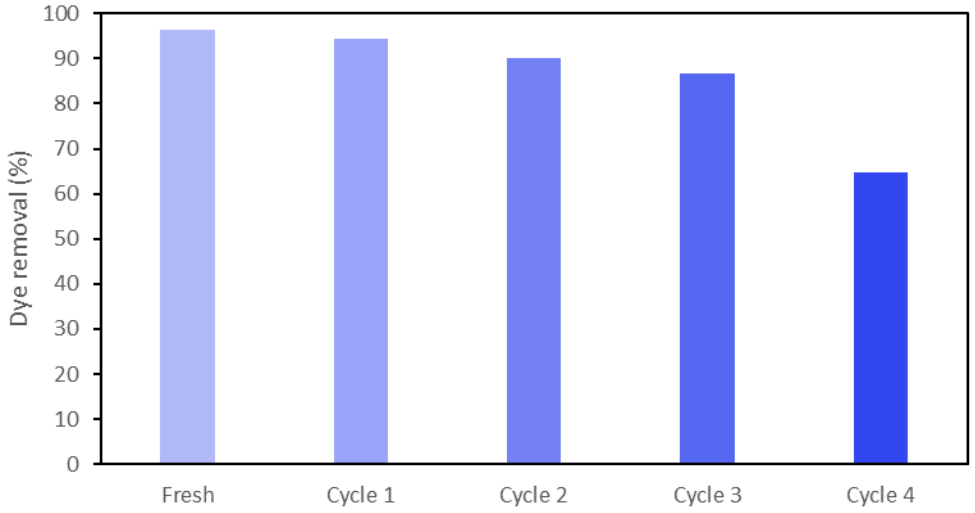

Figure 7-12. The removal efficiency of aminated CELF lignin for DB 1 dye after four adsorption-desorption cycles.

Aminated CELF lignin characterization after dye adsorption. The FTIR spectra of aminated CELF lignin before and after dye adsorption are shown in Fig. S10. After adsorption, two additional peaks at around 1200 and 1035 cm-1 representing the stretching vibration bands of the sulfonate group appear in the aminated lignin due to the attachment of the DB 1 dye. The N=N stretching vibration from DB 1 dye is unclear in the IR spectra since the direct dye is a symmetrical trans azo compound. SEM was also used to analyze the morphology of the aminated CELF lignin's surface after the adsorption of DB 1 dye (Fig. 13). Results showed that the shape of lignin particles did not change dramatically and remained as an aggregated cluster with irregular shapes and heterogeneous surface, but their size appeared to increase significantly after dye adsorption. These observations clearly revealed that the DB 1 dye is adsorbed on the surface of the modified CELF lignin.

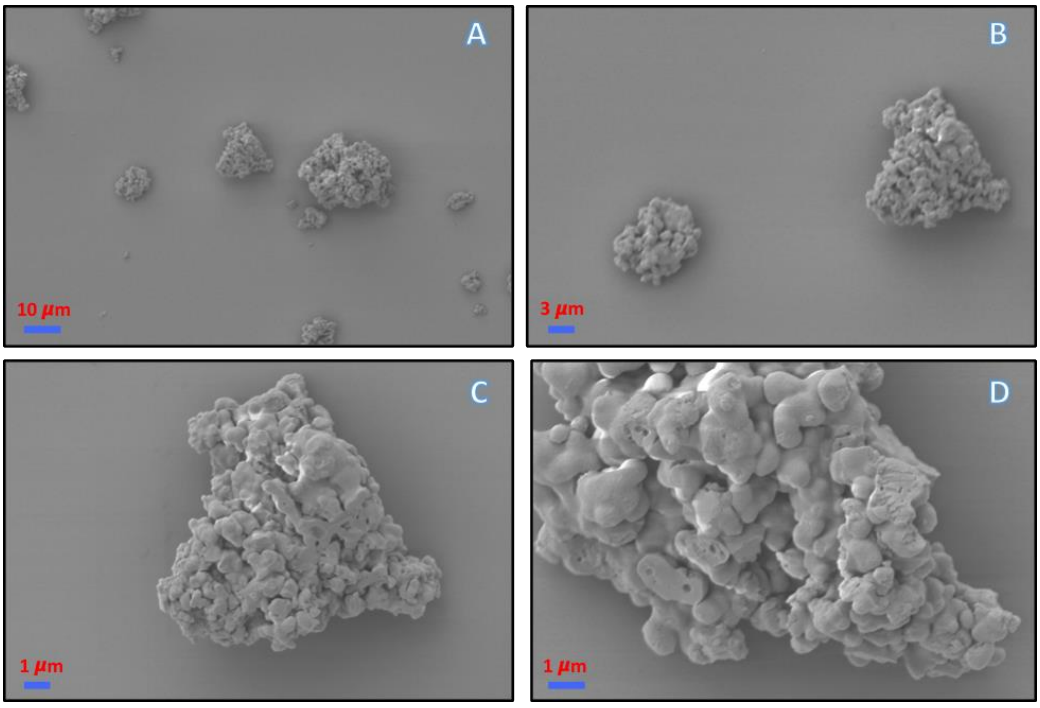

Figure 7-13. SEM images of aminated lignin after adsorption of DB 1 dye. (A. Mag. = 2K. B. Mag. = 5K. C. Mag. = 10K. D. Mag. = 20K.)

7.5 Conclusion

Development of low-cost renewable bio-adsorbents for removal of toxic dyes from contaminated water has been a topic of great interest but remains challenging. In this study, aminated corn stover lignin was synthesized via combinatorial CELF pretreatment and Mannich reaction to remove azo dyes from aqueous solutions. Under acid conditions, both the primary and secondary amines have high reactivity toward the $H_{3/5}$ and G_5 position of CELF lignin. SEM revealed that the original lignin particles are distributed in a large conglomerate, while the surface of aminated lignin becomes smoother and the nano-spheric particles of the modified lignin aggregate into nano- and micron-sized cluster with undefined shapes. The combination of CELF pretreatment and Mannich reaction

significantly increased the adsorption behavior of aminated lignin toward azo direct blue 1 dye with a maximum capacity of 502.7 mg/g, which is significantly higher than that of many adsorbent materials reported in the literature. Recycle studied suggested that once recovered, the bio-adsorbent was capable of maintaining a relatively high dye removal efficiency (>85%) even after three recycles. In conclusion, the proposed aminated CELF lignin could be considered as a cost-effective bio-adsorptive platform for the efficient removal of azo dyes from aqueous solutions.

7.6 References

Abdelhamid, H. N., & Zou, X. (2018). Template-free and room temperature synthesis of hierarchical porous zeolitic imidazolate framework nanoparticles and their dye and CO2 sorption. *Green Chemistry*, *20*(5), 1074–1084. https://doi.org/10.1039/C7GC03805D

Alatalo, S. M., Mäkilä, E., Repo, E., Heinonen, M., Salonen, J., Kukk, E., Sillanpää, M., & Titirici, M. M. (2016). Meso- and microporous soft templated hydrothermal carbons for dye removal from water. *Green Chemistry*, *18*(4), 1137–1146. https://doi.org/10.1039/C5GC01796C

Amore, A., Ciesielski, P. N., Lin, C. Y., Salvachuá, D., & Nogué, V. S. I. (2016). Development of Lignocellulosic Biorefinery Technologies: Recent Advances and Current Challenges. *Australian Journal of Chemistry*, *69*(11), 1201–1218. https://doi.org/10.1071/CH16022

Andrady, A. L., Pandey, K. K., & Heikkilä, A. M. (2019). Interactive effects of solar UV radiation and climate change on material damage. *Photochemical & Photobiological Sciences*, *18*(3), 804–825. https://doi.org/10.1039/C8PP90065E

Ataeefard, M., Shadman, A., Saeb, M. R., & Mohammadi, Y. (2016). A hybrid mathematical model for controlling particle size, particle size distribution, and color properties of toner particles. *Applied Physics A: Materials Science and Processing*, *122*(8). https://doi.org/10.1007/S00339-016-0242-1

Balakshin, M., & Capanema, E. (2015). On the Quantification of Lignin Hydroxyl Groups With 31P and 13C NMR Spectroscopy. *Http://Dx.Doi.Org/10.1080/02773813.2014.928328*, *35*(3), 220–237. https://doi.org/10.1080/02773813.2014.928328

Bian, H., Chen, L., Gleisner, R., Dai, H., & Zhu, J. Y. (2017). Producing wood-based nanomaterials by rapid fractionation of wood at 80 °C using a recyclable acid hydrotrope. *Green Chemistry*, *19*(14), 3370–3379. https://doi.org/10.1039/C7GC00669A

Budnyak, T. M., Aminzadeh, S., Pylypchuk, I. v., Sternik, D., Tertykh, V. A., Lindström, M. E., & Sevastyanova, O. (2018). Methylene Blue dye sorption by hybrid materials from technical lignins. *Journal of Environmental Chemical Engineering*, *6*(4), 4997–5007. https://doi.org/10.1016/J.JECE.2018.07.041

Buono, P., Duval, A., Verge, P., Averous, L., & Habibi, Y. (2016). New Insights on the Chemical Modification of Lignin: Acetylation versus Silylation. *ACS Sustainable Chemistry and Engineering*, *4*(10), 5212–5222. https://doi.org/10.1021/ACSSUSCHEMENG.6B00903/SUPPL_FILE/SC6B00903_SI_001.PDF

Cao, J., Xiao, G., Xu, X., Shen, D., & Jin, B. (2013). Study on carbonization of lignin by TG-FTIR and high-temperature carbonization reactor. *Fuel Processing Technology*, *106*, 41–47. https://doi.org/10.1016/J.FUPROC.2012.06.016

Chatterjee, M., Ishizaka, T., & Kawanami, H. (2016). Reductive amination of furfural to furfurylamine using aqueous ammonia solution and molecular hydrogen: an environmentally friendly approach. *Green Chemistry*, *18*(2), 487–496. https://doi.org/10.1039/C5GC01352F

Constant, S., Wienk, H. L. J., Frissen, A. E., Peinder, P. de, Boelens, R., van Es, D. S., Grisel, R. J. H., Weckhuysen, B. M., Huijgen, W. J. J., Gosselink, R. J. A., & Bruijnincx, P. C. A. (2016). New insights into the structure and composition of technical lignins: a comparative characterisation study. *Green Chemistry*, *18*(9), 2651–2665. https://doi.org/10.1039/C5GC03043A

Domínguez-Robles, J., Peresin, M. S., Tamminen, T., Rodríguez, A., Larrañeta, E., & Jääskeläinen, A. S. (2018). Lignin-based hydrogels with "super-swelling" capacities for dye removal. *International Journal of Biological Macromolecules*, *115*, 1249–1259. https://doi.org/10.1016/J.IJBIOMAC.2018.04.044

Du, X., Li, J., & Lindström, M. E. (2014). Modification of industrial softwood kraft lignin using Mannich reaction with and without phenolation pretreatment. *Industrial Crops and Products*, *52*, 729–735. https://doi.org/10.1016/J.INDCROP.2013.11.035

Figueiredo, P., Lintinen, K., Hirvonen, J. T., Kostiainen, M. A., & Santos, H. A. (2018). Properties and chemical modifications of lignin: Towards lignin-based nanomaterials for biomedical applications. *Progress in Materials Science*, *93*, 233–269. https://doi.org/10.1016/J.PMATSCI.2017.12.001

Gadioli, R., Waldman, W. R., & de Paoli, M. A. (2016). Lignin as a green primary antioxidant for polypropylene. *Journal of Applied Polymer Science*, *133*(45). https://doi.org/10.1002/APP.43558

Ge, Y., Song, Q., & Li, Z. (2015). A Mannich base biosorbent derived from alkaline lignin for lead removal from aqueous solution. *Journal of Industrial and Engineering Chemistry*, *23*, 228–234. https://doi.org/10.1016/J.JIEC.2014.08.021

Gillet, S., Aguedo, M., Petitjean, L., Morais, A. R. C., da Costa Lopes, A. M., Łukasik, R. M., & Anastas, P. T. (2017). Lignin transformations for high value applications: towards targeted modifications using green chemistry. *Green Chemistry*, *19*(18), 4200–4233. https://doi.org/10.1039/C7GC01479A

Hosseinnezhad, M., Shadman, A., Saeb, M. R., & Mohammadi, Y. (2017). A new direction in design and manufacture of co-sensitized dye solar cells: Toward concurrent

optimization of power conversion efficiency and durability. *Opto-Electronics Review*, *25*(3), 229–237. https://doi.org/10.1016/J.OPELRE.2017.06.003

Jiao, G. J., Peng, P., Sun, S. L., Geng, Z. C., & She, D. (2019). Amination of biorefinery technical lignin by Mannich reaction for preparing highly efficient nitrogen fertilizer. *International Journal of Biological Macromolecules*, *127*, 544–554. https://doi.org/10.1016/J.IJBIOMAC.2019.01.076

Konicki, W., Aleksandrzak, M., Moszyński, D., & Mijowska, E. (2017). Adsorption of anionic azo-dyes from aqueous solutions onto graphene oxide: Equilibrium, kinetic and thermodynamic studies. *Journal of Colloid and Interface Science*, *496*, 188–200. https://doi.org/10.1016/J.JCIS.2017.02.031

Langholtz, M., Downing, M., Graham, R., Baker, F., Compere, A., Griffith, W., Boeman, R., & Keller, M. (2014). Lignin-Derived Carbon Fiber as a Co-Product of Refining Cellulosic Biomass. *SAE International Journal of Materials and Manufacturing*, *7*(1), 115–121. https://doi.org/10.4271/2013-01-9092

Liu, L., Qian, M., Song, P., Huang, G., Yu, Y., & Fu, S. (2016). Fabrication of Green Lignin-based Flame Retardants for Enhancing the Thermal and Fire Retardancy Properties of Polypropylene/Wood Composites. *ACS Sustainable Chemistry and Engineering*, *4*(4), 2422–2431. https://doi.org/10.1021/ACSSUSCHEMENG.6B00112

Liu, Z., Lu, X., An, L., & Xu, C. (2016). A novel cationic lignin-amine emulsifier with high performance reinforced via phenolation and Mannich reactions. *BioResources*, *11*(3), 6438–6451. https://doi.org/10.15376/BIORES.11.3.6438-6451

Liu, Z., Zhao, L., Cao, S., Wang, S., & Li, P. (2013). Preparation and evaluation of a novel cationic amphiphilic lignin derivative with high surface activity. *BioResources*, *8*(4), 6111–6120. https://doi.org/10.15376/BIORES.8.4.6111-6120

Mahmoodi, N. M., Ghezelbash, M., Shabanian, M., Aryanasab, F., & Saeb, M. R. (2017). Efficient removal of cationic dyes from colored wastewaters by dithiocarbamate-functionalized graphene oxide nanosheets: From synthesis to detailed kinetics studies. *Journal of the Taiwan Institute of Chemical Engineers*, *81*, 239–246. https://doi.org/10.1016/J.JTICE.2017.10.011

Meng, X., Evans, B. R., Yoo, C. G., Pu, Y., Davison, B. H., & Ragauskas, A. J. (2017). Effect of in Vivo Deuteration on Structure of Switchgrass Lignin. *ACS Sustainable Chemistry and Engineering*, *5*(9), 8004–8010. https://doi.org/10.1021/ACSSUSCHEMENG.7B01527/SUPPL_FILE/SC7B01527_SI_001.PDF

Meng, X., Parikh, A., Seemala, B., Kumar, R., Pu, Y., Wyman, C. E., Cai, C. M., & Ragauskas, A. J. (2019). Characterization of fractional cuts of co-solvent enhanced lignocellulosic fractionation lignin isolated by sequential precipitation. *Bioresource Technology*, *272*, 202–208. https://doi.org/10.1016/J.BIORTECH.2018.09.130

Mirzaei, N., Mahvi, A. H., & Hossini, H. (2018). Equilibrium and kinetics studies of Direct blue 71 adsorption from aqueous solutions using modified zeolite. *Adsorption Science and Technology*, *36*(1–2), 80–94. https://doi.org/10.1177/0263617416684836

Oliveira, E. H. C. de, Marques Fraga, D. M. D. S., da Silva, M. P., Fraga, T. J. M., Carvalho, M. N., de Luna Freire, E. M. P., Ghislandi, M. G., & da Motta Sobrinho, M. A. (2019). Removal of toxic dyes from aqueous solution by adsorption onto highly recyclable xGnP® graphite nanoplatelets. *Journal of Environmental Chemical Engineering*, *7*(2), 103001. https://doi.org/10.1016/J.JECE.2019.103001

Peng, N., Hu, D., Zeng, J., Li, Y., Liang, L., & Chang, C. (2016). Superabsorbent Cellulose-Clay Nanocomposite Hydrogels for Highly Efficient Removal of Dye in Water. *ACS Sustainable Chemistry and Engineering*, *4*(12), 7217–7224. https://doi.org/10.1021/ACSSUSCHEMENG.6B02178/SUPPL_FILE/SC6B02178_SI_001.PDF

Prola, L. D. T., Machado, F. M., Bergmann, C. P., de Souza, F. E., Gally, C. R., Lima, E. C., Adebayo, M. A., Dias, S. L. P., & Calvete, T. (2013). Adsorption of Direct Blue 53 dye from aqueous solutions by multi-walled carbon nanotubes and activated carbon. *Journal of Environmental Management*, *130*, 166–175. https://doi.org/10.1016/J.JENVMAN.2013.09.003

Qiao, X., Zhao, C., Shao, Q., & Hassan, M. (2018). Structural Characterization of Corn Stover Lignin after Hydrogen Peroxide Presoaking Prior to Ammonia Fiber Expansion Pretreatment. *Energy & Fuels*, *32*(5), 6022–6030. https://doi.org/10.1021/ACS.ENERGYFUELS.8B00951

Ragauskas, A. J., Beckham, G. T., Biddy, M. J., Chandra, R., Chen, F., Davis, M. F., Davison, B. H., Dixon, R. A., Gilna, P., Keller, M., Langan, P., Naskar, A. K., Saddler, J. N., Tschaplinski, T. J., Tuskan, G. A., & Wyman, C. E. (2014). Lignin valorization: improving lignin processing in the biorefinery. *Science (New York, N.Y.)*, *344*(6185). https://doi.org/10.1126/SCIENCE.1246843

Ragauskas, A. J., Williams, C. K., Davison, B. H., Britovsek, G., Cairney, J., Eckert, C. A., Frederick, W. J., Hallett, J. P., Leak, D. J., Liotta, C. L., Mielenz, J. R., Murphy, R., Templer, R., & Tschaplinski, T. (2006). The path forward for biofuels and biomaterials. *Science (New York, N.Y.)*, *311*(5760), 484–489. https://doi.org/10.1126/SCIENCE.1114736

Seemala, B., Meng, X., Parikh, A., Nagane, N., Kumar, R., Wyman, C. E., Ragauskas, A., Christopher, P., & Cai, C. M. (2018). Hybrid Catalytic Biorefining of Hardwood Biomass to Methylated Furans and Depolymerized Technical Lignin. *ACS Sustainable Chemistry and Engineering*, *6*(8), 10587–10594. https://doi.org/10.1021/ACSSUSCHEMENG.8B01930/SUPPL_FILE/SC8B01930_SI_001.PDF

Singh, S., Sidhu, G. K., & Singh, H. (2017). Removal of methylene blue dye using activated carbon prepared from biowaste precursor. *Https://Doi.Org/10.1080/00194506.2017.1408431*, *61*(1), 28–39. https://doi.org/10.1080/00194506.2017.1408431

Sohni, S., Hashim, R., Nidaullah, H., Lamaming, J., & Sulaiman, O. (2019). Chitosan/nano-lignin based composite as a new sorbent for enhanced removal of dye pollution from aqueous solutions. *International Journal of Biological Macromolecules*, *132*, 1304–1317. https://doi.org/10.1016/J.IJBIOMAC.2019.03.151

Sun, M. J., Shi, L. S., Jin, Z. Y., Li, N., & Tao, X. (2014). Synthesis of novel cationic asphalt emulsifier and its investigation by online FTIR spectrophotometry. *Advanced Materials Research*, *989–994*, 189–193. https://doi.org/10.4028/WWW.SCIENTIFIC.NET/AMR.989-994.189

Sun, S., Huang, Y., Sun, R., & Tu, M. (2016). The strong association of condensed phenolic moieties in isolated lignins with their inhibition of enzymatic hydrolysis. *Green Chemistry*, *18*(15), 4276–4286. https://doi.org/10.1039/C6GC00685J

Wang, S., Kong, F., Fatehi, P., & Hou, Q. (2018). Cationic High Molecular Weight Lignin Polymer: A Flocculant for the Removal of Anionic Azo-Dyes from Simulated Wastewater. *Molecules 2018, Vol. 23, Page 2005*, *23*(8), 2005. https://doi.org/10.3390/MOLECULES23082005

Wang, X., Guo, Y., Zhou, J., & Sun, G. (2017). Structural changes of poplar wood lignin after supercritical pretreatment using carbon dioxide and ethanol–water as co-solvents. *RSC Advances*, *7*(14), 8314–8322. https://doi.org/10.1039/C6RA26122A

Wang, X., Zhang, Y., Hao, C., Dai, X., Zhou, Z., & Si, N. (2014). Ultrasonic-assisted synthesis of aminated lignin by a Mannich reaction and its decolorizing properties for anionic azo-dyes. *RSC Advances*, *4*(53), 28156–28164. https://doi.org/10.1039/C4RA03133D

Wang, Y. Y., Li, M., Wyman, C. E., Cai, C. M., & Ragauskas, A. J. (2018). Fast Fractionation of Technical Lignins by Organic Cosolvents. *ACS Sustainable Chemistry & Engineering*, *6*(5), 6064–6072. https://doi.org/10.1021/ACSSUSCHEMENG.7B04546

Wildschut, J., Smit, A. T., Reith, J. H., & Huijgen, W. J. J. (2013). Ethanol-based organosolv fractionation of wheat straw for the production of lignin and enzymatically digestible cellulose. *Bioresource Technology*, *135*, 58–66. https://doi.org/10.1016/J.BIORTECH.2012.10.050

Ye, X. X., Luo, W., Lin, L., Zhang, Y. Q., & Liu, M. H. (2017). Quaternized lignin-based dye dispersant: Characterization and performance research. *Journal of Dispersion Science and Technology*, *38*(6), 852–859. https://doi.org/10.1080/01932691.2016.1207545

Yoo, C. G., Li, M., Meng, X., Pu, Y., & Ragauskas, A. J. (2017). Effects of organosolv and ammonia pretreatments on lignin properties and its inhibition for enzymatic hydrolysis. *Green Chemistry*, *19*(8), 2006–2016. https://doi.org/10.1039/C6GC03627A

Yu, C., Wang, F., Zhang, C., Fu, S., & Lucia, L. A. (2016). The synthesis and absorption dynamics of a lignin-based hydrogel for remediation of cationic dye-contaminated effluent. *Reactive and Functional Polymers*, *106*, 137–142. https://doi.org/10.1016/J.REACTFUNCTPOLYM.2016.07.016

Zambare, R., Song, X., Bhuvana, S., Antony Prince, J. S., & Nemade, P. (2017). Ultrafast Dye Removal Using Ionic Liquid-Graphene Oxide Sponge. *ACS Sustainable Chemistry and Engineering*, *5*(7), 6026–6035. https://doi.org/10.1021/ACSSUSCHEMENG.7B00867/SUPPL_FILE/SC7B00867_SI_001.PDF

Zhang, L., Lu, H., Yu, J., McSporran, E., Khan, A., Fan, Y., Yang, Y., Wang, Z., & Ni, Y. (2019). Preparation of High-Strength Sustainable Lignocellulose Gels and Their Applications for Antiultraviolet Weathering and Dye Removal. *ACS Sustainable Chemistry and Engineering*, *7*(3), 2998–3009. https://doi.org/10.1021/ACSSUSCHEMENG.8B04413/SUPPL_FILE/SC8B04413_SI_001.PDF

Zhou, W., Chen, F., Zhang, H., & Wang, J. (2017). Preparation of a Polyhydric Aminated Lignin and Its Use in the Preparation of Polyurethane Film. *Journal of Wood Chemistry and Technology*, *37*(5), 323–333. https://doi.org/10.1080/02773813.2017.1299185

Chapter 8: Conclusions and Future Recommendations

8.1 Summary of Key Developments of this Dissertation

The overarching goals of this thesis were to investigate CELF-CBP synergy in order to maximize the deconstruction of woody lignocellulosic biomass at the lowest process severity: eliminating the need for exogenous enzymes, reducing the cost, and minimizing the degradation products inhibitory to downstream biological systems.

The CELF- CBP pairing produced 90%-100% glucan solubilization from 5-25 minutes CELF pretreated Poplar at the low severity of 2.17-2.87. This is the lowest severity and highest glucan solubilization CELF-CBP process reported in the literature. In-depth investigation by X-ray diffraction (XRD), Gel Permeation Chromatography (GPC), Stimulated Raman Spectroscopy (SRS), and NMR was done to gain insights into the physio-chemical changes that most influence yields and rates of glucan solubilization.

SRS imaging revealed extensive lignin depolymerization and aggregation that increased *C. thermocellum*'s accessibility to glucan, resulting into faster kinetics. Gel Permeation Chromatography (GPC) confirmed extensive lignin depolymerization, and NMR revealed extensive breakdown of β-*O*-4 linkages, lower Syringyl/Guaiacyl (S:G) ratios, and reduction of C-C linkages in lignin at the lowest process severity of 2.17, expanding the unique opportunity of CELF-*C. thermocellum C*BP pairing for lignin valorization.

Detailed characterization of CELF-solids, CELF-CBP solids, CELF-liquid, CBP-broth and CBP residue by 1D/2D NMR, GPC, XRD, SRS imaging, compositional analysis and then correlating physio-chemical modification at various severities to the glucan solubilization extent and rate, provided details of the factors that influence the high

performance of the CELF-CBP pairing. Chapter 2 details the experimental design and results of the characterization for the CELF-CBP paired system for Poplar biomass. Lignin phase change at CELF processing temperatures above lignin glass transition temperature (>150°C) and *C. thermocellum*'s ability to deconstruct crystalline cellulose together with its ligninolytic activity on the residual lignin in CELF solid seem to be the key factors.

In Chapter 3, the CELF process was investigated on two additional biological systems, namely fungal cellulase Ctec2 and *C. thermocellum secretome,* in addition to *C. thermocellum*. The objective of this study was to investigate the activities of each of these biological systems on CELF pretreated lignocellulosic woody biomass. This design of experiment for Poplar biomass at three different CELF severities, paired with three different biological systems, at two different enzyme loadings is a complex multi-factorial problem; therefore, to tease out similarities and distinctions of these promising biological systems for paired processes with CELF, a combined experimental and modeling approach was taken. Fractal kinetics models were applied to the rate of percent glucan solubilization by each system. The fractal exponent h decreased as pretreatment time and enzyme loadings were increased, except for CBP of 25 minutes CELF pretreated Poplar, where the fractal exponent h increased and k_t decreased rapidly, likely due to complete solubilization of the substrate. The transient rate coefficient k_t was 2x greater temporally for the CBP process using *C. thermocellum* than both fungal cellulase Ctec2 and the *C. thermocellum* secertome. These key parameters were then correlated with the physio-chemical change to the cellulose, xylan and lignin components in CELF solids and fermentation broth with total glucan solubilization as a performance metrics.

C. thermocellum was found to be least sensitive to the pretreatment severities and the resultant physio-chemical change to the CELF Poplar, whereas, C. *thermocellum* secretome showed similar performance *as C. thermocellum* only at high enzyme loading (15 mg/g glucan) and longer incubation times. When the fermentation broth was examined, an unexpected observation of this study was the more similarities between *C. thermocellum* secretome and fungal cellulase Ctec2 than between *C. thermocellum* secretome and *C. thermocellum* whole cell. At higher enzyme loadings of 15 mg/g of glucan and higher CELF severities, the glucan solubilization of CELF Poplar improved by fungal cellulase Ctec2 and *C. thermocellum* secretome, and started to match with *C. thermocellum* performance on lower severity CELF. Overall, for the CELF pretreated Poplar, the cellulolytic activities by the three biological systems studied were: *C. thermocellum* whole cell > fungal cellulase Ctec2> *C. thermocellum* secretome. *C. thermocellum* secretome appeared to be more impacted by the concentrations of xylan and lignin in the CELF pretreated Poplar substrate, whereas fungal cellulase seemed to be more influenced by cellulose accessibility.

The CELF-CBP pairing was then investigated at high solids loadings of 50-100 g/L to understand the limitations of the CELF-CBP paired process and the factors that may limit performance at very high solids loadings. Process intensification is a must for the commercial viability of any process. Chapter 4 reports on this research effort. The comparison of the extent of total carbohydrate solubilization as a function of solids loadings and as a function of CELF severity were compared. Total carbohydrate solubilization was comparable (>96%) when the solids loadings were increased from 20g/L

to 50g/L. For each 25g/L increased in solids loading, a ~ 15% drop in total glucan solubilization was observed for Poplar. NMR studies indicated an accumulation of oligomeric and monomeric xylose in the fermentation broth; therefore, it was hypothesized that the xylose and oligomeric xylan inhibited *C. thermocellum* activity, and that in turn further inhibited glucan solubilization. To test the hypothesis, a xylose metabolizing *Thermoanaerbacterium thermosaccharolyticum* bacterium was used as a co-culture strategy with *C. thermocellum.* The co-culture strategy resulted in a reduction of xylose accumulation by 45%, improving total glucan solubilization to >97% at the high solids loadings of 75 g/L. This is the first report of an optimized integrated CELF-CBP process for a woody biomass that leads to > 97% glucan solubilization from Poplar at high solids loadings of >75g/L.

Chapter 5 details the first reported study on renewable ester biosynthesis from a lignocellulosic biomass using an engineered *C. thermocellum* in a consolidated bioprocessing. This chapter focused on developing a robust *C. thermocellum* biocatalyst compatible with CELF pretreated Poplar and possible engineering strategies to enhance the CBP performance and metabolic/proteomic trade-offs from CELF biomass fermentation for the enhanced production of C4-derived alcohols and esters. Ethanol, acetic, lactic and ester intermediates, as well as ethyl- and isobutyl-isobutyrate and acetates were biosynthesized from CELF pretreated Poplar. Lignin removal from Poplar was correlated with higher cell density and higher esters biosynthesis, but was found to be less problematic than the xylan content.

Chapter 6 details the investigation into the utility of CELF process as a green manufacturing approach for the production of hemp-based sugars, hemp-fuel, and hemp-crete from the whole industrial hemp plant, eliminating the need for mechanical decortication. Using relatively milder CELF process, ~70% cellulose enriched CELF pulp was produced. High solids simultaneous saccharification and fermentation using Cellic® Ctec2 enzymes at 15 mg/g of glucan loading, and *S. cerevisiae* D5A, highly concentrated glucose (80 g/L) and a theoretical ethanol yield of 70% was demonstrated. CELF pulp was also formulated into 2X2 briquettes using biomass:binder:water ratios of 1:1:3. In addition to improved water retention (10.94 milliliters of water per gram of reacted fibers- an important property for building material), briquettes were also noticeably denser, less porous and less brittle compared to the briquettes molded from the raw decorticated hemp. This is the first study to demonstrate complete utilization of industrial hemp into multiple green products, and a milder, non-toxic process with potential to be utilized for processing large quantities of underutilized industrial hemp resources.

Lastly, Chapter 7 focused on the application of CELF lignin for the production of low-cost renewable bio-adsorbents for the removal of toxic dyes from contaminated water. CELF pretreatment and the Mannich reaction were combined to generate aminated CELF lignin which was then used for the removal of Methylene Blue and Direct Blue dyes from aqueous solution. The physicochemical, morphological, and thermal properties of the aminated CELF lignin were characterized to confirm the successful grafting of diethylenetriamine onto the lignin. The adsorbent properties of aminated CELF were attributed to the incorporated amine functionalities as well as the increased specific surface

area of the aminated CELF lignin. Under acid conditions, both the primary and secondary amines have high reactivity toward the $H_{3/5}$ and G_5 position of CELF lignin. CELF aminated lignin shows significantly higher adsorption behavior toward azo direct blue 1 dye with a maximum capacity of 502.7 mg/g, which is much higher than that of many adsorbent materials reported in the literature for this application.

8.2 Concluding Remarks and Future Recommendations

In summary, the results presented in this thesis demonstrate that the lignocellulosic biomass is a renewable sustainable resource that has the potential to be transformed as fuels, chemicals and materials, impacting GHG emission and greening of multiple sectors by providing alternatives for fossil derived fuels, chemical and materials. This thesis also demonstrates that biomass recalcitrance, although challenging, could be overcome by combining promising thermochemical pretreatment technologies with advanced biotechnology. Developing advanced technologies for transforming lignocellulose into high volume fuels and high value chemicals is a multi-factorial challenge. Therefore, understanding the details of the important factors and inter-dependence of these factors, both positive and negative, that influence and maximize lignocellulosic conversion is important. The work presented in this thesis provides novel insights on CELF pretreatment, especially when optimizing the CELF process for a woody lignocellulosic biomass at very low process severities by leveraging the cellulolytic machinery of *C. thermocellum.* Several questions arose throughout the duration of this thesis work. Many questions were further investigated and are reported in this dissertation. Some additional important questions to explore that could advance this field further are listed below as recommendations:

1. Develop a structure-function understanding of lignin residue and *C. thermocellum* activity for CELF enabled lignin-first strategies and CELF lignin upgrading. Further study is recommended to determine the fermentability of soluble lignin in CELF liquid streams. In general, a wider study spanning CELF on a variety of wild type and engineered-lignin feedstocks should be conducted to get a comprehensive picture of the opportunities of CELF pretreatment in lignin valorization. A modified-CELF should be developed with lignin in mind, specially taking advantage of the phase behavior/miscibility gap of THF:water system for product separation/concentration. And if needed, employing a ternary system to overcome the product separation that is one of the key hurdles in this field.
2. The liquid stream from CELF contains a large amount of C5 pentose sugars. A chemical or biological catalysis to maximize sugar utilization should be explored beyond HMF as a platform chemical.
3. Test and confirm, or refute the hypothesis that xylan accumulation led to glucose fermentation inhibition by *C. thermocellum* and that led to further reduction in total glucan solubilization by *C. thermocellum* at high solids loadings.
4. It is recommended that more fundamental studies of carefully built design of experiments that include the addition of exogenous measured quantities of expected deconstructed products (xylose, defined oligomeric xylose, expected depolymerized monomeric and dimeric lignin products from the wild type and engineered lignocellulosic feedstocks) be carried out with promising biocatalysts to advance the field for robust microbial chassis development. The presumption

that all xylose and all lignin deconstructed products negatively impact fermentative organisms is flawed, and will benefit tremendously by more systematic studies.

5. High amounts of formate build up was observed in the CELF pretreated poplar during CBP using *C. thermocellum* and should be examined further to identify upregulated gene expressions and pathways. Since, pyruvate is converted into several fermentation products depending on the enzyme that catalyzes the reaction (for example, pyruvate formate-lyase forms formate), multi-omics- especially functional proteomics- to gain a better understanding of upregulated pathways, proteins etc., during high solids loading deconstruction/fermentation of CELF pretreated Poplar with *C. thermocellum* could be very informative.
6. For ester work, it is recommended to investigate the metabolic and proteomic changes to *C. thermocellum* biocatalyst on a variety of CELF pretreated woody and herbaceous biomass and compare that to Avicel in order to gain a deeper understanding of the metabolic response. In addition, a better understanding of which components cause a longer lag phase for CELF poplar fermentation without strain adaption is essential. This line of work could further optimize the CELF process, and also develop bio-engineering strategies to build a more robust *C. thermocellum* strain for lignocellulose transformation.
7. When ester biosynthesis was compared for CELF pretreated Poplar in a Parr and steam jacketed reactor, we observed significant differences in the ester yield. It is suggested that the high solids loadings experiment be extended on CELF substrate generated using a steam jacketed reactor (with even lower xylan and maximized

glucan) as substrate for wild type *C. thermocellum,* and examine even higher solids loadings towards industrially relevant processes.

8. When working with CELF hydrolysate and an engineered *S. cerevisiae*, it was observed that the CELF hydrolysate had a stimulating effect on the rate of anaerobic xylose fermentation to ethanol as compared to sugar controls. This needs to be characterized further. The original findings hypothesized that side reactions during CELF between monomeric glucose and 1,4-butanediol broken down from tetrahydrofuran, the reaction solvent, produced a fermentation stimulant.
9. A detailed techno-economic analysis (TEA) should be conducted to understand the major cost contributions, and sensitivity analysis to understand the important factors for further optimization of the CELF process. Similarly, life cycle analysis (LCA) to understand the GHG, water, energy, waste disposal etc. is recommended.
10. A small-pilot scale study of the optimized CELF-CBP process to understand the scaling factor (any unexpected limitations etc.) to provide recommendations for further research should be conducted. Although specific to CELF-CBP, it's an important design-build-test-learn strategy that can be generally informative for technology development for cost competitive renewable fuels and chemicals.

In conclusion, the researchers working in this field are urged to take a systems approach, sensitive multi-modal analytics and machine learning to analyze and gain a deeper insight of the complex multivariate problem that includes inputs from:

- Feedstock attribute (wild type/engineered, composition, physical processing etc.)
- Influence of pretreatment conditions on resultant pretreated substrate (chemical, structural/physical, mechanical)
- Enzyme cocktail composition and loading
- Details of biocatalyst CBP chassis (engineered pathways)/microbial fermentation
- Lignin and hemicellulose fate, byproduct etc. and the influence thereof.

Chapter 9: Appendix

Enhanced Fermentation Rate Due to Compound Produced During CELF Pretreatment of Switchgrass.

* The work done in this section is an exploratory study following up on the work done by Patri et al. In reporting a boost compound. Some of this work has been filed in a provisional patent.

9.1 Introduction

Co-solvent Enhanced Lignocellulosic Fractionation (CELF) is a novel pretreatment technology that employs tetrahydrofuran (THF) as a co-solvent in an aqueous dilute sulfuric acid solution to produce highly digestible glucan-rich solids from lignocellulosic biomass (Cai et al., 2013; Kothari et al., 2018; A. Patri, 2018; A. S. Patri et al., 2019).

The liquid remaining after CELF pretreatment is rich in C5 sugars and lignin. When the CELF liquid is neutralized and THF is boiled off, a THF free CELF hydrolysate (TFCH) is produced. It has been observed that when small amounts of TFCH is incorporated into anaerobic fermentation with an engineered industrial strain, there is a significant boost in the rate of production of ethanol, reaching the maximum theoretical ethanol yield within 24 hours. Patri et al. reported that when TFCH produced from pretreatment of switchgrass, maple wood, and model cellulose, was fermented using an engineered *Sacchromyces cerevisiae* strain provided by Mascoma LLC. the fermentation enhancement was greatest when CELF hydrolysate was 2-33% of the total fermentation volume (A. Patri, 2018).

Further studies suggested that CELF pretreatment solubilizes glucose and hydrolyzes THF to 1,4-butanediol. The hypothesis provided by Patri et al. was that the combination of glucose and 1,4-butanediol in the presence of acid led to the formation of an alkyl glycoside, 4-hydroxybutyl glucopyranoside through the process of fisher glycosylation.

The experiments in this section of the appendix of this thesis were to evaluate three different reactions to validate the hypothesis provided by Patri et al. in order to replicate

the rate boost effect for fermentation. First, we tested the boost effect in anaerobic and aerobic seed flasks to investigate whether THF free CELF hydrolysate had the same impact on aerobic growth of two engineered *S. cerevisiae* strains. Additionally, this appendix explored testing industrially relevant sugar concentrations for fermentation in a model mixture based on the amount of sugars present in CELF liquid to understand the fermentation capabilities of the strain.

9.2 Materials and Methods

Alamo Switchgrass provided by the BioEnergy Sciecnes Center

Two strains of *Saccharomyces cerevisiae*

Strain 1: Industrial engineered to utilize both glucose (C6) and xylose (C5) sugars provided by Mascoma LLC.

Strain 2: D5A another common strain for ethanol conversion from glucose provided by the National Renewable Energy Laboratory.

Pretreatments were performed in a 1 L Hastelloy Parr® autoclave reactor (236HC Series, Parr Instruments Co., Moline, IL) equipped with a double stacked pitch blade impeller rotated at 200 rpm. The reactions were prepared by first adding the milled Switchgrass at 7.5 wt % solid loadings. A mixture of DI water and 0.5 wt% (based on liquid mass) 72 wt % sulfuric acid (Ricca Chemical Company, Arlington, TX). Tetrahydrofuran (>99% purity, Fisher Scientific, Pittsburgh, PA) was added in a 1:1 mass ratio with water in the fume hood. The reactions were left to soak overnight at 4 °C. Temperatures for CELF reactions was 150°C for 25 minutes. All reactions were maintained at reaction temperature (± 0.5°C) by convective heating with a 4 kW fluidized sand bath (Model SBL-2D, Techne, Princeton, NJ). The reaction temperature was directly measured by using an in-line K-type

thermocouple (Omega Engineering Inc., Stamford, Connecticut). When the reaction was complete, the Parr reactor was submerged into a room temperature water bath until the internal temperature reached 30-40°C. The reaction solids were separated from the liquid by vacuum filtration at room temperature through glass fiber filter paper. Sugar reactions were neutralized to a pH of 7 using 30 wt% Ammonium Hydroxide immediately following the reaction. Neutralized Sugar Reactions were filter sterilized and stored at 4 °C prior to fermentation. After sugar was added to each flask at the desired percentage, all flasks were brought up to the same final concentration of glucose, xylose, BDO using stock mixtures.

Fermentation

Composition: Xylose (40-50 g/L), Glucose (5-7 g/L), Other sugars (<10 g/L), Lignin derived phenolics (Low MW), 1-4 Butanediol (2 g/L), Mystery compound THF removal (4 g/L)

S. cerevisiae was grown aerobically on 50 g/L Glucose (control) and Glucose control supplemented with 1 ml TFCH @ 37°C that was agitated at 130 RPM in 500 mL baffled flasks (Innova 4000). Sampled periodically for the first 12-15 hours by OD measurements. Optical density readings taken at each sample point were used to measure growth rate at 600 nm. Samples were centrifuged and then diluted to 1:4 and the concentration of glucose consumption in (g/L) was measured using HPLC for each sample (Waters Alliance 2695, HPX-87X column)

Verification of boost effect on anaerobic and aerobic fermentation:

The boost effect was first observed in anerobic culture flasks. To further evaluate the rate enhancement, 1 mL of TFCH was added to aerobic seed cultures of *S. cerevisiae* strain 1 from Mascoma LLC and strain 2 D5A and was compared to control glucose consumption and OD 600 nm measurements.

Pure sugar reaction mixtures to target boost compound production:

Next, to further understand the glycosylation reaction, pure sugar mixtures were reacted to try and replicate the compound from TFCH. Each of the pure sugar mixture cases presented below were reacted at 150°C for 20 minutes prior to addition to fermentation with strain 1 from Mascoma. Each case was evaluated at 2, 15, and 33% of the total fermentation flask volume.

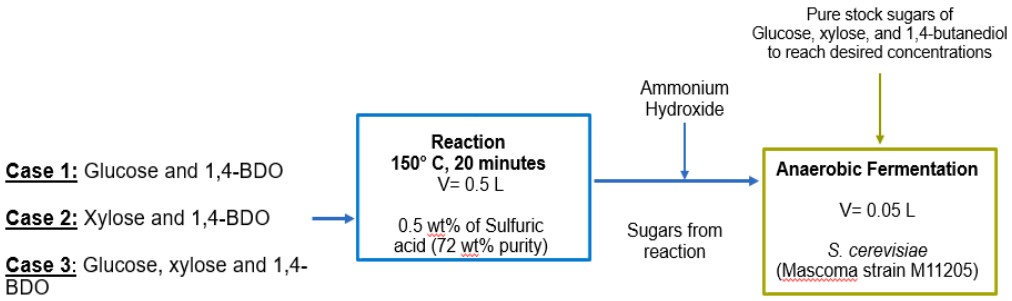

Figure 9-1. Process flow diagram of pure sugar reactions to target boost compound production

Strain 1 tolerance to higher concentration sugar mixtures:

Unreacted sugar mixtures at 1, 2, 3, and 5x the concentrations present in TFCH from switchgrass was also tested with the engineered strain with Mascoma to evaluate sugar tolerance for future studies. The concentrations are presented below.

Goal Starting Concentrations (g/L)			
Sample	Glucose	Xylose	1, 4-BDO
C1-1x	6.5	43	0
C2-1x	6.5	43	4.2
C3-2x	13.5	86	0
C4-3x	19.5	129	0
C5-5x	32.5	215	0

Table 9-1. Pure sugar fermentations for strain tolerance testing with strain 1.

9.3 Results

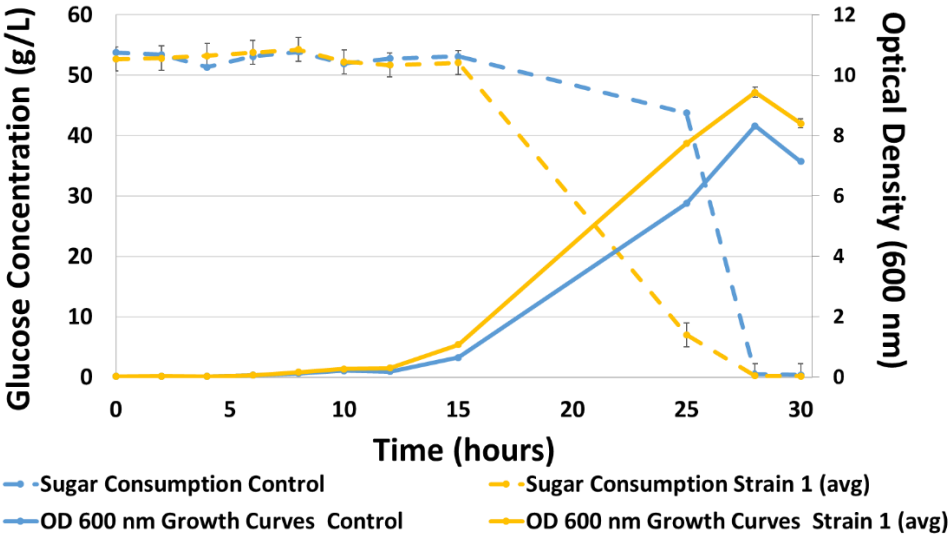

Figure 9-2. Glucose Concentration (Y1) and Optical Density (Y2) as a function of fermentation time for the aerobically grown Mascoma *S. cerevisiae* strain

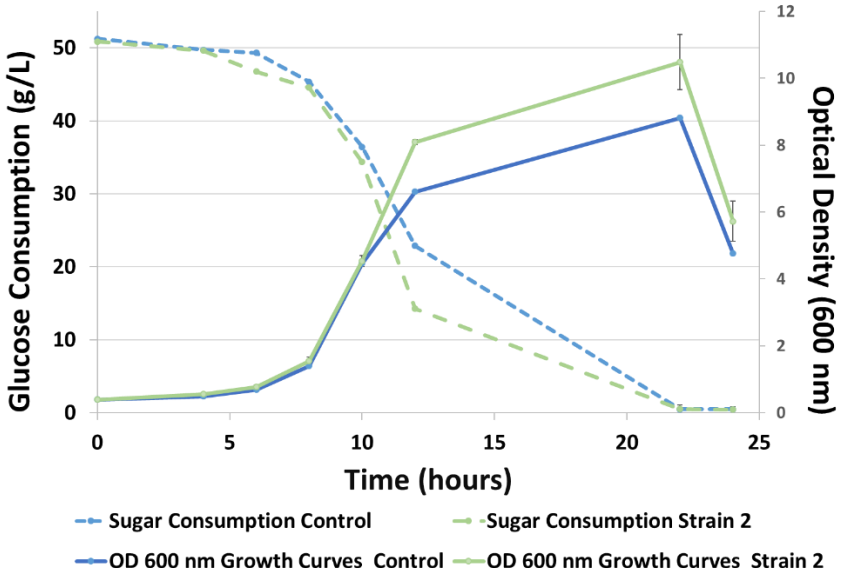

Figure 9-3 Glucose Concentration (Y1) and Optical Density (Y2) as a function of fermentation time for the aerobically grown D5A *S. cerevisiae* strain.

Adding as little as 1 mL of TFCH resulted in higher OD compared to control samples that were grown only on glucose in aerobic seed cultures. Growth rates were observed to be slightly higher for growth flasks that were supplemented with TFCH. Both *Saccharomyces cerevisiae* strains showed faster consumption of glucose with addition of TFCH.

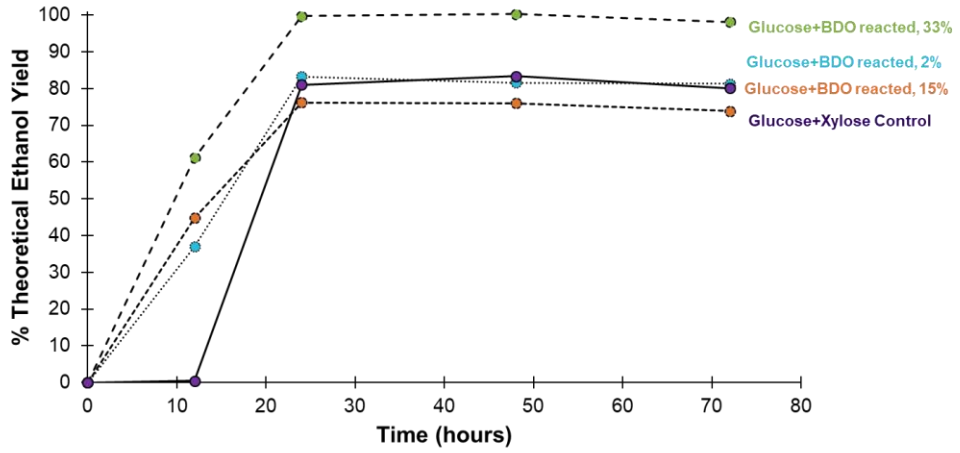

Figure 9-4. Glucose and 1,4-Butanediol reactions (reacted at 150°C for 25 minutes at 6.5 g/L glucose and 4.5 g/L 1,4-BDO) at varied percentages in shake flasks.

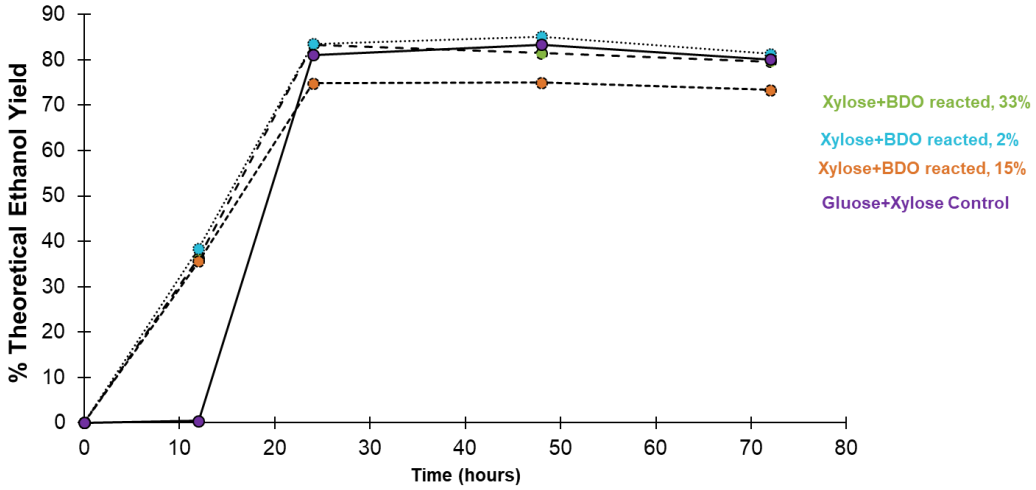

Figure 9-5. Xylose and 1,4-Butanediol reactions (reacted at 150°C for 25 minutes at 6.5 g/L glucose and 4.5 g/L 1,4-BDO) at varied percentages in shake flasks.

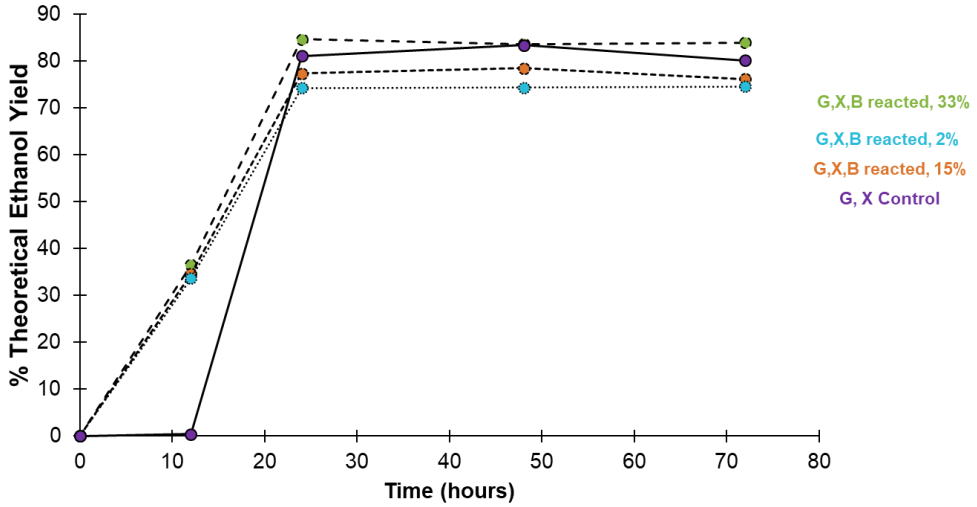

Figure 9-6. Glucose, xylose and 1,4-Butanediol reactions (reacted at 150°C for 25 minutes at 6.5 g/L glucose and 4.5 g/L 1,4-BDO) at varied percentages in shake flasks.

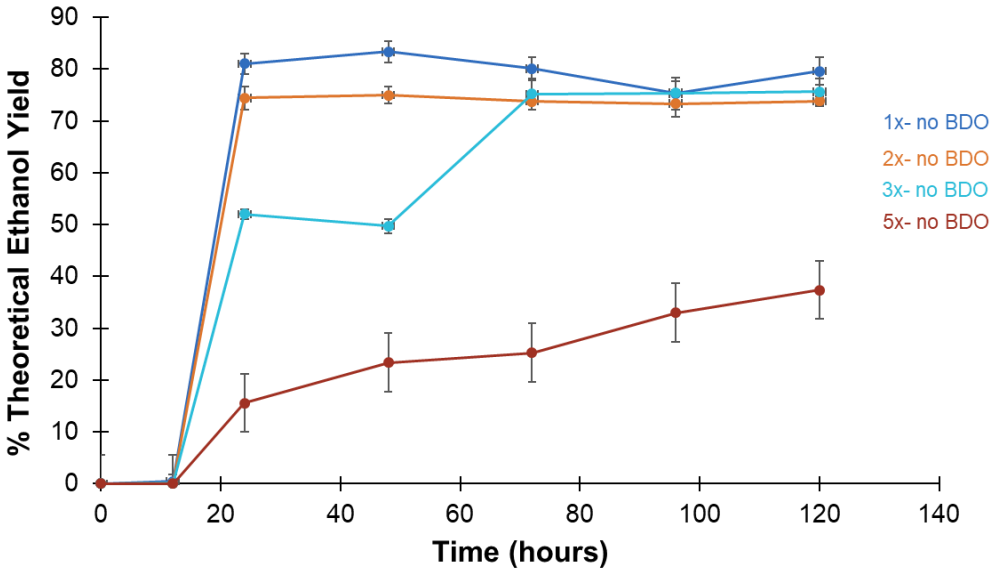

Figure 9-7. Testing strain tolerance to higher concentration mixtures of glucose and xylose based on concentrations found in TFCH from switchgrass.

9.4 Conclusions

Our results indicate that adding as little as 1 mL of TFCH (2% of the total fermentation volume) to aerobic seed cultures can impact two engineered strains of *S. cerevisiae* showing both higher optical density and glucose consumption as compared to controls.

Pure sugars reacted at 150°C for 25 minutes and targeted the production of the boost compound, with all mixtures added at varied volumes, showed a positive enhancement on the rate of fermentation. However, the fermentation rate enhancement effect was most prominent with the addition of reacted glucose and 1,4-BDO. Our working hypothesis still holds for the presented studies and should be further investigated and must be further validated.

9.5 References

Cai, C. M., Zhang, T., Kumar, R., & Wyman, C. E. (2013). THF co-solvent enhances hydrocarbon fuel precursor yields from lignocellulosic biomass. *Green Chemistry*, *15*(11), 3140–3145. https://doi.org/10.1039/c3gc41214h

Kothari, N., Holwerda, E. K., Cai, C. M., Kumar, R., & Wyman, C. E. (2018). Biomass augmentation through thermochemical pretreatments greatly enhances digestion of switchgrass by Clostridium thermocellum. *Biotechnology for Biofuels*, *11*(1), 1–14. https://doi.org/10.1186/s13068-018-1216-7

Patri, A. (2018). Biological Conversion of Alamo Switchgrass Carbohydrates Following Co-Solvent Pretreatment. *Thesis*, *June*, 158–185.

Patri, A. S., Mostofian, B., Pu, Y., Ciaffone, N., Soliman, M., Smith, M. D., Kumar, R., Cheng, X., Wyman, C. E., Tetard, L., Ragauskas, A. J., Smith, J. C., Petridis, L., & Cai, C. M. (2019). A Multifunctional Cosolvent Pair Reveals Molecular Principles of Biomass Deconstruction. *Journal of the American Chemical Society*, *141*(32), 12545–12557. https://doi.org/10.1021/jacs.8b10242